Some Studies of Thermal Degradation in an Ion Exchange System

by

John Thomas Klaschka, B.Sc., A.C.G.I.,

A Thesis submitted for the
Degree of Doctor of Philosophy
of the University of London

Nuclear Technology Laboratory,
Department of Chemical Engineering
and Chemical Technology,
Imperial College,
London, S.W.7.

January 1967.

Abstract

The thermal stability of four weak and five strong base exchange resins was measured at temperatures up to 180°C. The loss in strong base capacity, gain in weak base capacity, yields of trimethylamine and methanol, and the change in water regain were determined. The decomposition reaction followed a first order rate law with activation energies between 20 and 35 kcal/mole. The weak base exchangers were found to be stable at 180°C, for up to 10 days. The strong base exchangers were much less stable, and Deacidite FF was the most stable example.

The effect of degree of crosslinking, particle size and nature of the sorbed counter ion on the thermal decomposition of Deacidite FF was investigated. A higher degree of crosslinking resulted in a substantial decrease in stability; stability decreased with particle size significantly above 100°C and the most stable ionic form of a resin was that in which the most preferred counter ion was sorbed on the resin.

The behaviour of the Deacidite FF - hydroxide in a flow system was studied in a hot water test, specially constructed for this purpose. Thermal decomposition of the resin in a flowing system was found to be substantially the same as in a static system . Hydrodynamic studies in the test loop indicated that

the resin particles suffered no significant physical or mechanical damage. The Carman Cozeny correlation for pressure drop in fixed beds of particles was found to account for the observed pressure drop in the test loop. A maximum bed compaction of 5% occurred over a 70 day run.

Mass transfer studies in the region where both film and particle diffusion are significant were carried out with degraded samples of Deacidite FF, in a small packed column. Diffusion coefficients were calculated from a published mathematical theory; a Fortran IV computer programme was written to accomplish these calculations. The rate of exchange, and hence the particle diffusion coefficient as defined by the model, passed through a maximum value as the total capacity was reduced by thermal decomposition. The chemical reaction of exchange, the rate of which decreases with decreasing resin capacity, probably replaces the diffusional mechanism as the exchange rate controlling factor after the maximum has been passed.

Acknowledgements

It is a pleasure to thank Professor G.R. Hall for his constant encouragement and support throughout this work. I am also particularly grateful to Dr. M.Streat for contributing his experience and knowledge of Ion Exchange and for much sensible advice.

I am indebted to Dr. P.G. Clay for rewarding discussions on reaction mechanisms and advice on many chemical matters and to Dr. H. Sawistowski for stimulating the theoretical work on alternative models of Ion Exchange.

I wish to thank Mr. W. F. White , Senior Technician in the Department for his willing help during the erection of the test loop.

This work was made possible by a Research Bursary awarded by the United Kingdom Atomic Energy Authority.

Contents

Chapter 1

INTRODUCTION

Ion exchange resins were first developed for use in water treatment; lately they have found application in many other chemical engineering operations. The increasing use of these materials has opened a whole new field of study, concerned with measuring and improving their performance.

The development of nuclear power in particular has stimulated the use of ion exchanges, both in their traditional applications and where the more common separation processes have proved unsatisfactory for economic or technical reasons. In nuclear chemical operations ion exchange resins are used for refining new materials, reprocessing irradiated fuels and decontamination of primary coolant in water cooled reactors.

Ion exchange resins in common with all other engineering materials have disadvantages which limits their usefullness. The inorganic ion exchangers have poor resistance to chemical attack, while the more commonly used organic exchangers are seriously damaged by exposure to radiation and elevated temperature. Elevated temperature is taken as the range from 50°C to 180°C, for the purposes of this report.

The thermal instability of organic ion exchange materials (such as quaternary ammonium polystyrene based resins), in the hydroxide form is well known. In practical operations, manufacturers recommend that the temperature of process solutions should be kept below 60°C, to avoid serious chemical decomposition. Very little quantitative data exists at the present time on the precise nature of the decomposition reactions, and the degree of chemical decompositions that may ensue at operating conditions above 60°C.

Wheaton and Baumann(ref.W1) investigated the anion exchangers Dowex 1 and Dowex 2 and found little capacity loss after 26 hours when the hydroxide and chloride forms of these resins were heated at 125°C. Heating at 175°C for 26 hours caused a complete loss of capacity in the hydroxide form and a 75% loss in the chloride form of the resin. Results obtained by heating Dowex 2 in the hydroxide and chloride forms at 95°C for 50 days showed 60% capacity loss and no capacity loss respectively. Hall and Streat (ref.H1) working with the anion exchanger Deacidite FF hydroxide found 10% loss in capacity when the resin was heated at 100°C for 26 hours and only 20% loss after 100 hours. Marinsky and Potter (ref.M1) however observed a marked decrease in exchange capacity when Amberlite IRA 400 hydroxide was heated at temperatures of 117°C and 135°C for 100 hours. Amberlite IRA 400 and Dowex 1 are chemically similar. E.W. Baumann (ref.B1) conducted an investigation into the thermal decomposition of Amberlite IRA 400, in static and simulated flow system and found that the resin decomposed

on heating by 2 distinct reactions, suggested to be the following:-

1 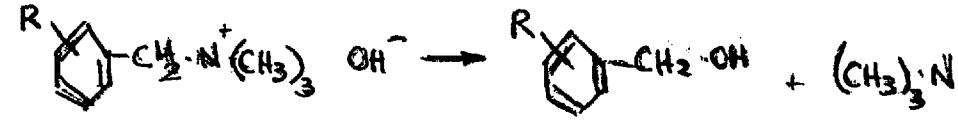

2 

where R denotes the resin matrix. Creed (ref.C1) heated Deacidite FF hydroxide at 150°C and reported total strong base capacity loss in less than 12 hours . Several other workers (ref.S1,J1,P1,P3) have reported results of experimental work on the thermal stability of anion exchange resins, but as yet no exhaustive work has been completed. The results to date are summarised in Table 1.1.

The results of the work described above are incomplete and therefore the first stage of the present work was a systematic study of the thermal stability of a variety of anion exchange resins under carefully controlled conditions, The second stage of the work was an investigation of the variation in the rate of exchange with temperature.

Ion exchange operations, whether in the laboratory or in plant scale processes are most frequently carried out in columns. A solution is passed through a fixed bed of ion exchange particles, where its composition is changed by sorption. The composition change with time, depends on the characteristics of the ion exchanger, and the operating conditions.

TABLE 1.1 RESULTS OF THERMAL STABILITY INVESTIGATIONS TO DATE.

WORKER	RESIN	TIME HEATED	HEATING TEMPERATURE	CAPACITY LOSS
W1	DOWEX 1 AND 2 HYDROXIDE	26 HRS	125°C	LITTLE
W1	DOWEX 1 AND 2 CHLORIDE	26 HRS	125°C	LITTLE
W1	DOWEX 1 AND 2 HYDROXIDE	26 HRS	175°C	100%
W1	DOWEX 1 AND 2 CHLORIDE	26 HRS	175°C	60%
W1	DOWEX 1 AND 2 HYDROXIDE	50 DAYS	95°C	60%
W1	DOWEX 1 AND 2 CHLORIDE	50 DAYS	95°C	NONE
H1	DEACIDITE FF HYDROXIDE	26 HRS	100°C	10%
H1	DEACIDITE FF HYDROXIDE	100 HRS	100°C	20%
M1	AMBERLITE IRA 400 HYDROXIDE	100 HRS	117°C	MARKED
M1	AMBERLITE IRA 400 CHLORIDE	100 HRS	135°C	MARKED
C1*	DEACIDITE FF HYDROXIDE	12 HRS	150°C	100%
B1	AMBERLITE IRA 400	see Chapter 1		

*STRONG BASE CAPACITY LOSS.

The characteristics of an ion exchange resin operating on a given binary ionic system, which affect its performance are resin capacity, selectivity, and the rate of sorption. Resin capacity changes significantly with sustained temperature above 50°C. The selectivity of an ion exchanger for a given ion decreases with temperature since selectivity results in most cases from association processes, which are suppressed by an increasing temperature. The rate of sorption is strongly dependent upon diffusion processes, the rates of which increase markedly with temparature (ref.B8,H6,B9), and are probably also affected by thermal damage.

The effects of temperature increase are therefore more rapid exchange, consequent greater column utilisation, but also an increased rate of resin decomposition. The most economic temperature for any resin operation occurs at the point where increased operating efficiency is balanced by reduced resin lifetime caused by thermal damage.

Anion exchange at temperatures above 50°C is accompanied by thermal decomposition of the resin, and the release of decomposition products. The latter may cause trouble in separation processes by contamination of the process solution. In application where mixed beds of resin are used (e.g. coolant cleanup), some decomposition products may reduce effective cation capacity,and the remainder accumulate in the process equipment. Salt forms of anion exchangers decompose less rapidly at any given temperature and have found application in elevated temperature chemical processing (ref.R1).

The work presented in this thesis had two aims. Firstly, to examine the feasibility of processing elevated temperature solutions without prior cooling, and secondly to determine whether ambient temperature exchange processes can be significantly improved by increasing the operating temperature. Quantitative information is not available on all the factors relevant to these problems, so the answers must be determined by experiment.

Chapter 2

THERMAL DECOMPOSITION OF ANION EXCHANGE RESINS UNDER STATIC CONDITIONS

2.1 Introduction.

2.1.1 Scope of work, (Table 2.1).

The object of this work was an extensive study of the effect of prolonged exposure to elevated temperatures on selected anion exchange resins (Table 2.2). The term elevated temperature is used in this report to describe the range between 50°C and 180°C.

The effect of time, temperature, sorbed counter ion, degree of crosslinking and particle size on thermal decomposition in anion exchange resins at elevated temperature was investigated. The nature and quantity of all significant decomposition products was determined. The reaction mechanisms were identified and characterised by velocity constants and activation energies. The factors affecting water regain were considered.

2.1.2 Structure of anion exchange resins.

Organic anion exchangers contain fixed, basic, ionic, functional groups attached to an inert, irregular, three dimensional matrix of hydrocarbon chains. The hydrophobic

TABLE 2.1 SCOPE OF STUDIES ON ANION EXCHANGE RESINS

TYPE OF RESIN	TIME	NATURE OF ION
IRA 400 IR 45	0-30 DAYS	$OH^-, Cl^-, B_2O_7^{1-}$;
IRA 900 IR 93		NO_3^-, SO_4^{2-}, CNS^-
EACIDITE FF DEACIDITE J		
DOWEX 1 DOWEX 3		
ERMUTIT-SK		

ORE STRUCTURE		NATURE OF GROUPS
RDINARY IRA 400	EFFECT ON RESIN	N^+-(ALKYL)$_3$ IRA 400
IACRORETICULAR IRA 900	DECOMPOSITION	N-(ALKYL)$_n$ IR 45
		PYRIDYL PERMUTIT SK

TYPE OF CROSSLINK	DEGREE OF CROSSLINKING
METHYLENE BRIDGE DEACIDITE FF	2-3%, 4-6%, 7-9%,
DVB TYPE IRA 400	

EMPERATURE	PARTICLE SIZE
50°C-180°C	14-52 MESH
	100-200 MESH

TABLE 2.2 LIST OF ANION EXCHANGERS USED IN THIS WORK

STRONG BASE EXCHANGERS

TRADE NAME	TYPE	S.B.CAPACITY	W.B.CAPACITY	WATER REGAIN
AMBERLITE IRA 400.	QUATERNARY AMMONIUM POLYSTYRENE	2.90	0.30	1.06
*AMBERLITE IRA 900		2.90	0.30	1.25
DEACIDITE FF		3.90	0.10	0.98
DOWEX 1		2.90	0.28	0.94
PERMUTIT SK	ALKYL VINYL POLYPYRIDINE	3.40	0.81	0.71

WEAK BASE EXCHANGERS

TRADE NAME	TYPE	S.B.CAPACITY	W.B.CAPACITY	WATER REGAIN
AMBERLITE IR 45	POLYAMINE POLYSTYRENE		5.48	0.51
*AMBERLITE IR 93			5.49	0.62
DEACIDITE J			5.22	0.40
DOWEX 3			5.55	0.30.

* MACRORETICULAR ION EXCHANGE RESINS

CAPACITY IN MEQ/G.
WATER REGAIN IN G. PER G. DRY RESIN.

matrix is insoluble but flexible and may swell to a limited extent by taking up water, depending on the degree of crosslinking. The hydrophilic functional groups are able to exchange ions selectively and may be weakly or strongly basic. The chemical, mechanical, and thermal properties of an ion exchange resin depend on the nature and degree of crosslinking and the nature and number of fixed ionic groups.

The early ion exchangers, now obsolete, were based on a phenol formaldehyde polycondensation matrix, crosslinked with unsubstituted phenol. The degree of crosslinking was controlled by the relative amount of phenol added to the reaction mixture, but this was not easily adjustable. Anion exchange properties were incorporated by the use of m-phenylene diamine. Resins prepared in this way were polyfunctional aliphatic amines with very variable properties.

A significant advance was afforded by the introduction of the second generation ion exchange resins based on a polystyrene matrix, and with which this work is entirely concerned. In these resins the degree of crosslinking is easily and accurately adjustable by the controlled addition of divinylbenzene. The matrix is chloromethylated in a carefully controlled reaction before quaternization with trimethylamine (type 1) or dimethylethanolamine (type 2). The resulting anion exchanger is almost monofunctional and has reproducible properties.

The following structure has been suggested for Amberlite IRA 400, a typical type 1 second generation strong base

exchanger, quaternised with trimethylamine (ref H3). (Strong base functional groups are those groups which are capable of exchange over the whole pH range, whereas weak base groups operate only at pH values less than 6).

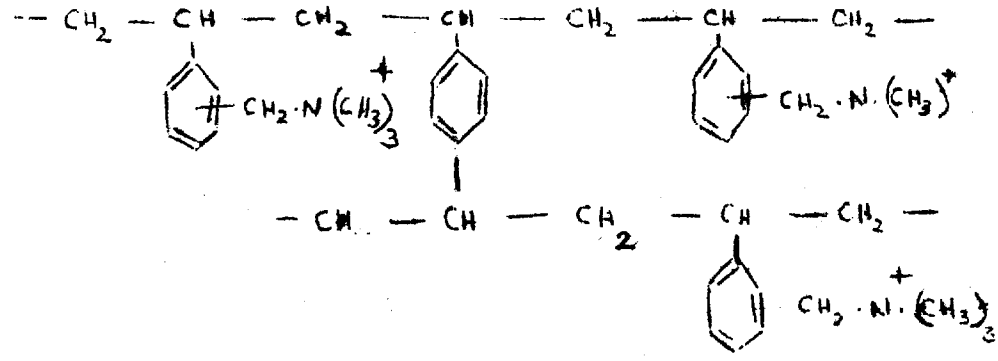

The resin contains strong base functional groups $-N^{+}(alkyl)_3$ type and a small proportion of weak base functional groups thought to be of the $-N(alkyl)_n$ type. Type 2 strong base exchangers differ from type 1 only in the type of strong base functional group. A typical example is Amberlite IRA 410:-

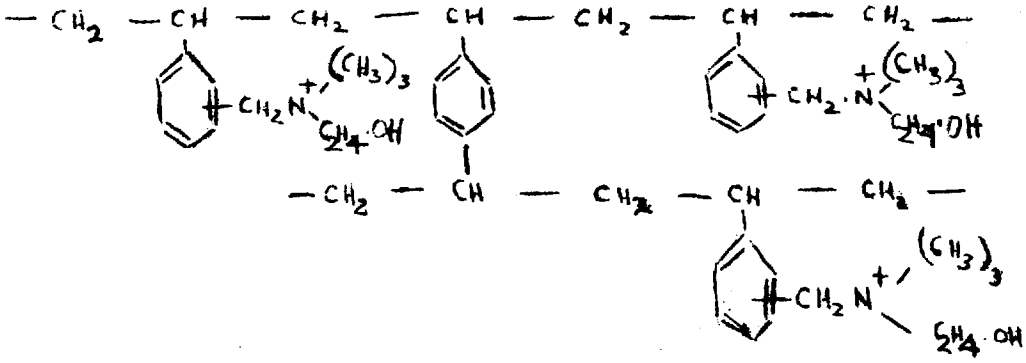

Weakly basic exchangers based on the polystyrene matrix are prepared by the amination of a chloromethylated matrix

with amines or ammonia. Examples of this type are Amberlite IR 45 and Dowex 3.

Deacidite FF is a type 1 strong base exchanger produced by the suspension copolymerisation of styrene with a divinyl aliphatic ester thought to be ethylene glycol dimethacrylate (ref.B6). Subsequent chloromethylation gives a matrix crosslinked by methylene bridges as in structure X although some typical DVB crosslinks are produced as in structure Y. The manufacturers of Deacidite FF claim that their resin contains mainly type X crosslinks, whereas in Amberlite IRA 400 and other type 1 strong base exchangers copolymerised with divinylbenzene the DVB crosslink predominates (ref. A1,H3).

STRUCTURE X

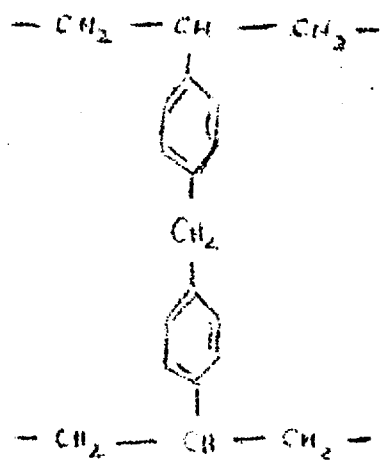

STRUCTURE Y

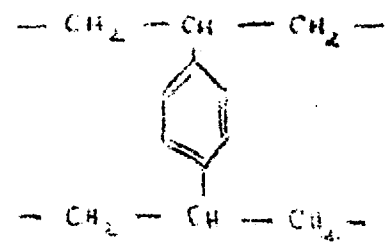

Functional groups are distributed throughout the whole resin matrix and if exchange capacity is to be fully utilised, the exchanging counter ions must be able to move freely through the particle. The pore structure of the conventional

anion exchangers is such that large complex molecules are unable to penetrate into the interior of the particle. Macroreticular resins were introduced to overcome this problem. These are highly porous materials with pores of several hundred Angstrom units diameter and a narrow pore size distribution, which guarantee access to the interior of the particle even when large molecules or non polar solvents are used. They are identical to the conventional resins in all other aspects. An example of this type of anion exchanger is Amberlite IRA 900 .

Samples of Deacidite FF used in this work were of the " isoporous" type introduced by the Permutit Co. in 1964 (ref.A2). "Isoporous"resins are claimed to have a uniform distribution of functional groups and pore sizes on the molecular scale.

2.2 Experimental.

2.2.1 Preparation of resin for experimental work.

Raw resin was obtained from the makers predominantly in the chloride form, and treated as follows before use. A large quantity of each resin was thoroughly mixed and divided into equal batches for further treatment. This procedure ensured constant properties in the resin used in this work, because a 10% variation in properties was sometimes found between resin taken from different bottles.

Each batch was conditioned by washing with 10 batch volumes of warm methanol (40°C) and an equal volume of fresh demineralised water, air dried and converted to the required ionic form as described in Appendix 1.

After 99.5% conversion (checked by capacity analysis) batches were stored under methanol in stoppered bottles until required. Immediately before use each batch was soaked in fresh demineralised water for 24 hours, washed with 10 batch volumes of fresh demineralised water and divided into samples of appropriate size.

Resin for mass transfer work was pretreated as follows before carrying out the above operations. The raw material was sieved after air drying and the fraction between 20 and 30 BSS mesh size was retained. Irregular and cracked particles were removed by careful inspection and water elutriation. A sample removed for examination under a microscope showed that this treatment was sufficient to reduce the fraction of undesirable particles to a negligible level (0.005).

2.2.2 Analytical techniques.

a) Capacity analysis.

Initially it had been decided to use the standard Fisher Kunin method for anion exchange capacity analysis. (ref.F1). However, at an early stage in the work a paper by Juracka and Stamberg (ref.J2) was published which demonstrated certain errors in the Fisher Kunin technique. The paper showed that values of strong base capacity obtained by the Fisher Kunin technique were too low and values of weak base capacity were too high. This was because the ammonium hydroxide reagent used, hydrolysed an appreciable fraction of the strong base capacity. Fisher and Kunin had assumed that ammonium hydroxide only reacted with the weak

base functional groups. The method of Juracka and Stamberg was tested against the Fisher Kunin method and the conclusions of the former confirmed. Results and discussion are given in Appendix 2. The former method was used for all subsequent analyses of capacity. Juracka's method was further modified by using a radiochemical technique to measure chloride, instead of the Volhard volumetric analysis. This technique, described fully in Appendix 2 , saved a considerable amount of time since counting could be carried out automatically while other analyses were being made.

b) Water regain.

Water regain was measured by the method of Pepper et al. (ref.P2). Samples were dried at 105°C for 48 hours to obtain the final dry weight. This sufficed to attain constant weight. Water regain was measured after carrying out capacity analysis and samples were therefore always in the sulphate form .

c) Soluble decomposition products.

After heating, resin samples were separated from the liquid in which they have been heated. The liquid and washings from rinsing the sample were analysed for soluble decomposition products. Trimethylamine, methanol, dimethylamine, methylamine and ammonia were expected. It soon became apparent that trimethylamine and methanol only were produced as a result of the decomposition. Trimethylamine was measured by the amine picrate method (ref.D1). In the past methanol has only been inferred as a decomposition product. Recently, however, quantitative

measurement using a Perkin Elmer vapour phase chromatograph has proved possible. A column containing DE 105K packing, (i.e. polyethylene glycol 155 supported on chromosorb P) was used, with a flame ionisation detector. Methanol yields were measured only in a few cases, by comparing the area under peaks produced from a sample of liquid and from a controlled sample of known methanol content.

2.2.3 Experimental method.

A large number of small samples (0.5g) of ion exchange resin were heated in demineralised water (5ml.) to provide experimental data. Samples and water were sealed in glass ampoules , to prevent the escape of volatile decomposition products. At temperatures up to 90°C the ampoules were heated in a constant temperature water bath, maintained to within ± 0.5°C of the required temperature by a thermostatically controlled 1kw. Heater and stirrer unit. At temperatures above 90°C a heavily lagged bath of silicone oil was used ; the temperature was maintained to ± 1°C of the required value. The ampoules were placed in a small autoclave for work above 100°C. A trial experiment was carried out to determine the time necessary for the interior of the autoclave to attain the bath temperature. This was found to be less than 2 minutes in all cases.

2.2.4 Sources of error and precautions.

a) Incomplete conversion.

Each bath of resin was checked by separate analysis and rejected if less than 99.5% converted to the desired ionic form.

b) Carbon dioxide absorption.

Streat (ref.H1) showed that anion exchange resins in the hydroxide form absorbe carbon dioxide rapidly on exposure to air. Hydroxide samples were accordingly stored under methanol in stoppered bottles.

c) Impurities in analytical reagents.

Methanol, sodium, sulphate and ammonium hydroxide were checked for chloride content before use in capacity determinations. (see Appendix 2). No chloride was detected.

d) Incomplete removal of sorbed chloride ions during capacity analysis.

The number of column volumes for complete elution of the chloride ions in the resin samples was determined beforehand by collecting successive 10ml. aliquots of column effluent and analysing each for eluted chloride ions, until no further amounts were detected.

e) Loss of volatile decomposition products.

Soluble products of thermal decomposition include volatile amines. Loss of these was avoided by heating resin samples in sealed ampoules. After heating, these ampoules were cooled to ambient temparature and broken under water.

2.3 Results and discussion.

2.3.1 Weak base exchangers.

No significant changes were observed over a 30 day heating period in the four weak base exchangers, which were heated in the chloride and free base forms, at temparatures up to 180°C. Results are shown in Table 2.3.

Limits of significance were taken as $\pm$ 0.05 meq/g. change

TABLE 2.3 THERMAL DECOMPOSITION, CAPACITY CHANGES
WEAK BASE EXCHANGERS, CHLORIDE AND FREE BASE FORMS
14-52 MESH. 7-9% CROSSLINKED.

TEMPERATURE	RESIN	IONIC FORM	CAPACITY AS % OF ORIGINAL
90 C*	IR 45	FREE BASE	99.8
	IR 93		99.8
	DEACIDITE J		99.8
	DOWEX 3		100.0
	IR 45	CHLORIDE	100.0
	IR 93		99.9
	DEACIDITE J		99.8
	DOWEX 3		99.8
180 C+	IR 45	FREE BASE	100.0
	IR 93		100.1
	DEACIDITE J		100.0
	DOWEX 3		99.9
	IR 45	CHLORIDE	99.8
	IR 93		100.0
	DEACIDITE J		100.0
	DOWEX 3		100.0

*30 DAYS HEATING
+10 DAYS HEATING

NO SIGNIFICANT CHANGE IN WATER REGAIN. ERROR ON MEASUREMENTS IS OF THE ORDER OF 1-2%.

in capacity, 0.01 meq/g. yield of decomposition products and ± 0.01 gH_2O/g. dry resin for water regain. Weak base functional groups in these anion exchangers are evidently stable up to 180°C for long periods of time.

Previous reports (ref.B10) had indicated good thermal stability in weak base exchangers up to 100°C. These new results suggest that certain exchangers with properties similar to weak base exchangers might be usefully applied to water coolant treatment. For example Amberlite IR 63 (which has become available since this work was finished) operates effectively over the whole pH range (ref.K3) yet has strong similarities to the weak base exchangers in all other respects suggesting that the above thermal stability results may well apply.

2.3.2 Strong base exchangers in the hydroxide form.

Strong base capacity decreases and the rate of capacity loss increases with increasing temperature above 50°C. In the hydroxide form Amberlite IRA 400 and Dowex 1 are stable at 50°C (Table 2.4) but have lost approximately 25% and 50% strong base capacity at 75°C and 90°C respectively after 30 days heating (Fig.2.1 and 2.4). Amberlite IRA 900 (Fig.2.2), a macroreticular resin is slightly more stable with strong base capacity losses of about 20% at 75°C and 40% at 90°C over the same period. Deacidite FF resin (Fig 2.3) has the greatest stability, losing only about 10% and 30% strong base capacity at 75°C and 90°C respectively after 30 days heating. The results for Amberlite IRA 400 are in good agreement with E.W. Baumann (ref.B1). At 120°C a more rapid loss of strong

TABLE 2.4 THERMAL DECOMPOSITION, CAPACITY CHANGES. STRONG BASE EXCHANGERS HYDROXIDE AND CHLORIDE

HYDROXIDE FORMS AT 50°C

RESIN	CAPACITY	BLANK	AFTER 30DAYS HEATING
IRA 400	S.B.	2.91	2.90
	W.B.	0.28	0.28
IRA 900	S.B.	3.01	3.02
	W.B.	0.21	0.20
DEACIDITE FF	S.B.	3.90	3.91
	W.B.	0.11	0.11
DOWEX 1	S.B.	2.81	2.81
	W.B.	0.21	0.21

CHLORIDE FORMS AT 90°C

RESIN	CAPACITY	BLANK	AFTER 30 DAYS HEATING
IRA 400	S.B.	2.90	2.91
	W.B.	0.28	0.28
IRA 900	S.B.	3.01	3.00
	W.B.	0.22	0.22
DEACIDITE FF	S.B.	3.91	3.92
	W.B.	0.11	0.13
DOWEX 1	S.B.	2.80	2.79
	W.B.	0.21	0.22

base capacity was noted. Considerable loss occurred in about 4 to 5 days, in all four strong base resins. Above 120°C loss in strong base capacity was very rapid; complete loss occurred in 12 hours at 150°C and in four hours at 180°C. Deacidite FF was again the most stable of the resins over the range 120°C to 180°C (Fig. 2.1-2.4). Marinsky and Potter's values for Amberlite IRA 400 at 117°C and 135°C are again in good agreement (ref.M1).

Significant increases in weak base capacity and yields of trimethylamine were measured when any loss in strong base capacity occurred. At temperatures up to 90°C, the weak base capacity increased steadily with time, reaching 120% of the original value in Amberlite IRA 400, Dowex 1 and Amberlite IRA 900 and 150% in Deacidite FF, after 30 days heating at 75°C (Fig.2.5-2.8). At 90°C values of 145% and 160% respectively were attained after the same heating period. A similar result was observed for the production of trimethylamine (Fig.2.9-2.12).

At temperatures of 120°C and above, the weak base capacity increased rapidly, reaching a maximum when all strong base capacity had been destroyed, after which a slow decrease in weak base capacity occurred. At higher temparatures six fold increases of weak base capacity were observed. Yields of trimethylamine continued to increase as the heating temperature was increased until all strong base capacity had been lost, after which no further change occurred. Weak base capacity changes are plotted on a logarithmic scale for the sake of presentation.

FIG 2.1

THERMAL DECOMPOSITION STRONG BASE CAPACITY CHANGES.

AMBERLITE IRA 400 - HYDROXIDE AND CHLORIDE

14-52 MESH, 7-9 % CROSSLINKING.

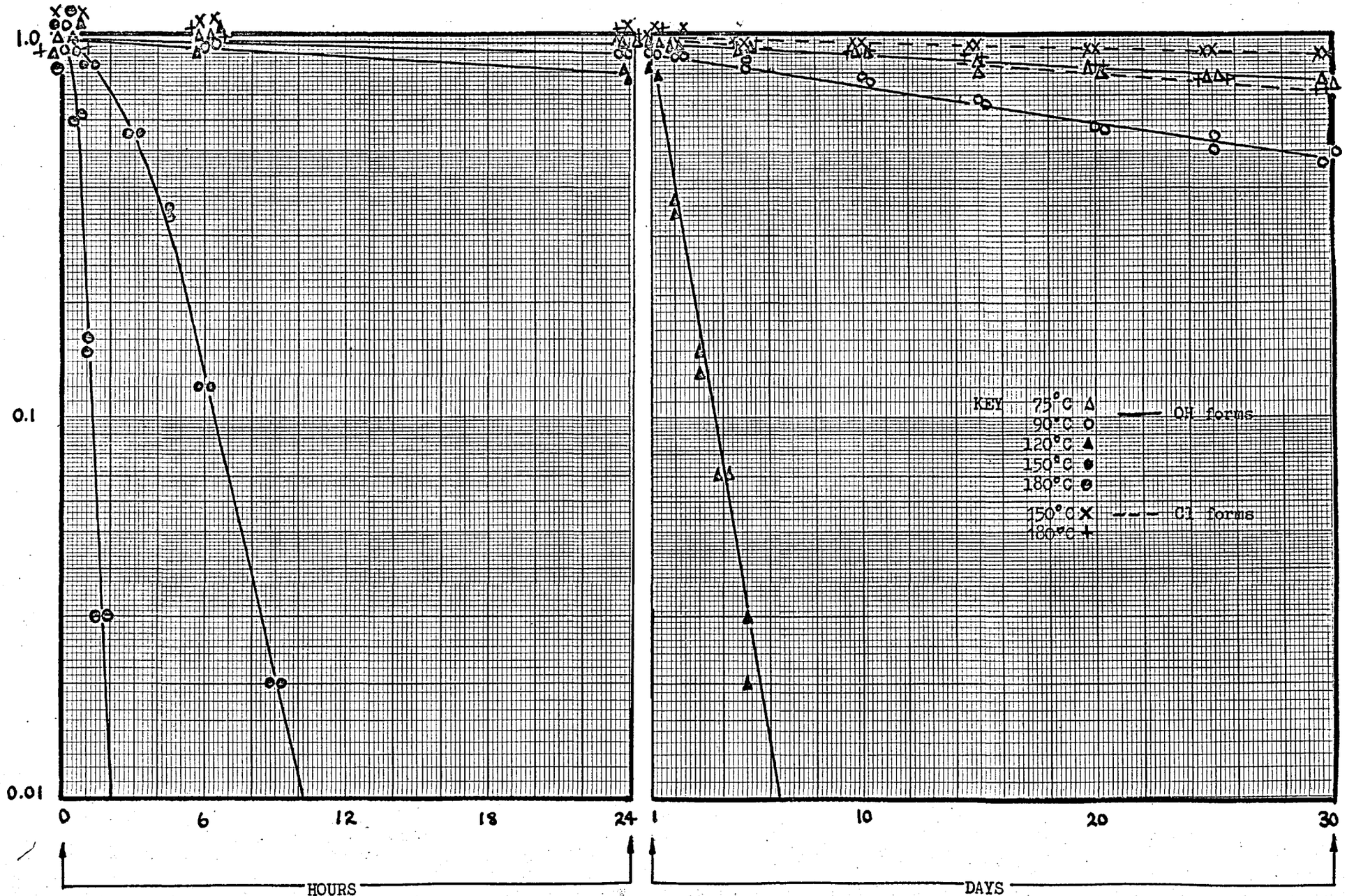

HEATING PERIOD

FIG 2.2

THERMAL DECOMPOSITION STRONG BASE CAPACITY CHANGES.

AMBERLITE IRA 900 - HYDROXIDE AND CHLORIDE

14-52 MESH, 7-9 % CROSSLINKING.

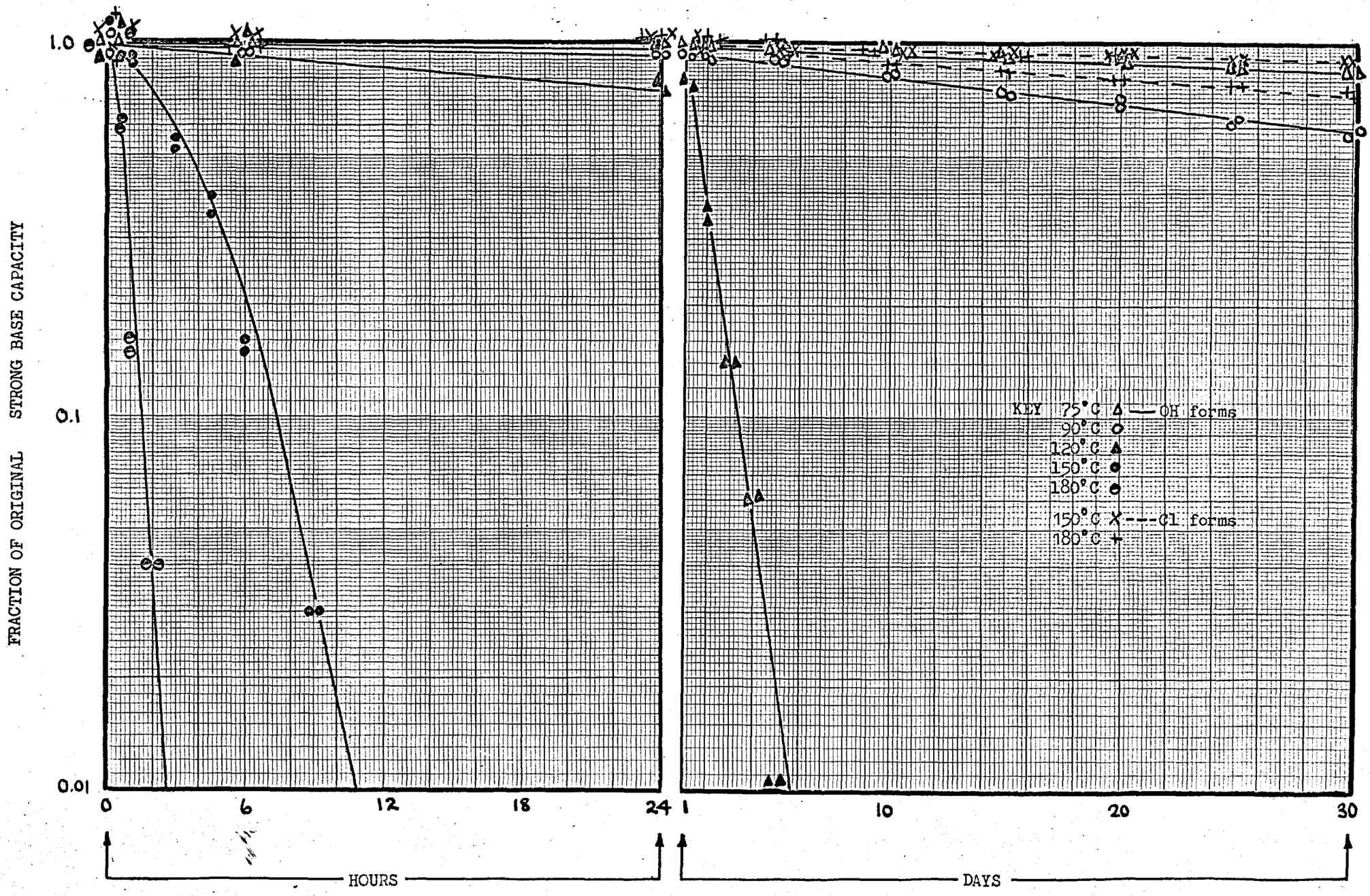

FIG 2.3

THERMAL DECOMPOSITION STRONG BASE CAPACITY CHANGES

DEACIDITE FF - HYDROXIDE AND CHLORIDE

14-52 MESH, 7-9 % CROSSLINKING.

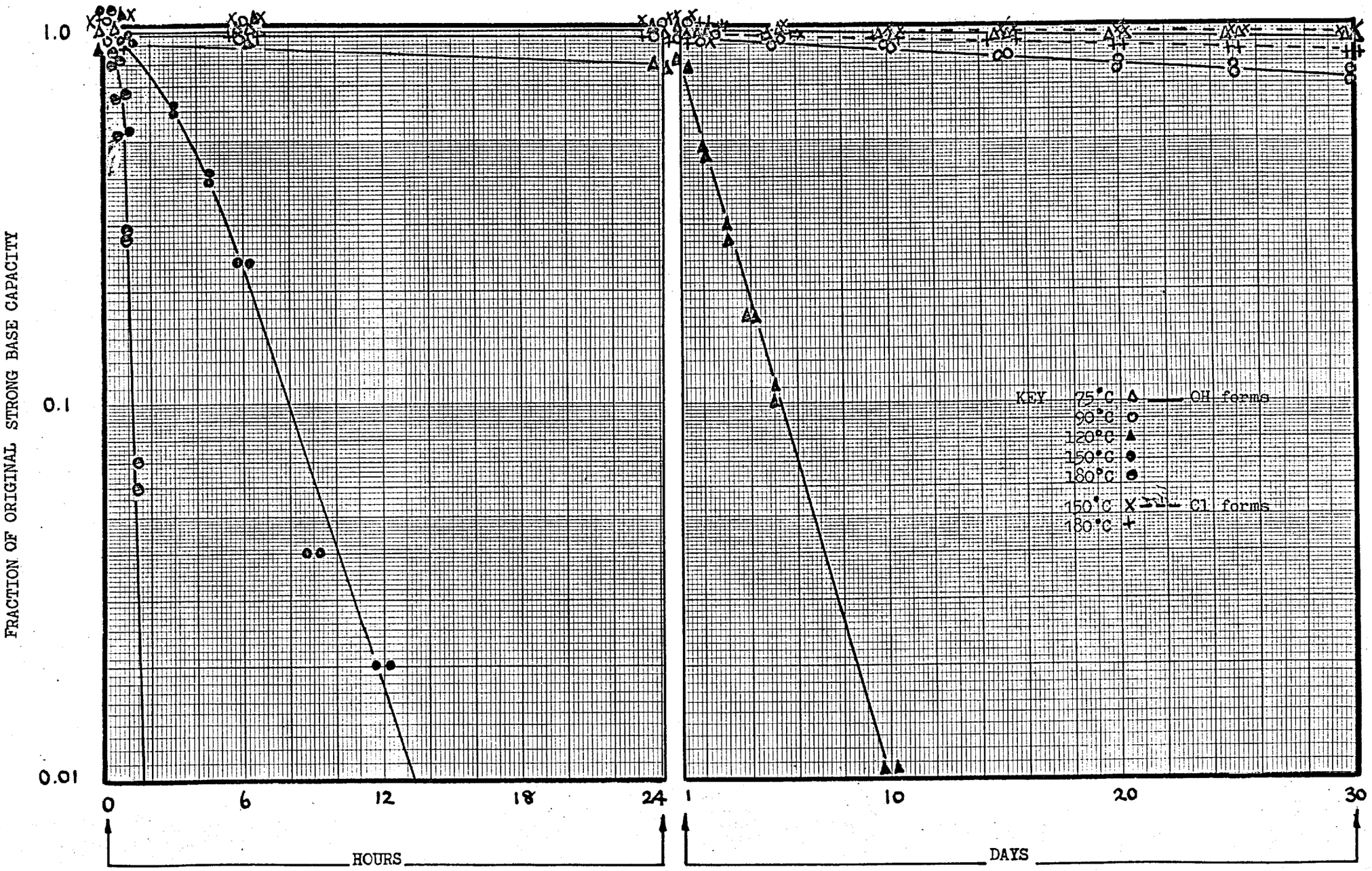

FIG 2.4

THERMAL DECOMPOSITION STRONG BASE CAPACITY CHANGES

DOWEX 1 - HYDROXIDE AND CHLORIDE

14-52 MESH, 7-9 % CROSSLINKING.

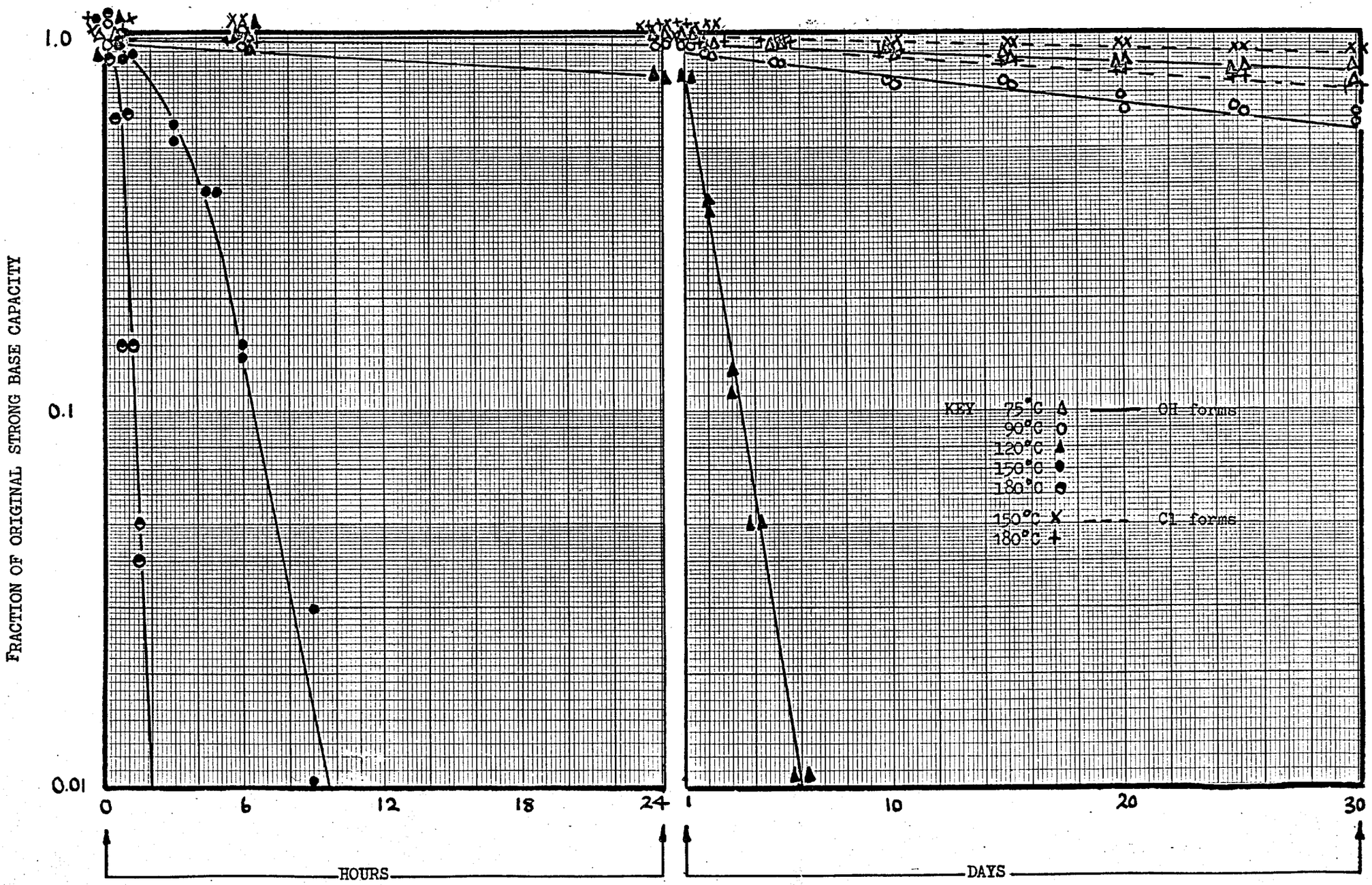

FIG. 2.5 THERMAL DECOMPOSITION WEAK BASE CAPACITY CHANGES.

AMBERLITE IRA 400 - HYDROXIDE AND CHLORIDE

14-52 MESH, 7-9 % CROSSLINKING.

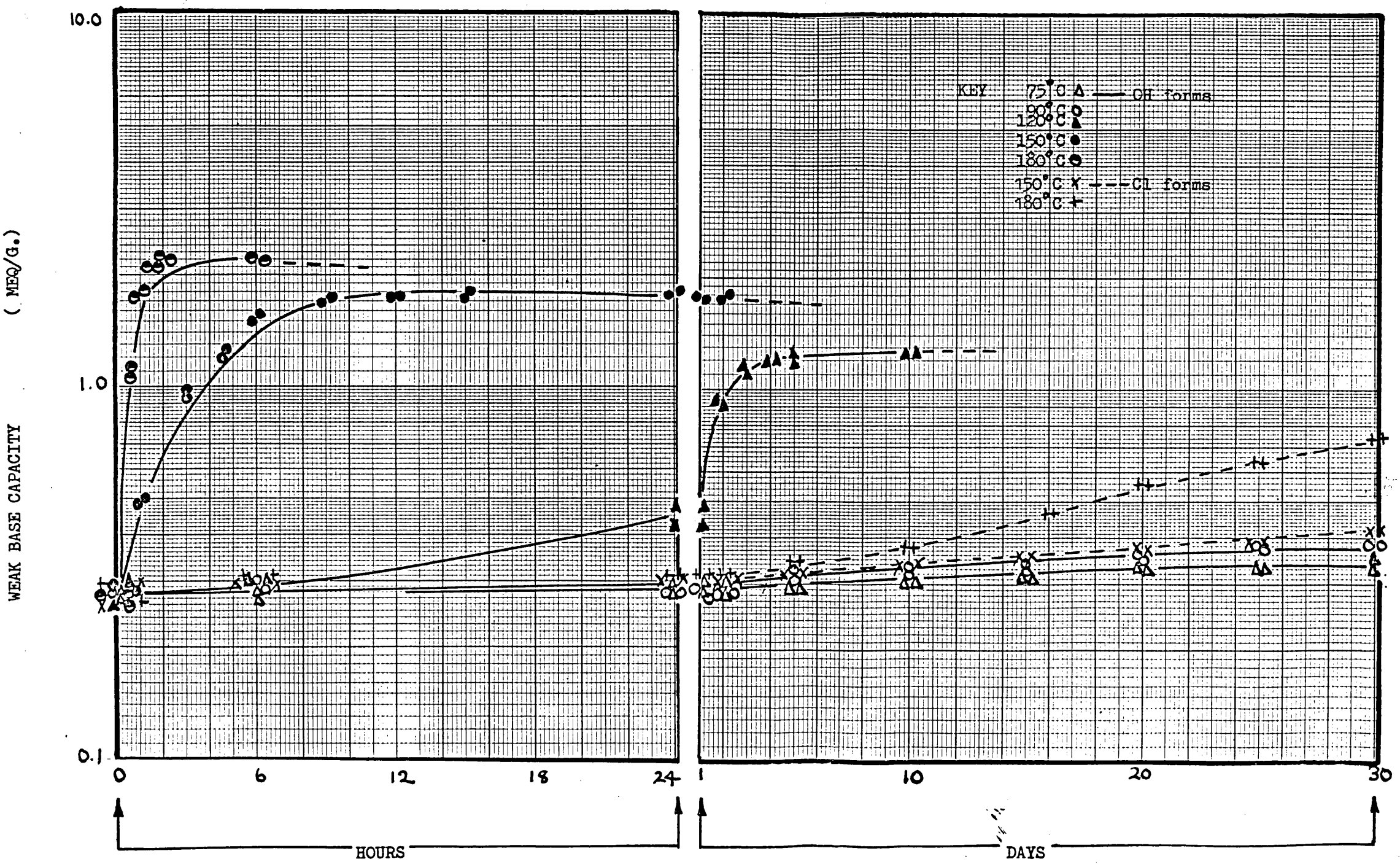

FIG 2.6

THERMAL DECOMPOSITION WEAK BASE CAPACITY CHANGES.

AMBERLITE IRA 900 - HYDROXIDE AND CHLORIDE

14-52 MESH, 7-9 % CROSSLINKING.

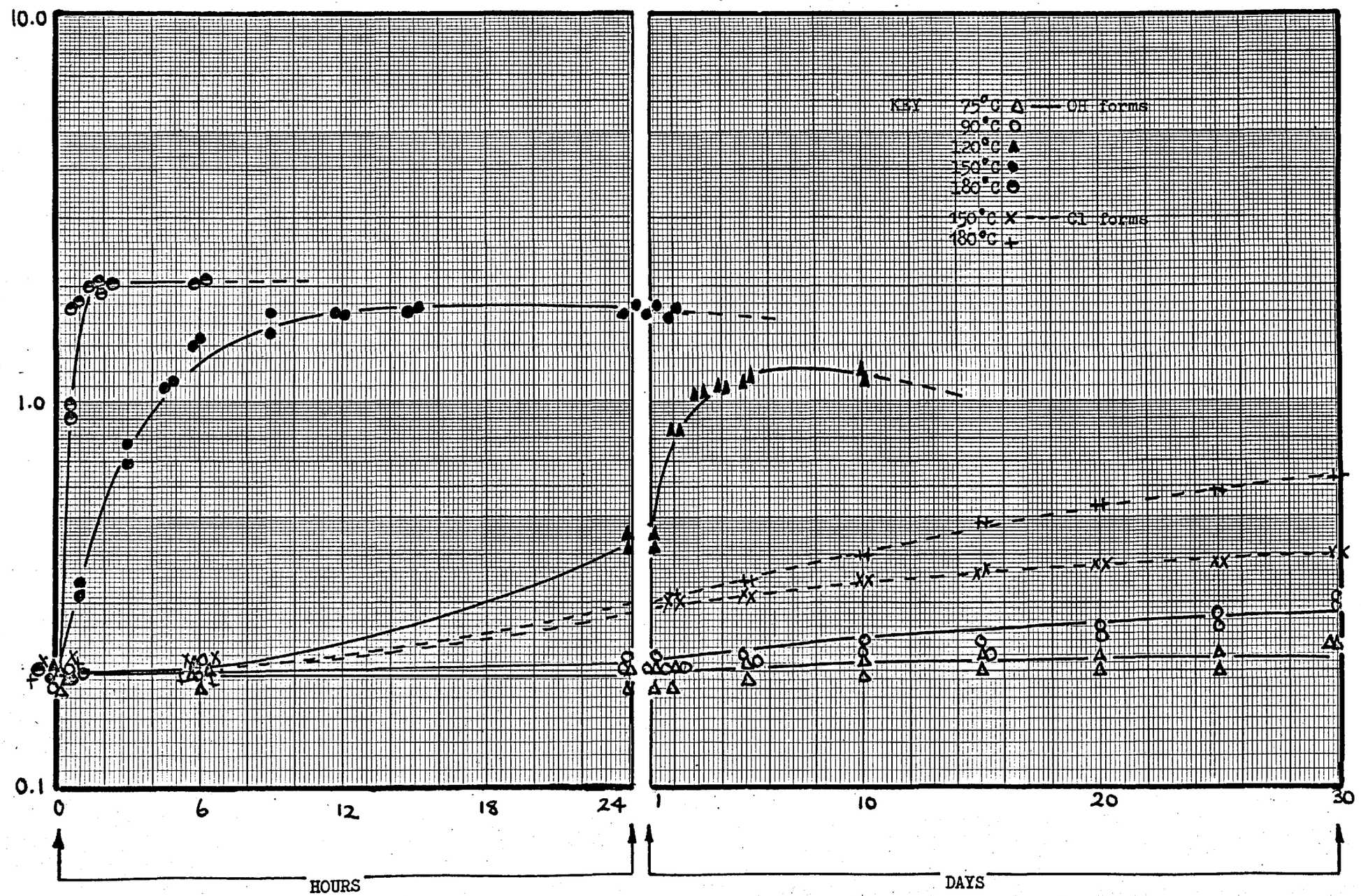

FIG 2.7

THERMAL DECOMPOSITION WEAK BASE CAPACITY CHANGES.

DEACIDITE FF - HYDROXIDE AND CHLORIDE

14-52 MESH, 7-9 % CROSSLINKING.

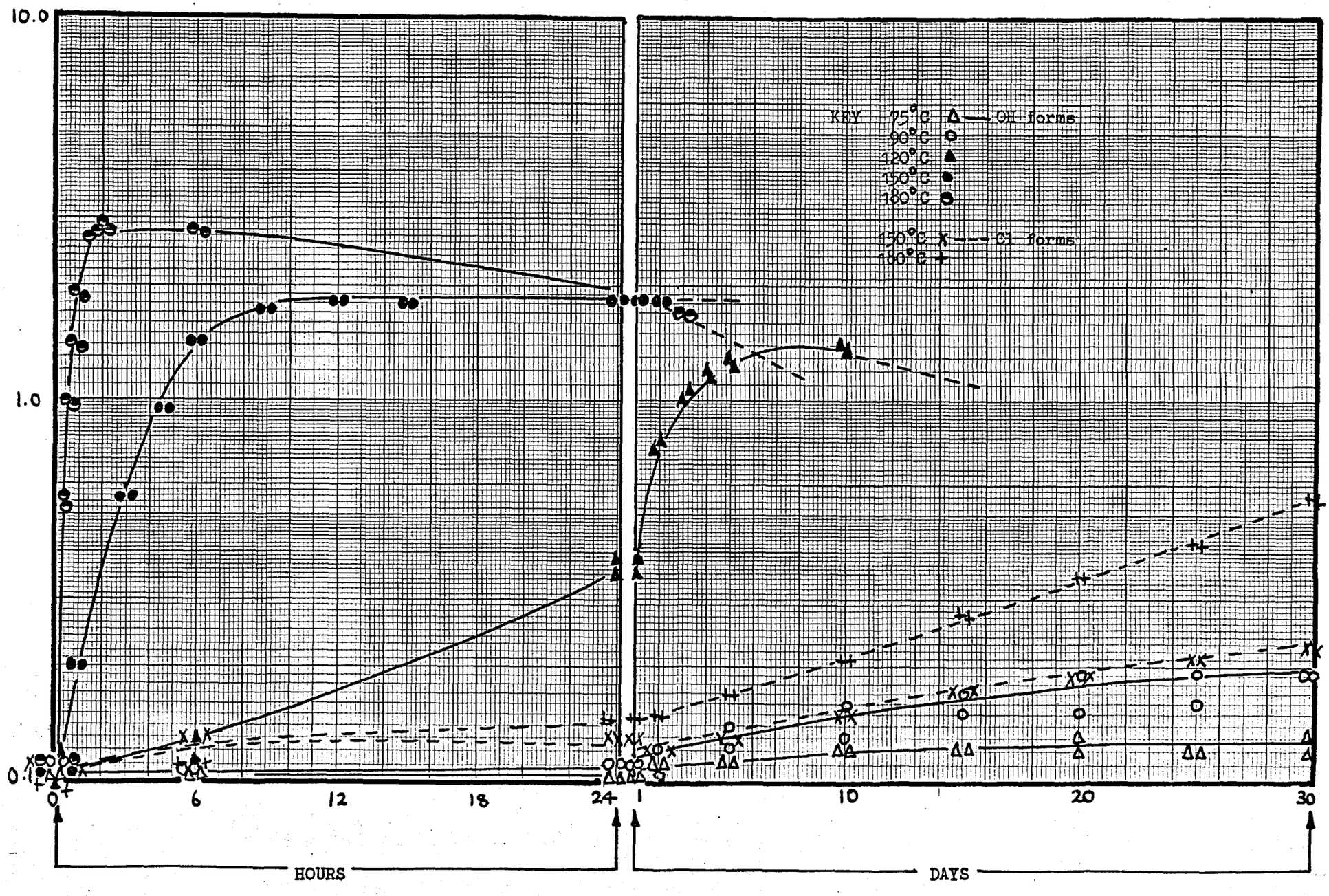

FIG 2.8

THERMAL DECOMPOSITION WEAK BASE CAPACITY CHANGES.

DOWEX 1 - HYDROXIDE AND CHLORIDE

14-52 MESH, 7-9 % CROSSLINKING.

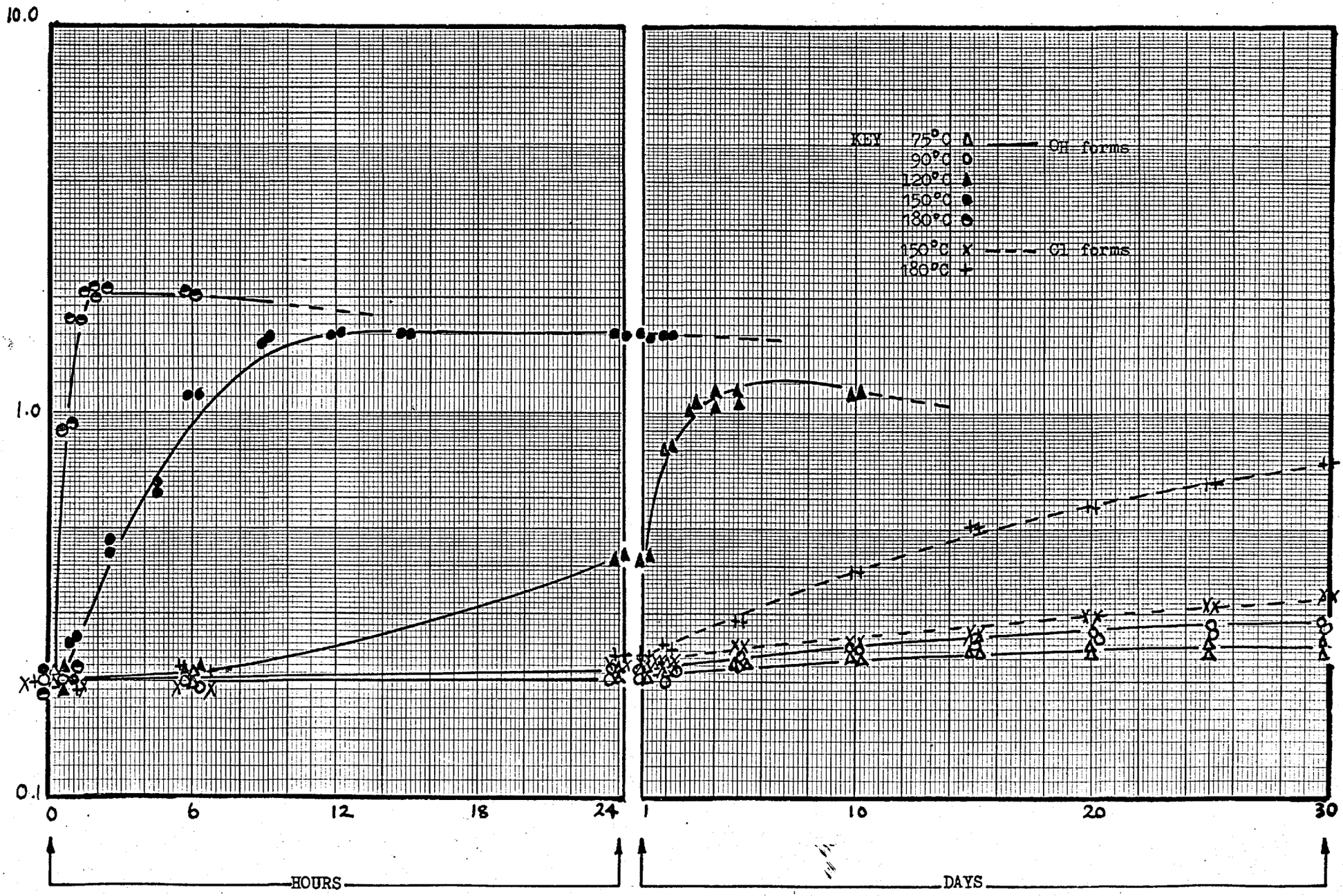

FIG 2.9

THERMAL DECOMPOSITION TRIMETHYLAMINE YIELD.

AMBERLITE IRA 400 - HYDROXIDE AND CHLORIDE

14-52 MESH, 7?9 % CROSSLINKING.

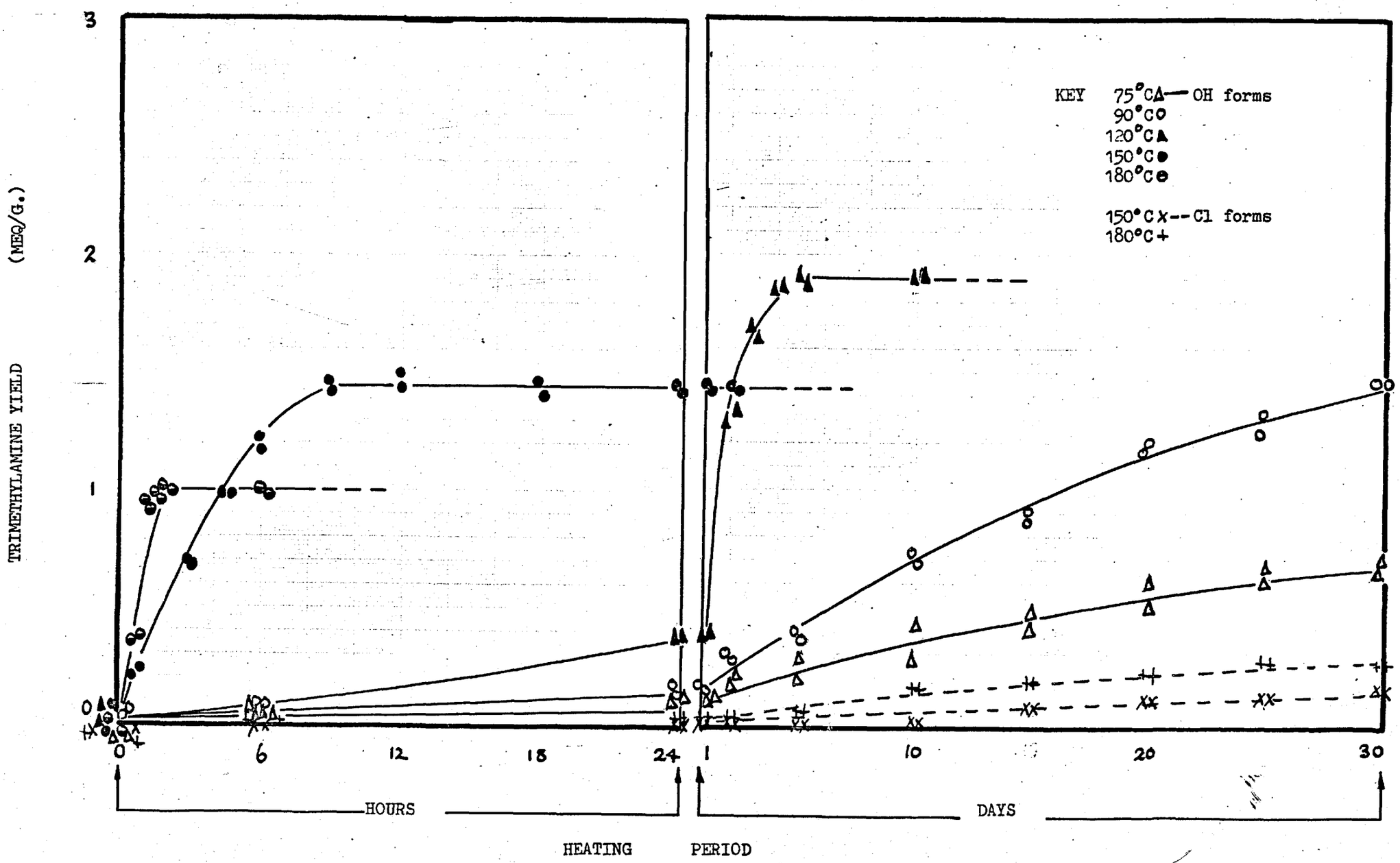

FIG 2.10 THERMAL DECOMPOSITION TRIMETHYLAMINE YIELD.

AMBERLITE IRA 900 - HYDROXIDE AND CHLORIDE

14-52 MESH, 7-9 % CROSS LINKING.

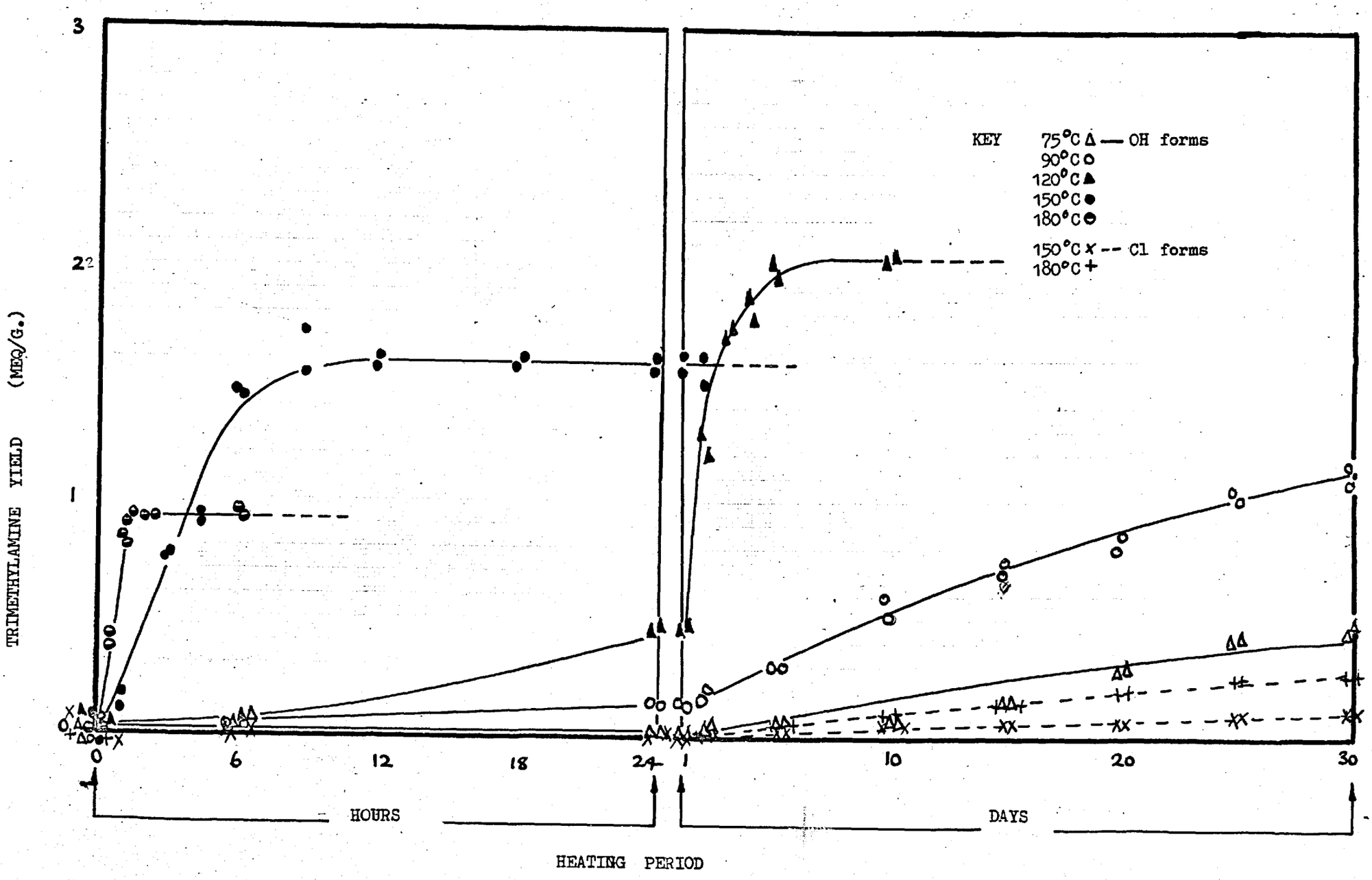

FIG 2.11

THERMAL DECOMPOSITION TRIMETHYLAMINE YIELD.

DEACIDITE FF - HYDROXIDE AND CHLORIDE

14-52 MESH, 7-9 % CROSSLINKING.

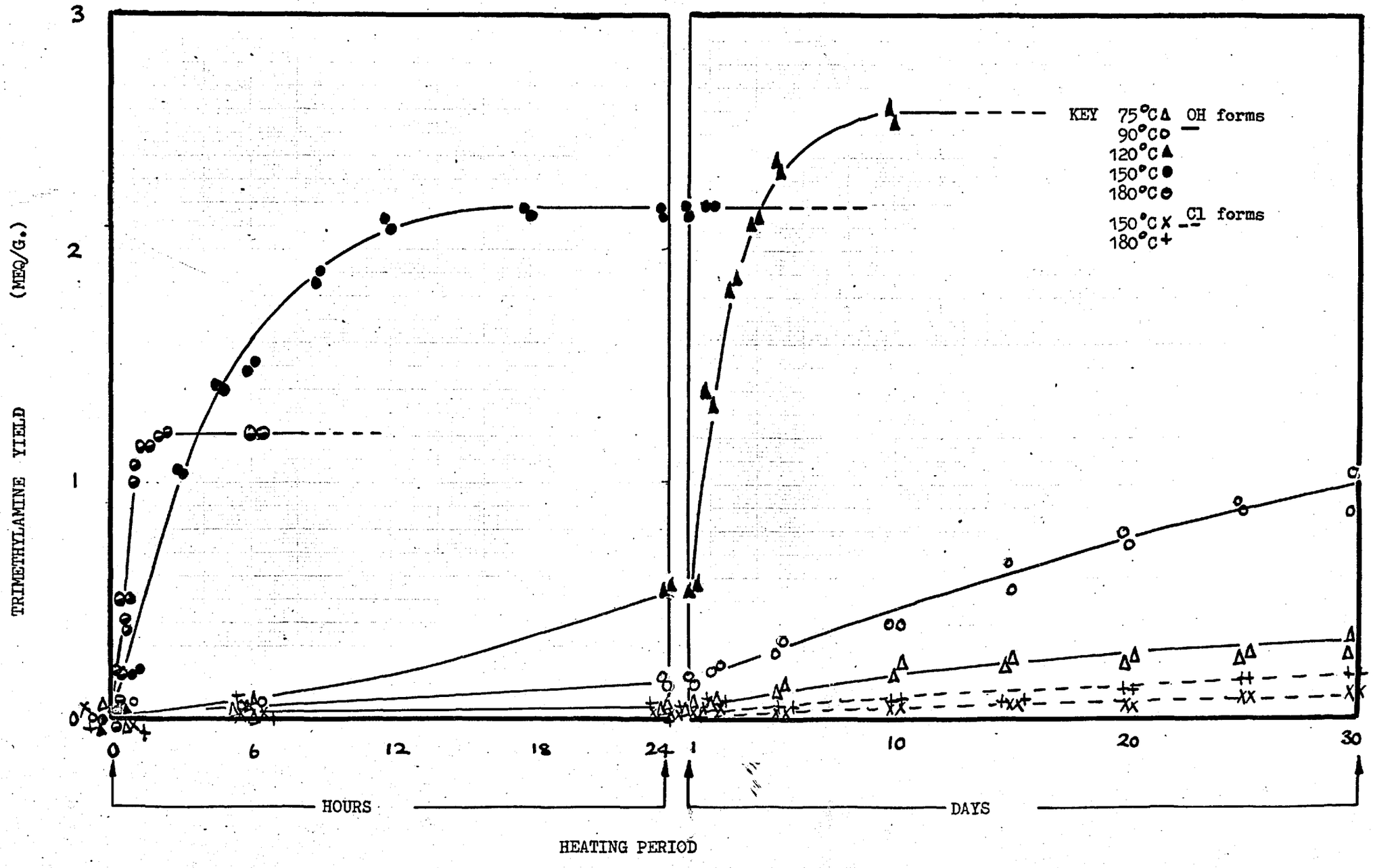

FIG 2.12

THERMAL DECOMPOSITION TRIMETHYLAMINE YIELD.

DOWEX 1 - HYDROXIDE AND CHLORIDE

14-52 MESH, 7-9 % CROSSLINKING.

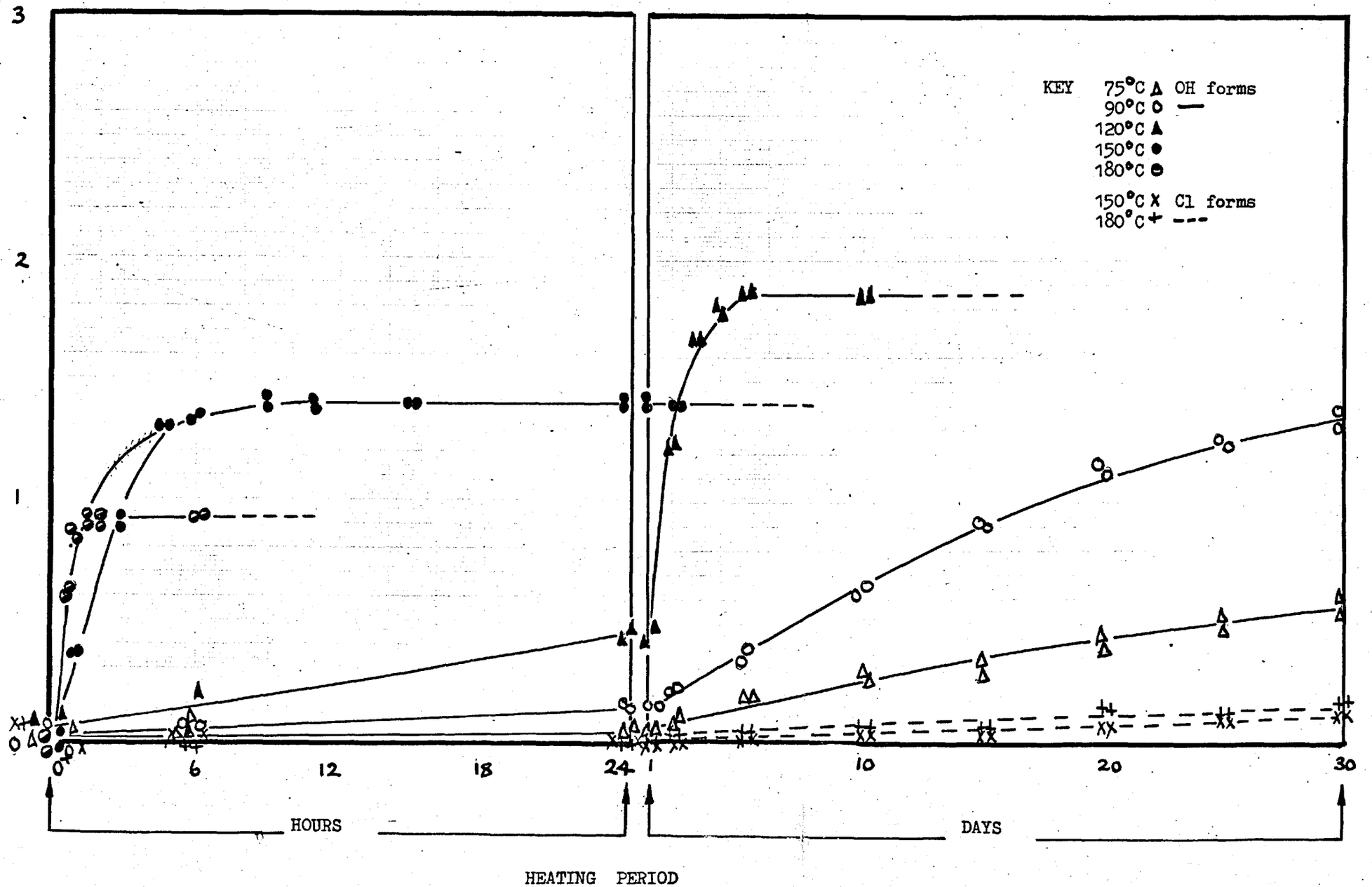

It is interesting to compare the slow decomposition of the weak base groups formed by the decomposition of strong base capacity in the strong base exchangers, with the completely stable weak base groups found in the weak base exchangers. These two types of group are evidently of a different nature, even though they both give a weak base capacity reaction during capacity analysis.

It was suspected that methanol would be present as a decomposition product at all temperatures, but actual measurements were only made at 150°C in the static experiments . Yields of methanol stoichiometrically equivalent to 10% of the increase in weak base capacity were measured in all four resins (Table 2.8). If the reaction scheme proposed by E.W. Baumann is correct then the yield of methanol should be stoichiometrically equivalent to the increase in weak base capacity. In fact this is not so, and Baumann's scheme must be modified to make allowance for this fact.

The changes observed during the heating of strong base exchange resins can be adequately described by the following three reactions. The proportion of the decomposition occurring by any one reaction varies with temparature.

1 

2 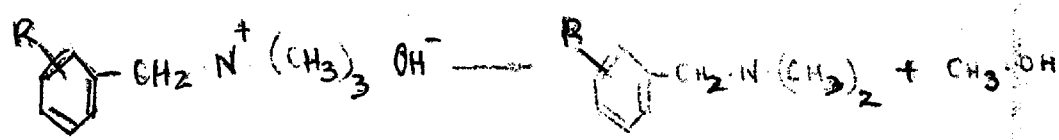

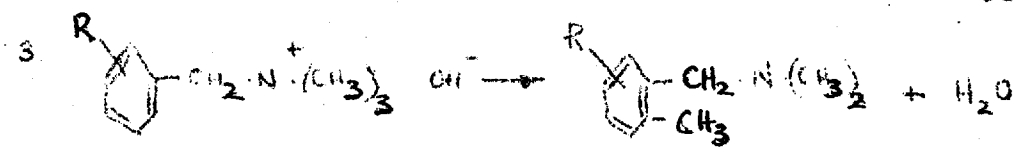

Further evidence in support of this scheme is given in Section 2.3.5.

The small loss in weight that occurred when resin samples were heated was slightly in excess of the measured weight of trimethylamine resulting from heating. The small yield of methanol, which was not measured in all cases, was not taken into account and is probably responsible for the discrepancy. The accuracy of the loss in weight experiments was poor and little inference can be made from them.

No significant change in the water regain was detected up to 90°C, but at 120°C, a 150°C and 180°C a rapid decrease in water regain accompanied the loss in strong base capacity (Fig. 2.13-2.16). In all cases it was noted that little change in water regain took place until between 30% and 50% of the strong base capacity loss occurred. The water regain attained a constant value, independent of heating temperature (within experimental error) when all strong base capacity was lost. This suggests that a definite fraction of the water regain of a dry resin is associated with the strong base functional groups, probably as water of hydration and that this fraction was lost when the strong base groups are destroyed.

Thermal decrosslinking can be discounted since it would cause an increase in water regain. The change in water regain corresponds completely with the change in

FIG 2.13

THERMAL DECOMPOSITION WATER REGAIN.

AMBERLITE IRA 400 - HYDROXIDE

14-52 MESH, 7-9 % CROSSLINKING.

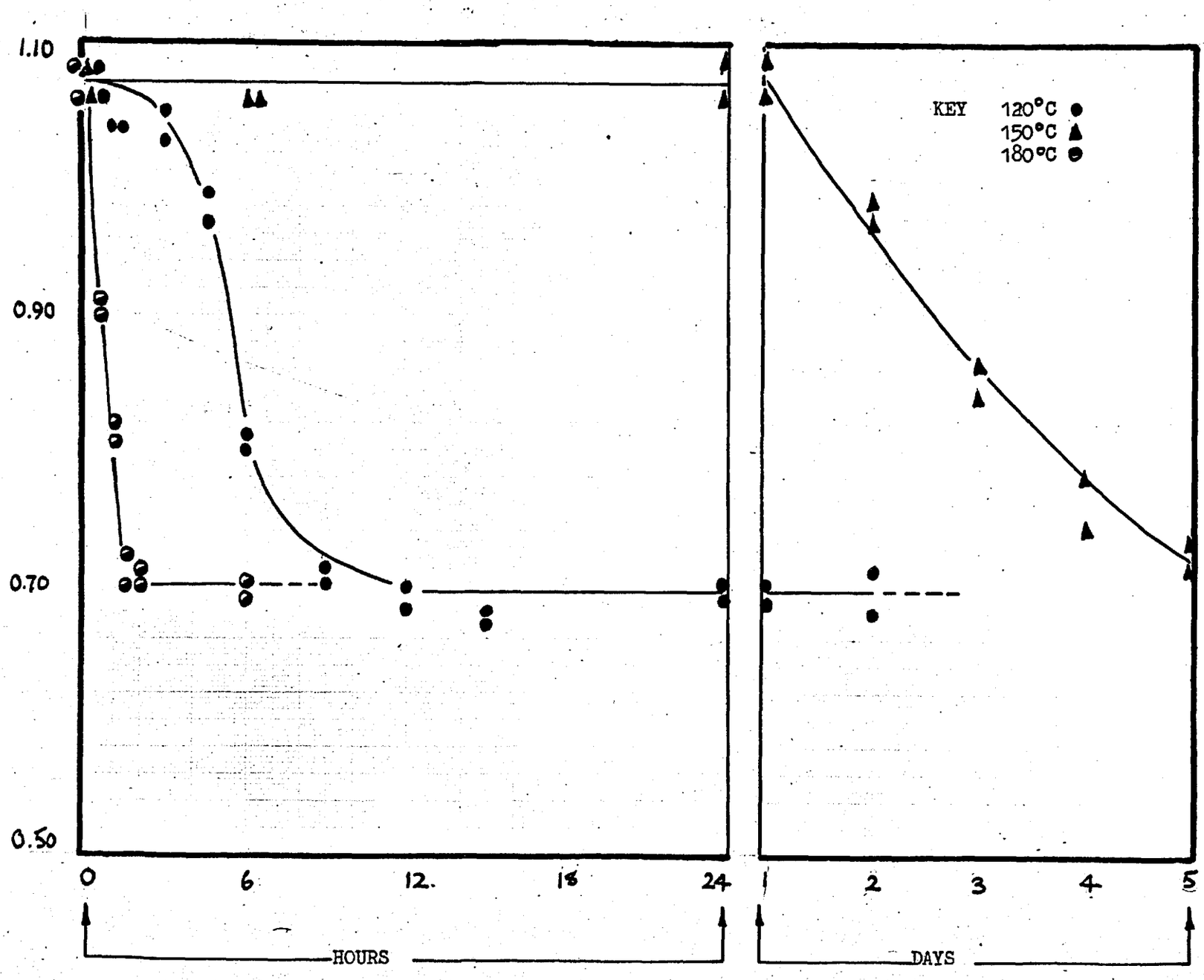

FIG 2.14

THERMAL DECOMPOSITION WATER REGAIN.

AMBERLITE IRA 900 - HYDROXIDE

14-52 MESH, 7-9 % CROSSLINKING.

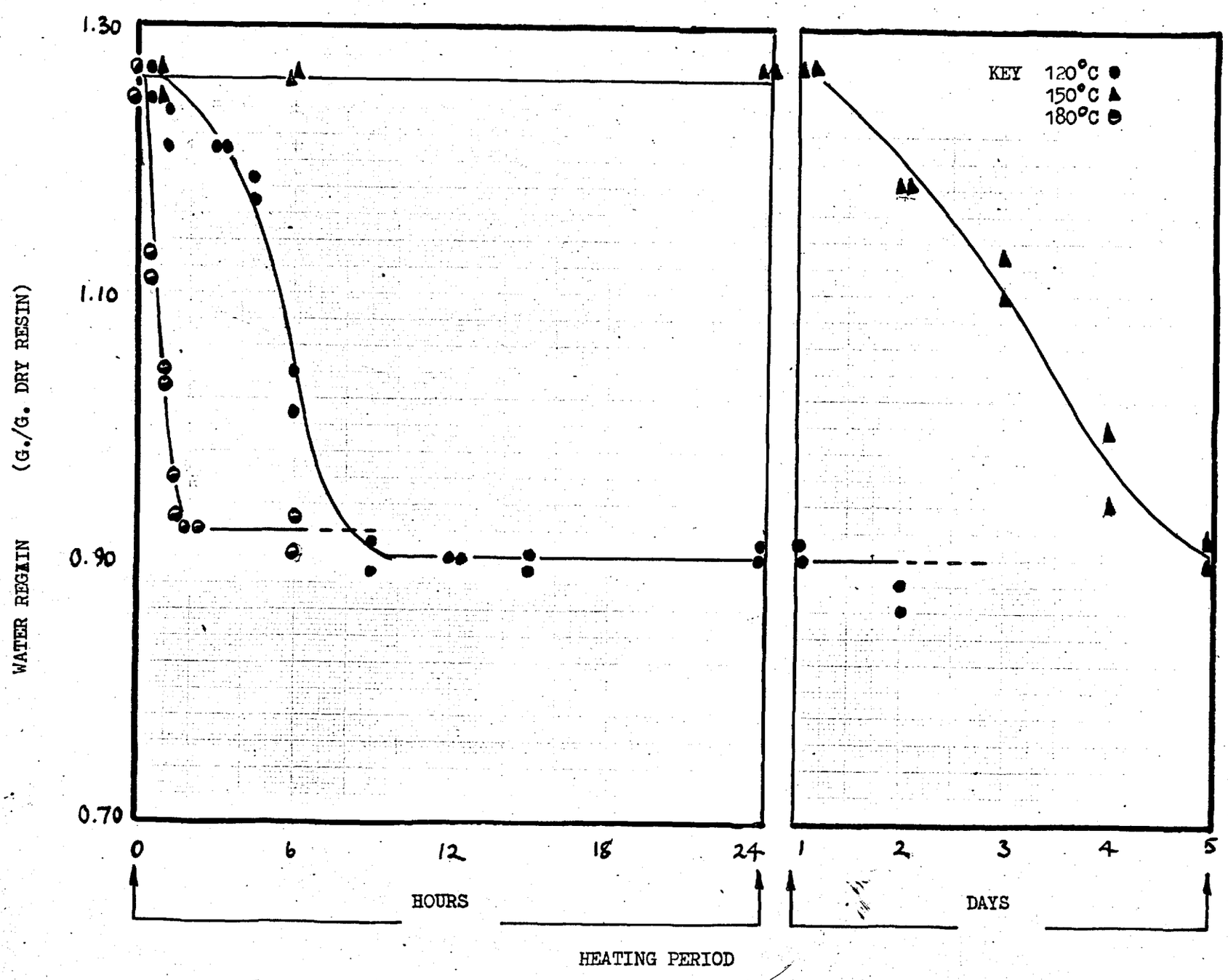

FIG 2.15

THERMAL DECOMPOSITION WATER REGAIN.

DEACIDITE FF - HYDROXIDE

14-52 MESH, 7-9 % CROSSLINKING.

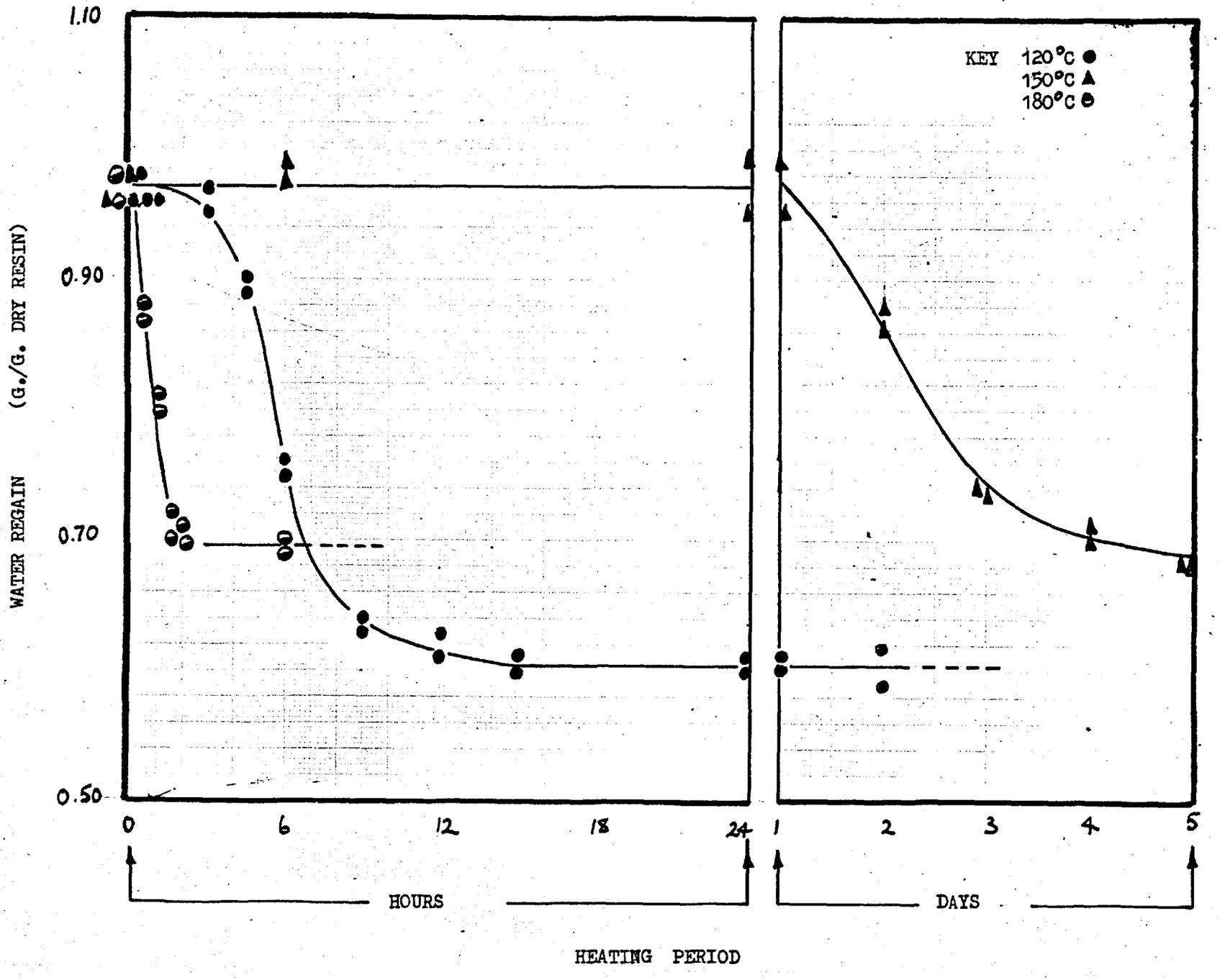

FIG 2.16

THERMAL DECOMPOSITION WATER REGAIN

DOWEX 1 - HYDROXIDE

14-52 MESH, 7-9 % CROSSLINKING.

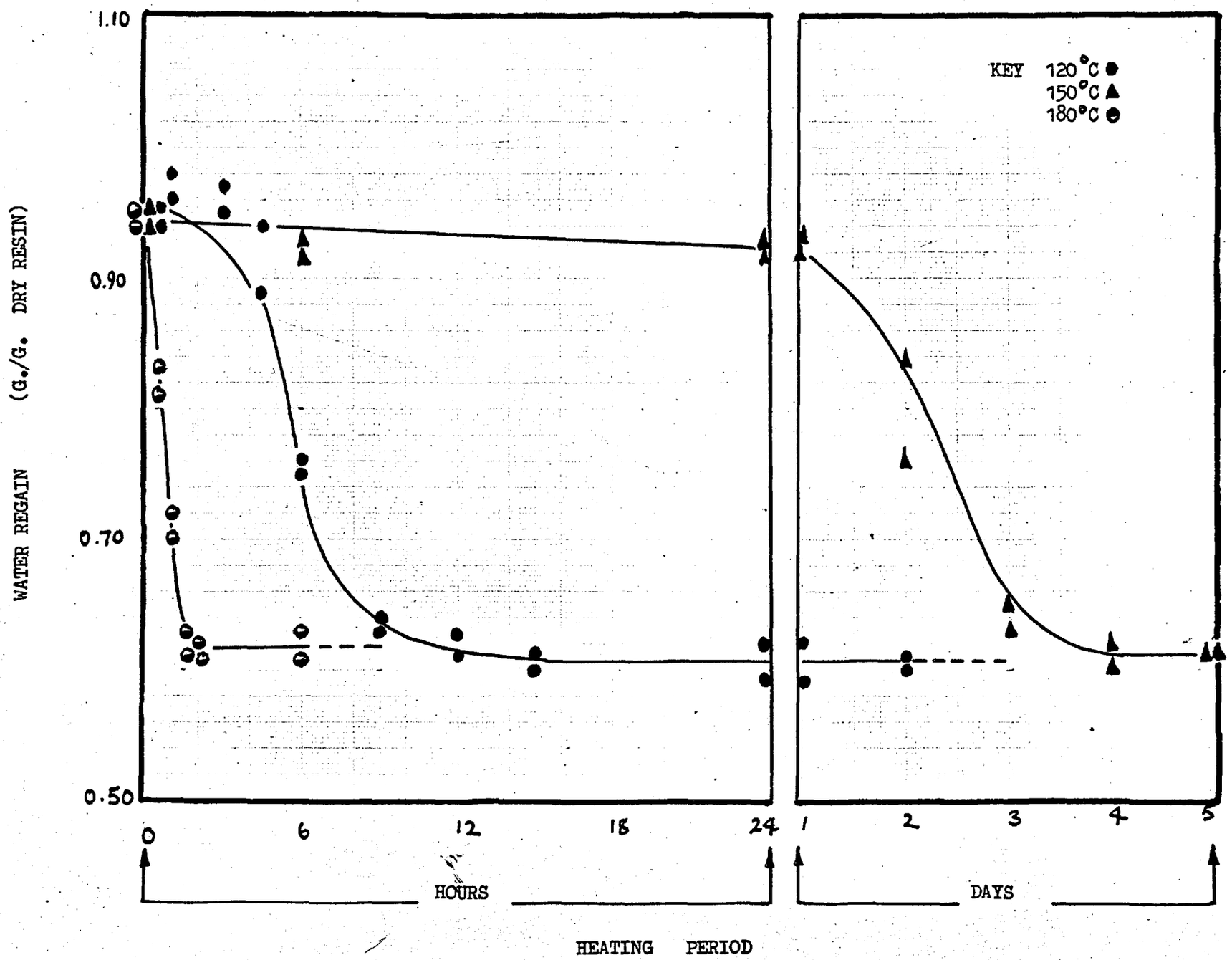

RESIN IN THE HYDROXIDE FORM

TEMPERATURE 75.0 C

TIME		DAYS	0	0.25	1.00	2.00	5.00	10.00	15.00	20.00	25.00	30.00
AMBERLITE	SB CAPACITY	MEQ/G	2.92	2.88	2.80	2.74	2.72	2.63	2.48	2.38	2.28	2.21
IRA 400	SB CAPACITY		1.00	0.99	0.96	0.94	0.93	0.90	0.85	0.82	0.78	0.76
	WB CAPACITY	MEQ/G	0.28	0.28	0.29	0.29	0.29	0.30	0.31	0.33	0.33	0.34
	TOTAL CAPACITY	MEQ/G	3.20	3.16	3.09	3.03	3.01	2.93	2.79	2.71	2.61	2.55
	TRIMETHYLAMINE	MEQ/G	0.	0.03	0.10	0.16	0.19	0.28	0.40	0.50	0.60	0.64
	METHANOL	MEQ/G										
	WTR REGAIN	GM/GM	1.06	1.07	1.06	1.09	1.06	1.07	1.06	1.07	1.06	1.08
AMBERLITE	SB CAPACITY	MEQ/G	3.02	3.01	3.01	2.98	2.96	2.94	2.85	2.70	2.60	2.56
IRA 900	SB CAPACITY		1.00	1.00	1.00	0.99	0.98	0.97	0.94	0.89	0.86	0.85
	WB CAPACITY	MEQ/G	0.20	0.20	0.20	0.20	0.21	0.21	0.21	0.22	0.22	0.23
	TOTAL CAPACITY	MEQ/G	3.22	3.21	3.21	3.18	3.17	3.15	3.06	2.92	2.82	2.79
	TRIMETHYLAMINE	MEQ/G	0.	0.01	0.01	0.02	0.06	0.06	0.15	0.28	0.40	0.43
	METHANOL	MEQ/G										
	WTR REGAIN	GM/GM	1.25	1.23	1.24	1.27	1.25	1.25	1.26	1.24	1.25	1.23
DEACIDITE	SB CAPACITY	MEQ/G	3.91	3.91	3.85	3.83	3.76	3.69	3.68	3.64	3.63	3.54
FF	SB CAPACITY		1.00	1.00	0.98	0.98	0.96	0.94	0.94	0.93	0.93	0.91
	WB CAPACITY	MEQ/G	0.10	0.10	0.10	0.11	0.11	0.12	0.12	0.12	0.12	0.13
	TOTAL CAPACITY	MEQ/G	4.01	4.01	3.95	3.94	3.87	3.81	3.80	3.76	3.75	3.67
	TRIMETHYLAMINE	MEQ/G	0.	0.	0.06	0.08	0.13	0.22	0.24	0.25	0.26	0.34
	METHANOL	MEQ/G										
	WTR REGAIN	GM/GM	0.98	0.96	0.98	0.96	0.96	0.97	0.96	0.99	0.98	0.99
DOWEX	SB CAPACITY	MEQ/G	2.82	2.78	2.76	2.68	2.61	2.54	2.48	2.37	2.31	2.27
1	SB CAPACITY		1.00	0.99	0.98	0.95	0.93	0.90	0.88	0.84	0.82	0.80
	WB CAPACITY	MEQ/G	0.21	0.21	0.22	0.22	0.22	0.23	0.24	0.25	0.25	0.25
	TOTAL CAPACITY	MEQ/G	3.03	2.99	2.98	2.90	2.83	2.77	2.72	2.62	2.56	2.52
	TRIMETHYLAMINE	MEQ/G	0.	0.03	0.05	0.12	0.19	0.27	0.30	0.40	0.48	0.52
	METHANOL	MEQ/G										
	WTR REGAIN	GM/GM	0.94	0.91	0.96	0.94	0.92	0.92	0.91	0.94	0.94	0.92

SAMPLE 2

RESIN IN THE HYDROXIDE FORM

TEMPERATURE 75.0 C

TIME		DAYS	0	0.25	1.00	2.00	5.00	10.00	15.00	20.00	25.00	30.00
AMBERLITE	SB CAPACITY	MEQ/G	2.92	2.87	2.77	2.75	2.68	2.62	2.34	2.36	2.27	2.25
IRA 400	SB CAPACITY		1.00	0.98	0.95	0.94	0.92	0.90	0.80	0.81	0.78	0.77
	WB CAPACITY	MEQ/G	0.27	0.27	0.28	0.28	0.29	0.30	0.31	0.33	0.33	0.35
	TOTAL CAPACITY	MEQ/G	3.19	3.14	3.05	3.03	2.97	2.92	2.65	2.69	2.60	2.60
	TRIMETHYLAMINE	MEQ/G	0.	0.05	0.12	0.15	0.22	0.29	0.41	0.47	0.60	0.64
	METHANOL	MEQ/G										
	WTR REGAIN	GM/GM	1.08	1.09	1.08	1.05	1.04	1.08	1.09	1.07	1.07	1.07
AMBERLITE	SB CAPACITY	MEQ/G	3.01	3.00	2.98	2.95	2.89	2.90	2.77	2.72	2.60	2.54
IRA 900	SB CAPACITY		1.00	1.00	0.99	0.98	0.96	0.96	0.92	0.90	0.86	0.84
	WB CAPACITY	MEQ/G	0.18	0.18	0.18	0.18	0.19	0.19	0.19	0.20	0.20	0.23
	TOTAL CAPACITY	MEQ/G	3.19	3.18	3.16	3.13	3.08	3.09	2.96	2.92	2.80	2.77
	TRIMETHYLAMINE	MEQ/G	0.	0.03	0.01	0.04	0.07	0.06	0.15	0.30	0.41	0.44
	METHANOL	MEQ/G										
	WTR REGAIN	GM/GM	1.27	1.26	1.26	1.27	1.27	1.27	1.29	1.26	1.25	1.27
DEACIDITE	SB CAPACITY	MEQ/G	3.87	3.86	3.85	3.83	3.78	3.67	3.64	3.60	3.60	3.60
FF	SB CAPACITY		1.00	1.00	0.99	0.99	0.98	0.95	0.94	0.93	0.93	0.93
	WB CAPACITY	MEQ/G	0.10	0.10	0.10	0.11	0.11	0.12	0.12	0.13	0.12	0.12
	TOTAL CAPACITY	MEQ/G	3.97	3.96	3.95	3.94	3.89	3.79	3.76	3.73	3.72	3.72
	TRIMETHYLAMINE	MEQ/G	0.	0.01	0.01	0.04	0.10	0.18	0.23	0.24	0.24	0.24
	METHANOL	MEQ/G										
	WTR REGAIN	GM/GM	0.96	0.97	0.98	0.98	0.98	0.98	0.97	0.98	0.97	0.96
DOWEX	SB CAPACITY	MEQ/G	2.80	2.77	2.79	2.73	2.58	2.46	2.41	2.32	2.25	2.16
1	SB CAPACITY		1.00	0.99	1.00	0.97	0.92	0.88	0.86	0.83	0.80	0.77
	WB CAPACITY	MEQ/G	0.20	0.20	0.21	0.21	0.22	0.23	0.24	0.24	0.24	0.24
	TOTAL CAPACITY	MEQ/G	3.00	2.97	3.00	2.94	2.80	2.69	2.65	2.56	2.49	2.40
	TRIMETHYLAMINE	MEQ/G	0.	0.01	0.03	0.07	0.20	0.30	0.34	0.45	0.52	0.60
	METHANOL	MEQ/G										
	WTR REGAIN	GM/GM	0.94	0.90	0.92	0.92	0.90	0.90	0.94	0.93	0.95	0.96

RESIN IN THE HYDROXIDE FORM

TEMPERATURE 90.0 C

TIME		DAYS	0	0.25	1.00	2.00	5.00	10.00	15.00	20.00	25.00	30.00
AMBERLITE	SB CAPACITY	MEQ/G	2.92	2.86	2.75	2.67	2.54	2.25	1.95	1.65	1.50	1.35
IRA 400	SB CAPACITY		1.00	0.98	0.94	0.91	0.87	0.77	0.67	0.57	0.51	0.46
	WB CAPACITY	MEQ/G	0.28	0.30	0.29	0.28	0.30	0.32	0.33	0.35	0.37	0.38
	TOTAL CAPACITY	MEQ/G	3.20	3.16	3.04	2.95	2.84	2.57	2.28	2.00	1.87	1.73
	TRIMETHYLAMINE	MEQ/G	0.	0.08	0.16	0.27	0.37	0.68	0.92	1.20	1.33	1.47
	METHANOL	MEQ/G										
	WTR REGAIN	GM/GM	1.06	1.08	1.04	1.04	1.01	1.04	1.07	1.06	1.04	1.04
AMBERLITE	SB CAPACITY	MEQ/G	3.02	2.97	2.88	2.84	2.72	2.45	2.27	2.16	1.87	1.78
IRA 900	SB CAPACITY		1.00	0.98	0.95	0.94	0.90	0.81	0.75	0.72	0.62	0.59
	WB CAPACITY	MEQ/G	0.20	0.21	0.21	0.21	0.22	0.24	0.25	0.26	0.28	0.31
	TOTAL CAPACITY	MEQ/G	3.22	3.18	3.09	3.05	2.94	2.69	2.52	2.42	2.15	2.09
	TRIMETHYLAMINE	MEQ/G	0.	0.02	0.14	0.16	0.30	0.60	0.70	0.80	1.06	1.08
	METHANOL	MEQ/G										
	WTR REGAIN	GM/GM	1.27	1.26	1.27	1.27	1.24	1.23	1.26	1.26	1.27	1.24
DEACIDITE	SB CAPACITY	MEQ/G	3.91	3.82	3.72	3.71	3.65	3.40	3.30	3.20	3.04	2.80
FF	SB CAPACITY		1.00	0.98	0.95	0.95	0.93	0.87	0.84	0.82	0.78	0.72
	WB CAPACITY	MEQ/G	0.10	0.10	0.11	0.12	0.14	0.16	0.17	0.19	0.19	0.19
	TOTAL CAPACITY	MEQ/G	4.01	3.92	3.83	3.83	3.79	3.56	3.47	3.39	3.23	2.99
	TRIMETHYLAMINE	MEQ/G	0.	0.06	0.15	0.22	0.34	0.40	0.54	0.74	0.88	0.94
	METHANOL	MEQ/G										
	WTR REGAIN	GM/GM	0.98	0.96	0.99	0.96	0.94	0.96	0.96	0.94	0.96	0.96
DOWEX	SB CAPACITY	MEQ/G	2.82	2.78	2.63	2.55	2.38	2.10	1.85	1.60	1.50	1.45
1	SB CAPACITY		1.00	0.99	0.93	0.90	0.84	0.74	0.66	0.57	0.53	0.51
	WB CAPACITY	MEQ/G	0.21	0.20	0.20	0.20	0.22	0.24	0.25	0.26	0.27	0.28
	TOTAL CAPACITY	MEQ/G	3.03	2.98	2.83	2.75	2.60	2.34	2.10	1.86	1.77	1.73
	TRIMETHYLAMINE	MEQ/G	0.	0.05	0.15	0.22	0.35	0.61	0.93	1.17	1.26	1.30
	METHANOL	MEQ/G										
	WTR REGAIN	GM/GM	0.94	0.96	0.91	0.94	0.97	0.96	0.95	0.96	0.95	0.96

SAMPLE 2

RESIN IN THE HYDROXIDE FORM

TEMPERATURE 90.0 C

TIME		DAYS	0	0.25	1.00	2.00	5.00	10.00	15.00	20.00	25.00	30.00
AMBERLITE	SB CAPACITY	MEQ/G	2.92	2.82	2.73	2.65	2.40	2.30	2.00	1.68	1.60	1.45
IRA 400	SB CAPACITY		1.00	0.97	0.93	0.91	0.82	0.79	0.68	0.58	0.55	0.50
	WB CAPACITY	MEQ/G	0.27	0.28	0.28	0.27	0.32	0.33	0.34	0.36	0.38	0.38
	TOTAL CAPACITY	MEQ/G	3.19	3.10	3.01	2.92	2.72	2.63	2.34	2.04	1.98	1.83
	TRIMETHYLAMINE	MEQ/G	0.	0.09	0.18	0.30	0.40	0.73	0.86	1.16	1.23	1.47
	METHANOL	MEQ/G										
	WTR REGAIN	GM/GM	1.08	1.06	1.01	1.04	1.03	1.07	1.02	1.02	1.02	1.01
AMBERLITE	SB CAPACITY	MEQ/G	3.01	2.92	2.88	2.77	2.68	2.47	2.20	2.07	1.90	1.76
IRA 900	SB CAPACITY		1.00	0.97	0.96	0.92	0.89	0.82	0.73	0.69	0.63	0.58
	WB CAPACITY	MEQ/G	0.18	0.19	0.20	0.21	0.21	0.22	0.24	0.25	0.26	0.29
	TOTAL CAPACITY	MEQ/G	3.19	3.11	3.08	2.98	2.89	2.69	2.44	2.32	2.16	2.05
	TRIMETHYLAMINE	MEQ/G	0.	0.04	0.14	0.20	0.30	0.51	0.75	0.85	1.00	1.16
	METHANOL	MEQ/G										
	WTR REGAIN	GM/GM	1.27	1.26	1.27	1.27	1.24	1.23	1.26	1.26	1.27	1.24
DEACIDITE	SB CAPACITY	MEQ/G	3.87	3.87	3.77	3.70	3.50	3.50	3.20	3.00	2.90	2.90
FF	SB CAPACITY		1.00	1.00	0.97	0.96	0.90	0.90	0.83	0.78	0.75	0.75
	WB CAPACITY	MEQ/G	0.10	0.10	0.11	0.10	0.12	0.13	0.15	0.15	0.16	0.19
	TOTAL CAPACITY	MEQ/G	3.97	3.97	3.88	3.80	3.62	3.63	3.35	3.15	3.06	3.09
	TRIMETHYLAMINE	MEQ/G	0.	0.04	0.17	0.20	0.28	0.41	0.67	0.80	0.91	0.88
	METHANOL	MEQ/G										
	WTR REGAIN	GM/GM	0.96	0.97	0.98	0.99	0.98	0.98	0.98	0.97	0.97	0.94
DOWEX	SB CAPACITY	MEQ/G	2.80	2.75	2.65	2.56	2.42	2.12	0.95	1.65	1.52	1.35
1	SB CAPACITY		1.00	0.98	0.95	0.91	0.86	0.76	0.34	0.59	0.54	0.48
	WB CAPACITY	MEQ/G	0.20	0.19	0.21	0.21	0.23	0.24	0.26	0.27	0.28	0.29
	TOTAL CAPACITY	MEQ/G	3.00	2.94	2.86	2.77	2.65	2.36	1.21	1.92	1.80	1.64
	TRIMETHYLAMINE	MEQ/G	0.	0.05	0.16	0.23	0.40	0.65	0.92	1.11	1.23	1.39
	METHANOL	MEQ/G										
	WTR REGAIN	GM/GM	0.94	0.97	0.93	0.91	0.94	0.91	0.97	0.94	0.97	0.96

RESIN IN THE HYDROXIDE FORM

TEMPERATURE 120.0 C

TIME		DAYS	0	0.25	1.00	2.00	3.00	4.00	5.00	10.00
AMBERLITE IRA 400	SB CAPACITY	MEQ/G	2.92	2.88	2.36	0.99	0.41	0.19	0.08	0.
	SB CAPACITY		1.00	0.99	0.81	0.34	0.14	0.07	0.03	0.
	WB CAPACITY	MEQ/G	0.28	0.29	0.47	0.92	1.11	1.18	1.21	1.24
	TOTAL CAPACITY	MEQ/G	3.20	3.17	2.83	1.91	1.52	1.37	1.29	1.24
	TRIMETHYLAMINE	MEQ/G	0	0.03	0.37	1.29	1.68	1.84	1.91	1.90
	METHANOL	MEQ/G								
	WTR REGAIN	GM/GM	1.06	1.06	1.06	0.97	0.84	0.74	0.71	0.72
AMBERLITE IRA 900	SB CAPACITY	MEQ/G	3.02	2.98	2.36	1.03	0.41	0.17	0.04	0.
	SB CAPACITY		1.00	0.99	0.78	0.34	0.14	0.06	0.01	0.
	WB CAPACITY	MEQ/G	0.20	0.21	0.46	0.83	1.06	1.10	1.16	1.20
	TOTAL CAPACITY	MEQ/G	3.22	3.19	2.82	1.86	1.47	1.27	1.20	1.20
	TRIMETHYLAMINE	MEQ/G	0	0.03	0.44	1.30	1.70	1.87	2.01	2.01
	METHANOL	MEQ/G								
	WTR REGAIN	GM/GM	1.25	1.26	1.27	1.18	1.13	0.94	0.91	0.91
DEACIDITE FF	SB CAPACITY	MEQ/G	3.91	3.85	3.13	1.88	1.18	0.66	0.39	0.04
	SB CAPACITY		1.00	0.98	0.80	0.48	0.30	0.17	0.10	0.01
	WB CAPACITY	MEQ/G	0.10	0.11	0.35	0.78	1.01	1.20	1.25	1.37
	TOTAL CAPACITY	MEQ/G	4.01	3.96	3.48	2.66	2.19	1.86	1.64	1.41
	TRIMETHYLAMINE	MEQ/G	0	0.04	0.51	1.40	1.83	2.12	2.38	2.61
	METHANOL	MEQ/G								
	WTR REGAIN	GM/GM	0.98	0.99	0.99	0.86	0.74	0.70	0.68	0.69
DOWEX 1	SB CAPACITY	MEQ/G	2.82	2.79	2.20	0.96	0.31	0.13	0.05	0.
	SB CAPACITY		1.00	0.99	0.78	0.34	0.11	0.05	0.02	0.
	WB CAPACITY	MEQ/G	0.21	0.22	0.41	0.81	1.04	1.14	1.08	1.12
	TOTAL CAPACITY	MEQ/G	3.03	3.01	2.61	1.77	1.35	1.27	1.13	1.12
	TRIMETHYLAMINE	MEQ/G	0	0.02	0.41	1.22	1.66	1.81	1.86	1.85
	METHANOL	MEQ/G								
	WTR REGAIN	GM/GM	0.94	0.93	0.92	0.80	0.65	0.62	0.61	0.60

SAMPLE 2

RESIN IN THE HYDROXIDE FORM

TEMPERATURE 120.0 C

TIME		DAYS	0	0.25	1.00	2.00	3.00	4.00	5.00	10.00
AMBERLITE IRA 400	SB CAPACITY	MEQ/G	2.92	2.85	2.27	1.08	0.43	0.20	0.07	0.
	SB CAPACITY		1.00	0.98	0.78	0.37	0.15	0.07	0.02	0.
	WB CAPACITY	MEQ/G	0.27	0.30	0.42	0.91	1.14	1.19	1.24	1.26
	TOTAL CAPACITY	MEQ/G	3.19	3.15	2.69	1.99	1.57	1.39	1.31	1.26
	TRIMETHYLAMINE	MEQ/G	0	0.04	0.37	1.32	1.65	1.85	1.87	1.92
	METHANOL	MEQ/G								
	WTR REGAIN	GM/GM	1.08	1.06	1.09	0.98	0.85	0.76	0.73	0.71
AMBERLITE IRA 900	SB CAPACITY	MEQ/G	3.01	2.96	2.30	1.12	0.43	0.17	0.02	0.
	SB CAPACITY		1.00	0.98	0.76	0.37	0.14	0.06	0.01	0.
	WB CAPACITY	MEQ/G	0.18	0.20	0.41	0.85	1.06	1.09	1.14	1.16
	TOTAL CAPACITY	MEQ/G	3.19	3.16	2.71	1.97	1.49	1.26	1.16	1.16
	TRIMETHYLAMINE	MEQ/G	0	0.05	0.45	1.21	1.74	1.78	1.96	2.04
	METHANOL	MEQ/G								
	WTR REGAIN	GM/GM	1.27	1.27	1.27	1.18	1.10	0.96	0.90	0.90
DEACIDITE FF	SB CAPACITY	MEQ/G	3.87	3.78	3.06	1.82	1.04	0.66	0.41	0.04
	SB CAPACITY		1.00	0.98	0.79	0.47	0.27	0.17	0.11	0.01
	WB CAPACITY	MEQ/G	0.10	0.13	0.38	0.77	1.05	1.17	1.24	1.36
	TOTAL CAPACITY	MEQ/G	3.97	3.91	3.44	2.59	2.09	1.83	1.65	1.40
	TRIMETHYLAMINE	MEQ/G	0	0.07	0.52	1.39	1.88	2.14	2.32	2.56
	METHANOL	MEQ/G								
	WTR REGAIN	GM/GM	0.96	0.98	0.95	0.88	0.74	0.71	0.68	0.68
DOWEX 1	SB CAPACITY	MEQ/G	2.80	2.74	2.10	0.98	0.36	0.13	0.04	0.
	SB CAPACITY		1.00	0.98	0.75	0.35	0.13	0.05	0.01	0.
	WB CAPACITY	MEQ/G	0.20	0.22	0.43	0.80	1.01	1.03	1.13	1.13
	TOTAL CAPACITY	MEQ/G	3.00	2.96	2.53	1.78	1.37	1.16	1.17	1.13
	TRIMETHYLAMINE	MEQ/G	0	0.20	0.46	1.24	1.66	1.79	1.86	1.85
	METHANOL	MEQ/G								
	WTR REGAIN	GM/GM	0.94	0.92	0.93	0.76	0.63	0.60	0.61	0.60

RESIN IN THE HYDROXIDE FORM

TEMPERATURE 150.0 C

TIME		HRS	0	1.00	3.00	4.50	6.00	9.00	12.00	15.00	24.00	48.00
AMBERLITE IRA 400	SB CAPACITY	MEQ/G	2.92	2.45	1.60	1.00	0.36	0.06	0	0	0	0
	SB CAPACITY		1.00	0.84	0.55	0.34	0.12	0.02	0	0	0	0
	WB CAPACITY	MEQ/G	0.28	0.50	0.94	1.20	1.50	1.70	1.75	1.78	1.74	1.76
	TOTAL CAPACITY	MEQ/G	3.20	2.95	2.54	2.20	1.86	1.76	1.75	1.78	1.74	1.76
	TRIMETHYLAMINE	MEQ/G	0	0.24	0.68	0.98	1.16	1.41	1.43	1.40	1.44	1.42
	METHANOL	MEQ/G	0				0.12		0.14		0.15	
	WTR REGAIN	GM/GM	1.06	1.04	1.05	0.99	0.81	0.70	0.70	0.67	0.70	0.68
AMBERLITE IRA 900	SB CAPACITY	MEQ/G	3.02	2.81	1.96	1.18	0.48	0.10	0	0	0	0
	SB CAPACITY		1.00	0.93	0.65	0.39	0.16	0.03	0	0	0	0
	WB CAPACITY	MEQ/G	0.20	0.31	0.69	1.10	1.44	1.70	1.70	1.74	1.76	1.70
	TOTAL CAPACITY	MEQ/G	3.22	3.12	2.65	2.28	1.92	1.80	1.70	1.74	1.76	1.70
	TRIMETHYLAMINE	MEQ/G	0	0.10	0.74	0.94	1.47	1.54	1.56	1.57	1.55	1.50
	METHANOL	MEQ/G	0				0.15		0.13		0.12	
	WTR REGAIN	GM/GM	1.25	1.24	1.21	1.17	1.01	0.91	0.90	0.89	0.91	0.88
DEACIDITE FF	SB CAPACITY	MEQ/G	3.91	3.62	2.57	1.59	0.92	0.17	0.06	0.	0.	0.
	SB CAPACITY		1.00	0.93	0.66	0.41	0.24	0.04	0.02	0.	0.	0.
	WB CAPACITY	MEQ/G	0.10	0.20	0.55	0.94	1.43	1.72	1.81	1.78	1.84	1.83
	TOTAL CAPACITY	MEQ/G	4.01	3.82	3.12	2.53	2.35	1.89	1.87	1.78	1.84	1.83
	TRIMETHYLAMINE	MEQ/G	0	0.19	1.04	1.41	1.53	1.90	2.10	2.16	2.16	2.20
	METHANOL	MEQ/G	0				0.15		0.20		0.20	
	WTR REGAIN	GM/GM	0.98	0.96	0.97	0.90	0.75	0.64	0.61	0.60	0.60	0.62
DOWEX 1	SB CAPACITY	MEQ/G	2.82	2.40	1.66	1.08	0.42	0.04	0	0	0	0
	SB CAPACITY		1.00	0.85	0.59	0.38	0.15	0.01	0	0	0	0
	WB CAPACITY	MEQ/G	0.21	0.25	0.47	0.62	1.11	1.54	1.60	1.61	1.59	1.61
	TOTAL CAPACITY	MEQ/G	3.03	2.65	2.13	1.70	1.53	1.58	1.60	1.61	1.59	1.61
	TRIMETHYLAMINE	MEQ/G	0	0.36	0.88	1.30	1.33	1.43	1.41	1.40	1.42	1.40
	METHANOL	MEQ/G	0				0.13		0.14		0.14	
	WTR REGAIN	GM/GM	0.94	0.96	0.97	0.94	0.75	0.64	0.61	0.60	0.62	0.61

SAMPLE 2

RESIN IN THE HYDROXIDE FORM

TEMPERATURE 150.0 C

TIME		HRS	0	1.00	3.00	4.50	6.00	9.00	12.00	15.00	24.00	48.00
AMBERLITE IRA 400	SB CAPACITY	MEQ/G	2.92	2.47	1.61	1.01	0.36	0.07	0	0	0	0
	SB CAPACITY		1.00	0.85	0.55	0.35	0.12	0.02	0	0	0	0
	WB CAPACITY	MEQ/G	0.27	0.51	0.98	1.23	1.52	1.71	1.73	1.76	1.77	1.79
	TOTAL CAPACITY	MEQ/G	3.19	2.98	2.59	2.24	1.88	1.78	1.73	1.76	1.77	1.79
	TRIMETHYLAMINE	MEQ/G	0	0.21	0.69	0.99	1.22	1.46	1.50	1.47	1.46	1.44
	METHANOL	MEQ/G	0				0.12		0.16		0.14	
	WTR REGAIN	GM/GM	1.08	1.04	1.03	0.97	0.80	0.71	0.68	0.68	0.69	0.71
AMBERLITE IRA 900	SB CAPACITY	MEQ/G	3.01	2.74	1.84	1.08	0.45	0.09	0	0	0	0
	SB CAPACITY		1.00	0.91	0.61	0.36	0.15	0.03	0	0	0	0
	WB CAPACITY	MEQ/G	0.18	0.34	0.77	1.13	1.47	1.51	1.71	1.73	1.71	1.69
	TOTAL CAPACITY	MEQ/G	3.19	3.08	2.61	2.21	1.92	1.60	1.71	1.73	1.71	1.69
	TRIMETHYLAMINE	MEQ/G	0	0.17	0.77	0.91	1.46	1.71	1.50	1.51	1.51	1.51
	METHANOL	MEQ/G	0				0.13		0.16		0.16	
	WTR REGAIN	GM/GM	1.27	1.21	1.21	1.19	1.04	0.89	0.90	0.90	0.90	0.86
DEACIDITE FF	SB CAPACITY	MEQ/G	3.87	3.60	2.31	1.51	0.91	0.15	0.04	0	0	0
	SB CAPACITY		1.00	0.93	0.60	0.39	0.24	0.04	0.01	0	0	0
	WB CAPACITY	MEQ/G	0.10	0.20	0.55	0.94	1.43	1.72	1.81	1.78	1.84	1.83
	TOTAL CAPACITY	MEQ/G	3.97	3.80	2.86	2.45	2.34	1.87	1.85	1.78	1.84	1.83
	TRIMETHYLAMINE	MEQ/G	0	0.18	1.05	1.41	1.48	1.86	2.13	2.17	2.18	2.18
	METHANOL	MEQ/G	0				0.13		0.19		0.20	
	WTR REGAIN	GM/GM	0.96	0.98	0.95	0.89	0.76	0.63	0.63	0.61	0.61	0.59
DOWEX 1	SB CAPACITY	MEQ/G	2.80	2.43	1.63	1.06	0.38	0.08	0	0	0	0
	SB CAPACITY		1.00	0.87	0.58	0.38	0.14	0.03	0	0	0	0
	WB CAPACITY	MEQ/G	0.20	0.27	0.44	0.65	1.11	1.55	1.62	1.61	1.62	1.61
	TOTAL CAPACITY	MEQ/G	3.00	2.70	2.07	1.71	1.49	1.63	1.62	1.61	1.62	1.61
	TRIMETHYLAMINE	MEQ/G	0	0.37	0.94	1.30	1.35	1.38	1.39	1.40	1.39	1.41
	METHANOL	MEQ/G	0				0.12		0.15		0.15	
	WTR REGAIN	GM/GM	0.94	0.98	0.95	0.89	0.76	0.63	0.63	0.61	0.59	1.60

RESIN IN THE HYDROXIDE FORM

TEMPERATURE 180.0 C

TIME		HRS	0	0.25	0.50	0.45	1.00	1.50	2.00	6.00
AMBERLITE IRA 400	SB CAPACITY	MEQ/G	2.92		1.79		0.47	0.09	0	0
	SB CAPACITY		1.00		0.61		0.16	0.03	0	0
	WB CAPACITY	MEQ/G	0.28		1.07		1.78	2.11	2.19	2.19
	TOTAL CAPACITY	MEQ/G	3.20		2.86		2.25	2.20	2.19	2.19
	TRIMETHYLAMINE	MEQ/G	0		0.35		0.94	0.98	1.01	1.01
	METHANOL	MEQ/G								
	WTR REGAIN	GM/GM	1.06		0.90		0.82	0.72	0.71	0.69
AMBERLITE IRA 900	SB CAPACITY	MEQ/G	3.02		1.83		0.46	0.13	0	0
	SB CAPACITY		1.00		0.61		0.15	0.04	0	0
	WB CAPACITY	MEQ/G	0.20		0.92		1.78	2.01	2.04	2.03
	TOTAL CAPACITY	MEQ/G	3.22		2.75		2.24	2.14	2.04	2.03
	TRIMETHYLAMINE	MEQ/G	0		0.39		0.81	0.91	0.93	0.92
	METHANOL	MEQ/G								
	WTR REGAIN	GM/GM	1.25		1.11		1.03	0.93	0.92	0.90
DEACIDITE FF	SB CAPACITY	MEQ/G	3.91	3.17	2.55	2.05	1.07	0.28	0	0
	SB CAPACITY		1.00	0.81	0.65	0.52	0.27	0.07	0	0
	WB CAPACITY	MEQ/G	0.10	0.62	0.99	1.40	1.92	2.74	2.85	2.80
	TOTAL CAPACITY	MEQ/G	4.01	3.79	3.54	3.45	2.99	3.02	2.85	2.80
	TRIMETHYLAMINE	MEQ/G	0	0.20	0.42	0.52	1.01	1.16	1.20	1.21
	METHANOL	MEQ/G								
	WTR REGAIN	GM/GM	0.98		0.88		0.80	0.72	0.71	0.69
DOWEX 1	SB CAPACITY	MEQ/G	2.82		1.70		0.42	0.13	0	0
	SB CAPACITY		1.00		0.60		0.15	0.05	0	0
	WB CAPACITY	MEQ/G	0.21		0.90		1.78	2.03	2.11	2.09
	TOTAL CAPACITY	MEQ/G	3.03		2.60		2.20	2.16	2.11	2.09
	TRIMETHYLAMINE	MEQ/G	0		0.62		0.86	0.90	0.91	0.93
	METHANOL	MEQ/G								
	WTR REGAIN	GM/GM	0.94		0.81		0.70	0.61	0.61	0.61

SAMPLE 2

RESIN IN THE HYDROXIDE FORM

TEMPERATURE 180.0 C

TIME		HRS	0	0.25	0.50	0.75	1.00	1.50	2.00	6.00
AMBERLITE IRA 400	SB CAPACITY	MEQ/G	2.92		1.75		0.45	0.08	0	0
	SB CAPACITY		1.00		0.60		0.15	0.03	0	0
	WB CAPACITY	MEQ/G	0.27		1.10		1.81	2.15	2.20	2.21
	TOTAL CAPACITY	MEQ/G	3.19		2.85		2.26	2.23	2.20	2.21
	TRIMETHYLAMINE	MEQ/G	0		0.36		0.92	0.96	1.00	0.99
	METHANOL	MEQ/G								
	WTR REGAIN	GM/GM	1.08		0.91		0.81	0.70	0.70	0.70
AMBERLITE IRA 900	SB CAPACITY	MEQ/G	3.01		1.79		0.47	0.11	0	0
	SB CAPACITY		1.00		0.59		0.16	0.04	0	0
	WB CAPACITY	MEQ/G	0.18		0.99		1.81	2.04	2.01	2.06
	TOTAL CAPACITY	MEQ/G	3.19		2.78		2.28	2.15	2.01	2.06
	TRIMETHYLAMINE	MEQ/G	0		0.41		0.83	0.93	0.91	0.95
	METHANOL	MEQ/G								
	WTR REGAIN	GM/GM	1.27		1.13		1.04	0.96	0.92	0.93
DEACIDITE FF	SB CAPACITY	MEQ/G	3.87	3.08	2.56	2.01	1.11	0.23	0	0
	SB CAPACITY		1.00	0.80	0.66	0.52	0.29	0.06	0	0
	WB CAPACITY	MEQ/G	0.10	0.66	0.98	1.42	1.93	2.73	2.83	2.83
	TOTAL CAPACITY	MEQ/G	3.97	3.74	3.54	3.43	3.04	2.96	2.83	2.83
	TRIMETHYLAMINE	MEQ/G	0	0.21	0.38	0.50	1.08	1.16	1.21	1.20
	METHANOL	MEQ/G								
	WTR REGAIN	GM/GM	0.96		0.87		0.81	0.70	0.70	0.70
DOWEX 1	SB CAPACITY	MEQ/G	2.80		1.68		0.43	0.10	0	0
	SB CAPACITY		1.00		0.60		0.15	0.04	0	0
	WB CAPACITY	MEQ/G	0.20		0.92		1.79	2.08	2.12	2.08
	TOTAL CAPACITY	MEQ/G	3.00		2.60		2.22	2.18	2.12	2.08
	TRIMETHYLAMINE	MEQ/G	0		0.60		0.84	0.87	0.88	0.92
	METHANOL	MEQ/G								
	WTR REGAIN	GM/GM	0.94		0.83		0.72	0.63	0.62	0.63

TABLE 2.10

SAMPLE 3

RESIN IN THE CHLORIDE FORM

TEMPERATURE 150.0 C

TIME		DAYS	0	0.25	1.00	2.00	5.00	10.00	15.00	20.00	25.00	30.00
AMBERLITE IRA 400	SB CAPACITY	MEQ/G	2.91	2.91	2.90	2.90	2.88	2.83	2.75	2.70	2.66	2.61
	SB CAPACITY		1.00	1.00	1.00	1.00	0.99	0.97	0.95	0.93	0.91	0.90
	WB CAPACITY	MEQ/G	0.28	0.28	0.30	0.30	0.31	0.33	0.35	0.37	0.39	0.41
	TOTAL CAPACITY	MEQ/G	3.19	3.19	3.20	3.20	3.19	3.16	3.10	3.07	3.05	3.02
	TRIMETHYLAMINE	MEQ/G	0	0	0	0	0	0.02	0.08	0.11	0.13	0.16
AMBERLITE IRA 900	SB CAPACITY	MEQ/G	3.01			2.98	2.92	2.86	2.83	2.77	2.74	2.74
	SB CAPACITY		1.00			0.99	0.97	0.95	0.94	0.92	0.91	0.91
	WB CAPACITY	MEQ/G	0.28			0.31	0.32	0.35	0.36	0.38	0.38	0.40
	TOTAL CAPACITY	MEQ/G	3.29			3.29	3.24	3.21	3.19	3.15	3.12	3.14
	TRIMETHYLAMINE	MEQ/G	0			0.01	0.03	0.05	0.06	0.06	0.09	0.10
DEACIDITE FF	SB CAPACITY	MEQ/G	3.92	3.87	3.88	3.87	3.87	3.84	3.80	3.78	3.74	3.70
	SB CAPACITY		1.00	0.99	0.99	0.99	0.99	0.98	0.97	0.96	0.95	0.94
	WB CAPACITY	MEQ/G	0.11	0.14	0.13	0.12	0.13	0.15	0.17	0.19	0.21	0.23
	TOTAL CAPACITY	MEQ/G	4.03	4.01	4.01	3.99	4.00	3.99	3.97	3.97	3.95	3.93
	TRIMETHYLAMINE	MEQ/G	0	0.02	0.02	0.04	0.03	0.04	0.06	0.06	0.08	0.10
DOWEX 1	SB CAPACITY	MEQ/G	2.79	2.78	2.77	2.77	2.75	2.70	2.66	2.61	2.56	2.50
	SB CAPACITY		1.00	1.00	0.99	0.99	0.99	0.97	0.95	0.94	0.92	0.90
	WB CAPACITY	MEQ/G	0.19	0.19	0.21	0.22	0.25	0.25	0.27	0.30	0.32	0.34
	TOTAL CAPACITY	MEQ/G	2.98	2.97	2.98	2.99	3.00	2.95	2.93	2.91	2.88	2.84
	TRIMETHYLAMINE	MEQ/G	0	0.01	0	0	0	0.03	0.05	0.07	0.10	0.13

SAMPLE 4

RESIN IN THE CHLORIDE FORM

TEMPERATURE 150.0 C

TIME		DAYS	0	0.25	1.00	2.00	5.00	10.00	15.00	20.00	25.00	30.00
AMBERLITE IRA 400	SB CAPACITY	MEQ/G	2.91	2.89	2.88	2.90	2.89	2.81	2.72	2.69	2.67	2.63
	SB CAPACITY		1.00	0.99	0.99	1.00	0.99	0.97	0.93	0.92	0.92	0.90
	WB CAPACITY	MEQ/G	0.28	0.29	0.30	0.31	0.31	0.34	0.35	0.35	0.39	0.42
	TOTAL CAPACITY	MEQ/G	3.19	3.18	3.18	3.21	3.20	3.15	3.07	3.04	3.06	3.05
	TRIMETHYLAMINE	MEQ/G	0	0.01	0.01	0	0	0.04	0.12	0.15	0.13	0.14
AMBERLITE IRA 900	SB CAPACITY	MEQ/G	3.01			2.98	2.95	2.92	2.83	2.83	2.77	2.74
	SB CAPACITY		1.00			0.99	0.98	0.97	0.94	0.94	0.92	0.91
	WB CAPACITY	MEQ/G	0.29			0.31	0.33	0.35	0.37	0.38	0.39	0.41
	TOTAL CAPACITY	MEQ/G	3.30			3.29	3.28	3.27	3.20	3.21	3.16	3.15
	TRIMETHYLAMINE	MEQ/G	0			0.01	0.03	0.06	0.06	0.08	0.10	0.11
DEACIDITE FF	SB CAPACITY	MEQ/G	3.92	3.89	3.88	3.88	3.87	3.85	3.81	3.76	3.73	3.69
	SB CAPACITY		1.00	0.99	0.99	0.99	0.99	0.98	0.97	0.96	0.95	0.94
	WB CAPACITY	MEQ/G	0.11	0.13	0.13	0.13	0.14	0.16	0.18	0.20	0.22	0.24
	TOTAL CAPACITY	MEQ/G	4.03	4.02	4.01	4.01	4.01	4.01	3.99	3.96	3.95	3.93
	TRIMETHYLAMINE	MEQ/G	0	0	0.02	0.01	0.01	0.01	0.03	0.06	0.07	0.13
DOWEX 1	SB CAPACITY	MEQ/G	2.79	2.79	2.78	2.78	2.76	2.71	2.65	2.60	2.54	2.47
	SB CAPACITY		1.00	1.00	1.00	1.00	0.99	0.97	0.95	0.93	0.91	0.89
	WB CAPACITY	MEQ/G	0.19	0.20	0.20	0.24	0.25	0.26	0.28	0.31	0.33	0.37
	TOTAL CAPACITY	MEQ/G	2.98	2.99	2.98	3.02	3.01	2.97	2.93	2.91	2.87	2.84
	TRIMETHYLAMINE	MEQ/G	0	0.04	0.05	0.01	0.02	0.06	0.10	0.12	0.16	0.1

TABLE 2.11

SAMPLE 3

RESIN IN THE CHLORIDE FORM

TEMPERATURE 180.0 C

TIME		DAYS	0	0.25	1.00	2.00	5.00	10.00	15.00	20.00	25.00	30.00
AMBERLITE	SB CAPACITY	MEQ/G	2.91	2.86	2.84	2.81	2.77	2.64	2.52	2.38	2.27	2.17
IRA 400	SB CAPACITY		1.00	0.98	0.98	0.97	0.95	0.91	0.87	0.82	0.78	0.75
	WB CAPACITY	MEQ/G	0.28	0.31	0.32	0.33	0.35	0.38	0.47	0.56	0.65	0.74
	TOTAL CAPACITY	MEQ/G	3.19	3.17	3.16	3.14	3.12	3.02	2.99	2.94	2.92	2.91
	TRIMETHYLAMINE	MEQ/G	0	0.01	0.02	0.04	0.06	0.16	0.19	0.22	0.27	0.26
AMBERLITE	SB CAPACITY	MEQ/G	3.01			2.92	2.80	2.65	2.53	2.44	2.35	2.29
IRA 900	SB CAPACITY		1.00			0.97	0.93	0.88	0.84	0.81	0.78	0.76
	WB CAPACITY	MEQ/G	0.28			0.32	0.35	0.40	0.48	0.54	0.58	0.63
	TOTAL CAPACITY	MEQ/G	3.29			3.24	3.15	3.05	3.01	2.98	2.93	2.92
	TRIMETHYLAMINE	MEQ/G	0			0.05	0.10	0.15	0.20	0.24	0.24	0.25
DEACIDITE	SB CAPACITY	MEQ/G	3.92	3.87	3.85	3.83	3.78	3.69	3.60	3.48	3.37	3.29
FF	SB CAPACITY		1.00	0.99	0.98	0.98	0.96	0.94	0.92	0.89	0.86	0.84
	WB CAPACITY	MEQ/G	0.11	0.15	0.15	0.17	0.21	0.28	0.35	0.42	0.49	0.56
	TOTAL CAPACITY	MEQ/G	4.03	4.02	4.00	4.00	3.99	3.97	3.95	3.90	3.86	3.85
	TRIMETHYLAMINE	MEQ/G	0	0.01	0.01	0.08	0.04	0.06	0.08	0.13	0.17	0.19
DOWEX	SB CAPACITY	MEQ/G	2.79	2.77	2.75	2.70	2.65	2.52	2.40	2.24	2.17	2.04
1	SB CAPACITY		1.00	0.99	0.99	0.97	0.95	0.90	0.86	0.80	0.78	0.73
	WB CAPACITY	MEQ/G	0.19	0.22	0.23	0.25	0.29	0.39	0.51	0.58	0.67	0.76
	TOTAL CAPACITY	MEQ/G	2.98	2.99	2.98	2.95	2.94	2.91	2.91	2.82	2.84	2.80
	TRIMETHYLAMINE	MEQ/G	0	0	0	0.03	0.04	0.07	0.07	0.16	0.14	0.18

SAMPLE 4

RESIN IN THE CHLORIDE FORM

TEMPERATURE 180.0 C

TIME		DAYS	0	0.25	1.00	2.00	5.00	10.00	15.00	20.00	25.00	30.00
AMBERLITE	SB CAPACITY	MEQ/G	2.91	2.82	2.81	2.79	2.73	2.62	2.50	2.41	2.24	2.14
IRA 400	SB CAPACITY		1.00	0.97	0.97	0.96	0.94	0.90	0.86	0.83	0.77	0.74
	WB CAPACITY	MEQ/G	0.27	0.32	0.32	0.32	0.33	0.39	0.49	0.56	0.68	0.76
	TOTAL CAPACITY	MEQ/G	3.18	3.14	3.13	3.11	3.06	3.01	2.99	2.97	2.92	2.90
	TRIMETHYLAMINE	MEQ/G	0	0.05	0.06	0.08	0.13	0.18	0.20	0.22	0.27	0.25
AMBERLITE	SB CAPACITY	MEQ/G	3.01			2.89	2.95	2.92	2.89	2.83	2.77	2.74
IRA 900	SB CAPACITY		1.00			0.96	0.98	0.97	0.96	0.94	0.92	0.91
	WB CAPACITY	MEQ/G	0.29			0.33	0.36	0.42	0.50	0.54	0.59	0.64
	TOTAL CAPACITY	MEQ/G	3.30			3.22	3.31	3.34	3.39	3.37	3.36	3.38
	TRIMETHYLAMINE	MEQ/G	0			0.05	0.11	0.16	0.23	0.26	0.25	0.27
DEACIDITE	SB CAPACITY	MEQ/G	3.89	3.85	3.85	3.86	3.76	3.67	3.58	3.50	3.40	3.30
FF	SB CAPACITY		1.00	0.99	0.99	0.99	0.97	0.94	0.92	0.90	0.87	0.85
	WB CAPACITY	MEQ/G	0.13	0.17	0.17	0.18	0.24	0.29	0.37	0.44	0.50	0.58
	TOTAL CAPACITY	MEQ/G	4.02	4.02	4.02	4.04	4.00	3.96	3.95	3.94	3.90	3.88
	TRIMETHYLAMINE	MEQ/G	0	0	0	0	0.02	0.06	0.07	0.08	0.12	0.16
DOWEX	SB CAPACITY	MEQ/G	2.82	2.76	2.77	2.69	2.64	2.52	2.41	2.27	2.15	2.01
1	SB CAPACITY		1.00	0.98	0.98	0.95	0.94	0.89	0.85	0.80	0.76	0.71
	WB CAPACITY	MEQ/G	0.21	0.24	0.24	0.25	0.30	0.42	0.50	0.59	0.69	0.78
	TOTAL CAPACITY	MEQ/G	3.03	3.00	3.01	2.94	2.94	2.94	2.91	2.86	2.84	2.79
	TRIMETHYLAMINE	MEQ/G	0	0.02	0.02	0.09	0.09	0.10	0.12	0.19	0.19	0.24

strong base capacity, so there is no evidence to support thermal crosslinking, which is anyway an unlikely process.

2.3.3 Strong base exchangers in the chloride form.

The strong base exchangers in the chloride form were more stable than in the hydroxide form and no measuraable decomposition occurred over the 30 day heating period at 90°C (Table 2.4) . Above 90°C strong base capacity losses were observed in all four resins. At 120°C, losses were approximately 1-2% in Amberlite IRA 400 and Dowex 1, 1% in Amberlite IRA 900 and Deacidite FF, after 30 days heating but at 150°C strong base capacity losses of 10% in Amberlite IRA 400 and Dowex 1, 5% in Deacidite FF and 10% in Amberlite IRA 900 were measured, over the same period. At 180°C Amberlite IRA 400 and Dowex 1 lost 30%, Deacidite FF, 20%, and Amberlite IRA 900, 25%, strong base capacity after 30 days heating (Fig.2.1 - 2.4).

Degradation of strong base capacity resulted in the formation of weak base capacity in the heated samples (Fig. 2.5 - 2.12), and the formation of trimethylamine. No significant change was observed in the water regain in any of the chloride form samples, presumably because the loss in strong base capacity never exceeded 30%. A slight loss in weight was observed during thermal decomposition. No attempt was made to determine any decomposition products other than trimethylamine.

By analogy with the hydroxide form the following set of reactions probably account for the thermal decomposition of chloride form strong base exchange resins.

1. 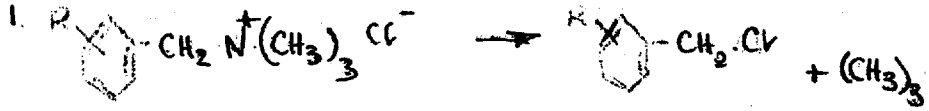

2. 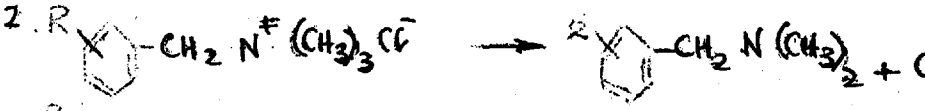

3. 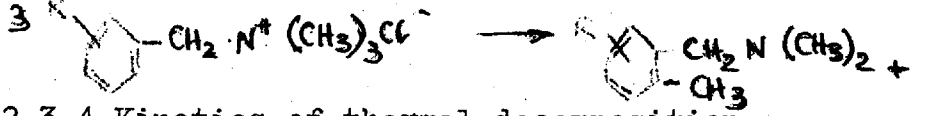

2.3.4 Kinetics of thermal decomposition.

Loss of strong base capacity in the hydroxide and chloride forms of the four strong base exchangers followed a first order rate law, as observed by E.W. Baumann and Marinsky and Potter (ref.B1,M1). At 150°C and 180°C the first order law is obeyed after transient decomposition has been passed (see Section 2.3.9). Activation energies for decomposition calculated with the Arrhenius equation are given in Table 2.12. Values are of the order 25 to 35 kcal/mole as compared with 29 to 33 kcal/mole reported by Marinsky and Potter.

The decomposition of Deacidite FF was analysed in more detail and activation energies for each of the three reactions occurring during thermal decomposition are given. A plot of velocity constants versus reciprocal temperature for each reaction (Fig. 2.17) shows that reaction (1) predominates over the range investigated, but that reaction (2) becomes more important as the temperature increases and reaction (3) becomes less important as the temparature increases.

2.3.5 Heating of model compounds.

Thermal decomposition in anion exchange resins detaches simple molecules from the main matrix structure. Identification of the simple molecules is easy. The

TABLE 2.12 THERMAL DECOMPOSITION KINETIC DATA.
RESIN-HYDROXIDE AND CHLORIDE
14-52 MESH. 7-9% CROSSLINKED.

		VELOCITY CONSTANT OF REACTION (DAYS^{-1})					ACTIVATION ENERGY
	TEMP	75°C	90°C	120°C	150°C	180°C	KCAL/MOLE
IRA 400	OH TOT	7.4×10^{-3}	2.5×10^{-2}	7.2×10^{-1}	1.5×10^{1}	7.4×10^{1}	24.5
	CL TOT	--	--	$< 10^{-4}$	0.9×10^{-3}	2.4×10^{-2}	33.7
IRA 900	OH TOT	5.8×10^{-3}	1.9×10^{-2}	8.4×10^{-1}	1.3×10^{1}	6.2×10^{1}	24.7
	CL TOT	--	--	$< 10^{-4}$	1.2×10^{-3}	8.0×10^{-2}	29.2
DOWEX 1	OH TOT	7.4×10^{-3}	2.5×10^{-2}	8.2×10^{-1}	1.4×10^{1}	6.4×10^{1}	24.5
	CL TOT	--	--	$< 10^{-4}$	0.8×10^{-3}	1.7×10^{-3}	33.7
DEACIDITE FF	OH TOT	3.4×10^{-3}	1.1×10^{-2}	4.6×10^{-1}	9.9×10^{0}	5.4×10^{1}	26.8
	OH R1		8.9×10^{-3}		1.2×10^{0}		35.2
	OH R2		5.5×10^{-3}		5.2×10^{-2}		36.6
	OH R3		1.0×10^{-4}		5.4×10^{-1}		22.7
	CL TOT	--	--	$< 10^{-4}$	1.0×10^{-3}	1.6×10^{-3}	35.3

DEACIDITE FF IS ANALYSED IN MORE DETAIL

FIG 2.17

THERMAL DECOMPOSITION REACTION KINETICS

DEACIDITE FF - HYDROXIDE 14-52 mesh, 7-9% crosslinked

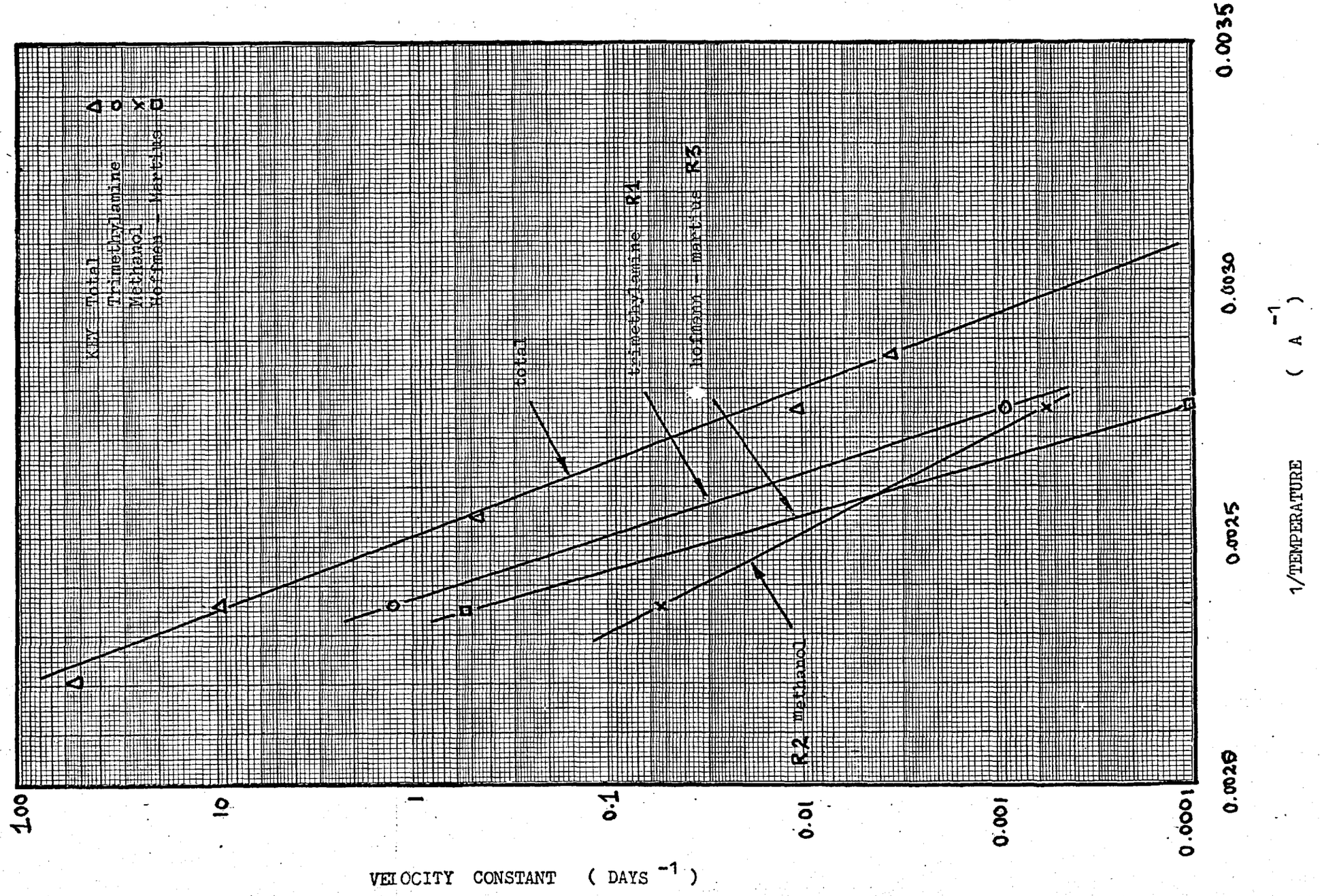

configuration remaining on the matrix after removal of the simple molecules cannot be found by analysis, but may be inferred by proposing reaction schemes, which account for the formation of the simple molecules.

Alternatively a model compound may be used. This is a simple molecule identical with the suspected part of the resin structure where thermal decomposition occurs. Manufacturing processes give some idea of the resin structure and enable suitable model compounds to be chosen.

The method of production of the anion exchanger Deacidite FF, suggests that the strong base functional groups are substituted benzyltrimethylammonium salts or bases linked to the main structure by methylene groups:-

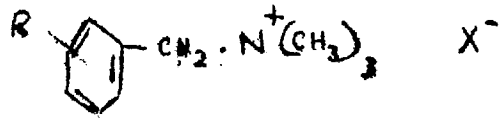

Hence a useful model compound is a benzyltrimethylammonium salt or base . This splits into two simple molecules on heating, both of which are readily identifiable. The

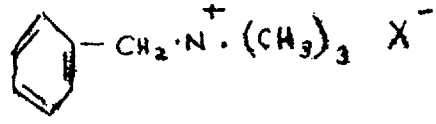

configuration remaining on the matrix after thermal decomposition may be inferred from model compound heating results with some confidence.

Collie and Schryver (ref.C2) have reported the formation of benzyldimethylamine and trimethylamine when the compound benzyltrimethylammonium hydroxide was heated.

They found a similar reaction in the salt forms of the compound, though at substantially higher temperatures.

Similar experiments were carried out as part of this work. A 2 molar solution of the model compound (i.e. with the same concentration as that of the functional groups in Deacidite FF), was prepared, and heated at 90°C, 120°C,150°C and 180°C. No decomposition was observed at 90°C but at 120°C and above increasing amounts of trimethylamine, methanol benzyldimethylamine and benzyl alcohol were detected by vapour phase chromatography. Results are shown in Fig. 2.18. No other significant products were observed over the temperature range indicated. The reactions occurring in the thermal decomposition of the model compound are therefore:-

1. 

2. 

No attempts to measure the quantitative yields of decomposition products were made, but some indications of the relative increase in yield as the temperature increases can be gained by comparing peak areas on the chromatograph record (Fig. 2.18).

The following conclusions were drawn from the model compound heating work.

a. The model compound yields the same decomposition products as the equivalent resin form, thus justifying the choice of model and confirming the suspected resin

FIG 2.18 THERMAL DECOMPOSITION OF 2M AQUEOUS BENZYLTRIMETHYLAMMONIUM HYDROXIDE

VAPOUR PHASE CHROMATOGRAMS OF DECOMPOSED SOLUTION

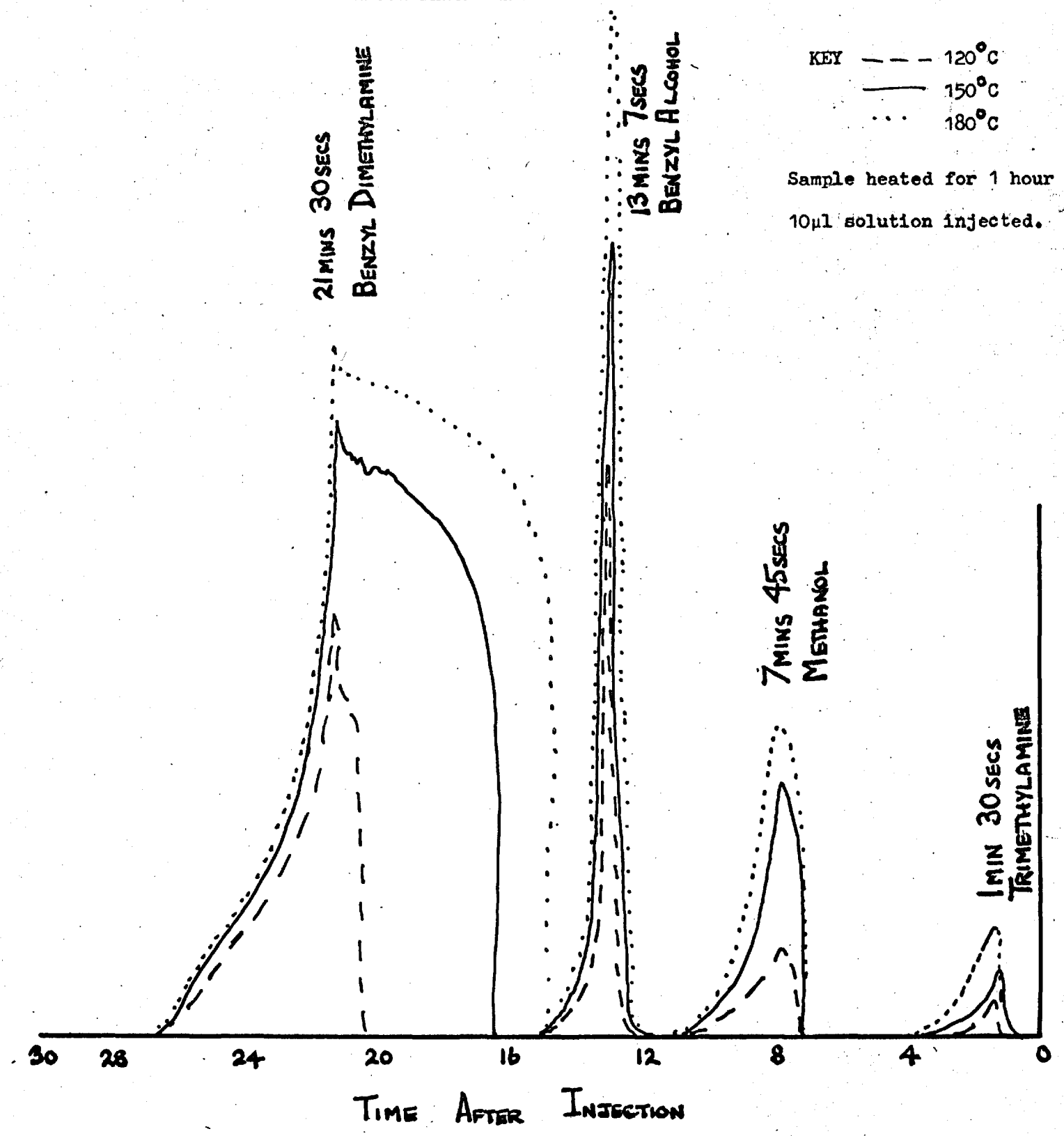

The model compound has substantially better thermal stability than the resin.

b. The configuration remaining on the resin after thermal decomposition is either a substituted benzyl alcohol group or a substituted benzyldimethylamine group. The latter most probably accounts for the increased weak base capacity and suggests the structure of one type of weak base group.

c. The Hofmann Martius rearrangement reaction (ref.M3) given below has been observed in compounds similar to the model at temperatures between 200°C and 300°C. In the resin analogous reactions to (1) and (2) occur at some 50°C lower than in the model compound, and it is probable that

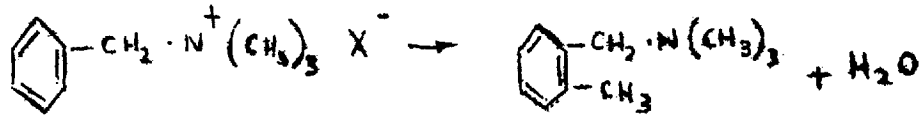

the Hofmann Martius reaction will occur in the resin at temparatures substantially lower than 200°C.

2.3.6 The reaction mechanism of thermal decomposition.

The results of the present work have shown that the simple Hofmann degradation scheme proposed by E.W. Baumann (ref.B1) requires some modification if it is to fully describe the thermal decomposition of anion exchange resins. In quaternary ammonium compounds, thermal decomposition occurs by the abstraction of an electron by the quaternary nitrogen atom, from one of the groups attached to it. This may result in substitution or elimination reactions.

The nature of the functional group in the quaternary ammonium polystyrene based anion exchangers precludes the elimination reaction.

Collie and Schryver (ref.C2) and Hanhart and Ingold (ref.H7) have heated many different quaternary ammonium compounds and have arrived at the following sequence of organic groups arranged in order of increasing electron affinity:-

$$(C_6H_5)_3C^- : (C_6H_5)_2CH^- : C_6H_5CH_2^- : CH_3^- : C_6H_5^-$$

From the sequence it can bee seen that a quaternary ammonium nitrogen atom can abstract an electron from a benzyl group with greater ease than from a methyl group. Now , in the strong base exchangers under study, there are only methyl and substituted benzyl groups attached to the quaternary nitrogen, which leads to the conclusion that both the reactions suggested by E.W. Baumann should occur, but that the trimethylamine producing reaction should predominate.

E.W. Baumann's reaction scheme was as follows :-

1. 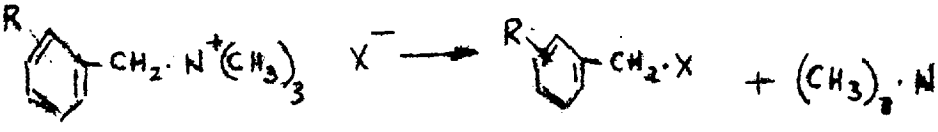

2. 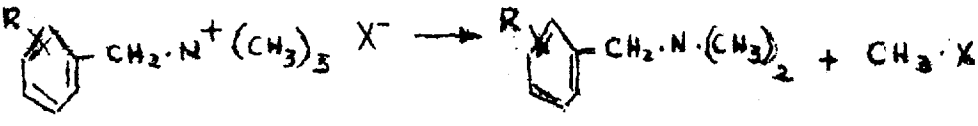

The existence of methanol as a product of decomposition was only inferred, no actual measurements being possible.

In the present work a special experiment was carried out as described below to provide detailed information on the reaction mechanisms. In addition a search for methanol

was made and this product was detected and measured, though in substantially smaller quantities than expected.

a. The loss in weight experiment.

The object of this experiment was to provide additional information about the mechanism of thermal decomposition in Deacidite FF .

Samples of Deacidite FF (approx.,10g.) In the hydroxide form (14-52 mesh, 7-9% crosslinking) were dried in a desiccator over silica gel to constant weight. The drying time needed was three weeks. This method of drying has been found to be equivalent to heating the resin salt forms at 105°C for 48 hours. Accurately weighed dried samples were placed in weighed ampoules and heated for 24 hours at 150°C. Subsequently the ampoules and contents were cooled and frozen in liquid nitrogen prior to opening. The ampoule and frozen contents were transferred to a vacuum distillation apparatus (Fig.2.19) and the volatile products, i.e. methanol, trimethylamine and water separated from the decomposed resin. The volatile products were condensed in the cooler part of the apparatus and collected. The separated resin was analysed for strong and weak base capacity by the method described earlier and dried in the sulphate form at 105°C to constant weight.

The condensed products (Approx., 1ml.) were weighed. To separate organic products from the water a simple fractional crystallisation was performed by freezing the solution in a salt-ice bath at - 10°C. In this way it was possible to separate ice crystals from the mother liquor

FIG 2.19

VACUUM DISTILLATION APPARATUS

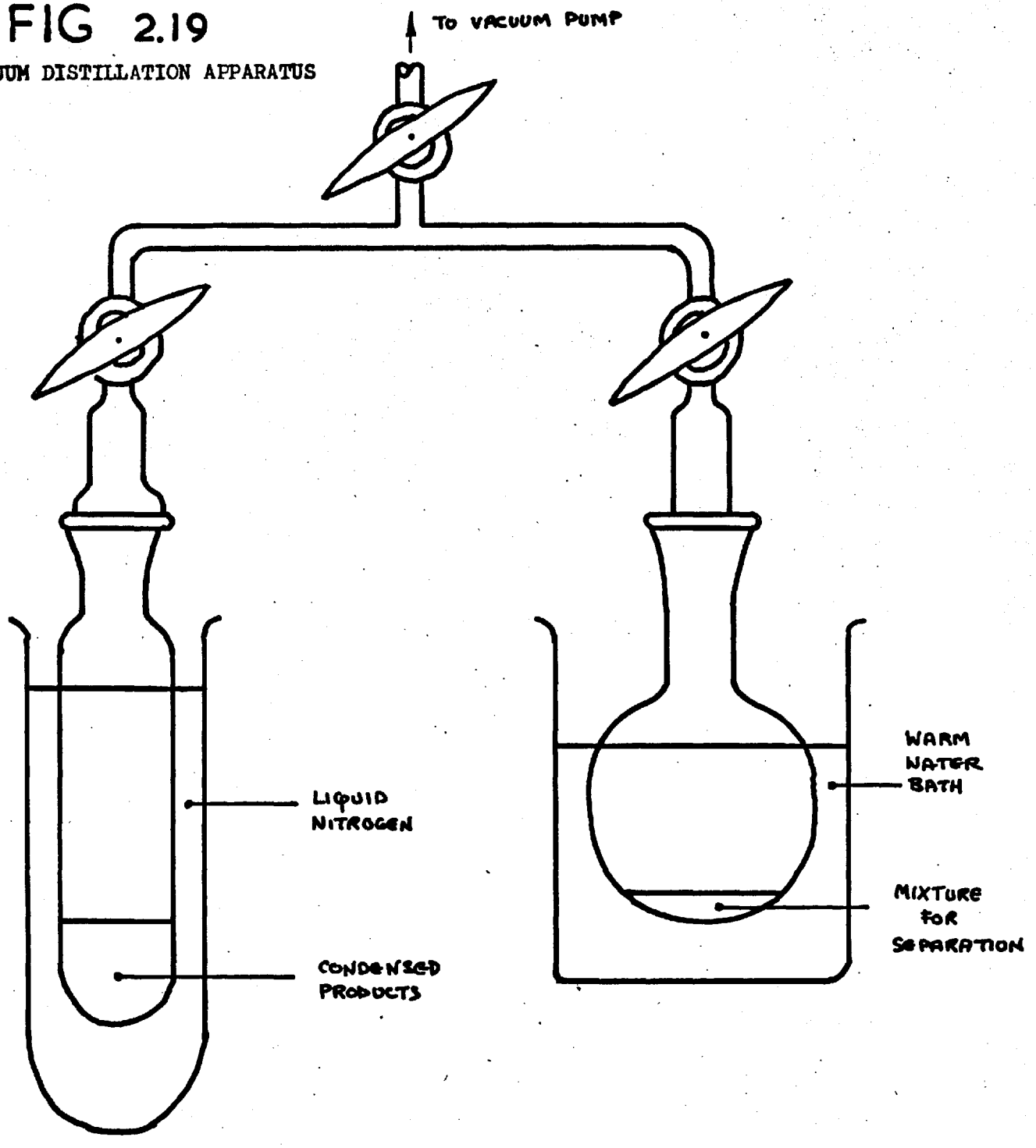

containing methanol and trimethylamine. The latter were analysed by vapour phase chromatography and colorimetry respectively. The ice was melted, checked for organic products and weighed. Results of the experiment are shown in Table 2.13.

The capacity measurements were reproducible to 1%, whereas there was greater scatter in the measurement of decomposition products. Trimethylamine was measured to ± 5% and the yield of methanol was averaged from five independent measurements. The scatter on the methanol determinations is between ± 10% of the arithmetic mean. The measured amount of water given in Table 2.13 may possibly be higher than the true yield from decomposition. This is because the resin is expected to contain some tightly bound water , which may be released during heating and subsequent vacuum distillation.

b. Conclusions.

The following evidence is extracted from Table 2.13:-

i. Approximately half the decomposition results in the formation of trimethylamine .

ii. The yield of water is approximately nine times the yield of methanol.

iii . The loss in strong base capacity equals the gain in weak base capacity plus the yield of trimethylamine.

iv. The yield of methanol is approximately 10% of the increase in weak base capacity.

v. The only significant decomposition products are methanol, trimethylamine and water.

TABLE 2.13 THERMAL DECOMPOSITION. ACCURATE LOSS IN WEIGHT EXPT.
DEACIDITE FF-HYDROXIDE, 14-52 MESH, 7-9 % CROSSLINKED.
TEMPERATURE 90°C, HEATING PERIOD 24 HOURS.

		UNHEATED SAMPLE	SAMPLE 1	SAMPLE 2	SAMPLE 3	SAMPLE 4
CAPACITY (MEQ/G.)	STRONG BASE	3.92	0.00	0.00	0.00	0.00
	WEAK BASE	0.10	1.83	1.81	1.82	1.83
	TOTAL	4.02	1.83	1.81	1.82	1.83
PRODUCT YIELD (MEQ/G.)	TRIMETHYLAMINE	0.00	2.20	2.25	2.20	2.20
	METHANOL	0.00	0.2±.02	0.2±.02	0.2±.02	0.2±.02
	WATER	0.00	1.70	1.65	1.70	1.75
WEIGHTS (G.)	INITIAL	13.7091	12.6142	14.3010	13.7111	12.8703
	FINAL	13.6979	10.6313	12.0629	11.5544	10.8342
LOSS IN WEIGHT		0.0112	1.9829	2.2381	2.1567	2.0361
GRAMS LOST PER GRAM		0.001	0.157	0.157	0.157	0.158
GRAMS PRODUCTS PER GRAM		0.000	0.167	0.169	0.167	0.168

The two reactions suggested by E.W. Baumann can satisfactorily account for the production of trimethylamine and methanol. However, these two reactions alone cannot account for the proportion of weak base capacity to methanol, as in (iv) . To account for those proportions there must be at least another reaction, which results in the formation of weak base capacity and water.

The following three reactions account for all the points of evidence:-

1. 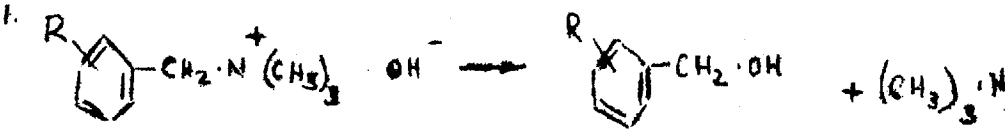

2. 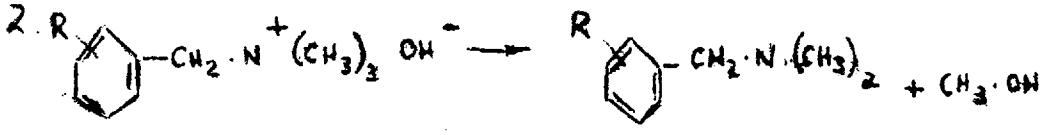

3. 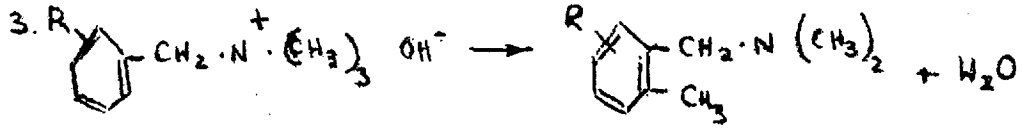

The discrepancy of 0.2 m moles/g between the observed and expected yield of water based on the above scheme (1.7 m moles/g) is more likely due to the loss of tightly bound water from the resin matrix, than to any other undetected reaction. At other temperatures, though the overall contribution to decomposition from each reaction is different (Table 2.14), the pattern of reactions should be the same.

2.3.7 Effect of the sorbed counter ion on thermal stability.

It is known that the quaternary ammonium strong base functional groups in anion exchange resin are less stable

TABLE 2.14 THERMAL DECOMPOSITION, RATIO OF TRIMETHYLAMINE YIELD TO INCREASE IN WEAK BASE CAPACITY ON HEATING AT VARIOUS TEMPERATURES
DEACIDITE FF-HYDROXIDE, 14-52 MESH, 7-9% CROSSLINKED.

HEATING TEMPERATURE	TRIMETHYLAME YIELD WEAK BASE CAPACITY INCREASE
50°C+	
75°C+	10:1
90°C+	8:1
120°C*	2:1
150°C*	1:1
180°C*	2:3

+RATIO AFTER 30 DAYS HEATING
*RATIO AFTER TOTAL COSS IN STRONG BASE CAPACITY

than the corresponding tertiary amine weak base groups. A possible explanation for this is the electron drift caused by the positively charged nitrogen atom in the quaternary group, which tends to weaken the bonds between nitrogen, the three methyl groups and the resin matrix. The substituted benzyl group between the nitrogen atom and the resin matrix is a better electron donor than the methyl groups and reaction (1) is favoured.

The negatively charged counter ion will tend to neutralise the electron drift caused by the nitrogen atom. The magnitude of any effect depends upon ionic charge, ionic size, distance of nearest approach and any specific interactions between the counter ion and resin functional group. Similar criteria apply to the selectivity of the resin for a given counter ion. The counter ion of the greatest selectivity is the most closely bound to the functional group, and hence the most effective in neutralising the effect of the nitrogen atom. This explanation predicts that the order of increasing thermal stability should be identical with the order of selectivity. The results of testing this hypothesis are shown in Table 2.15.

The order of stability was:-

$$B_2O_7^{4-} > SO_4^{2-} > NO_3^- > CNS^- > Cl^- > OH^-$$

The difference in stability between borate, sulphate, nitrate, thiocyanate and chloride is small though outside the range of experimental error, whereas the difference between these forms and hydroxide is large.

TABLE 2.15 THERMAL DECOMPOSITION. STRONG BASE CAPACITY CHANGES
DEACIDITE FF. 14-52 MESH. 7-9 % CROSSLINKED.
TEMPERATURE 150° C.
EFFECT OF NATURE OF SORBED COUNTER ION.

IONIC FORM	PER CENT LOSS IN STRONG BASE CAPACITY	HEATING TIME (DAYS)
$B_2O_7^{4-}$	17.0	60.0
SO_4^{2-}	18.0	60.0
NO_3^-	20.0	60.0
CNS^-	21.5	60.0
Cl^-	24.0	60.0
OH^-	100.0	12 HOURS *

*HYDROXIDE FORM HEATED TILL ALL STRONG BASE CAPACITY LOST.

2.3.8 Effect of degree of crosslinking on thermal stability.

Results obtained by heating Deacidite FF hydroxide samples of 2-3%, 4-6% and 7-9% crosslinking are shown in Fig.2.20 and 2.21. It can beseen that the loss in capacity is greatest in the sample of greatest degree of crosslinking at any given time.

A possible explamation of these effects is as follows. A greater degree of crosslinking results in a more closely knit matrix, with functional groups much closer to one another. As the degree of crosslinking increases there will be an increasing tendency for the sorbed counter ion to move continuously between adjacent functional groups. On average the counter ion will be further from any given functional group, and hence have less effect in neutralising the bond weakening action of the nitrogen atom, discussed in the previous section.

Further, if a comparison is made between the stability of Deacidite FF and Amberlite IRA 400, the former is found to be more stable. The crosslinks in Deacidite FF are longer than in the latter resin, so resulting in a greater separation between functional groups and an increased thermal stability for the reason given above. In Amberlite IRA 900 the slightly greater thermal stability, when compared with Amberlite IRA 400, could be caused by a greater functional group separation resulting from the wider pores.

2.3.9 Effect of particle size on thermal stability.

Samples of Deacidite FF in the hydroxide form, 7-9% crosslinked were heated at 90°C, 150°C and 180°C for 30 days

FIG 2.20

THERMAL DECOMPOSITION STRONG BASE CAPACITY CHANGES.

DEACIDITE FF - HYDROXIDE, 14-52 MESH,

TEMPERATURE 90°C,

EFFECT OF DEGREE OF CROSSLINKING.

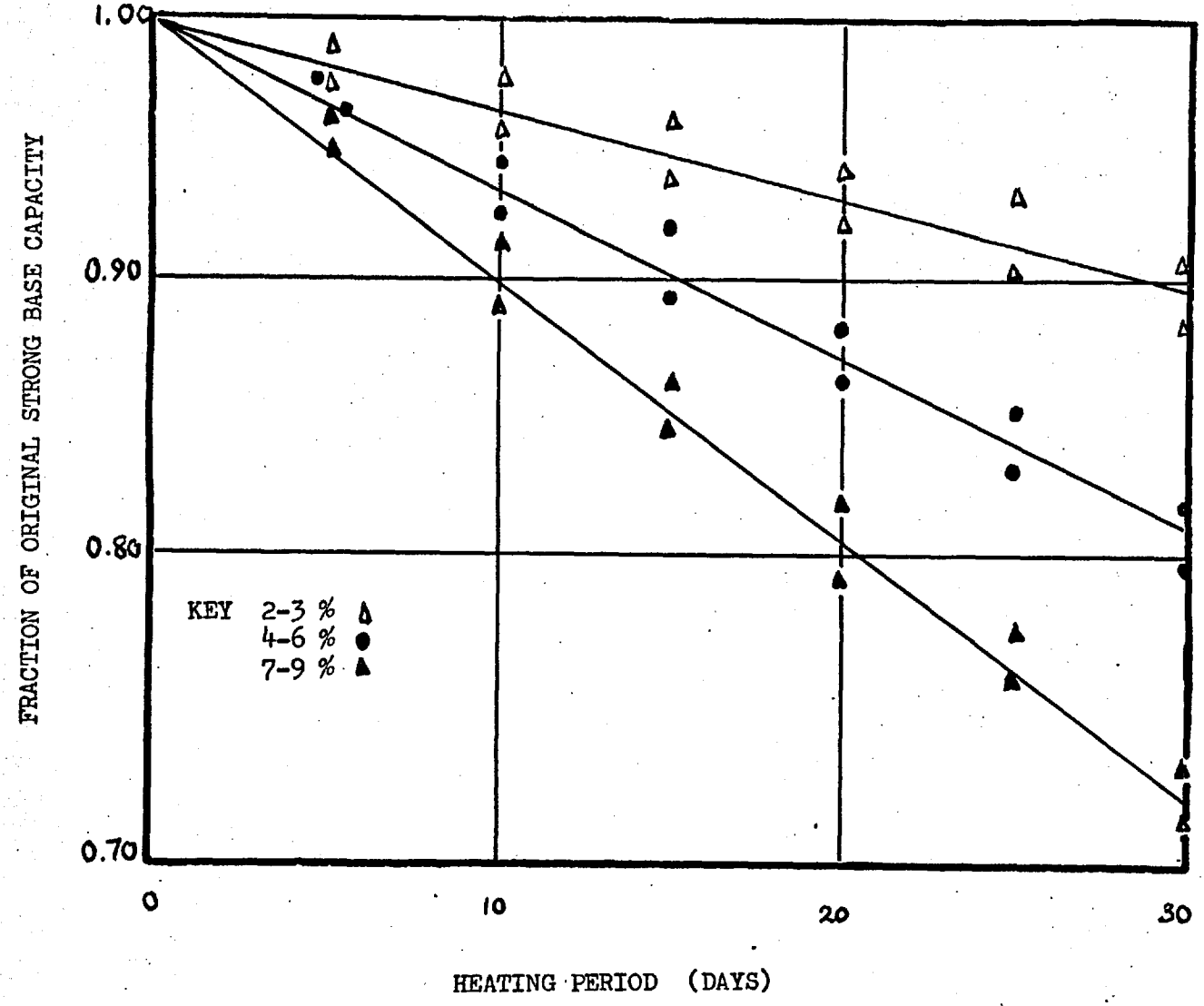

FIG 2.21 THERMAL DECOMPOSITION WEAK BASE CAPACITY CHANGES.

DEACIDITE FF - HYDROXIDE, 14-52 MESH,

TEMPERATURE 90°C,

EFFECT OF DEGREE OF CROSSLINKING.

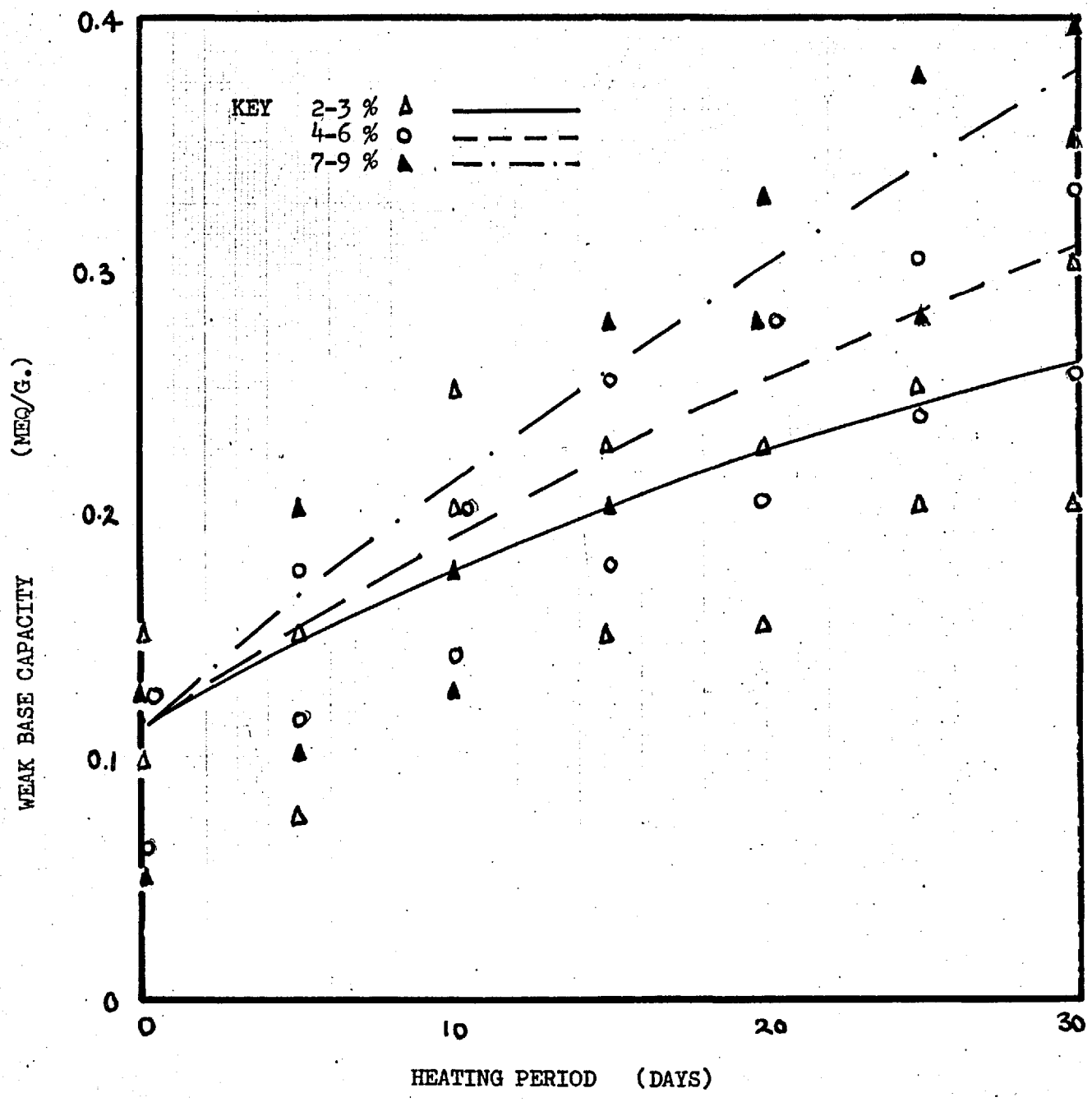

or until all strong base capacity had been destroyed. Resin samples in the BSS size ranges 14-52 mesh and 100-200 mesh were used (i.e. 0.05 to 0.01 in. and 0.006 to 0.003 in., respectively). Strong base capacity changes were measured.

At 90°C, no significant difference between resin samples of different particle sizes (ratio approximately 7:1) was observed, but at 150°C and 180°C, the smaller particles lost their entire strong base capacity in about three quarters of the time taken by the larger particles (Fig. 2.22). It was noted that the strong base capacity loss did not follow the first order rate law at the start of the heating period.

It is possible that heating of an ion exchange particle occurs in two stages, i.e. firstly, a transient period during which the bead is raised to the surrounding temperature, followed by a steady state period when the entire bead is at the surrounding temparature. During such a transient period, decomposition would occur more slowly in the cooler inner part of the bead. Hence the average rate of decomposition would increase at first during the transient period, attaining a first order rate when the entire bead has attained constant temparature. The duration of the transient period would increase with particle size.

At 150°C and 180°C a particle size effect is observed in Deacidite FF which may be explained in terms of transient periods lasting about five hours and one hour respectively in the larger particles. The smaller particles show shorter transient periods. After the transient period, decomposition proceeds at the same rate irrespective of particle size.

FIG 2.22 THERMAL DECOMPOSITION STRONG BASE CAPACITY CHANGES. DEACIDITE FF - HYDROXIDE, 7-9 % CROSSLINKED, EFFECT OF PARTICLE SIZE.

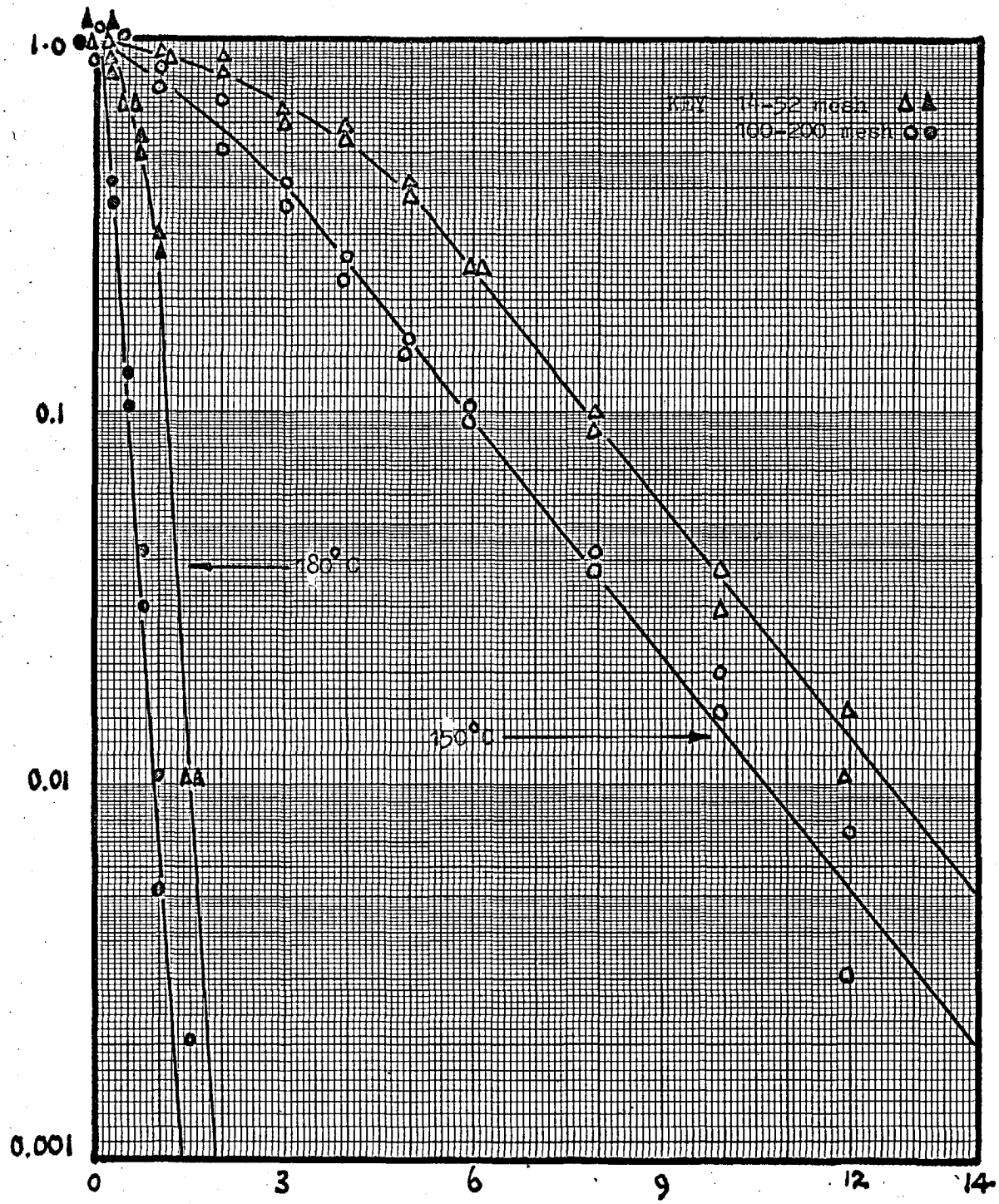

At 90°C the duration of the transient period would be small compared with the time for significant damage to occur, and therefore no detectable difference would be expected. Particle size effects based on this explanation would only be important when the transient period is appreciable compared with the time for significant thermal damage to occur.

2.3.10 Thermal decomposition of Permutit SK.

Permutit SK (ref.G3) is a polysubstituted pyridine, based, polyfunctional anion exchange resin which is thought to be prepared by chlorinating a crosslinked polymer of an alkyl vinylpyridine, aminating the chloro-alkyl group and finally alkylating the tertiary nitrogen atom in the pyridine ring. This results in a measured weak and strong base capacity of 3.40 meq/g.and 0.81 meq/g. respectively.

The thermal stability of Permutit SK in the hydroxide and chloride forms was studied at 90°C, 120°C, 150°C and 180°C. Samples were heated in demineralised water for periods up to seven days and analysed for strong and weak base capacity. A few determinations of the nature and yield of soluble decomposition products were made.

At 90°C , this resin is stable in the hydroxide form for at least 24 hours (Fig. 2.23) and in the chloride form for at least 7 days (Fig. 2.24). Above 90°C, strong base capacity decreases and the rate of capacity loss increases with increasing temperatur. At 120°C no significant capacity changes occur in the chloride form up to 7 days, whereas the hydroxide form showed a strong base

FIG 2.2 3 THERMAL DECOMPOSITION STRONG BASE CAPACITY CHANGES.

PERMUTIT S.K. - HYDROXIDE

14-52 MESH, 4-9% CROSSLINKING.

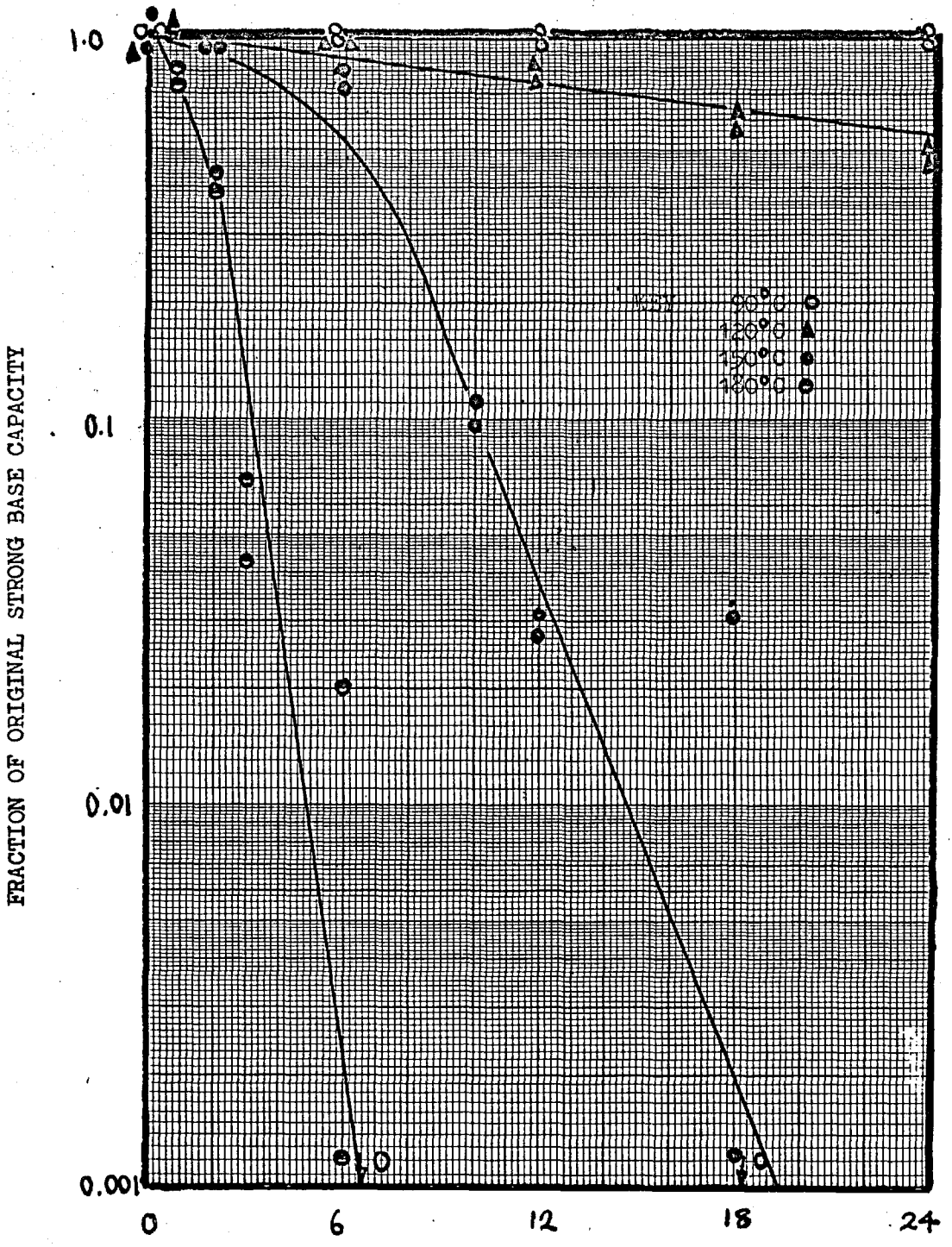

FIG 2.24 THERMAL DECOMPOSITION STRONG BASE CAPACITY CHANGES.

PERMUTIT S.K. - CHLORIDE, 14-52 MESH, 4-9 % CROSSLINKED,

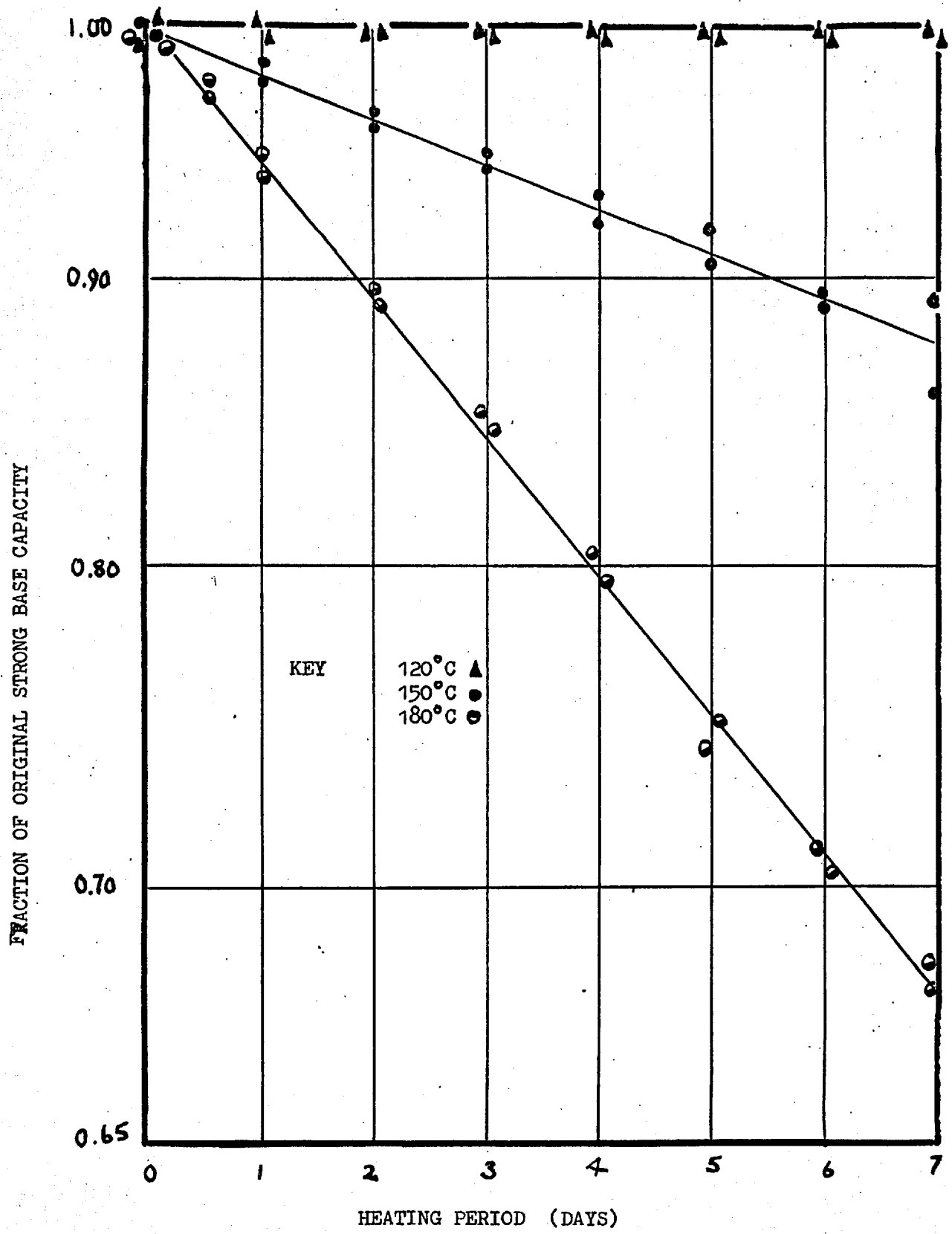

RESIN IN THE HYDROXIDE FORM

TABLE 2.16

TEMPERATURE 90.0 C

TIME		HRS	0	1.00	2.00	3.00	6.00	8.00	10.00	12.00	18.00	24.00
PERMUTIT	SB CAPACITY	MEQ/G	3.40				3.40			3.33		3.33
SK	SB CAPACITY		1.00				1.00			0.98		0.98
	WB CAPACITY	MEQ/G	0.85				0.85			0.88		0.85
	TOTAL CAPACITY	MEQ/G	4.25				4.25			4.21		4.18

TEMPERATURE 120.0 C

TIME		HRS	0	1.00	2.00	3.00	6.00	8.00	10.00	12.00	18.00	24.00
PERMUTIT	SB CAPACITY	MEQ/G	3.37				3.06			2.52		1.56
SK	SB CAPACITY		0.99				0.90			0.74		0.46
	WB CAPACITY	MEQ/G	0.85				1.26			1.80	2.38	2.86
	TOTAL CAPACITY	MEQ/G	4.22				4.32			4.32	2.38	4.42

TEMPERATURE 150.0 C

TIME		HRS	0	1.00	2.00	3.00	6.00	8.00	10.00	12.00	18.00	24.00
PERMUTIT	SB CAPACITY	MEQ/G	3.37			2.62	2.62	1.53	0.37	0.14	0	0
SK	SB CAPACITY		0.99			0.77	0.77	0.45	0.11	0.04	0	0
	WB CAPACITY	MEQ/G	0.88			1.29	2.01	2.79	3.91	4.15	4.22	4.25
	TOTAL CAPACITY	MEQ/G	4.25			3.91	4.63	4.32	4.28	4.29	4.22	4.25

TEMPERATURE 180.0 C

TIME		HRS	0	1.00	2.00	3.00	6.00	8.00	10.00	12.00	18.00	24.00
PERMUTIT	SB CAPACITY	MEQ/G	3.40	2.58	1.39	0.24	0			0	0	0
SK	SB CAPACITY		1.00	0.76	0.41	0.07	0			0	0	0
	WB CAPACITY	MEQ/G	0.88	1.80	2.89	4.08	4.25			4.25	4.22	4.25
	TOTAL CAPACITY	MEQ/G	4.28	4.38	4.28	4.32	4.25			4.25	4.22	4.25

SAMPLE 6

RESIN IN THE HYDROXIDE FORM

TEMPERATURE 90.0 C

TIME		HRS	0	1.00	2.00	3.00	6.00	8.00	10.00	12.00	18.00	24.00
PERMUTIT	SB CAPACITY	MEQ/G	3.40				3.33			3.37		3.40
SK	SB CAPACITY		1.00				0.98			0.99		1.00
	WB CAPACITY	MEQ/G	0.82				0.82			0.85		0.78
	TOTAL CAPACITY	MEQ/G	4.22				4.15			4.22		4.18

TEMPERATURE 120.0 C

TIME		HRS	0	1.00	2.00	3.00	6.00	8.00	10.00	12.00	18.00	24.00
PERMUTIT	SB CAPACITY	MEQ/G	3.40				6.39			2.38		1.36
SK	SB CAPACITY		1.00				1.88			0.70		0.40
	WB CAPACITY	MEQ/G	0.82				1.15			1.70	2.24	2.65
	TOTAL CAPACITY	MEQ/G	4.22				7.54			4.08	2.24	4.01

TEMPERATURE 150.0 C

TIME		HRS	0	1.00	2.00	3.00	6.00	8.00	10.00	12.00	18.00	24.00
PERMUTIT	SB CAPACITY	MEQ/G	3.40			2.65	2.38	1.33	0.31	0.10	0	0
SK	SB CAPACITY		1.00			0.78	0.70	0.39	0.09	0.03	0	0
	WB CAPACITY	MEQ/G	0.82			1.22	1.94	2.72	3.81	4.01	4.15	4.15
	TOTAL CAPACITY	MEQ/G	4.22			3.87	4.32	4.05	4.12	4.11	4.15	4.15

TEMPERATURE 180.0 C

TIME		HRS	0	1.00	2.00	3.00	6.00	8.00	10.00	12.00	18.00	24.00
PERMUTIT	SB CAPACITY	MEQ/G	3.37	2.38	1.26	0.14	0			0	0	0
SK	SB CAPACITY		0.99	0.70	0.37	0.04	0			0	0	0
	WB CAPACITY	MEQ/G	0.82	1.70	2.79	3.98	4.15			4.15	4.15	4.11
	TOTAL CAPACITY	MEQ/G	4.19	4.08	4.05	4.12	4.15			4.15	4.15	4.11

SAMPLE 7

RESIN IN THE CHLORIDE FORM

TABLE 2.17

TEMPERATURE 120.0 C

TIME		DAYS	0	1.00	2.00	3.00	4.00	5.00	6.00	7.00	8.00	9.00
PERMUTIT	SB CAPACITY	MEQ/G	3.40	3.47	3.47	3.43	3.40	3.33	3.26			
SK	SB CAPACITY		1.00	1.02	1.02	1.01	1.00	0.98	0.96			
	WB CAPACITY	MEQ/G	0.71	0.71	0.71	0.75	0.78	0.75	0.78			
	TOTAL CAPACITY	MEQ/G	4.11	4.18	4.18	4.18	4.18	4.08	4.04			

TEMPERATURE 150.0 C

TIME		DAYS	0	1.00	2.00	3.00	4.00	5.00	6.00	7.00	8.00	9.00
PERMUTIT	SB CAPACITY	MEQ/G	3.40	3.33	3.30	3.23	3.16	3.13	3.06	3.03		
SK	SB CAPACITY		1.00	0.98	0.97	0.95	0.93	0.92	0.90	0.89		
	WB CAPACITY	MEQ/G	0.75	0.82	0.92	0.95	1.02	1.09	1.16	1.29		
	TOTAL CAPACITY	MEQ/G	4.15	4.15	4.22	4.18	4.18	4.22	4.22	4.32		

TEMPERATURE 180.0 C

TIME		DAYS	0	1.00	2.00	3.00	4.00	5.00	6.00	7.00	8.00	9.00
PERMUTIT	SB CAPACITY	MEQ/G	3.40	3.23	3.03	2.89	2.72	2.52	2.41	2.31		
SK	SB CAPACITY		1.00	0.95	0.89	0.85	0.80	0.74	0.71	0.68		
	WB CAPACITY	MEQ/G	0.71	0.95	1.16	1.38	1.50	1.67	1.77	1.94		
	TOTAL CAPACITY	MEQ/G	4.11	4.18	4.19	4.27	4.22	4.19	4.18	4.25		

SAMPLE 8

RESIN IN THE CHLORIDE FORM

TEMPERATURE 120.0 C

TIME		DAYS	0	1.00	2.00	3.00	4.00	5.00	6.00	7.00	8.00	9.00
PERMUTIT	SB CAPACITY	MEQ/G	3.40	3.43	3.43	3.43	3.43	3.33	3.50	3.40		
SK	SB CAPACITY		1.00	1.01	1.01	1.01	1.01	0.98	1.03	1.00		
	WB CAPACITY	MEQ/G	0.75	0.75	0.75	0.78	0.82	0.75	0.75	0.78		
	TOTAL CAPACITY	MEQ/G	4.15	4.18	4.18	4.21	4.25	4.08	4.25	4.18		

TEMPERATURE 150.0 C

TIME		DAYS	0	1.00	2.00	3.00	4.00	5.00	6.00	7.00	8.00	9.00
PERMUTIT	SB CAPACITY	MEQ/G	3.40	3.33	3.26	3.23	3.13	3.09	3.03	2.92		
SK	SB CAPACITY		1.00	0.98	0.96	0.95	0.92	0.91	0.89	0.86		
	WB CAPACITY	MEQ/G	0.75	0.85	0.95	0.95	1.05	1.12	1.19	1.29		
	TOTAL CAPACITY	MEQ/G	4.15	4.18	4.21	4.18	4.18	4.21	4.22	4.21		

TEMPERATURE 180.0 C

TIME		DAYS	0	1.00	2.00	3.00	4.00	5.00	6.00	7.00	8.00	9.00
PERMUTIT	SB CAPACITY	MEQ/G	3.40	3.20	3.06	2.89	2.69	2.55	2.45	2.28		
SK	SB CAPACITY		1.00	0.94	0.90	0.85	0.79	0.75	0.72	0.67		
	WB CAPACITY	MEQ/G	0.75	1.02	1.16	1.33	1.50	1.67	1.77	2.01		
	TOTAL CAPACITY	MEQ/G	4.15	4.22	4.22	4.22	4.19	4.22	4.22	4.29		

capacity loss of 45% in 24 hours. At 150°C and 180°C total loss of strong base capacity takes place in less than 24 hours in the hydroxide form (Fig 2.23), whereas the chloride form is appreciably more stable, showing a strong base capacity loss of about 10% and 30% respectively, after 7 days heating (Fig.2.24). Increases in weak base capacity were measured in cases where decomposition occurred (Fig.2.25 and 2.26).

Methanol was the only significant decomposition product detected; the yield was measured in several cases and found to be comparable with the increase in weak base capacity. The precise chemical structure of Permutit SK is not known, but the results of this work suggest that the most likely configuration is:-

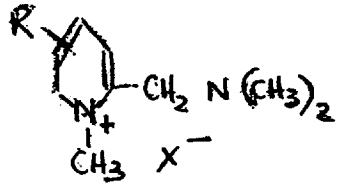

Although some quaternary side chains may exist, these are small in number compared with the N-methyl groups. A suggested mechanism of decomposition is as follows:-

1.

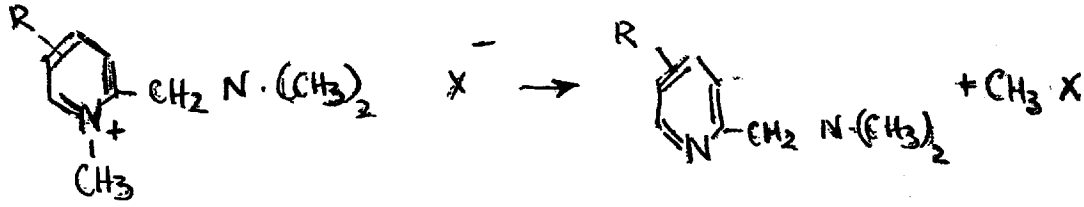

The removal of methyl groups from the quaternary nitrogen atom results in the conversion of strong base capacity to

FIG 2.25 THERMAL DECOMPOSITION WEAK BASE CAPACITY CHANGES.

PERMUTIT S.K. - HYDROXIDE,

14-52 MESH, 7-9 % CROSSLINKED.

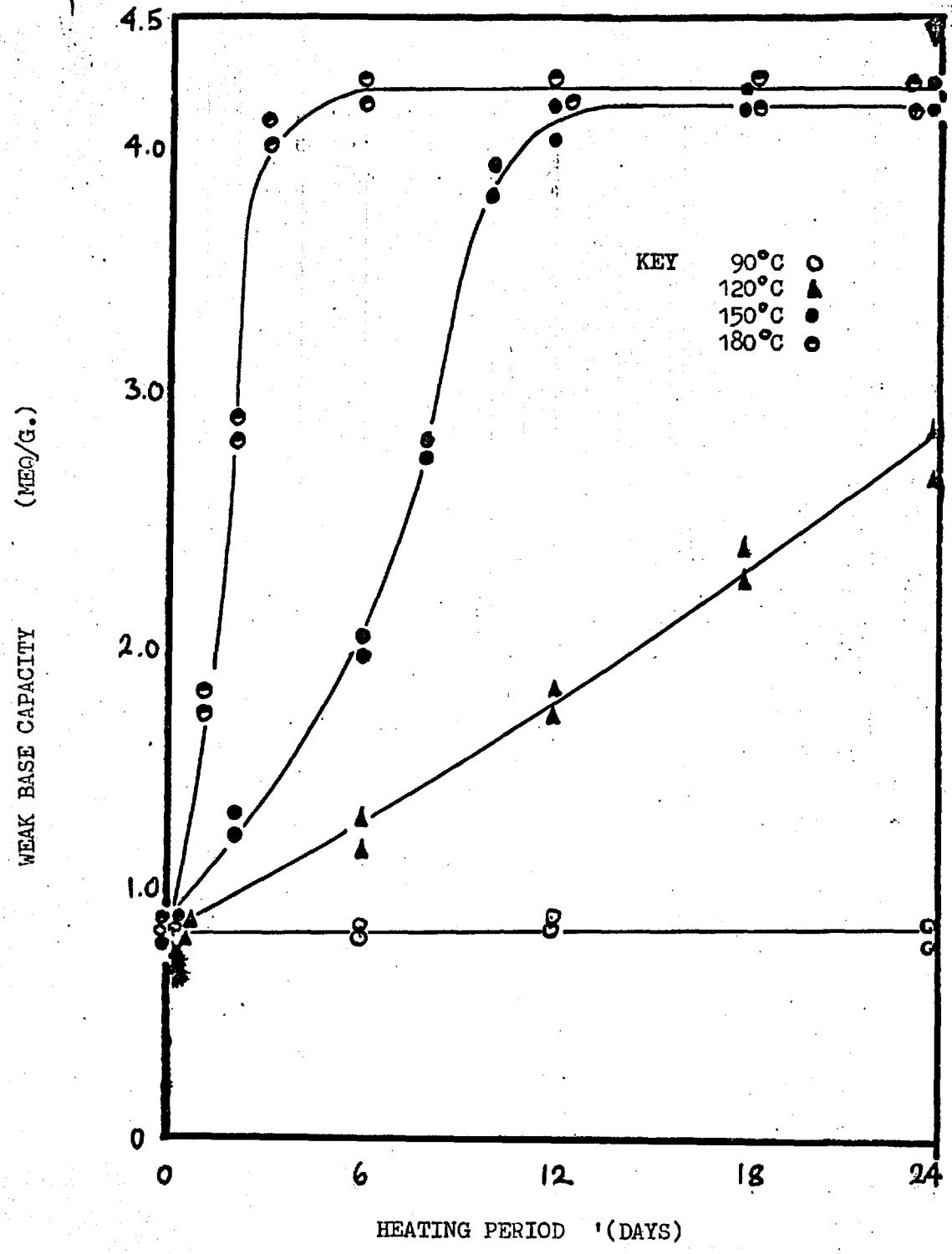

FIG 2.26 THERMAL DECOMPOSITION WEAK BASE CAPACITY CHANGES.

PERMUTIT S.K. - CHLORIDE

14-52 MESH, 4-9 % CROSSLINKING.

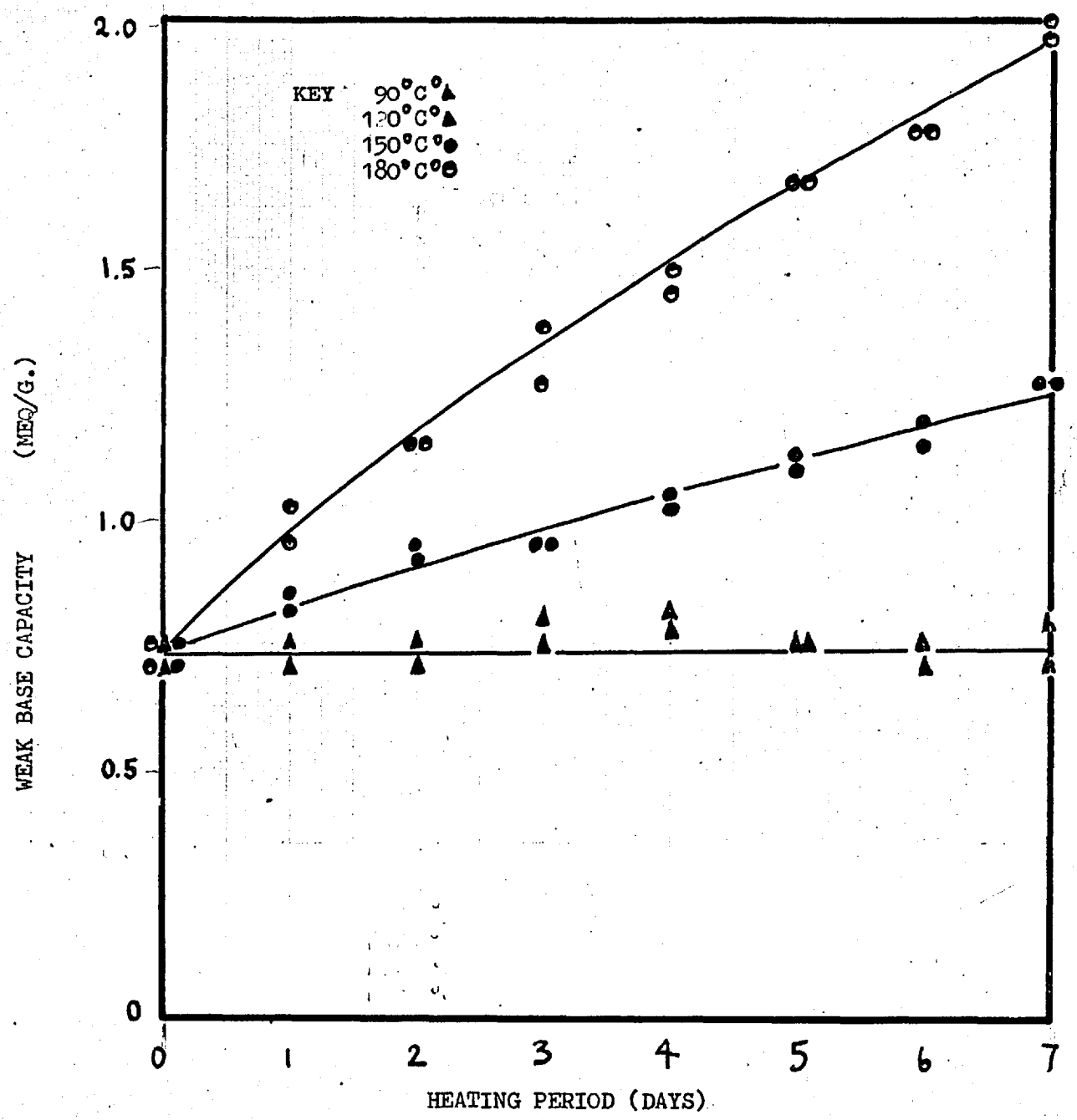

weak base capacity and the production of methanol.

The activation energy for thermal decomposition of Permutit SK and the velocity constant at each temperature are given in Table 2.18.

2.4 Conclusion.

The following conclusions were drawn from the work described in this chapter :-

a. Organic anion exchangers with strong base capacity of the quaternary ammonium type are generally unstable above 50°C. Limited improvements may be attained by changing the matrix structure and the groups attached to the quaternary nitrogen atom.

b. Weak base capacity in the weak base exchangers is thermally stable up to 180°C, whereas weak base capacity resulting from the decomposition of strong base capacity is slowly destroyed at temperatures below 180°C. Hence there are at least two kinds of weak base capacity groups.

c. Trimethylamine bases and salts, methanol and its derivatives and water result as products of the thermal decomposition of strong base capacity. Of the two organic products trimethylamine is the main product and the yield of methanol decreases with temperature.

d. Particle size, degree and nature of cross linking and the nature of the sorbed counter ion have a limited effect on the thermal stability of strong base capacity. Thermal stability increases with decreasing degree of crosslinking of increasing length of crosslinks. The most stable ionic form of resin is that where the affinity between counter ion

TABLE 2.18 THERMAL DECOMPOSITION KINETIC DATA.
PERMUTIT SK HYDROXIDE AND CHLORIDE.
14-52 MESH. 4-9% CROSSLINKED

	VELOCITY CONSTANT OF REACTION (DAYS-1)			ACTIVATION ENERGY
TEMP	120°C	150°C	180°C	KCALE/MOLE
OH TOT	5.9×10^{-1}	1.4×10^{1}	3.7×10^{1}	10.3
CL TOT	$< 10^{-4}$	1.9×10^{-2}	5.6×10^{-2}	14.1

and functional group is greatest. The lifetime of an ion exchange resin increases with particle size at temperatures in excess of 100°C.

e. Decomposition of strong base capacity proceeds by a Hofmann degradation and a rearrangement reaction. The reactions are:-

1. 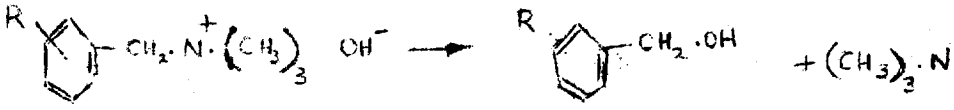

2. 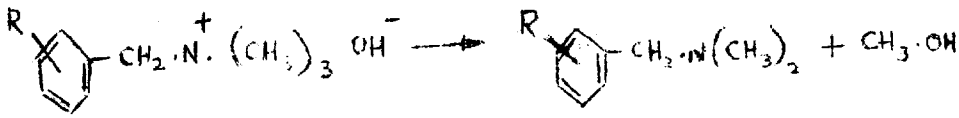

3. 

Activation energies are of the order of 30 kcal/mole.

Chapter 3

DESIGN, COMMISSIONING AND OPERATION OF A TEST LOOP.

3.1 Introduction.

The aim of this work was to investigate the behaviour of Deacidite FF-hydroxide in a flow system at elevated temperatures. To this end it was neccessary to design and construct a continuously operating test loop and to specify in line measuring-instruments and automatic control circuitry to allow unattended operations.

A glass lined, cast iron system was considered at first, to enable operation at temperatures up to 200°C. However, feasibility studies indicated that the cost of such a loop would be beyond the financial resources of the project. In view of financial and also safety considerations it was decided that a 90°C all glass loop was feasible and would produce useful data.

The apparatus was put to the following uses, during a test run of 71 days at 90°C:-

a. Measurement of changes in strong and weak base capacity with time in order to compare these changes with thermal decomposition in a static system.

b. Analysis of the ionic form of the resin under test at various times during the run to determine whether the

sample remained in the hydroxide form.

c. Identification of the decomposition products and measuremer of yields of :-

i. organic products.

ii. inorganic ions, in the loop water,if any.

d. Measurement of the particle size distribution before and after a run.

e. Measurement of the pressure drop across the test beds of anion exchange resin as a function of time and determination of changes in voidage and bed compaction during the run. Assessment of any physical damage to the resin

f. Measurement of the pH of the circulating water, upstream and downstream of the test beds as a function of time.

g. Degradation of larger quantities of anion exchange resin for mass transfer work as described in chapter 4.

3.2 The test loop.

3.2.1 Description.

The entire circulating loop (Fig.3.1) is constructed of Q.V.F. glass pipeline, fittings, valves and pump. Water only comes into contact with glass and plastic materials, hence maintaining a system where undissolved and dissolved impurities are reduced to a minimum. A schematic flowsheet of the system is enclosed in the wallet.

The circulating pump can deliver water at up to 20 g.p.m. against a head of 30 p.s.i.g. measured by a Bourdon gauge (P1). Water from the pump outlet is heated by a 1kw. booster heater section (A3) before passing through either of two 4 in. deep by 3 in. diameter clean

MEM
OFF

up beds, included to remove decomposition products. These beds contain Zeokarb 225 cation exchange resin and can be isolated from the loop by valves (SV1,SV2,SV3, SV4), when regeneration is necessary. Water flow through the main circuit is measured by a 65X glass rotameter with a korranite float, having a maximum capacity of 25 g.p.m. water at 25°C. The flow rate in the main circuit is controlled by the valve VB2 which regulates the flow through the by-pass line. Beyond the rotameter two further heater sections are incorporated; a 1kw. booster heater section (A2)and an 1kw trimmer heater section (A1), controlled by a sensitive mercury in glass temperature sensor (TC1). The booster heater sections are operated at a constant power level, which may be adjusted by a "variac" autotransformer. Water continues in down flow through a 6 in. diameter column containing the resin under test, before returning to the suction side of the pump. PTFE bellows are incorporated in the pipeline at the suction and delivery side of the pump to allow for misalignment in the pipe work and to ensure minimum transmission of pump vibration to the loop pipe lines and components.

A header tank of 100 litres capacity provides make up water to compensate for small leaks in the loop, and maintains the reference pressure at the circulating pump suction side at 4 p.s.i.g. For this purpose water may flow from the header tank through a manual stop valve (SV7) and a pressure operating shut off

FIG 3.2 RESIN LOADING

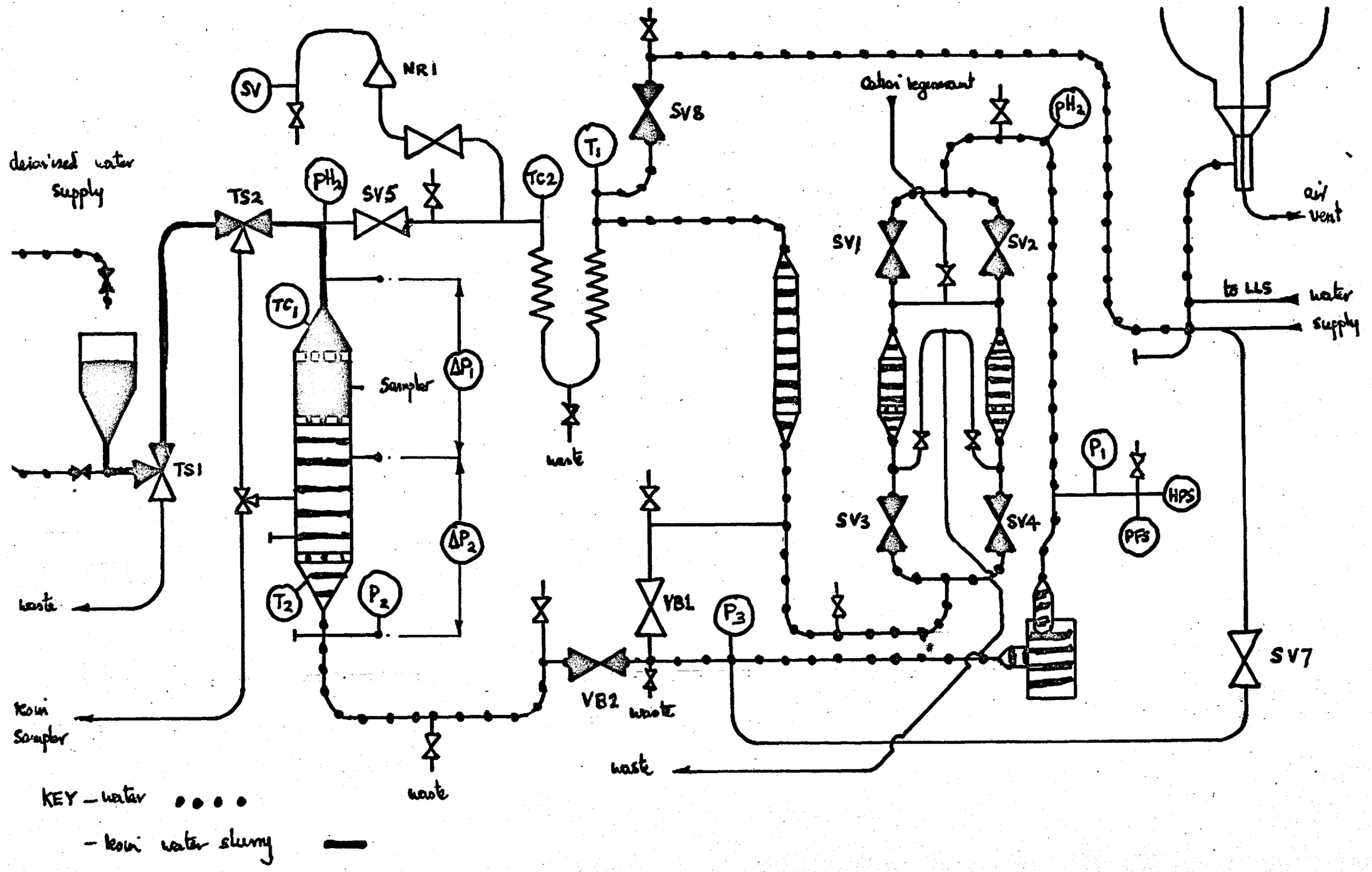

FIG 3.3 RESIN UNLOADING

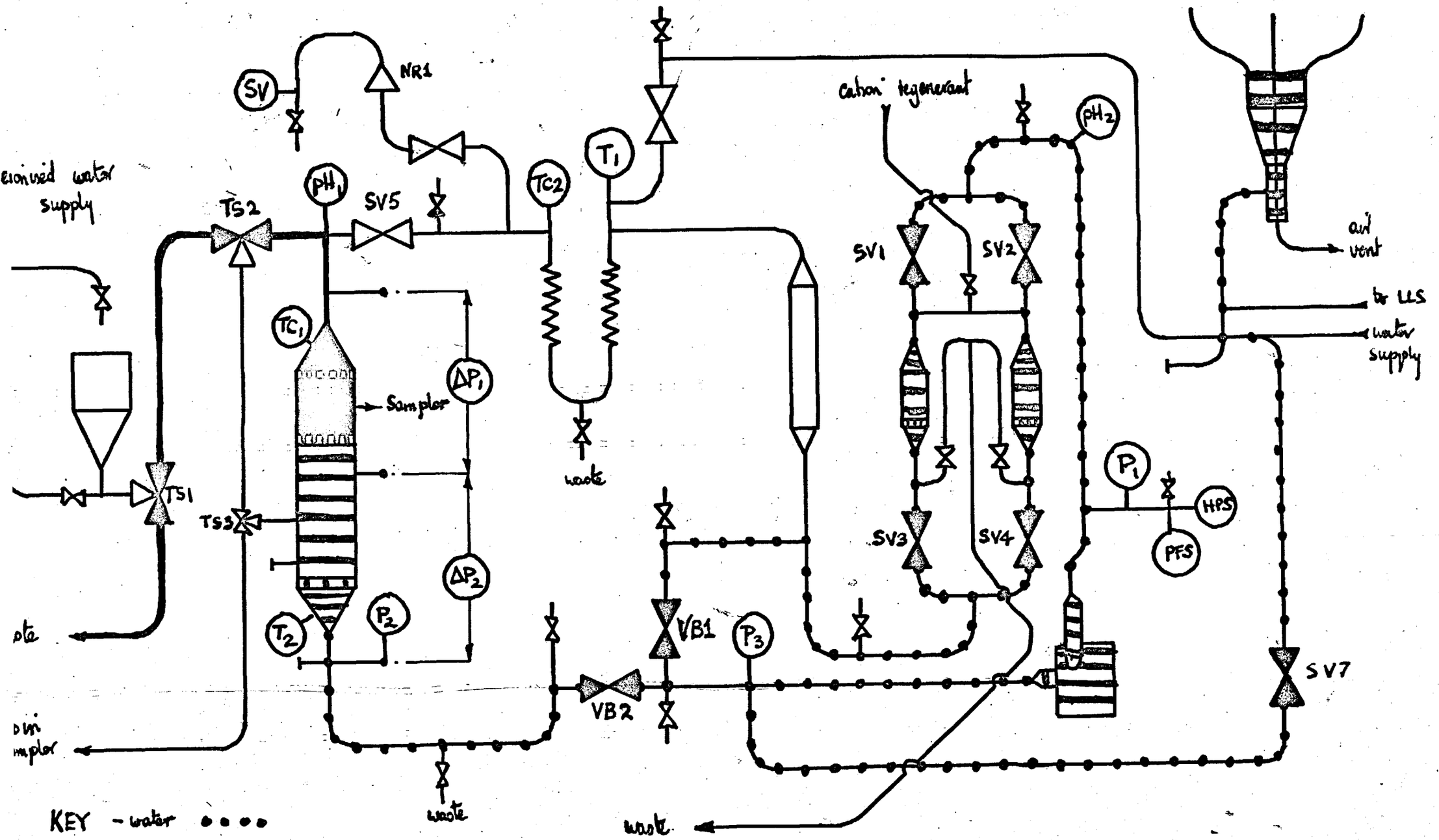

valve (PV1) into the loop through a tee immediately before the circulating pump. Suitable ventcocks and drain cocks for filling and emptying the system are provided.

The 6 in. diameter test column contains two fixed beds of anion exchange resin. The upper 4 in. deep bed consists of 20-30 mesh, 7-9% crosslinked Deacidite EF in the hydroxid form. The lower bed is of the same resin, in a 4 in. deep layer, except that the resin is 2-3% crosslinked. Resin may be loaded and unloaded by hydraulic conveying as shown in Fig. 3.2 and 3.3. Mercury manometers are incorporated for accurate pressure measurement across each bed.

Provision is made for temperature measurement by a mercury in glass thermometer (T1) and a chrome alumel thermocouple (T2) in a glass jacket. The pH of the flowing water is monitored by in-line electrodes (pH1 and pH2). Safety devices are designed to take action in the event of low header tank level, excess system pressure , serious leakage, circulating pump failure, excess temperature and failure of the safety circuitry. A clock is incorporated for measurements of the running time.

3.2.2 Important design considerations.

Trace quantities of metallic and other ions are reported to have an appreciable effect on the thermal decomposition of ion exchange resins (ref.A2), and the circulating loop was therefore designed to reduce unwanted impurities to a minimum.

Water was deionised to a conductivity less than 1 micromho/cm. and thereafter allowed to come into contact

with only glass, plastic and other non contaminating materials. The leaching of silica from glass(ref.A3) was expected and taken into account in assessing the results of loop experiments. Where possible measuring devices and sensors were specified in glass or plastic (pH probes, resistance thermometers, mercury in glass thermometers and temperature sensors), or specially manufactured in glass (level sensor, Fig.3.4). In cases where metallic components were unavoidable they were enclosed in glass sheaths filled with mercury (fail safe temperature overload cutout), or in plain glass sheaths (thermocoupled), or separated from the system by PVC diaphragms (pressure switches, Fig. 3.5). The bronze spring safety valve was situated at the end of a long dead leg and separated from the circulating water by a non return valve (NR1). This allowed water to flow from the system with a pressure overload occurred. In practice a small quantity of water leaked past the non return valve and accumulated in the dead leg from which it was periodically removed before the leg become full. The pressure shut off valve used to separate the header tank from the loop (PV1) was a rubber lined, cast iron 1 in. Saunders valve. All glass pipelines and components were Q.V.F. borosilicate glass to BSS 2598 (ref.Q1). The beds of ion exchange resin were supported on a glass and nylon mesh grid. Asbestos gaskets with PTFE sheaths or plain neoprene rubber gaskets were used at all joints. Stop cocks, ventcocks and draincocks were lubricated with non metallic "Apiezon" grease. Mercury

FIG 3.4 FLOAT SWITCH FITTING

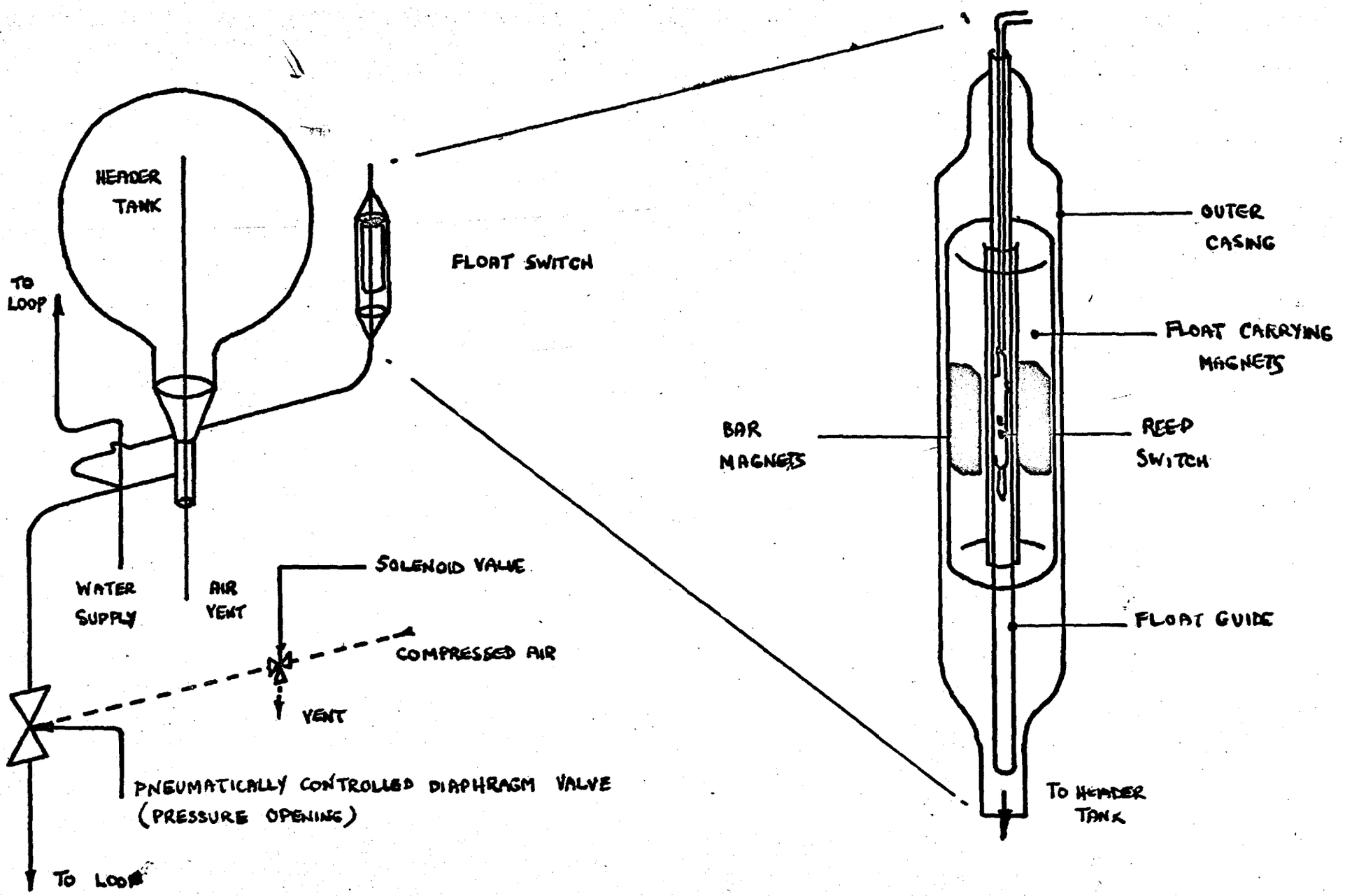

FIG 3.5 PRESSURE SWITCH FITTING

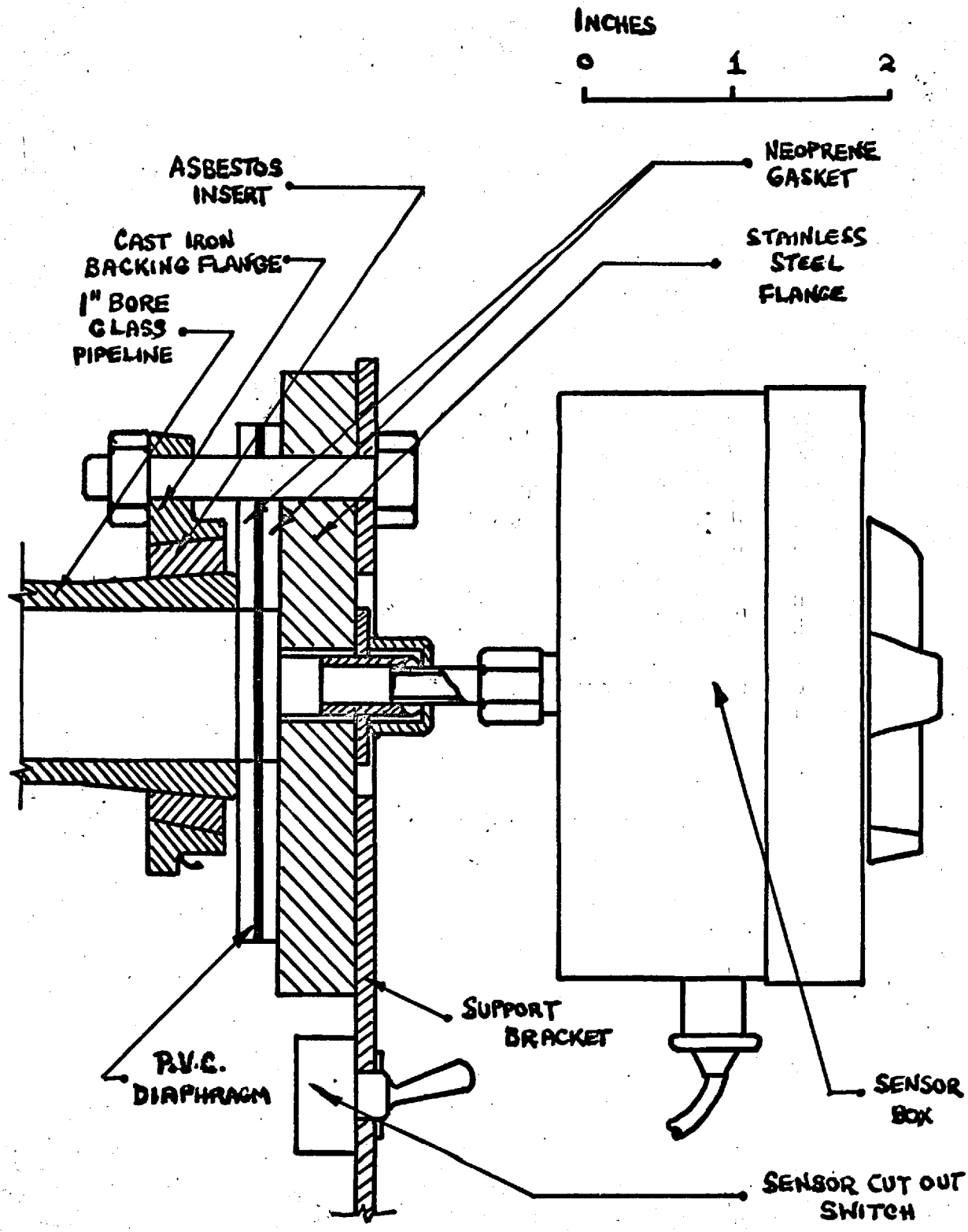

manometers were separated from the loop water by a small column of carbon tetrachloride .

Each of the three original heater sections consisted of 960 watt " thermocord " heating cord wound round a 2 ft. length of 1 in. bore pipe line. A 2 in. layer of asbestos string was wound over the heating cord to cut down heat loss to atmosphere. This type of heater was liable to burn out if accidental drainage of the system occurred, so each was later replaced by two 500 watt silica " red rod" heaters inserted into the loop through tee pieces . The red rod heaters were much more efficient, required no lagging and did not burn out under any conditions. In addition fusible links were cemented on to the outside wall of the pipeline in the heater sections, to provide an additional safety measure. The links melted if the outside wall temperature exceeded 100°C, because of accidental drainage of the loop.

3.2.3. Choice of equipment and operating conditions.

The materials in contact with the loop water were chosen to minimise undesirable impurities. A centrifugal circulating pump was chosen because it provided a constant output of the required capacity and could be obtained in glass as a standard item. The glass rotameter was chosen because it was obtainable already calibrated. Calibration would have been difficult had the alternative orifice plate meter been used because of the large flow rates involved. 1½ in., 1 in. and ⅝ in. nominal bore pipelines were considered. The 1 in. pipeline gave the best safety factor (i.e.6)under the internal pressure of the loop.

Only the 1 in. and $\frac{5}{8}$ in. pipeline systems would fit in the space allocated for construction. There was no significant difference in the cost of the 1 in. and $\frac{5}{8}$ in. pipeline system, and the former would degrade twice as much resin as the latter in one run. These factors made the 1 in. system the obvious choice.

Valves were chosen on two counts. Firstly, ease of operation and secondly, minimum pressure drop. The pressure drop through a 1 in. Q.V.F. stopcock and the 1 in. DVS diaphragm valve (ref. Q1) is approximately the same, but the stopcock barrel is likely to seize unless frequent maintenance is undertaken. The DVS valve was therefore used where stop valves were required. The more expensive VB type screw down valve was used where flow rate adjustment was required because of its better characteristic. Sensitive adjustment was achieved by using two of these valve one in the by pass circuit and one in the main circuit (VB1 and VB2).

The maximum superficial flow rate was 100 g.p.m./sq. ft. through the 6 in. diameter test column, this being the maximum output of the larger Q.V.F. glass pump. This superficial flow rate range was chosen to extend the work of Creed (ref.C1). He worked up to approximately 20 g.p.m./sq ft. in a $\frac{5}{8}$ in. diameter bed. The test bed dimensions (4 in. deep by 6 in.diameter) in this work was chosen to avoid difficulties encountered by Creed and to provide 1.5 litres of resin for mass transfer work, reported in chapter 4.

Beds of cation exchange resin (4 in. deep by 3 in. diameter) were necessary to give sufficient clean up capacity for a minimum of 10 days operation with an acceptab pressure drop at the flow rates used. The clean up beds consisted of 14-52 mesh, 8% crosslinked Zeokarb 225 initially in the hydrogen form, and were used to absorbe trimethylamine produced by decomposition of the resin in the test section. Methanol, the other significant product was not sorbed, and was allowed to accumulate in the system for 10 days. After this period the loop was drained and filled with fresh deionised water.

The maximum working pressure in the loop was 26 p.s.i.g. Pressure at the pump inlet was maintained at 4 p.s.i.g. by the 8 ft. water column connecting the loop to the header tank. The maximum working pressure was sufficient to prevent cavitation in the circulating pump at the maximum operating temperature. The heating capacity was calculated from formulae given by Colburn (ref.C5,C6) with modifications. The calculated figure was 1.5kw., but this was doubled in view of the approximate nature of the calculation. In practice 2kw. was sufficient for sustained operation at 90°C, but the extra power was useful for rapid attainment of operating temperature. When the loop was operating, the maximum variations of temperature over the test column were $\pm$ 2°C .

3.2.4 Safety circuitry.

The circulating loop was designed to run continuously without the presence of an operator, and

appropriate safety circuitry was designed to prevent damage caused by maloperation. The following fault conditions were considered.

a. Total loss of water caused by either a rapid leak or a slow leak (less than 0.5 litres per hour).

Damage would be caused by water spraying over personnel and apparatus , and by possible overheating and burn out of the heaters. In addition the circulating pump would overspeed, causing damage to its seals and bearings.

A float switch (Fig.3.5) was incorporated in the loop and arranged to discriminate between a rapid and slow leak. A rapid leak caused a suction action which lowered the float rapidly and actuated cutout circuits before much water had drained from the system. Slow leaks were made up by water from the header tank, causing a gradual drop in the level in the tank and the float switch chamber. Eventually, the float activated cutout circuits. The cutout circuits shut down the heaters and circulating pump and closed the pressure operating valve between the loop and the header tank. Additional safety features were incorporated in case the electrical cutout circuits failed. The heater sections were individually protected by fusible links and designed so that dry running would not cause damage. The pump was not additionally protected since overspeeding control would have been difficult to achieve reliably, and damage through overspeeding would have been confined to easily replaceable PTFE seals. The whole system was placed in a drip tray of sufficient capacity

to contain twice the volume of water in the loop and header tank, and was surrounded by an aluminium and perspex shield to prevent spraying of the adjacent area.

b. Failure of the circulating pump.

In this case water circulation would cease and boiling would occur in the heater sections causing pressure in the loop to rise beyond the design limit. A pressure sensor was provided to detect lowered pressure, consequent on pump failure and a second pressure sensor detected pressure in excess of the design limit, caused by boiling and other factors. In addition fusible links in the heater sections would melt before boiling temperatures were reached. In practice, boiling would also be prevented by the temperature sensors in the system, which were set at 90°C and 95°C respectively.

c. Water temperature in excess of the desired value.

Water temperature in the system was maintained by two booster heater sections switched on continuously and a trimmer heater section controlled by a sensitive mercury in glass temperature sensor. The operation of this sensor completed a circuit when the set temperature was reached, thereby initiating control action and hence failure of this device would usually result in an uncontrolled temperature rise. A coarse bimetallic strip sensor was also incorporated in the system to prevent excess temperature due to this cause. This stand by sensor breaks the circuit when the set temperature is reached.

Signals from the sensors were transferred to relays

designed to bring about appropriate control action. The relay systems were arranged so that a power failure would cause shut down of the circulating loop. Duplicate relays were included were necessary to safeguard against relay failures. Temperature control was self resetting but the other safety circuits had to be reset manually.

3.3 Results and discussions.

3.3.1 General considerations.

The pH of the circulating water remained at 7 ± 0.2 units during the 70 day running period, showing that trimethylamine was completely sorbed from solution by the cation exchange clean up beds. Methanol was not significantly sorbed, and was detected in the loop water.

Sorbed trimethylamine was eluted from the clean up beds by a 15% hydrochloric acid solution (ref.J3) every 10 days. 46% of the total capacity was utilised, without significant leakage. This is in agreement with the work of Juracka and Kaspar (ref.J3) and Creed (ref.C1) who reported 90% capacity utilisation in controlled experiments with cation exchangers and trimethylamine. Creed's work was carried out at superficial flow rates of up to 17.5 g.p.m./sq.ft. approximately 20% of the maximum in this work. The present results show that the decrease in efficiency of clean up is very small if the superficial flow rate is increased beyond 20 g.p.m./sq.ft. up to 100 g.p.m./sq.ft.

The observations regarding methanol sorption are in agreement with E.W. Baumann (ref.B1) who reported no

significant sorbtion in a simulated flow system. At higher methanol concentrations (50 g./litre) Wheaton and Bauman (ref.W5) achieved methanol sorption on Dowex 50-H^+; however it is unlikely that methanol sorbtion on cation exchangers will occur in a predominantly aqueous environment such as exists in water circulating systems.

The size distribution of fully swollen particles in the two resin beds before and after heating is shown in Fig. 3.6. No significant damage was observed. Microscopic examination before and after heating revealed less than 0.1% broken fragments. These results show that no significant physical damage has occurred. The majority of the particles in the 2-3% and 7-9% crosslinked samples have a diameter of 0.070 ± 0.001 and 0.067 ± 0.001 cm. The close tolerance was achieved by careful grading of the particles as described in chapter 2.

Measurement of the cation exchanger capacity showed that no thermal decomposition occurred in the clean up beds.

3.3.2. Thermal decomposition in a flow system.

The rate of loss of strong base capacity compared with that in static heating experiments (see chapter 2) is shown in Fig. 3.7. As found by E.W. Baumann (ref.B1) no significant difference was observed. The important difference between the circulating system and static experiments was that in the former the pH was maintained close to 7.0, whereas in the latter the pH increased as a result of the accumulation of trimethylamine. Of the possible SN_1 and SN_2 reactions (ref.H7), only the latter

FIG 3.6

THERMAL DECOMPOSITION IN A FLOW SYSTEM

DEACIDITE FF - HYDROXIDE

20 - 30 mesh,

PARTICLE SIZE DISTRIBUTION BEFORE AND AFTER HEATING FOR 70 DAYS AT 90°C.

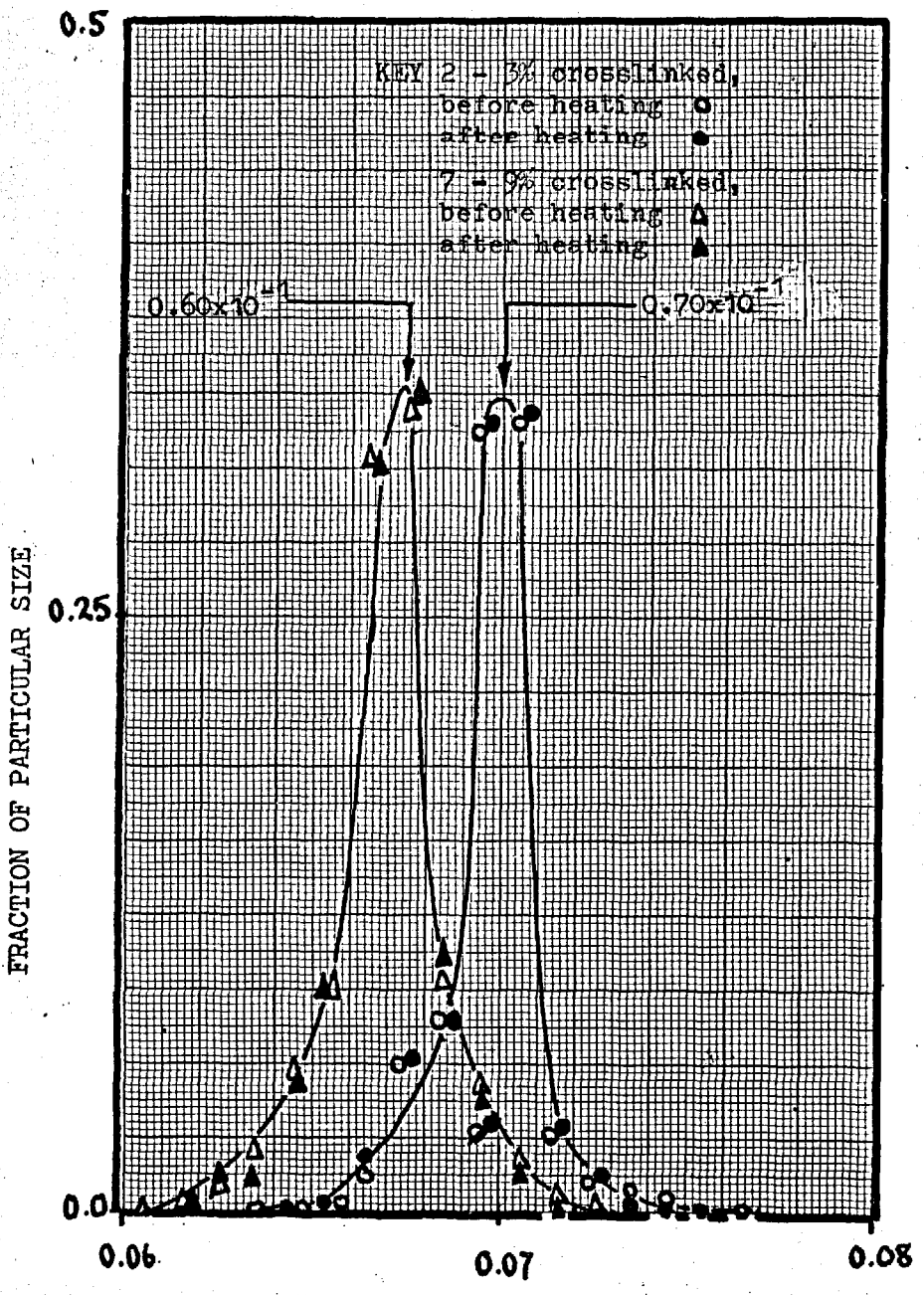

FIG 3.7 THERMAL DECOMPOSITION STRONG BASE CAPACITY CHANGES DEACIDITE FF - HYDROXIDE TEMPERATURE 90°C, COMPARISON OF STATIC AND FLOW EXPERIMENTS.

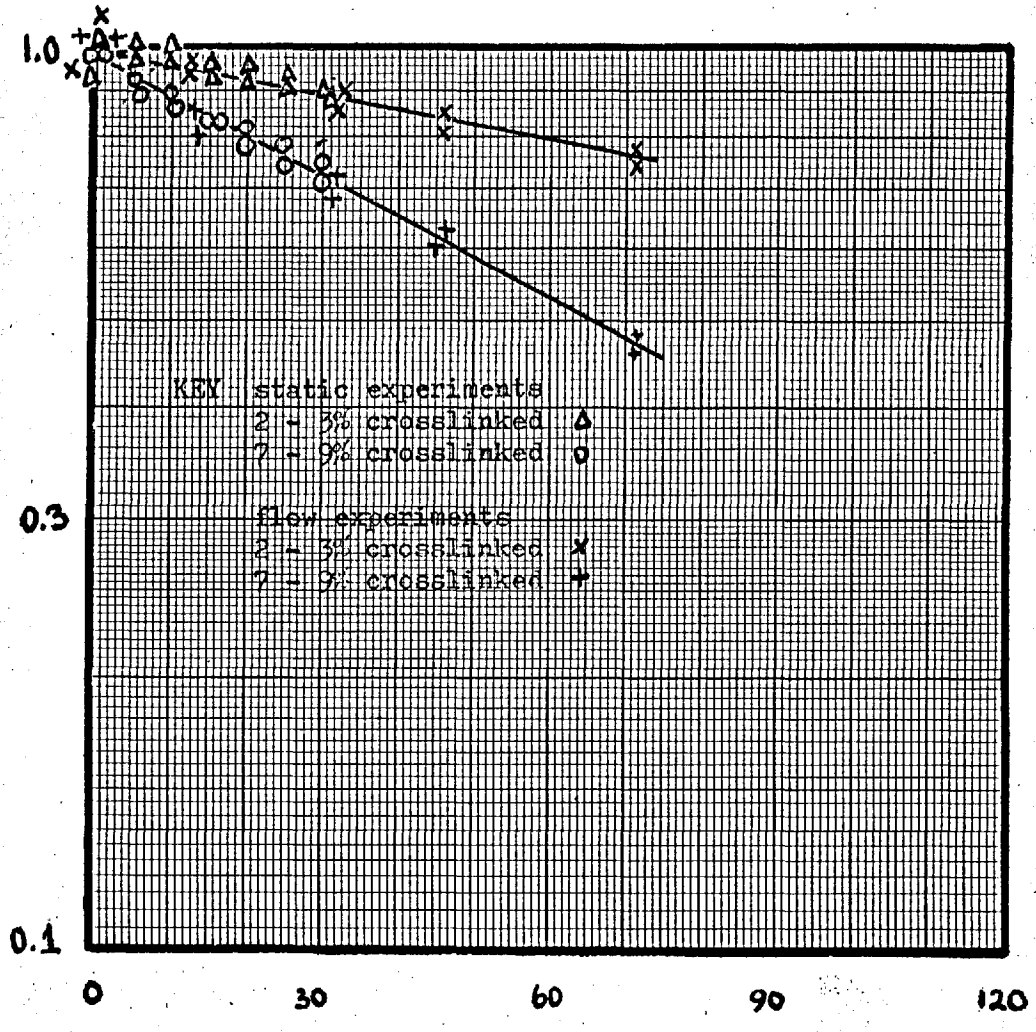

is pH dependent since the hydroxyl ion is one of the reactants. Hence an SN_2 reaction would occur more rapidly in the static experiments because of the resultant increase in basicity.

SN_1

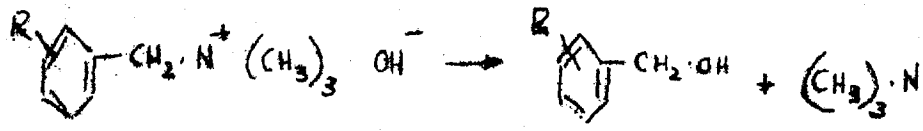

SN_2

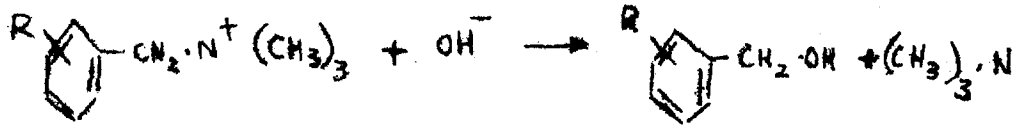

The methanol yield from the flow experiments is shown in Fig. 3.9. The 2-3% crosslinked resin is the more stable thermally. Changes in trimethylamine yields of the heated samples (Fig. 3.8) again show no difference between the static and flow experiments . This confirms the evidence of the strong base capacity results, that there is no difference in the rate of thermal decomposition in static and flow systems.

Two Canadian workers (ref.A3) observed that silica dissolved in water at 270°C. If silica also dissolves at 90°C it is probable that the dissolved silica would be sorbed by the anion exchange resin in the test bed. However, analysis of the heated samples from the test bed indicated that no more than 0.5% of sorbed silicate was present (Table 3.1). This means either that silica was not

FIG 3.8

THERMAL DECOMPOSITION AMINE YIELD

DEACIDITE FF - HYDROXIDE TEMPERATURE 90°C.

COMPARISON OF STATIC AND FLOW EXPERIMENTS.

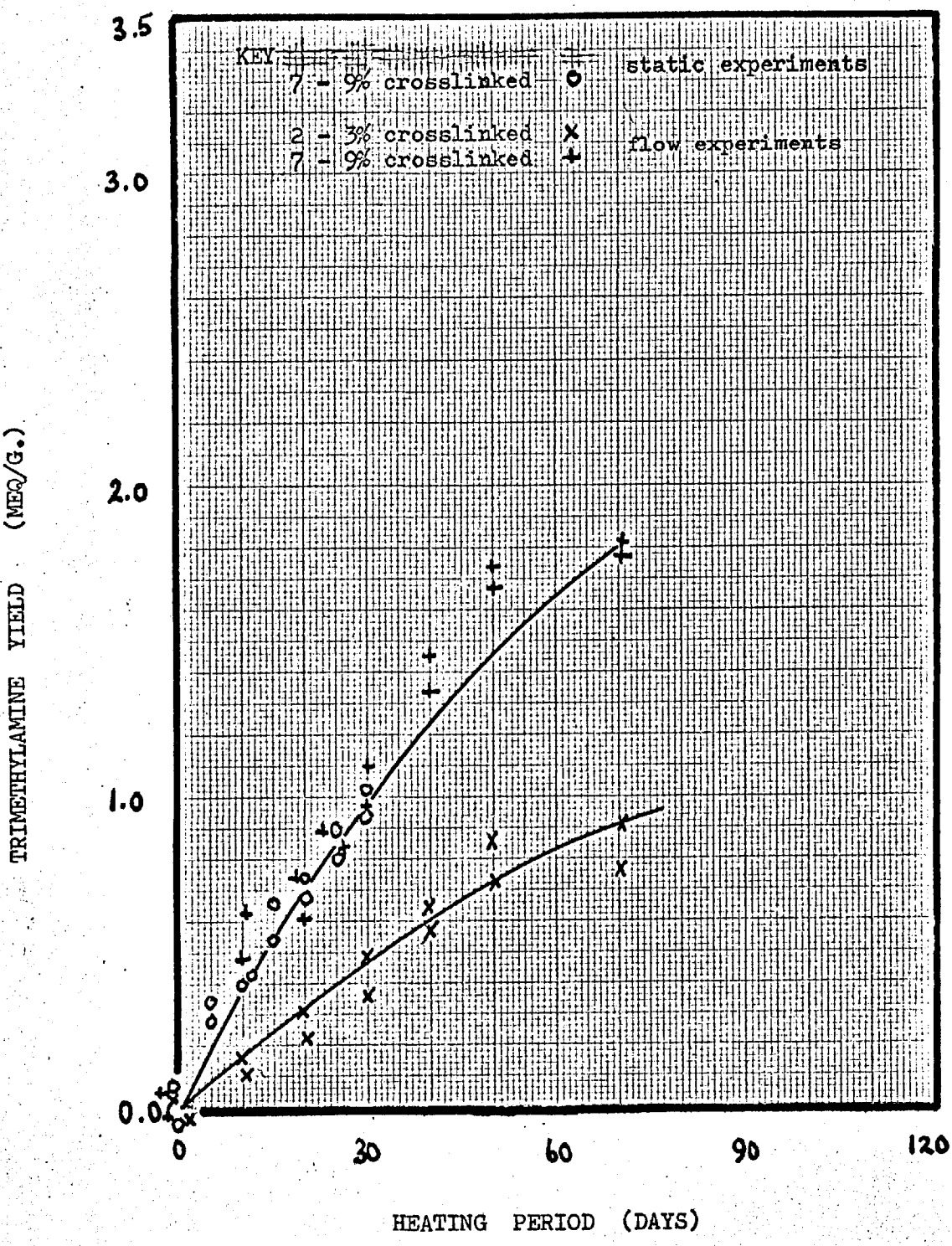

FIG 3.9

THERMAL DECOMPOSITION METHANOL YIELD

DEACIDITE - FF TEMPERATURE 90°C.

FLOW SYSTEM EXPERIMENTS.

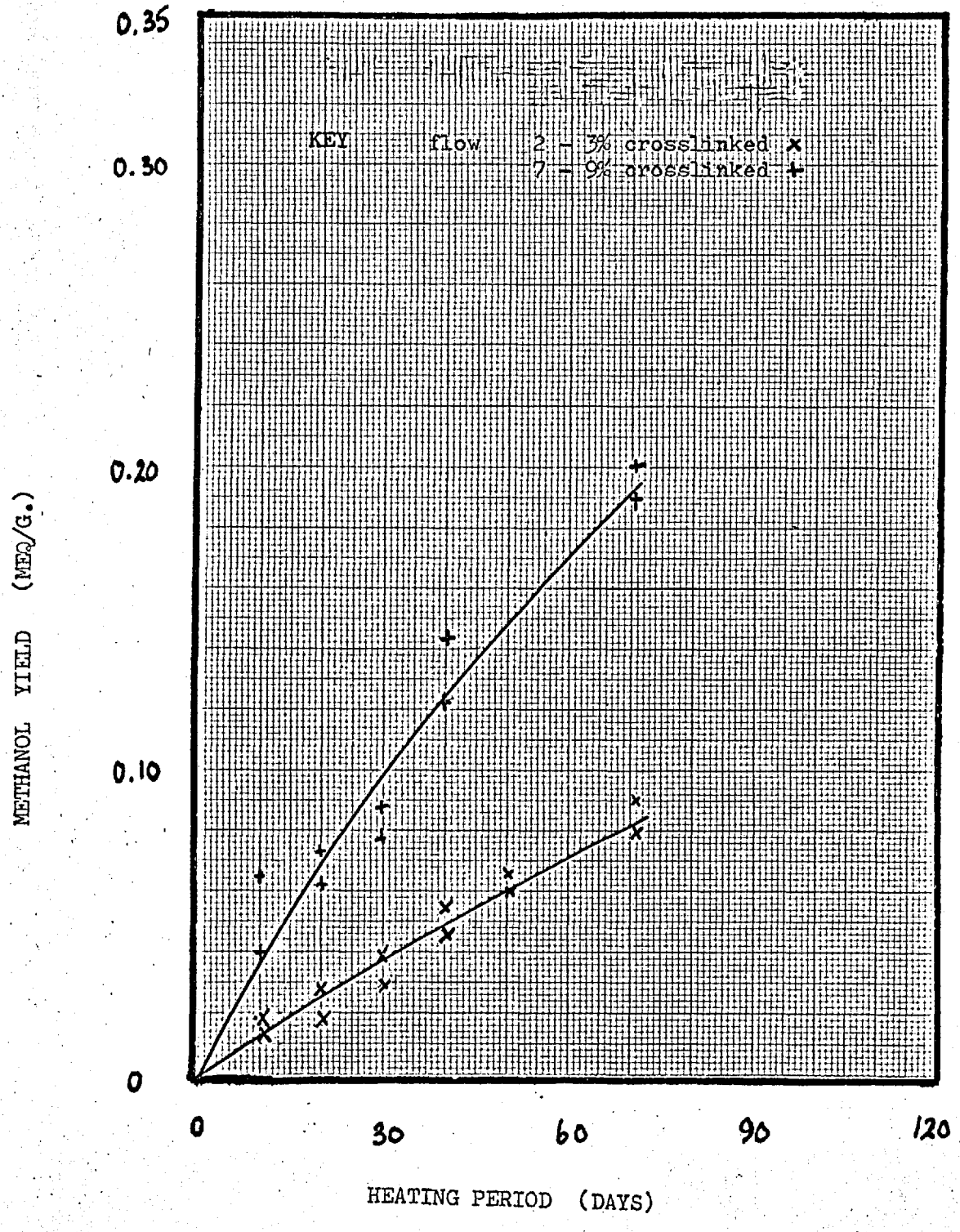

TABLE 3.1 THERMAL DECOMPOSITION IONIC COMPOSITION OF RESIN SAMPLES AFTER HEATING AT 90° C. DEACIDITE FF-HYDROXIDE. 20-30 MESH.

2-3 CROSSLINKING

TIME (DAYS)	0.0	13.5	32.0	45.0	71.0
CAPACITY (MEQ/G.)					
HYDROXIDE	4.00	3.76	3.60	3.40	3.11
CARBONATE	0.01	0.01	0	0	0.01
OTHERS	0	0	0.01	0.01	0.01
TOTAL	4.01	3.77	3.61	3.41	3.13

7-9 CROSSLINKING

TIME (DAYS)	0.0	13.5	32.0	45.0	71.0
CAPACITY (MEQ/G.)					
HYDROXIDE	3.99	3.20	2.72	1.97	1.82
CARBONATE	0.01	0.01	0.01	0.01	0.01
OTHERS	0.01	0	0	0.02	0.01
TOTAL	4.01	3.21	2.73	2.00	1.84

TABLE 3.2 THERMAL DECOMPOSITION FLOW SYSTEM DATA.
DEACIDITE FF-HYDROXIDE, 20-30 MESH,
TEMPERATURE 90° C.

2-3% CROSSLINKING

TIME (DAYS)	0.0	13.5	32.0	45.0	71.0
STRONG BASE*	1.00	0.94	0.90	0.85	0.78
CAPACITY	1.00	0.94	0.88	0.81	0.74
TRIMETHYLAMINE	0.00	0.20	0.55	0.67	0.76
(MEQ/G.)	0.00	0.21	0.36	0.51	0.91
METHANOL	0.00	0.02	0.04	0.06	0.08
(MEQ/G.)	0.00	0.01	0.03	0.05	0.09

7-9% CROSSLINKING

TIME (DAYS)	0.0	13.5	32.0	45.0	71.0
STRONG BASE*	1.00	0.80	0.68	0.50	0.46
CAPACITY	1.00	0.86	0.72	0.53	0.48
TRIMETHYLAMINE	0.00	0.51	0.98	1.65	1.79
(MEQ/G.)	0.00	0.70	1.13	1.74	1.81
METHANOL	0.00	0.05	0.08	1.14	0.19
(MEQ/G.)	0.00	0.07	0.09	1.16	0.20

* STRONG BASE CAPACITY IS EXPRESSED IN TERMS OF THE ORIGINAL STRONG BASE CAPACITY

leached from the glass in significant quantities or that silica was leached from the glass but that it was not sorbed by the anion exchange resin. Samples of loop water were analysed to decide between those possibilities, and no silica was detected. (Table. 3.2).

3.3.3 Pressure drop across the resin test beds.

Pressure drops per unit bed depth versus superficial velocity are plotted for various times after the beginning of the 70 days running period (Fig. 3.10 and 3.11). After the start of a run the pressure drop at a given superficial velocity increased for several hours, till a steady value was reached. At 13.5, 31, 45, and 71 days small samples of resin were removed from the bed by fluidisation. Immediately after this operation the pressure drop corresponded to the value at the beginning of the run. A steady rise to the original constant value independent of time then occurred. The change in pressure drop per unit bed depth with time at a superficial velocity of 0.016 ft./sec. is shown in Fig. 3.12. The basic pattern after the beginning of the run is repeated after each sampling time.

Several correlations between pressure drop and superficial velocity are currently accepted as accurate. The Carman Cozeny relation (ref.C7) was chosen instead of the more usually used Chilton Colburn plot (ref.C8) because the former allows the calculation of bed voidage, which was one of the aims of the experiment. In view of the narrow particle size distribution in the test beds, the necessary assumption of uniform particle size did

FIG 3.10

PRESSURE DROP VERSUS FLOW RATE IN A 6 in DIAMETER BED OF THERMALLY DEGRADED ION EXCHANGE RESIN. DEACIDITE FF , 2 - 3% crosslinked, 20 - 30 mesh, TEMPERATURE 90°C.

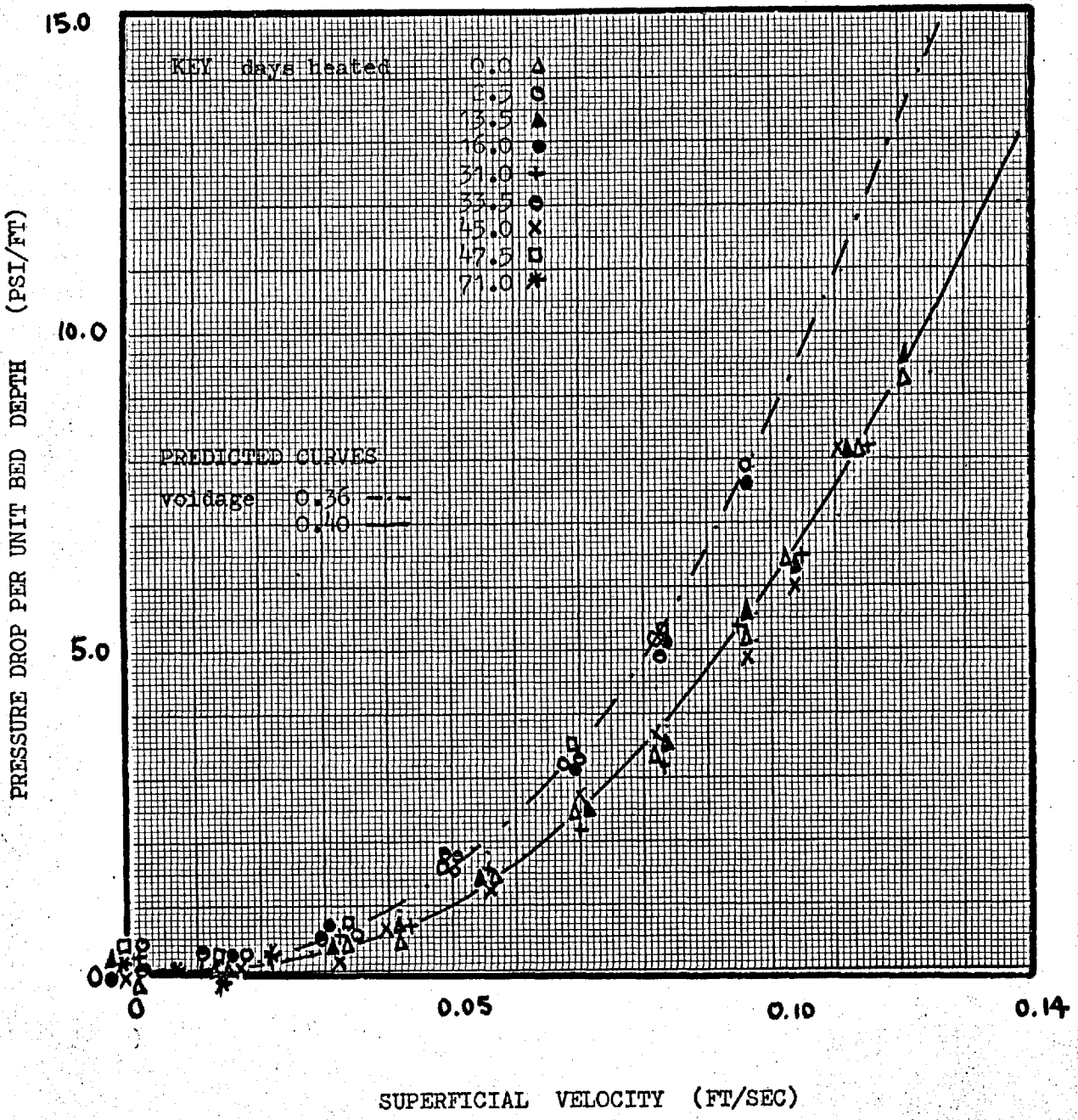

FIG 3.11 PRESSURE DROP VERSUS FLOW RATE IN A 6 in DIAMETER BED OF THERMALLY DEGRADED ION EXCHANGE RESIN. DEACIDITE FF, 7 - 9% crosslinked, 20 - 30 mesh, TEMPERATURE 90°C.

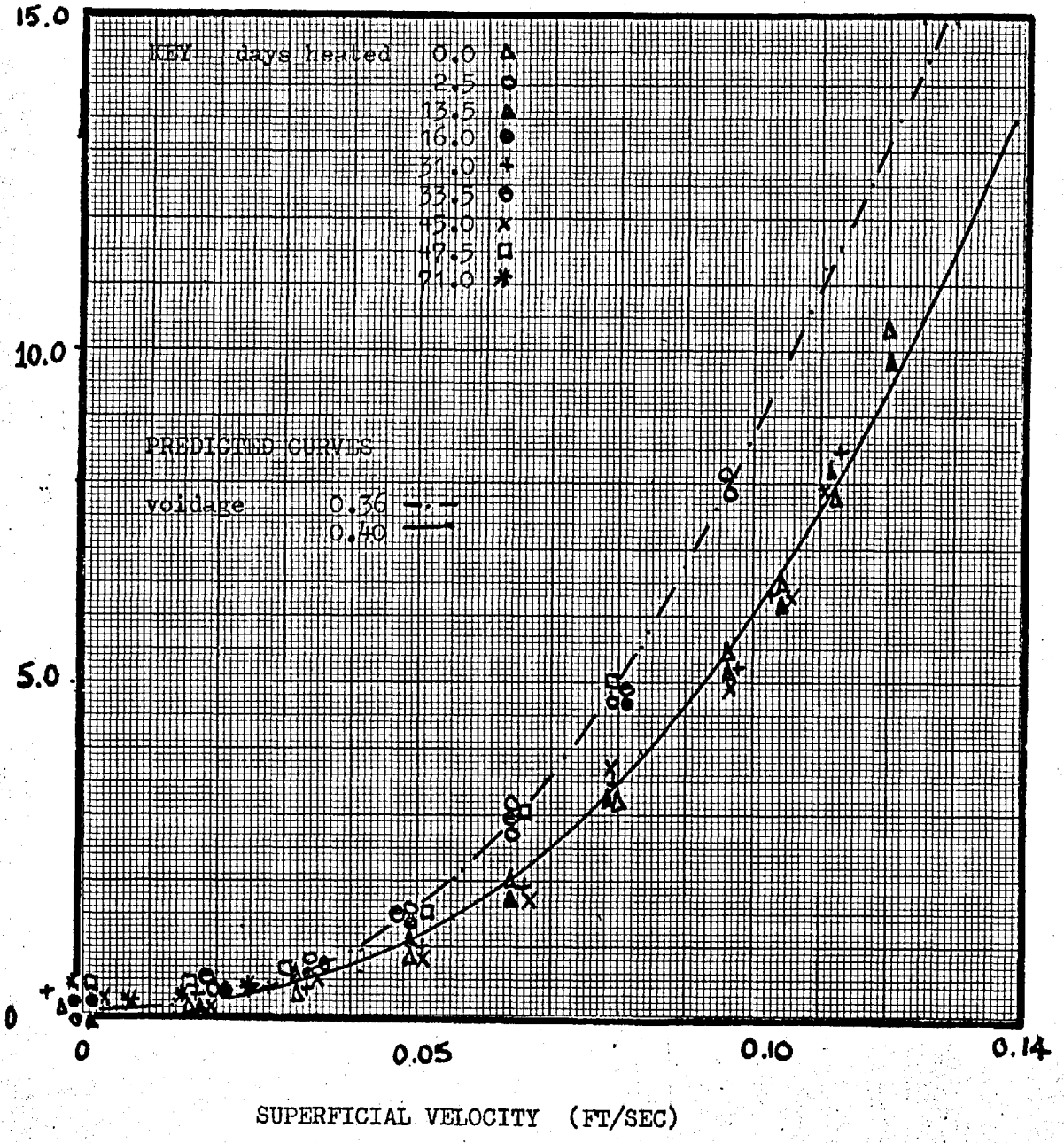

FIG 3.12 PRESSURE DROP VERSUS TIME IN A BED OF THERMALLY DEGRADED ION EXCHANGE RESIN.

DEACIDITE FF, 20 - 30 mesh, 7 - 9% crosslinked,

TEMPERATURE 90°C, BED DIAMETER 6 in.

SUPERFICIAL VELOCITY 0.016 ft/sec.

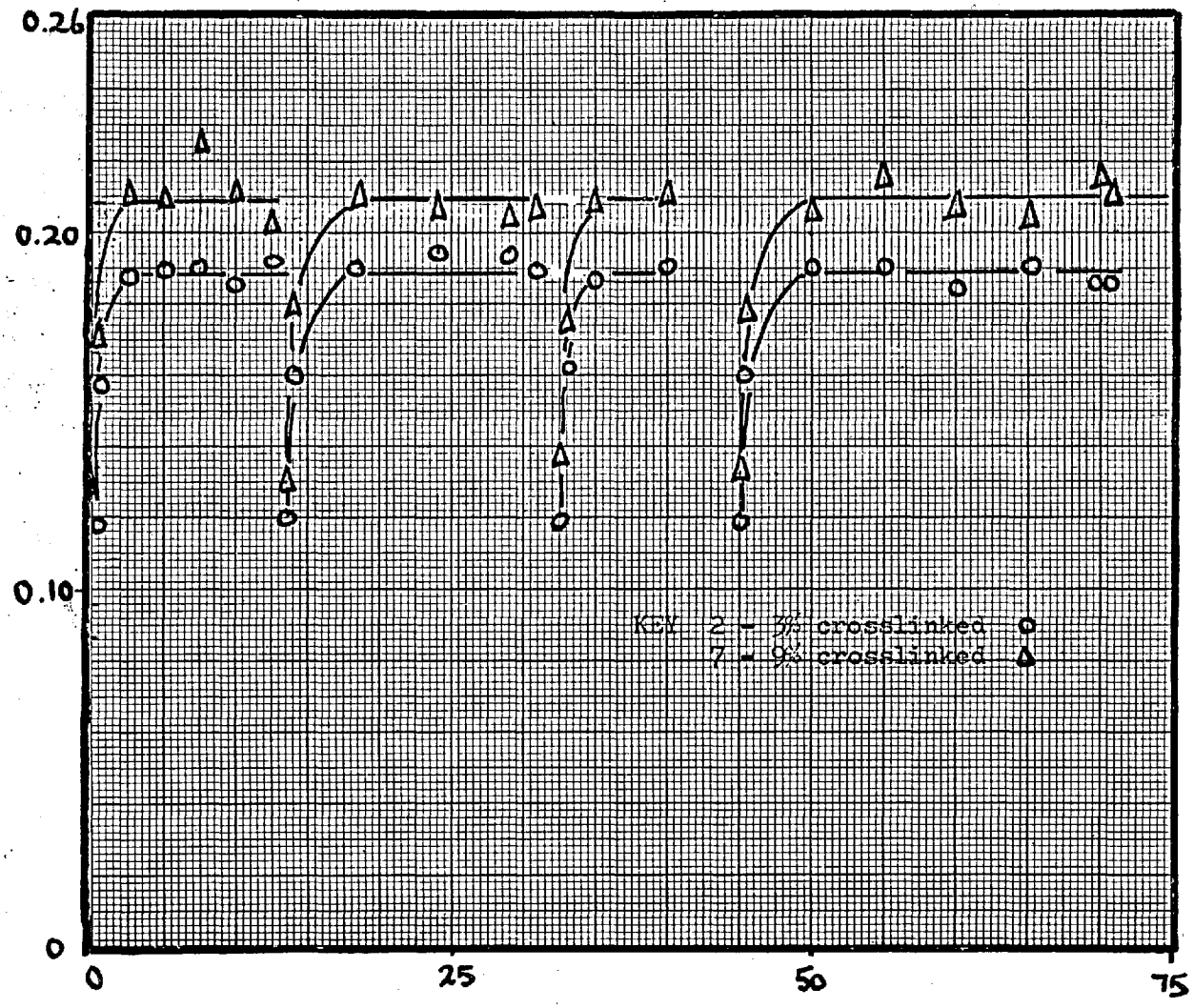

not result in important errors. This might not hold in beds with a wide particle size distribution although Demmitt's results (ref.D3) are encouraging.

The correlation was based on the mean diameters given in Section 3.3.1, and used to determine the bed voidage initially and after the steady pressure drop stage had been reached. This was accomplished by visually matching experimental curves and computed Carman Cozeny curves for several voidages. At the beginning of the run the voidage was approximately 0.40 in both beds. When the time independent pressure drop stage was reached the voidage was found to be approximately 0.36. The agreement between predicted and experimental curves was good. The decrease in bed voidage implies a bed compaction of 4% which agrees well with the measured 5% decrease in bed height.

3.4 Conclusions.

1. The rate of thermal decomposition is the same in static and flow systems. Thermal decomposition in anion exchangers occurs by SN_1 spontaneous decomposition reactions.

2. No physical damage occurs to the resin particles at temperatures up to 90°C and flow rates up to 100 g.p.m./sq.ft. over a 70 day running period .

3. Of the two significant decomposition products , methanol is not sorbed and trimethylamine is completely sorbed , with no clean up bed leakage at up to 46% capacity utilisation.

4. No silica was leached from the glass tubing at 90°C

during the 70 day running period.

5. Bed voidage decreased from an initial value of 0.40 to a steady state value of 0.36 after two days running so that a maximum of 4% bed compaction occurs.

Chapter 4

MASS TRANSFER STUDIES IN PACKED BEDS OF ANION EXCHANGE RESIN

4.1 Introduction.

4.1.1. General.

In this stage of the project the effects were investigated of temperature and solution concentration on the mass transfer performance of Deacidite FF at various stages of thermal decomposition. A theoretical model was assumed so that derived parameters of the resin could be calculated from the experimental results.

The kinetics of column processes are complex. Numerous theories have been published, some based on unrealistic assumptions and semi empirical approaches. Careful choice of one of these theories based on a sound understanding of the important factors can provide a good approximation of the operation of a given column and the most likely range of optimum operating conditions. Contrary to occasional claims, a general and quantitative theory of ion exchange column processes does not yet exist.

4.1.2 performance.

Consider a system comprising a column filled with uniformly sized ion exchange resin beads initially saturated with ion A. A solution containing ions B is

passed through the column at a constant flow rate. Ions A are transferred to the solution and ions B enter the resin until equilibrium is reached. The factors affecting the separation performance of the column are:-

a. Equilibrium.

The equilibrium between ions of equal valence in the particle and solution phases can be represented by a simple mass action equation, the use of which has been justified by Bauman and Eichorn (ref.B4) and (Boyd ref.B5). The

$$RA + B^- = RB + A^-$$

selectivity coefficient K is a measure of the equilibrium; K is defined as:-

$$K = \frac{[RB][A^-]}{[RA][B^-]}$$

K has also been called the equilibrium constant and separation factor, and varies with external solution concentration, temperature and ionic composition of the resin, in a given system (ref. K1,K2,W4,G1).

b. Stoichiometric capacity.

The exchange capacity of the resin in a column has an important effect on performance.

c. Rate behaviour.

The sequence of molecular scale processes involved in the exchange of an ion between the external solution and a resin particle can be grouped into four steps.

i. Fluid phase external diffusion (film diffusion).

Counter diffusion takes place of ion B from the bulk external solution to the surface of the particle, and

ion A from the surface into the bulk solution. The overall effect of fluid phase diffusion can be accounted for by a hypothetical film as in the Nernst concept (ref.B7).

ii. Phase change at the particle surface.

Ions A and B cross the particle surface. Spalding (ref. S5) has shown that provided this step is a purely physical process it occurs very rapidly.

iii. Solid phase internal diffusion (particle diffusion).

Counter diffusion of A and B occurs within the resin particle between the surface and the site of exchange .

iv. Chemical reaction of exchange.

The sorbed ion B reacts with the functional group, resulting in the release of ion A. This process follows a second order law, but in ion exchange not involving complexing reactions it is much more rapid than either of the diffusional steps.

In most ion exchange operations only the diffusional steps acting alone or together need be considered, when calculating the rate of ion exchange.

4.1.3. Theories of column performance.

The various theories of column performance can be divided into two main groups, the equilibrium theories and the rate theories.

a. Equilibrium theories.

These fall into two groups. In the discontinuous models the column is treated as a series of theoretical stages in which the solution attains equilibrium before entering the next stage. The effluent consists of a series

of finite solution packets each equal in volume to a theoretical stage. These packets undergo a series of equilibriations on their way through the column. Deviations from equilibrium are accounted for by a semi empirical stage height (ref.F2,M2,S2,S3). The disadvantages of these theories are their inability to predict stage height and the fact that the stage height is different for each species.

In the second group of theories local equilibrium is assumed in the column. These theories are inadequate for linear and favourable isotherms because the spreading effect of a finite exchange rate persists even after the boundary has travelled a considerable distance. Good approximation is attained for the case of unfavourable equilibrium (ref.C3,D2,W2,W3).

The only advantage of the equilibrium theories is their much greater simplicity. However, in the present work they are clearly inadequate.

b. Rate theories.

These are based on continuous flow through the column with a finite exchange rate and give a more realistic approach to the problem. The mathematics of these rate theories is difficult, but they allow the prediction of column performance from fundamental data without the use of empirical quantities. The various theories differ in their simplifying assumptions about rate processes and equilibria. A general survey of theories of column performance based on rate processes is given by

Vermeulen (ref.V1). From the point of view of this work, only certain general theories are of interest, and discussion of published work is restricted to these alone.

Furnas (ref.B3) adapted his heat transfer solution (ref.F3) to ion exchange, with a linear equilibrium (K=1). The result is more general than previous theories. Rosen (ref.R2) derived a model for the linear equilibrium case based on diffusional processes. This model accounts for ion exchange where both film and particle diffusion are important.

Thomas (ref.T1) assumed the rate of ion exchange to follow a second order reaction with a constant selectivity coefficient (K=constant) and derived the most general result to date. The main short-coming of Thomas's solution is that ion exchange does not follow a second order reaction.

The region in which both film and particle diffusion are important has not been satisfactorily analysed for anion exchange with a constant selectivity coefficient. The compounding of the individual rates into the overall rate is very difficult because of the discontinuity in the concentration profile at the interface between particle and solution. All attempts to date involve simplifying assumptions that restrict validity to varying degrees. Gilliland and Baddour (ref.G2) and others (ref.S4) equated the second order rate constant defined by Thomas with an overall mass transfer resistance. This resistance was calculated from the individual resistances to diffusion in the film and particle by an equation

valid only for linear equilibrium. Hiester et al. (ref.H5) introduced a correction term based upon local conditions at the interface which enabled them to extend Gilliland and Baddour's treatment to the case of a constant selectivity coefficient. The correction term can be evaluated if $0.4 < K < 7$, where it is insensitive to changes in local bed conditions; outside this range only a very approximate value can be obtained since the interfacial conditions are unknown. Rosen's model (ref.R2) accounts for the interfacial concentration by the use of an integrodifferential boundary condition. His differential equations can only be solved by numerical integration, requiring several hours time on high speed electronic computers.

Other rate theories have been proposed with first or second order reversible and irreversible reactions. Rosen's work has recently been extended to isotherms of the Freundlich type (ref.T2) . Electronic computers were used to tackle the lengthy complications involved. The most rigorous approaches to date consider ion exchange in terms of diffusional steps.

The majority of these rate models are designed to enable the prediction of column performance over a wide range of conditions from a few experimental measurements and as such have considerable value. However, mass transfer and diffusion coefficients used in such models are necessarily defined by the assumptions in the k model and do not necessarily coincide with conventionally

accepted meanings of these parameters, and hence cannot be expected to agree with independently determined values.

Since one of the aims of this work was to determine conventional diffusion coefficients from column experiments, the formulation of an improved model was attempted (see Appendix 3).

4.2 Experimental.

4.2.1. Scope of work.

The aims of the work described in this chapter were :-

a. To investigate a case of favourable and a case of unfavourable ion exchange in the region where particle and film diffusion are significant, in order to calculate the diffusional parameters in the particle and solution phases and to study to effect of changes in temperature, solution concentration and thermal degradation on the diffusion parameter.

b. To formulate an improved model of ion exchange in a column , if possible.

4.2.2. Design of experiments.

Ion exchange measurements may be carried out either in column or batch experiments. In a batch experiment, the progress of exchange is followed by removing samples of the resin at regular intervals, for subsequent analysis. The analytical proceedure is time consuming and restricts the number of expriments which can be carried out in a given time. At temperatures in excess of $60^{o}C$ exchange occurs very rapidly and it is impossible to remove sufficient samples to follow the process accurately.

The concentration of ions in the effluent from a column experiment can be monitored and recorded with good accuracy. A large body of data can be rapidly accumulated giving added confidence to the final result. Rapid exchange at elevated temperatures can be followed with a responsive system. Finally, most practical ion exchange operations are carried out in columns. These considerations led to the choice of a column system in preference to a batch system.

Hydroxide-chloride exchange with Deacidite FF resin was chosen for several reasons. Firstly, thermal decomposition of Deacidite FF in these forms has been thoroughly investigated (see chapter 2). Secondly, the hydroxide-chloride cycle is of interest in practical ion exchange operations at elevated temperature, such as coolant circuit clean up. Thirdly, the effluent concentration change may be followed by pH measurement. Fourthly, Deacidite FF shows a marked preference for chloride ions , giving favourable exchange in one direction and unfavourable exchange in the reverse direction.

Experimental apparatus was designed to reduce unwanted impurities to a minimum. The apparatus (Fig. 4.1) was constructed of glass and plastic with the exception of the feed pump. This was a DCL "M" plunger head type pump with a pumping head constructed of Hastelloy "B" to prevent corrosion by hydrochloric acid used in the experimental work (ref. C4).

Deacidite FF was used with a particle size range between 20 and 30 BSS mesh size (see Fig. 3.6.).

FIG 4.1

APPARATUS FOR THE MEASUREMENT OF BREAKTHROUGH CURVES.

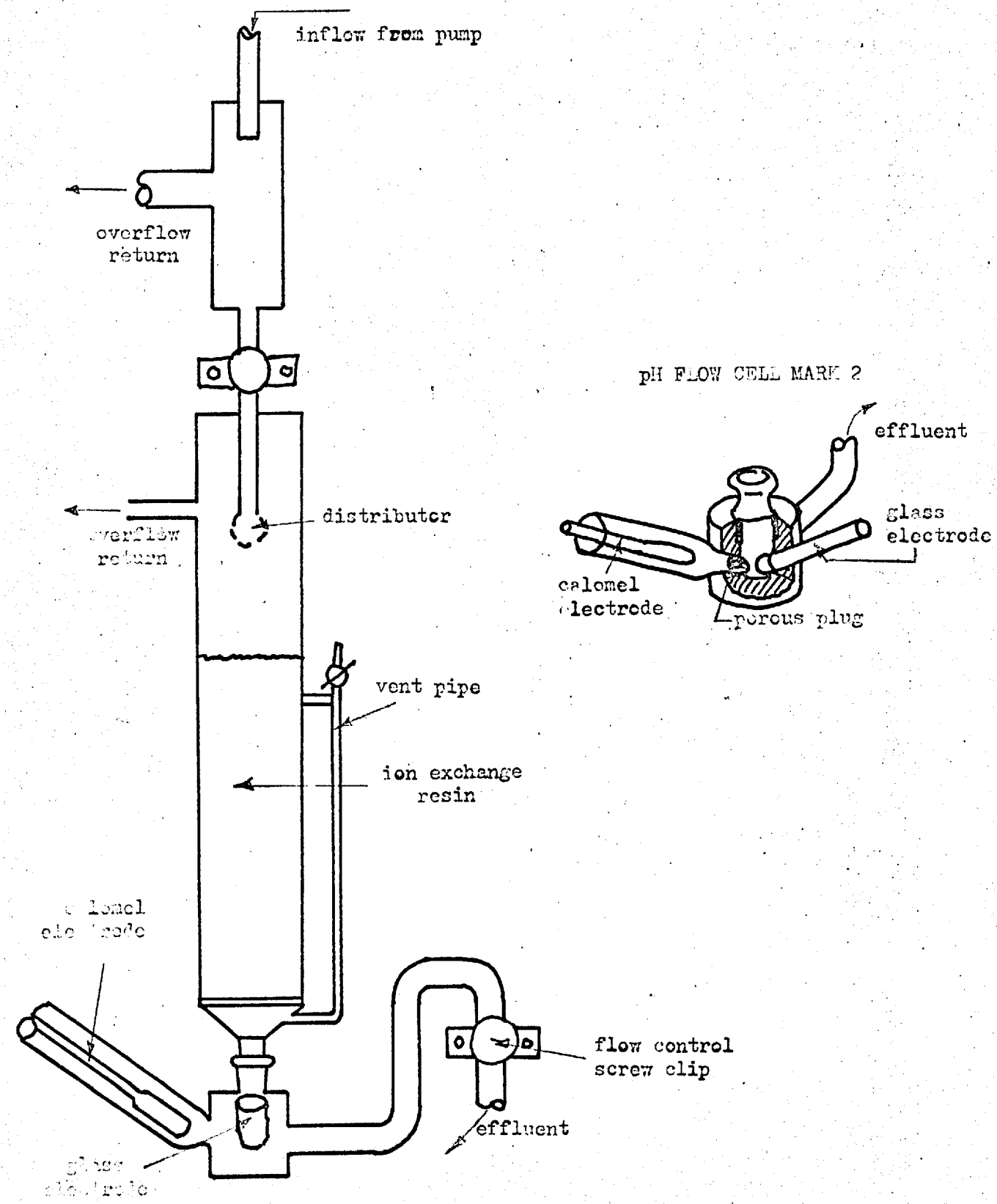

pH FLOW CELL MARK 2

This was chosen as a good compromise between practical resins (14-52 mesh) and applicability of the results to a model based on uniform particles. Measurements were made on samples of 2-3% and 7-9% crosslinked Deacidite FF.

The solution concentration range was between 0.01 and 0.1 molar. This is the region where both solution and particle diffusion are important rate controlling factors, and includes the region of greatest practical importance in chemical processing. The probable maximum operating temperature of anion exchange resins in the hydroxide form is 90°C. Experiments were therefore carried out at room temperature and at 50°C and at 90°C.

In a binary ionic system with a fixed bed of ion exchange resin , the rate of exchange varies with the solution flow rate, when film diffusion is significant. A typical case, sodium hydrogen exchange on Dowex 50 is shown in figure 4.2 (ref.G2). At high flow rates, particle diffusion contributes the major resistance, with film diffusion resistance attaining greater importance as the flow rate is decreased. The diffusion regions are shown in Fig. 4.2. Vermeulen (ref. V1) recommends an empirical correlation due to Wilke and Hougen (ref.W7) for the calculation of film transfer resistance. The range of flow rates applicable to this work was determined by using this correlation.

Economy of time and materials prescribes a fixed bed system of minimum size. A small system allows rapid approach to equilibrium at a given flow rate and is easier

FIG 4.2

TYPICAL FLOW DEPENDENCE OF THE FILM AND OVERALL MASS TRANSFER RESISTANCES

DOWEX 50-H^+, Na^+-H^+ exchange.

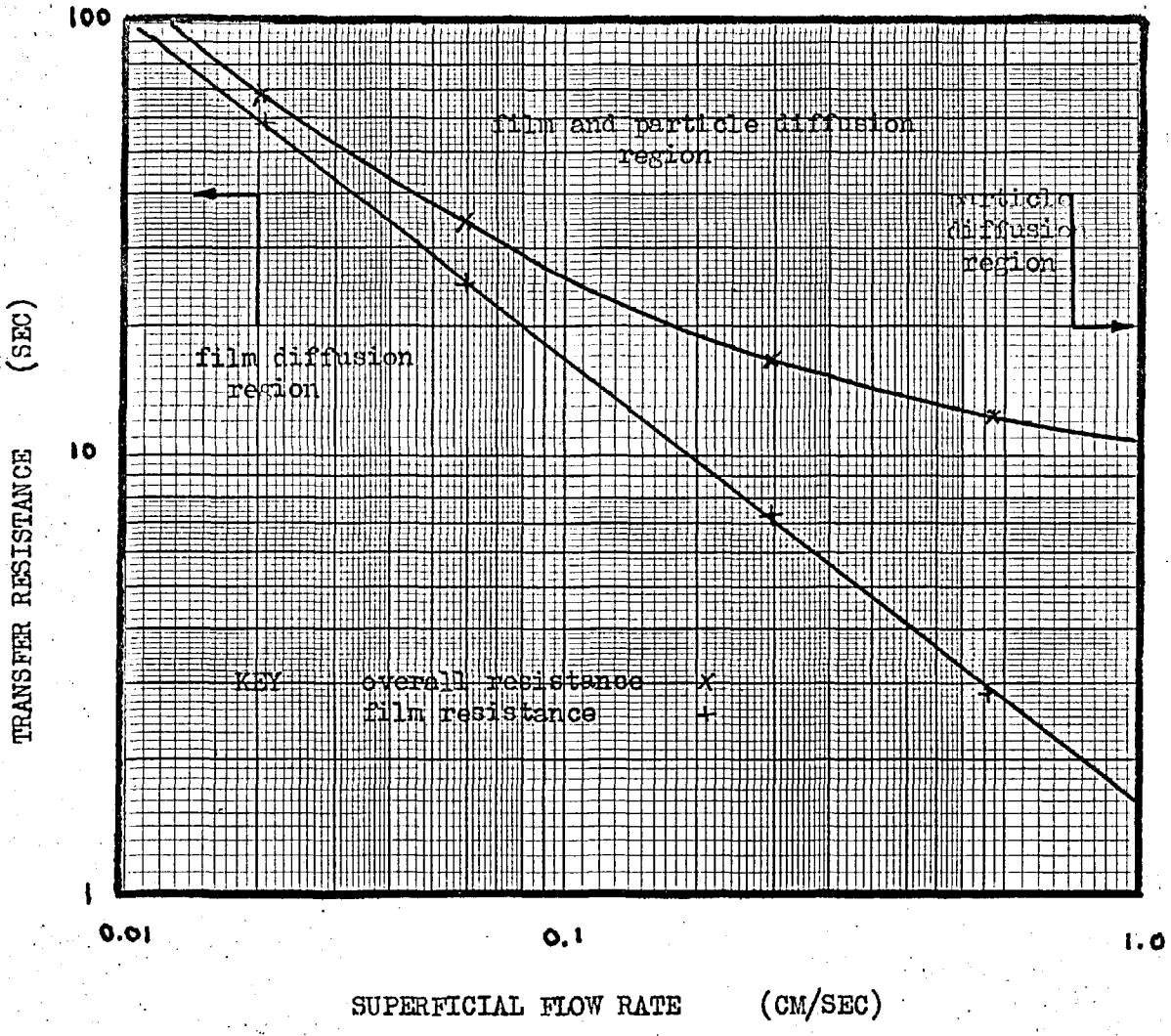

from GILLILAND and BADDOUR (ref.G2).

to maintain at a uniform temperature. The dimensions of the fixed bed must be large enough to avoid significant wall and entry effects. The minimum column diameter is given by Boyd (ref.B11) as greater than 20 particle diameters. No effect of column height was observed by Gilliland and Baddour as long as the minimum height diameter ratio was greater than 6. Therefore the bed dimensions were fixed at 1.5cm.diameter and about 12cm. height.

The effluent concentration from the column was monitored continuously by a pH flow cell, which was carefully designed to avoid mixing and turbulence .

4.2.3. Experimental method.

a) Measurement of effluent concentration histories.

Resin samples were prepared and stored as described in Section 2.2.1 and soaked in deionised water (CO_2 free) for 24 hours prior to use. Solutions of sodium hydroxide and hydrochloric acid were stirred thoroughly before use to ensure even concentration.

At the beginning of each day's experimental work the following procedure was carried out. The pH meter and recorder were switched on one hour before work was due to begin. Simultaneously , the pH cell was filled with a buffer solution (pH 4), the solution temperature noted and the meter controls adjusted until a reading of pH 4 was obtained. Half an hour later the meter was readjusted if necessary. The pH cell was then filled with deionised water and the column loaded with approximately 12cm. height

of resin. The column and pH cell were assembled and allowed to stand for one minute so that the resin might reach a settled state, after which the bed height was noted, meanwhile the pump controls and scew clips were adjusted to give the desired flow rate and the pump and recorder were started. The recorder scale was adjusted to include the expected concentration change. Finally the column outlet valve was opened to allow flow through the resin bed and the zero time marker on the recorder actuated at the same time. The flow rate of the solution through the column was measured by collecting solution for one minute. Three successive measurements were taken to check the constancy of flow. The experiment was continued till the influent and effluent concentration were equal. The temperature of the effluent was observed during the experiment. Experiments were repeated at several solution flow rates, temperatures and concentrations. Both forward and reverse exchange were examined and resin samples of 2-3% and 7-9% crosslinking were used.

Sources of error and precautions taken against them were as follows:-

i) Temparature constancy.

The pH meter was used on an expanded scale of two theoretical pH units and temperature constancy of $\pm$ 0.05°C was necessary to avoid errors in pH measurement. Where experiments were carried out at elevated temperature, the exchange column was lagged and heated to the required temperature by pumping deionised water through it,

before beginning the experiment. Temperature constancy in all work was maintained to the above limits.

ii) Distortion of the pH scale in high concentration region.

At pH values greater than 11.0 and less than 3.0 it was found that the observed pH equation deviated from the theoretical pH-concentration relation. The following empirical relations were found to hold:-

pH 11.0

$$pH = 12.425 - 0.475 \log_{10}(\text{concentration})$$

pH 3.0

$$pH = 0.30 - 0.67 \log_{10} (\text{concentration})$$

iii) Distortion of the effluent concentration history curves by turbulence and mixing in the pH cell, and axial dispersion in the column.

In experiments of this kind it is vital that the effluent concentration history curves should be caused only by ion exchange. Unless distortion of the curves by hydrodynamic effects such as axial dispersion in the resin column or mixing in the pH cell are eliminated, the results are meaningless.

The pH flow cell and resin column were tested by pumping a solution of hydrochloric acid through a bed of chloride form resin at the maximum and minimum flow rates to be used in the work. The resulting curves are shown in Fig. 4.3. Distortion of the input step is shown to be negligible.

FIG 4.3

TESTING OF MARK 2 pH FLOW CELL
FLOW RATE 3.5×10^{-4} litre/sec, 0.1 N HCl.

a) Column filled with Chloride form Deacidite FF, 20-30 mesh, 7-9% crosslinked.

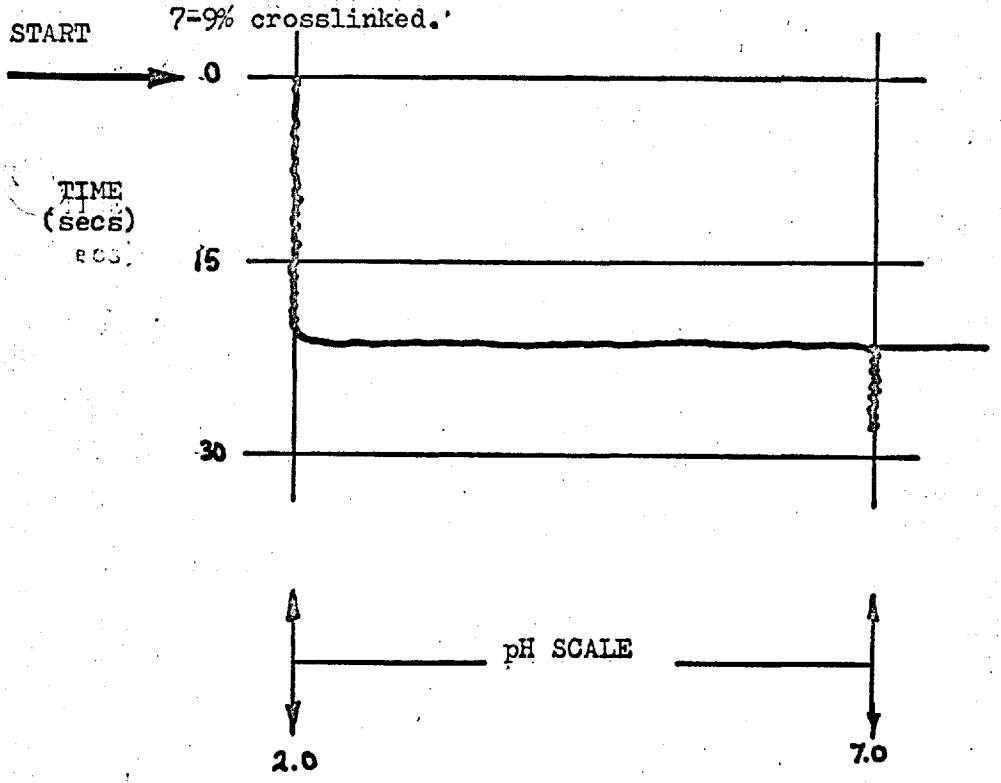

b) Empty column:

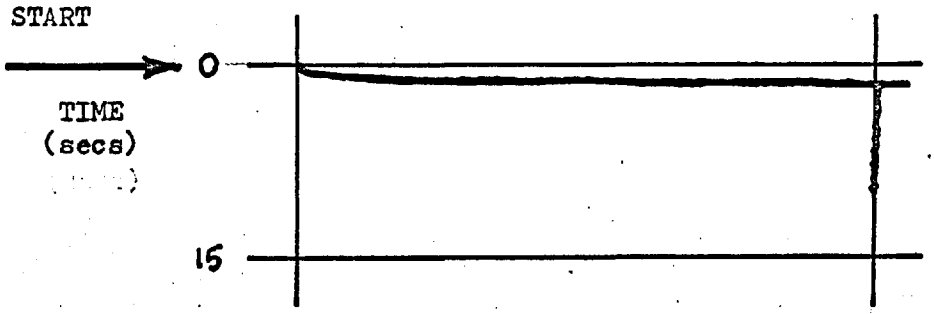

iV) Meter and recorder response.

A full scale deflection occurred in less than 0.5 sec., compared with at least 1 min. for the most rapid effluent concentration change.

v) Flow rate constancy.

The instantaneous output of the DCL pump varied with time, and a system of tanks (Fig. 4.4) was used to smooth the pulsations before solution was passed to the column. Flow through the column could be varied by adjustment of a screw clip on the effluent line. Excess liquid delivered by the pump was returned to supply via overflow pipes.

b) Determination of selectivity coefficient.

Experimental values of the selectivity coefficient for forward and reverse exchange in the hydroxide and chloride system were determined as follows: 100 g. batches of resin in the hydroxide and chloride form, prepared as described in chapter 2 were soaked in demineralised water for 24 hours prior to use. The capacity of a sample of each batch was measured as described previously. Approximately 100 g. of resin was added to 25 ml. standard solution in a clean conical flask, tightly stoppered and left for 24 hours in a constant temperature bath, after which the solution was drained off and replaced by a further 25 ml. of standard solution. This procedure was repeated four times after which equilibrium was attained and the solution concentration remained unchanged. The resin and solution were separated by centrifuging (ref.P2) for 30 minutes, which sufficed to remove adherent liquid films from the

FIG 4.4

SYSTEM OF SMOOTHING AND OTHER TANKS USED IN THE BREAKTHROUGH CURVE MEASUREMENTS.

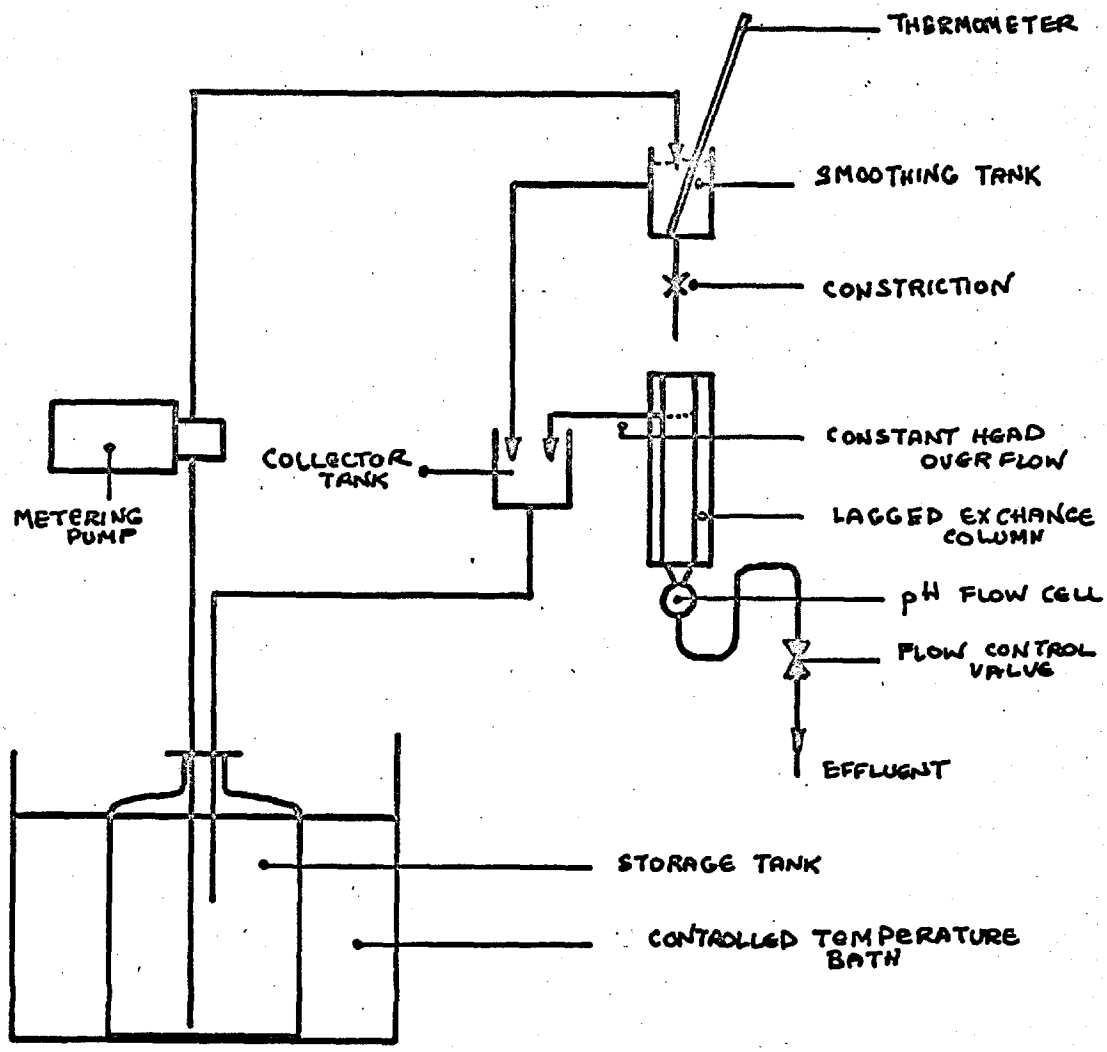

resin particles. The resin selectivity coefficients were calculated from equation 4.1,

$$ROH + Cl^- \rightleftharpoons RCL + OH^-$$

$$q_A \quad C_B \qquad q_B \quad C_A$$

$$K = \frac{(q_B/Q)/(C_B/C_0)}{(1-q_B/Q)/(1-C_B/C_0)} \qquad ---4.1$$

which gives K in terms of one ion and the total solution concentration C_0

Measurements were made at external solution concentrations of 0.01, 0.05 and 0.1 N, temperatures of 18, 50 and 90°C and 2-3% and 7-9% resin crosslinking; each equilibration was repeated three times.

Chloride resin samples were equilibrated with sodium hydroxide solution and hydroxide samples with hydrochloric acid solution.

The effect of ionic composition of the resin on the selectivity coefficient was investigated by equilibrating resin samples with mixtures of sodium chloride and sodium hydroxide solution. Two samples, one initially saturated with hydroxide ions and one saturated with chloride ions were equilibriated in each case.

Sources of error and precautions taken to avoid them were as follows:-

i) Disturbance of equilibrium during separation.

Equilibriation is a relatively rapid process (30 mins. required for strong acid and base resins of less than 10% DVB crosslinking), and therefore small traces of solution can cause considerable error (ref. F5), with high capacity and dilute solutions. Care was taken to

separate resin and solution rapidly. In practice most of the liquid was removed from the solid in less than 15 secs. after removal from the constant temperature bath.

ii) Disturbance of equilibrium by cooling before separation.

At elevated temperature, the container in which the resin and solution was separated was immersed in the constant temperature bath before use. This meant that most of the liquid had been separated from the solid before a significant temperature drop had occurred. Since the standard enthalpy of ion exchange is of the order of 2 kcal/mole., small changes in temperature do not cause significant changes in equilibrium between resin and solution.

iii) Changes in capacity caused by equilibration at elevated temperature.

The total time of heating was 96 hours. At the maximum temperature investigated the loss in capacity during this period of heating was small. Where thermal damage was likely to occur, the capacity of the sample was determined before and after equilibration and an average of the initial and final values taken.

iv) Contamination by glassware.

Soda glass is reported to exhibit ion exchange properties, therefore pyrex glass was used in all experimental glass ware.

4.3 Assessment of results.

4.3.1. General.

Since the attempted model development was not accomplished, a suitable published model was selected for the assessment of experimental results. The model was that of Gilliland and Baddour (ref.G2) as modified by Hiester and Vermeulen (ref. H5).

4.3.2. Gilliland and Baddour's model.

A short resume of the mathematical development is given here and the sources of error are indicated in more detail. The basic assumptions in the model are:-

i. The rate of exchange in a given resin ion system follows a second order reaction with a velocity constant dependent on particle size, solution flow rate and diffusional parameters. In fact ion exchange does not obey a second order rate law in most cases, so the velocity constant varies with time during exchange and is a rate parameter defined by the model, for use only with the model.

ii. The velocity constant may be equated to the combined film and particle mass transfer coefficients, based on diffusional mechanisms.

The rate in each individual phase is given by:-

$$\text{Rate} = kA(C-C_i) \qquad \text{--- 4.2}$$

where k is a general mass transfer coefficient per unit interfacial area. Equation 4.2 assumes a constant linear concentration gradient, which is accurate for film diffusion but unrealistic for particle diffusion. In Gilliland and Baddour's model the velocity constant is related to the individual transfer coefficients by

equation 4.3:-

$$\frac{1}{k_{kin}} = \frac{Q}{k_L} + \frac{C_o}{Kk_p} \qquad \text{--- 4.3}$$

equation 4.3 is only mathematically true when K equals unity. Hiester and Vermeulen (ref.H5) have modified equation 4.3 so that it holds more closely for all values of K, by the inclusion of a correction term b. The modified equation is:-

$$\frac{b\epsilon}{k_{kin}Q(1-\epsilon)} = \frac{1}{k_L A} + \frac{1}{k_p A D} \qquad \text{--- 4.4}$$

The correction term is related to a mechanism parameter as shown in Fig. 4.5. The mechanism parameter can be calculated from a knowledge of the interfacial concentration or the diffusion coefficients of the system. In practice b is not constant since the interfacial concentration varies with time as exchange proceeds.

iii. Equilibrium at the particle solution interface is assumed to be described by a selectivity coefficient K. The equilibrium in the system is :-

$$K = \frac{[RA][B^-]}{[RB][A^-]} \qquad \text{--- 4.5}$$

where R represents the resin matrix, and K is assumed independent of the ionic composition of the resin which is not strictly accurate.

The rate of exchange based on these assumptions is:-

$$\frac{dq_A}{dt} = k_{kin}\left[C_A(Q-q_A) - \frac{q_A}{K}(C_o - C_A)\right] \qquad \text{--- 4.6}$$

The use of equation 4.3 to relate the velocity constant and the individual coefficients can give values of the latter an order too low or high if Kidiffers greatly from unity.

In evaluating diffusion coefficients from experimental data the value of the correction factor b cannot be calculated, since neither the diffusion coefficients nor the interfacial concentrations are known. For the case of favourable exchange K lies between 5 and 15 and b is fortunately substantially independent of the mechanism parameter, and has a value of 1.8. In the unfavourable direction of exchange where K lies between 0.2 and 0.1, b varies considerably during exchange and the best compromise is to assume an average value of 0.35.

Combining equation 4.6 with the continuity equation for a column* and making use of Thomas's result (ref.T1) gives equation 4.7, which describes the effluent concentration history from a column:-

$$C_A/C_o = 1/\left[1 + G \exp\left[(K-1)\ (Kw-u)/K\right]\right] \qquad \text{--- 4.7}$$

where $u = k_{kin}C_o\theta$; $w = k_{kin}\bar{x}/Kv$;

It has been shown by past work that the mid point slope of the effluent concentration history curve can be used as a measure of the whole curve for the purposes of calculating transfer and diffussion coefficients (ref.T1,G2).

* see Appendix 3.

The mid point slope of the effluent concentration history curve is the gradient of the curve at the point where the effluent concentration has attained half the value of the influent concentration. Differentiating equation 4.7 with respect to θ gives the mid point slope in terms of time:-

$$\frac{1}{R}\frac{\partial(C_A/C_0)}{\partial\theta} = \frac{\bar{k}C_0}{4v} + \sigma \qquad \text{--- 4.8a}$$

where $\theta = t - x/v$ and is time measured from the instant when the solution front reaches a cross section x units from the column entry, and $\bar{k} = k_{kin}(K-1)/K$. Written in terms of, y, the volume of effluent collected, equation 4.8a becomes 4.8b:-

$$\frac{(C_A/C_0)}{\partial y} = \frac{(K-1)}{K}\frac{k_{kin}C_0}{4v} + \sigma \qquad \text{--- 4.8b}$$

where σ is a function of k_{kin}.

While this treatment is not strictly rigorous, the introduction of Hiester's correction term yields diffusion coefficients of the right order in both liquid and particle phase.

4.3.3. Calculation of the diffusion coefficients.

It is not possible to obtain an explicit relation for the diffusion coefficients in terms of the effluent concentration histories, so the former must be calculated by a controlled trial and error process. This computation can be substantially reduced by assuming that the concentration histories are fully characterised by their mid point slopes, so that equation 4.8b may be used for calculations. This assumption should be checked by

FIG 4.5

CORRECTION FACTOR FOR THE COMBINATION OF INDIVIDUAL TRANSFER RESISTANCES INTO THE OVERALL RESISTANCE.

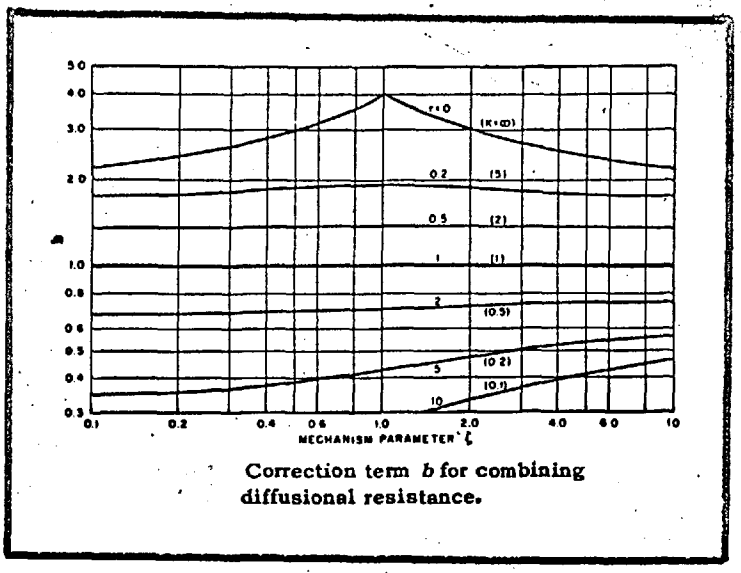

Correction term *b* for combining diffusional resistance.

from HIESTER et al. (ref.H5)

comparing experimental concentration history curves with model curves when the derived diffusion coefficients are substituted. In most cases good agreement will be found.

The mid point slope and the volume of effluent collected at the time at which the mid point slope occurred were estimated from each concentration time curve, obtained from the recorder. Equation 4.8b was then used to evaluate the velocity constant of exchange. The trial and error process was accomplished as follows. A value of k_{kin} was assumed and the mid point slope for that value calculated and compared with the observed mid point slope. The assumed value of k_{kin} was then corrected in equal steps of $k_{kin}/10$ until the difference between the observed and calculated mid point slopes passed the minimum and began to increase. The direction of change in k_{kin} was reversed and the step magnitude changed to $k_{kin}/100$ until the minimum was again passed. Finally, a third traverse was carried out with steps of $k_{kin}/1000$. This procedure was programmed for a computer and gave an accurate value of k_{kin} corresponding to the observed mid point slope.

A further trial and error calculation was performed using the results of five runs in which only solution flow rate was varied. This was intended to separate the velocity constant into the individual film and particle transfer coefficients, which was possible because the particle transfer coefficient is independent of flow rate, and the film transfer coefficient varies with flow rate according to a known law.

Film transfer resistance is proportional to the Reynolds number to a known exponent. When the film transfer resistance and flow rate are plotted on log-log paper they should give a straight line of known slope. To determine the value of the particle transfer resistance , trial and error values of the particle transfer resistance are subtracted from the total resistance, until the plot of the logarithm of the difference against the logarithm of flow rate gives a straight line of the required slope. The application of this technique to a sample set of results is shown in Fig. 4.6. The results of the other runs are summarised in Tables 4.1-4.16.

The liquid diffusion coefficient was calculated from the film transfer resistance using the correlation of Wilke and Hougen (ref. W7) .

$$k_L = 1.82v\ Re^{-0.51}\ Sc^{-0.67} \qquad \text{--- 4.9}$$

The diffusion coefficient in the particle is calculated from equation 4.10, which is based on a constant surface concentration.

$$D_P = \frac{k_P d_0^2}{4\pi^2} \qquad \text{---- 4.10}$$

A Fortran IV programme was developed to perform these calculations (see Appendix 3). Computation was carried out on the IBM 7090 system at Imperial College .

4.3.4. Effect of a varying selectivity coefficient on the break through curve predicted assuming a constant value.

In general there is some variation of selectivity with the ionic composition of the resin, and since the

FIG 4.6

SEPARATION OF TRANSFER RESISTANCES
FOR THIS WORK
DEACIDITE FF-CHLORIDE
20-30 MESH, 7-9% CROSSLINKING,
EXTERNAL SOLUTION CONCENTRATION 0.1 N.
TEMPERATURE 18.5°C.
PERCENTAGE DEGRADATION 0.0%.

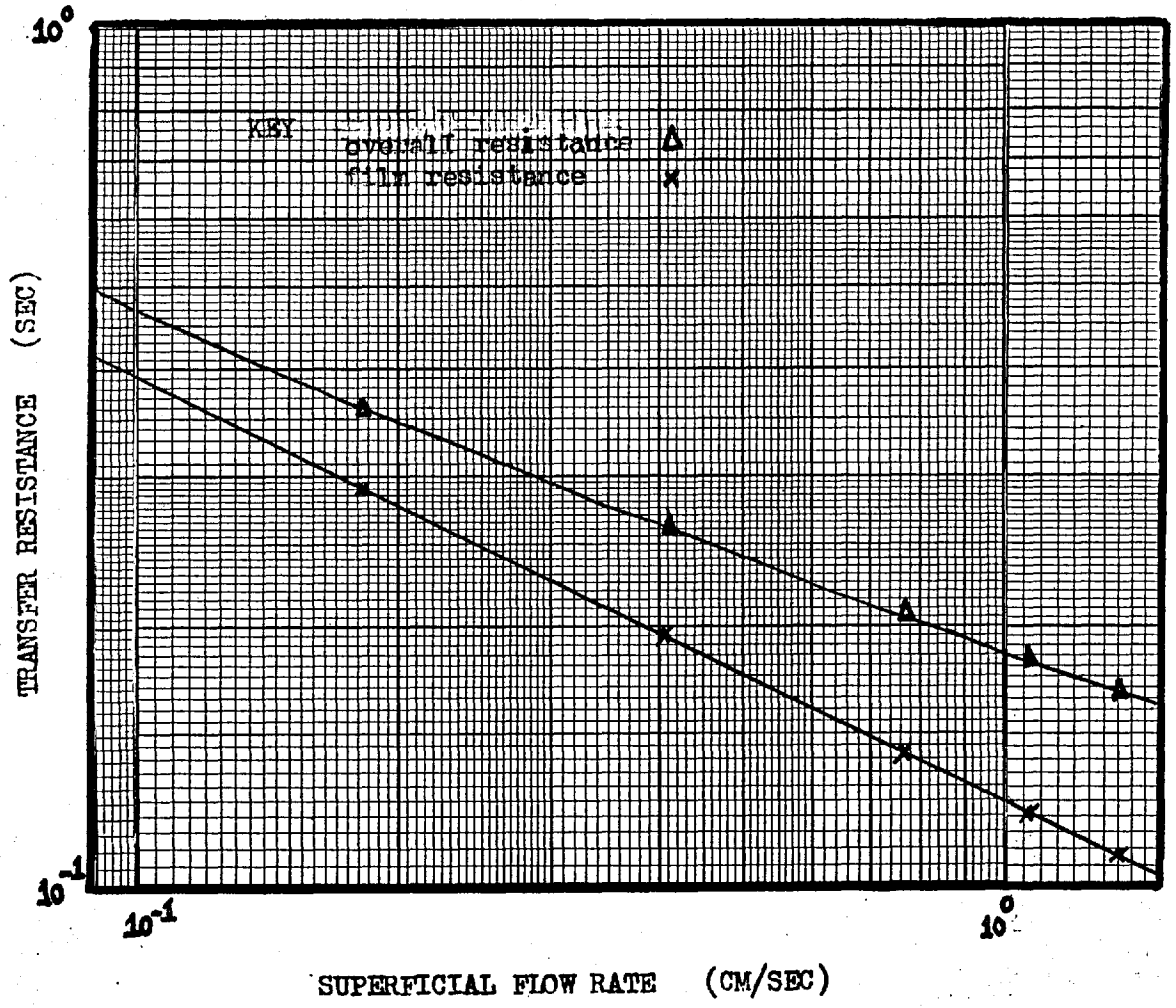

The following Tables are photocopies of off line computer output. As such they contain certain notations peculiar to the computer output system. The character E denotes the number 10.

For example 0.318E 03 means 0.318×10^3.

Tables 4.1 to 4.10 refer to Deacidite FF, 20 - 30 mesh, 7 - 9% crosslinking.

Tables 4.1 - 4.2 are reproducibility measurements.

Tables 4.3 and 4.4 show the effect of temperature.

Tables 4.5 and 4.6 show the effect of concentration.

Tables 4.7 to 4.10 show the effect of thermal degradation.

Tables 4.11 - 4.16 refer to Deacidite FF, 20-30 mesh, 2-3% crosslinking.

Tables 4.11 and 4.12 show the effect of temperature .

Tables 4.13 to 4.16 show the effect of Thermal degradation.

TABLE 4.1

OBSERVED RESULTS
HYDROXIDE SOLUTION - CHLORIDE RESIN

SERIES	GROUP	RUN	BREAKTHROUGH CURVE OBSERVED MID POINT VOLUME	BREAKTHROUGH CURVE OBSERVED MID POINT SLOPE	BREAKTHROUGH CURVE CALCULATED MID POINT SLOPE	SPECIFIC SOLUTION FLOW RATE	RADIUS OF ACTUAL PARTICLE	DIFFUSION COEFFICIENTS IN PARTICLE	DIFFUSION COEFFICIENTS IN FILM
			ML	1/SEC	1/SEC	ML/SEC	CM	CM*CM/SEC	CM*CM/SEC
1	1	1	0.318E 03	0.188E-01	0.188E-01	0.182E 00	0.335000E-01	0.140E-05	0.173E-04
1	1	2	0.287E 03	0.116E-01	0.116E-01	0.408E 00	0.335000E-01	0.140E-05	0.173E-04
1	1	3	0.312E 03	0.781E-02	0.781E-02	0.764E 00	0.335000E-01	0.140E-05	0.173E-04
1	1	4	0.253E 03	0.593E-02	0.593E-02	0.116E 01	0.335000E-01	0.140E-05	0.173E-04
1	1	5	0.293E 03	0.461E-02	0.461E-02	0.170E 01	0.335000E-01	0.140E-05	0.173E-04
	CONCENTRATION	0.106 N	TEMPERATURE	18.70 C	PERCENTAGE DEGRADATION	0.	PARTICLE DIAMETER	0.6700E-01 CM	
1	2	6	0.331E 03	0.190E-01	0.190E-01	0.180E 00	0.335000E-01	0.140E-05	0.173E-04
1	2	7	0.307E 03	0.118E-01	0.118E-01	0.398E 00	0.335000E-01	0.140E-05	0.173E-04
1	2	8	0.331E 03	0.783E-02	0.783E-02	0.762E 00	0.335000E-01	0.140E-05	0.173E-04
1	2	9	0.314E 03	0.592E-02	0.592E-02	0.117E 01	0.335000E-01	0.140E-05	0.173E-04
1	2	10	0.312E 03	0.455E-02	0.455E-02	0.173E 01	0.335000E-01	0.140E-05	0.173E-04
	CONCENTRATION	0.106 N	TEMPERATURE	18.70 C	PERCENTAGE DEGRADATION	0.	PARTICLE DIAMETER	0.6700E-01 CM	
1	3	11	0.301E 03	0.189E-01	0.189E-01	0.181E 00	0.335000E-01	0.140E-05	0.173E-04
1	3	12	0.295E 03	0.118E-01	0.118E-01	0.398E 00	0.335000E-01	0.140E-05	0.173E-04
1	3	13	0.309E 03	0.781E-02	0.781E-02	0.764E 00	0.335000E-01	0.140E-05	0.173E-04
1	3	14	0.286E 03	0.579E-02	0.579E-02	0.121E 01	0.335000E-01	0.140E-05	0.173E-04
1	3	15	0.283E 03	0.422E-02	0.422E-02	0.193E 01	0.335000E-01	0.140E-05	0.173E-04
	CONCENTRATION	0.106 N	TEMPERATURE	18.70 C	PERCENTAGE DEGRADATION	0.	PARTICLE DIAMETER	0.6700E-01 CM	

TABLE 4.2

OBSERVED RESULTS
CHLORIDE SOLUTION - HYDROXIDE RESIN

SERIES	GROUP	RUN	BREAKTHROUGH CURVE OBSERVED MID POINT VOLUME	BREAKTHROUGH CURVE OBSERVED MID POINT SLOPE	BREAKTHROUGH CURVE CALCULATED MID POINT SLOPE	SPECIFIC SOLUTION FLOW RATE	RADIUS OF ACTUAL PARTICLE	DIFFUSION COEFFICIENTS IN PARTICLE	DIFFUSION COEFFICIENTS IN FILM
			ML	1/SEC	1/SEC	ML/SEC	CM	CM*CM/SEC	CM*CM/SEC
1	4	16	0.334E 03	0.219E-01	0.219E-01	0.179E 00	0.335000E-01	0.540E-05	0.213E-04
1	4	17	0.326E 03	0.140E-01	0.140E-01	0.410E 00	0.335000E-01	0.540E-05	0.213E-04
1	4	18	0.290E 03	0.988E-02	0.988E-02	0.762E 00	0.335000E-01	0.540E-05	0.213E-04
1	4	19	0.339E 03	0.779E-02	0.779E-02	0.116E 01	0.335000E-01	0.540E-05	0.213E-04
1	4	20	0.365E 03	0.621E-02	0.621E-02	0.171E 01	0.335000E-01	0.540E-05	0.213E-04
	CONCENTRATION	0.100 N	TEMPERATURE	18.90 C	PERCENTAGE DEGRADATION	0.	PARTICLE DIAMETER	0.6700E-01 CM	
1	5	21	0.331E 03	0.219E-01	0.219E-01	0.180E 00	0.335000E-01	0.540E-05	0.213E-04
1	5	22	0.331E 03	0.142E-01	0.142E-01	0.397E 00	0.335000E-01	0.540E-05	0.213E-04
1	5	23	0.362E 03	0.989E-02	0.989E-02	0.761E 00	0.335000E-01	0.540E-05	0.213E-04
1	5	24	0.341E 03	0.775E-02	0.775E-02	0.117E 01	0.335000E-01	0.540E-05	0.213E-04
1	5	25	0.336E 03	0.609E-02	0.609E-02	0.177E 01	0.335000E-01	0.540E-05	0.213E-04
	CONCENTRATION	0.100 N	TEMPERATURE	18.90 C	PERCENTAGE DEGRADATION	0.	PARTICLE DIAMETER	0.6700E-01 CM	
1	6	26	0.357E 03	0.218E-01	0.218E-01	0.180E 00	0.335000E-01	0.540E-05	0.213E-04
1	6	27	0.336E 03	0.141E-01	0.141E-01	0.400E 00	0.335000E-01	0.540E-05	0.213E-04
1	6	28	0.354E 03	0.984E-02	0.984E-02	0.768E 00	0.335000E-01	0.540E-05	0.213E-04
1	6	29	0.367E 03	0.764E-02	0.764E-02	0.120E 01	0.335000E-01	0.540E-05	0.213E-04
1	6	30	0.359E 03	0.615E-02	0.615E-02	0.174E 01	0.335000E-01	0.540E-05	0.213E-04
	CONCENTRATION	0.100 N	TEMPERATURE	18.90 C	PERCENTAGE DEGRADATION	0.	PARTICLE DIAMETER	0.6700E-01 CM	

TABLE 4.3

OBSERVED RESULTS
HYDROXIDE SOLUTION - CHLORIDE RESIN

SERIES	GROUP	RUN	BREAKTHROUGH CURVE OBSERVED MID POINT VOLUME	BREAKTHROUGH CURVE OBSERVED MID POINT SLOPE	BREAKTHROUGH CURVE CALCULATED MID POINT SLOPE	SPECIFIC SOLUTION FLOW RATE	RADIUS OF ACTUAL PARTICLE	DIFFUSION COEFFICIENTS IN PARTICLE	DIFFUSION COEFFICIENTS IN FILM
			ML	1/SEC	1/SEC	ML/SEC	CM	CM*CM/SEC	CM*CM/SEC
2	1	1	0.318E 03	0.188E-01	0.188E-01	0.182E 00	0.335000E-01	0.140E-05	0.173E-04
2	1	2	0.287E 03	0.116E-01	0.116E-01	0.408E 00	0.335000E-01	0.140E-05	0.173E-04
2	1	3	0.312E 03	0.781E-02	0.781E-02	0.764E 00	0.335000E-01	0.140E-05	0.173E-04
2	1	4	0.253E 03	0.593E-02	0.593E-02	0.116E 01	0.335000E-01	0.140E-05	0.173E-04
2	1	5	0.293E 03	0.461E-02	0.461E-02	0.170E 01	0.335000E-01	0.140E-05	0.173E-04
CONCENTRATION 0.106 N TEMPERATURE 18.70 C PERCENTAGE DEGRADATION 0. PARTICLE DIAMETER 0.6700E-01 CM									
2	2	6	0.320E 03	0.201E-01	0.201E-01	0.179E 00	0.335000E-01	0.412E-05	0.315E-04
2	2	7	0.315E 03	0.126E-01	0.126E-01	0.411E 00	0.335000E-01	0.412E-05	0.315E-04
2	2	8	0.314E 03	0.874E-02	0.874E-02	0.769E 00	0.335000E-01	0.412E-05	0.315E-04
2	2	9	0.311E 03	0.673E-02	0.673E-02	0.119E 01	0.335000E-01	0.412E-05	0.315E-04
2	2	10	0.312E 03	0.547E-02	0.547E-02	0.167E 01	0.335000E-01	0.412E-05	0.315E-04
CONCENTRATION 0.101 N TEMPERATURE 50.00 C PERCENTAGE DEGRADATION 0. PARTICLE DIAMETER 0.6700E-01 CM									
2	3	11	0.331E 03	0.185E-01	0.185E-01	0.177E 00	0.335000E-01	0.136E-04	0.542E-04
2	3	12	0.342E 03	0.118E-01	0.118E-01	0.407E 00	0.335000E-01	0.136E-04	0.542E-04
2	3	13	0.329E 03	0.833E-02	0.833E-02	0.773E 00	0.335000E-01	0.136E-04	0.542E-04
2	3	14	0.329E 03	0.653E-02	0.653E-02	0.119E 01	0.335000E-01	0.136E-04	0.542E-04
2	3	15	0.327E 03	0.520E-02	0.520E-02	0.179E 01	0.335000E-01	0.136E-04	0.542E-04
CONCENTRATION 0.101 N TEMPERATURE 90.00 C PERCENTAGE DEGRADATION 0. PARTICLE DIAMETER 0.6700E-01 CM									

TABLE 4.4

OBSERVED RESULTS
CHLORIDE SOLUTION - HYDROXIDE RESIN

SERIES	GROUP	RUN	BREAKTHROUGH CURVE OBSERVED MID POINT VOLUME	BREAKTHROUGH CURVE OBSERVED MID POINT SLOPE	BREAKTHROUGH CURVE CALCULATED MID POINT SLOPE	SPECIFIC SOLUTION FLOW RATE	RADIUS OF ACTUAL PARTICLE	DIFFUSION COEFFICIENTS IN PARTICLE	DIFFUSION COEFFICIENTS IN FILM
			ML	1/SEC	1/SEC	ML/SEC	CM	CM*CM/SEC	CM*CM/SEC
2	4	16	0.334E 03	0.219E-01	0.219E-01	0.179E 00	0.335000E-01	0.540E-05	0.213E-04
2	4	17	0.326E 03	0.140E-01	0.140E-01	0.410E 00	0.335000E-01	0.540E-05	0.213E-04
2	4	18	0.290E 03	0.988E-02	0.988E-02	0.762E 00	0.335000E-01	0.540E-05	0.213E-04
2	4	19	0.292E 03	0.779E-02	0.779E-02	0.116E 01	0.335000E-01	0.540E-05	0.213E-04
2	4	20	0.365E 03	0.621E-02	0.621E-02	0.171E 01	0.335000E-01	0.540E-05	0.213E-04
CONCENTRATION 0.100 N TEMPERATURE 18.90 C PERCENTAGE DEGRADATION 0. PARTICLE DIAMETER 0.6700E-01 CM									
2	5	21	0.283E 03	0.396E-01	0.396E-01	0.178E 00	0.335000E-01	0.233E-04	0.476E-04
2	5	22	0.283E 03	0.256E-01	0.256E-01	0.409E 00	0.335000E-01	0.233E-04	0.476E-04
2	5	23	0.283E 03	0.183E-01	0.183E-01	0.768E 00	0.335000E-01	0.233E-04	0.476E-04
2	5	24	0.283E 03	0.147E-01	0.147E-01	0.115E 01	0.335000E-01	0.233E-04	0.476E-04
2	5	25	0.321E 03	0.118E-01	0.118E-01	0.173E 01	0.335000E-01	0.233E-04	0.476E-04
CONCENTRATION 0.103 N TEMPERATURE 50.00 C PERCENTAGE DEGRADATION 0. PARTICLE DIAMETER 0.6700E-01 CM									
2	6	26	0.324E 03	0.492E-01	0.492E-01	0.180E 00	0.335000E-01	0.728E-04	0.813E-04
2	6	27	0.324E 03	0.326E-01	0.326E-01	0.399E 00	0.335000E-01	0.728E-04	0.813E-04
2	6	28	0.324E 03	0.232E-01	0.232E-01	0.771E 00	0.335000E-01	0.728E-04	0.813E-04
2	6	29	0.329E 03	0.184E-01	0.184E-01	0.120E 01	0.335000E-01	0.728E-04	0.813E-04
2	6	30	0.326E 03	0.152E-01	0.152E-01	0.173E 01	0.335000E-01	0.728E-04	0.813E-04
CONCENTRATION 0.103 N TEMPERATURE 90.00 C PERCENTAGE DEGRADATION 0. PARTICLE DIAMETER 0.6700E-01 CM									

TABLE 4.5

OBSERVED RESULTS
HYDROXIDE SOLUTION - CHLORIDE RESIN

SERIES	GROUP	RUN	BREAKTHROUGH CURVE OBSERVED MID POINT VOLUME	BREAKTHROUGH CURVE OBSERVED MID POINT SLOPE	BREAKTHROUGH CURVE CALCULATED MID POINT SLOPE	SPECIFIC SOLUTION FLOW RATE	RADIUS OF ACTUAL PARTICLE	DIFFUSION COEFFICIENTS IN PARTICLE	DIFFUSION COEFFICIENTS IN FILM
			ML	1/SEC	1/SEC	ML/SEC	CM	CM*CM/SEC	CM*CM/SEC
3	1	1	0.316E 03	0.133E-01	0.133E-01	0.182E 00	0.335000E-01	0.140E-05	0.164E-04
3	1	2	0.283E 03	0.835E-02	0.835E-02	0.408E 00	0.335000E-01	0.140E-05	0.164E-04
3	1	3	0.306E 03	0.574E-02	0.574E-02	0.764E 00	0.335000E-01	0.140E-05	0.164E-04
3	1	4	0.245E 03	0.443E-02	0.443E-02	0.116E 01	0.335000E-01	0.140E-05	0.164E-04
3	1	5	0.284E 03	0.349E-02	0.349E-02	0.170E 01	0.335000E-01	0.140E-05	0.164E-04
CONCENTRATION 0.106 N TEMPERATURE 18.70 C PERCENTAGE DEGRADATION 0. PARTICLE DIAMETER 0.6700E-01 CM.									
3	2	6	0.653E 03	0.634E-02	0.634E-02	0.179E 00	0.335000E-01	0.910E-06	0.170E-04
3	2	7	0.672E 03	0.398E-02	0.398E-02	0.409E 00	0.335000E-01	0.910E-06	0.170E-04
3	2	8	0.608E 03	0.276E-02	0.276E-02	0.767E 00	0.335000E-01	0.910E-06	0.170E-04
3	2	9	0.616E 03	0.214E-02	0.214E-02	0.117E 01	0.335000E-01	0.910E-06	0.170E-04
3	2	10	0.586E 03	0.170E-02	0.170E-02	0.170E 01	0.335000E-01	0.910E-06	0.170E-04
CONCENTRATION 0.051 N TEMPERATURE 17.00 C PERCENTAGE DEGRADATION 0. PARTICLE DIAMETER 0.6700E-01 CM									
3	3	11	0.286E 04	0.762E-03	0.762E-03	0.183E 00	0.335000E-01	0.470E-06	0.173E-04
3	3	12	0.273E 04	0.503E-03	0.503E-03	0.398E 00	0.335000E-01	0.470E-06	0.173E-04
3	3	13	0.268E 04	0.350E-03	0.350E-03	0.770E 00	0.335000E-01	0.470E-06	0.173E-04
3	3	14	0.258E 04	0.274E-03	0.274E-03	0.120E 01	0.335000E-01	0.470E-06	0.173E-04
3	3	15	0.253E 04	0.214E-03	0.214E-03	0.185E 01	0.335000E-01	0.470E-06	0.173E-04
CONCENTRATION 0.011 N TEMPERATURE 17.60 C PERCENTAGE DEGRADATION 0. PARTICLE DIAMETER 0.6700E-01 CM									

TABLE 4.6

OBSERVED RESULTS
CHLORIDE SOLUTION - HYDROXIDE RESIN

SERIES	GROUP	RUN	BREAKTHROUGH CURVE OBSERVED MID POINT VOLUME	BREAKTHROUGH CURVE OBSERVED MID POINT SLOPE	BREAKTHROUGH CURVE CALCULATED MID POINT SLOPE	SPECIFIC SOLUTION FLOW RATE	RADIUS OF ACTUAL PARTICLE	DIFFUSION COEFFICIENTS IN PARTICLE	DIFFUSION COEFFICIENTS IN FILM
			ML	1/SEC	1/SEC	ML/SEC	CM	CM*CM/SEC	CM*CM/SEC
3	4	16	0.334E 03	0.154E-01	0.154E-01	0.179E 00	0.335000E-01	0.540E-05	0.213E-04
3	4	17	0.326E 03	0.991E-02	0.991E-02	0.410E 00	0.335000E-01	0.540E-05	0.213E-04
3	4	18	0.290E 03	0.707E-02	0.707E-02	0.762E 00	0.335000E-01	0.540E-05	0.213E-04
3	4	19	0.339E 03	0.561E-02	0.561E-02	0.116E 01	0.335000E-01	0.540E-05	0.213E-04
3	4	20	0.364E 03	0.451E-02	0.451E-02	0.171E 01	0.335000E-01	0.540E-05	0.213E-04
CONCENTRATION 0.100 N TEMPERATURE 18.90 C PERCENTAGE DEGRADATION 0. PARTICLE DIAMETER 0.6700E-01 CM									
3	5	21	0.640E 03	0.933E-02	0.933E-02	0.177E 00	0.335000E-01	0.410E-05	0.239E-04
3	5	22	0.635E 03	0.604E-02	0.604E-02	0.404E 00	0.335000E-01	0.410E-05	0.239E-04
3	5	23	0.640E 03	0.428E-02	0.428E-02	0.768E 00	0.335000E-01	0.410E-05	0.239E-04
3	5	24	0.640E 03	0.341E-02	0.341E-02	0.117E 01	0.335000E-01	0.410E-05	0.239E-04
3	5	25	0.639E 03	0.272E-02	0.272E-02	0.177E 01	0.335000E-01	0.410E-05	0.239E-04
CONCENTRATION 0.051 N TEMPERATURE 17.00 C PERCENTAGE DEGRADATION 0. PARTICLE DIAMETER 0.6700E-01 CM									
3	6	26	0.325E 04	0.211E-02	0.211E-02	0.181E 00	0.335000E-01	0.351E-05	0.258E-04
3	6	27	0.320E 04	0.141E-02	0.141E-02	0.398E 00	0.335000E-01	0.351E-05	0.258E-04
3	6	28	0.318E 04	0.999E-03	0.999E-03	0.773E 00	0.335000E-01	0.351E-05	0.258E-04
3	6	29	0.323E 04	0.794E-03	0.794E-03	0.120E 01	0.335000E-01	0.351E-05	0.258E-04
3	6	30	0.325E 04	0.646E-03	0.646E-03	0.179E 01	0.335000E-01	0.351E-05	0.258E-04
CONCENTRATION 0.010 N TEMPERATURE 17.60 C PERCENTAGE DEGRADATION 0. PARTICLE DIAMETER 0.6700E-01 CM									

TABLE 4.7

OBSERVED RESULTS
HYDROXIDE SOLUTION - CHLORIDE RESIN

SERIES	GROUP	RUN	BREAKTHROUGH CURVE OBSERVED MID POINT VOLUME	BREAKTHROUGH CURVE OBSERVED MID POINT SLOPE	BREAKTHROUGH CURVE CALCULATED MID POINT SLOPE	SPECIFIC SOLUTION FLOW RATE	RADIUS OF ACTUAL PARTICLE	DIFFUSION COEFFICIENTS IN PARTICLE	DIFFUSION COEFFICIENTS IN FILM
			ML	1/SEC	1/SEC	ML/SEC	CM	CM*CM/SEC	CM*CM/SEC
4	1	1	0.260E 03	0.215E-01	0.215E-01	0.182E 00	0.335000E-01	0.140E-05	0.173E-04
4	1	2	0.310E 03	0.178E-01	0.178E-01	0.248E 00	0.335000E-01	0.140E-05	0.173E-04
4	1	3	0.244E 03	0.125E-01	0.125E-01	0.441E 00	0.335000E-01	0.140E-05	0.173E-04
4	1	4	0.265E 03	0.603E-02	0.603E-02	0.133E 01	0.335000E-01	0.140E-05	0.173E-04
4	1	5	0.216E 03	0.476E-02	0.476E-02	0.187E 01	0.335000E-01	0.140E-05	0.173E-04
CONCENTRATION 0.108 N TEMPERATURE 19.00 C PERCENTAGE DEGRADATION 0. PARTICLE DIAMETER 0.6700E-01 CM									
4	2	6	0.241E 03	0.264E-01	0.264E-01	0.182E 00	0.335000E-01	0.202E-05	0.173E-04
4	2	7	0.237E 03	0.211E-01	0.211E-01	0.266E 00	0.335000E-01	0.202E-05	0.173E-04
4	2	8	0.284E 03	0.152E-01	0.152E-01	0.461E 00	0.335000E-01	0.202E-05	0.173E-04
4	2	9	0.221E 03	0.730E-02	0.730E-02	0.147E 01	0.335000E-01	0.202E-05	0.173E-04
4	2	10	0.221E 03	0.536E-02	0.536E-02	0.233E 01	0.335000E-01	0.202E-05	0.173E-04
CONCENTRATION 0.108 N TEMPERATURE 19.00 C PERCENTAGE DEGRADATION 7.20 PARTICLE DIAMETER 0.6700E-01 CM									
4	3	11	0.219E 03	0.373E-01	0.373E-01	0.186E 00	0.335000E-01	0.244E-05	0.173E-04
4	3	12	0.237E 03	0.334E-01	0.334E-01	0.224E 00	0.335000E-01	0.244E-05	0.173E-04
4	3	13	0.208E 03	0.213E-01	0.213E-01	0.477E 00	0.335000E-01	0.244E-05	0.173E-04
4	3	14	0.188E 03	0.114E-01	0.114E-01	0.128E 01	0.335000E-01	0.244E-05	0.173E-04
4	3	15	0.244E 03	0.820E-02	0.820E-02	0.211E 01	0.335000E-01	0.244E-05	0.173E-04
CONCENTRATION 0.108 N TEMPERATURE 19.00 C PERCENTAGE DEGRADATION 23.60 PARTICLE DIAMETER 0.6700E-01 CM									

TABLE 4.8

OBSERVED RESULTS
CHLORIDE SOLUTION - HYDROXIDE RESIN

SERIES	GROUP	RUN	BREAKTHROUGH CURVE OBSERVED MID POINT VOLUME	OBSERVED MID POINT SLOPE	CALCULATED MID POINT SLOPE	SPECIFIC SOLUTION FLOW RATE	RADIUS OF ACTUAL PARTICLE	DIFFUSION COEFFICIENTS IN PARTICLE	IN FILM
			ML	1/SEC	1/SEC	ML/SEC	CM	CM*CM/SEC	CM*CM/SEC
4	4	16	0.321E 03	0.252E-01	0.252E-01	0.175E 00	0.335000E-01	0.540E-05	0.214E-04
4	4	17	0.315E 03	0.179E-01	0.179E-01	0.328E 00	0.335000E-01	0.540E-05	0.214E-04
4	4	18	0.323E 03	0.150E-01	0.150E-01	0.451E 00	0.335000E-01	0.540E-05	0.214E-04
4	4	19	0.308E 03	0.919E-02	0.919E-02	0.107E 01	0.335000E-01	0.540E-05	0.214E-04
4	4	20	0.310E 03	0.699E-02	0.699E-02	0.170E 01	0.335000E-01	0.540E-05	0.214E-04
	CONCENTRATION	0.100 N	TEMPERATURE	19.00 C	PERCENTAGE DEGRADATION	0.	PARTICLE DIAMETER	0.6700E-01 CM	
4	5	21	0.282E 03	0.275E-01	0.275E-01	0.172E 00	0.335000E-01	0.556E-05	0.214E-04
4	5	22	0.279E 03	0.208E-01	0.208E-01	0.285E 00	0.335000E-01	0.556E-05	0.214E-04
4	5	23	0.284E 03	0.161E-01	0.161E-01	0.457E 00	0.335000E-01	0.556E-05	0.214E-04
4	5	24	0.274E 03	0.980E-02	0.980E-02	0.109E 01	0.335000E-01	0.556E-05	0.214E-04
4	5	25	0.289E 03	0.711E-02	0.711E-02	0.187E 01	0.335000E-01	0.556E-05	0.214E-04
	CONCENTRATION	0.100 N	TEMPERATURE	19.00 C	PERCENTAGE DEGRADATION	7.20	PARTICLE DIAMETER	0.6700E-01 CM	
4	6	26	0.247E 03	0.333E-01	0.333E-01	0.178E 00	0.335000E-01	0.796E-05	0.214E-04
4	6	27	0.243E 03	0.232E-01	0.232E-01	0.347E 00	0.335000E-01	0.796E-05	0.214E-04
4	6	28	0.241E 03	0.219E-01	0.219E-01	0.385E 00	0.335000E-01	0.796E-05	0.214E-04
4	6	29	0.213E 03	0.117E-01	0.117E-01	0.117E 01	0.335000E-01	0.796E-05	0.214E-04
4	6	30	0.237E 03	0.845E-02	0.845E-02	0.206E 01	0.335000E-01	0.796E-05	0.214E-04
	CONCENTRATION	0.100 N	TEMPERATURE	19.00 C	PERCENTAGE DEGRADATION	23.60	PARTICLE DIAMETER	0.6700E-01 CM	

TABLE 4.9

OBSERVED RESULTS
HYDROXIDE SOLUTION - CHLORIDE RESIN

SERIES	GROUP	RUN	BREAKTHROUGH CURVE OBSERVED MID POINT VOLUME	BREAKTHROUGH CURVE OBSERVED MID POINT SLOPE	BREAKTHROUGH CURVE CALCULATED MID POINT SLOPE	SPECIFIC SOLUTION FLOW RATE	RADIUS OF ACTUAL PARTICLE	DIFFUSION COEFFICIENTS IN PARTICLE	DIFFUSION COEFFICIENTS IN FILM
			ML	1/SEC	1/SEC	ML/SEC	CM	CM*CM/SEC	CM*CM/SEC
5	1	1	0.142E 04	0.671E-02	0.671E-02	0.154E 00	0.335000E-01	0.316E-05	0.173E-04
5	1	2	0.160E 04	0.550E-02	0.550E-02	0.226E 00	0.335000E-01	0.316E-05	0.173E-04
5	1	3	0.163E 04	0.365E-02	0.365E-02	0.497E 00	0.335000E-01	0.316E-05	0.173E-04
5	1	4	0.167E 04	0.284E-02	0.284E-02	0.806E 00	0.335000E-01	0.316E-05	0.173E-04
5	1	5	0.158E 04	0.185E-02	0.185E-02	0.182E 01	0.335000E-01	0.316E-05	0.173E-04
	CONCENTRATION 0.011 N		TEMPERATURE 19.00 C		PERCENTAGE DEGRADATION 33.10		PARTICLE DIAMETER 0.6700E-01 CM		
5	2	6	0.131E 04	0.713E-02	0.713E-02	0.181E 00	0.335000E-01	0.225E-05	0.173E-04
5	2	7	0.174E 04	0.476E-02	0.476E-02	0.391E 00	0.335000E-01	0.225E-05	0.173E-04
5	2	8	0.174E 04	0.429E-02	0.429E-02	0.478E 00	0.335000E-01	0.225E-05	0.173E-04
5	2	9	0.180E 04	0.337E-02	0.337E-02	0.753E 00	0.335000E-01	0.225E-05	0.173E-04
5	2	10	0.163E 04	0.210E-02	0.210E-02	0.182E 01	0.335000E-01	0.225E-05	0.173E-04
	CONCENTRATION 0.011 N		TEMPERATURE 19.00 C		PERCENTAGE DEGRADATION 48.60		PARTICLE DIAMETER 0.6700E-01 CM		

TABLE 4.10

OBSERVED RESULTS
CHLORIDE SOLUTION - HYDROXIDE RESIN

SERIES	GROUP	RUN	BREAKTHROUGH CURVE OBSERVED MID POINT VOLUME	BREAKTHROUGH CURVE OBSERVED MID POINT SLOPE	BREAKTHROUGH CURVE CALCULATED MID POINT SLOPE	SPECIFIC SOLUTION FLOW RATE	RADIUS OF ACTUAL PARTICLE	DIFFUSION COEFFICIENTS IN PARTICLE	DIFFUSION COEFFICIENTS IN FILM
			ML	1/SEC	1/SEC	ML/SEC	CM	CM*CM/SEC	CM*CM/SEC
5	4	16	0.202E 03	0.375E-01	0.375E-01	0.184E 00	0.335000E-01	0.658E-05	0.214E-04
5	4	17	0.201E 03	0.297E-01	0.297E-01	0.279E 00	0.335000E-01	0.658E-05	0.214E-04
5	4	18	0.185E 03	0.232E-01	0.232E-01	0.435E 00	0.335000E-01	0.658E-05	0.214E-04
5	4	19	0.194E 03	0.112E-01	0.112E-01	0.152E 01	0.335000E-01	0.658E-05	0.214E-04
5	4	20	0.213E 03	0.983E-02	0.983E-02	0.187E 01	0.335000E-01	0.658E-05	0.214E-04
CONCENTRATION 0.100 N TEMPERATURE 19.00 C PERCENTAGE DEGRADATION 33.10 PARTICLE DIAMETER 0.6700E-01 CM									
5	5	21	0.200E 03	0.396E-01	0.396E-01	0.181E 00	0.335000E-01	0.554E-05	0.214E-04
5	5	22	0.199E 03	0.299E-01	0.299E-01	0.298E 00	0.335000E-01	0.554E-05	0.214E-04
5	5	23	0.200E 03	0.241E-01	0.241E-01	0.433E 00	0.335000E-01	0.554E-05	0.214E-04
5	5	24	0.192E 03	0.133E-01	0.133E-01	0.117E 01	0.335000E-01	0.554E-05	0.214E-04
5	5	25	0.171E 03	0.894E-02	0.894E-02	0.221E 01	0.335000E-01	0.554E-05	0.214E-04
CONCENTRATION 0.100 N TEMPERATURE 19.00 C PERCENTAGE DEGRADATION 48.60 PARTICLE DIAMETER 0.6700E-01 CM									

TABLE 4.11

OBSERVED RESULTS
HYDROXIDE SOLUTION - CHLORIDE RESIN

SERIES	GROUP	RUN	BREAKTHROUGH CURVE OBSERVED MID POINT VOLUME	BREAKTHROUGH CURVE OBSERVED MID POINT SLOPE	BREAKTHROUGH CURVE CALCULATED MID POINT SLOPE	SPECIFIC SOLUTION FLOW RATE	RADIUS OF ACTUAL PARTICLE	DIFFUSION COEFFICIENTS IN PARTICLE	DIFFUSION COEFFICIENTS IN FILM
			ML	1/SEC	1/SEC	ML/SEC	CM	CM*CM/SEC	CM*CM/SEC
6	1	1	0.313E 03	0.185E-01	0.185E-01	0.178E 00	0.350000E-01	0.370E-05	0.173E-04
6	1	2	0.313E 03	0.111E-01	0.111E-01	0.410E 00	0.350000E-01	0.370E-05	0.173E-04
6	1	3	0.289E 03	0.740E-02	0.740E-02	0.770E 00	0.350000E-01	0.370E-05	0.173E-04
6	1	4	0.281E 03	0.561E-02	0.561E-02	0.116E 01	0.350000E-01	0.370E-05	0.173E-04
6	1	5	0.284E 03	0.436E-02	0.436E-02	0.168E 01	0.350000E-01	0.370E-05	0.173E-04
CONCENTRATION 0.102 N TEMPERATURE 18.60 C PERCENTAGE DEGRADATION 0. PARTICLE DIAMETER 0.7000E-01 CM									
6	2	6	0.317E 03	0.216E-01	0.216E-01	0.176E 00	0.350000E-01	0.789E-05	0.315E-04
6	2	7	0.319E 03	0.130E-01	0.130E-01	0.423E 00	0.350000E-01	0.789E-05	0.315E-04
6	2	8	0.321E 03	0.927E-02	0.927E-02	0.740E 00	0.350000E-01	0.789E-05	0.315E-04
6	2	9	0.287E 03	0.694E-02	0.694E-02	0.118E 01	0.350000E-01	0.789E-05	0.315E-04
6	2	10	0.300E 03	0.537E-02	0.537E-02	0.175E 01	0.350000E-01	0.789E-05	0.315E-04
CONCENTRATION 0.102 N TEMPERATURE 48.60 C PERCENTAGE DEGRADATION 0. PARTICLE DIAMETER 0.7000E-01 CM									
6	3	11	0.315E 03	0.195E-01	0.195E-01	0.180E 00	0.350000E-01	0.140E-04	0.542E-04
6	3	12	0.318E 03	0.123E-01	0.123E-01	0.410E 00	0.350000E-01	0.140E-04	0.542E-04
6	3	13	0.310E 03	0.858E-02	0.858E-02	0.763E 00	0.350000E-01	0.140E-04	0.542E-04
6	3	14	0.305E 03	0.661E-02	0.661E-02	0.118E 01	0.350000E-01	0.140E-04	0.542E-04
6	3	15	0.301E 03	0.527E-02	0.527E-02	0.171E 01	0.350000E-01	0.140E-04	0.542E-04
CONCENTRATION 0.103 N TEMPERATURE 90.10 C PERCENTAGE DEGRADATION 0. PARTICLE DIAMETER 0.7000E-01 CM									

TABLE 4.12

OBSERVED RESULTS
CHLORIDE SOLUTION - HYDROXIDE RESIN

SERIES	GROUP	RUN	BREAKTHROUGH CURVE OBSERVED MID POINT VOLUME	OBSERVED MID POINT SLOPE	CALCULATED MID POINT SLOPE	SPECIFIC SOLUTION FLOW RATE	RADIUS OF ACTUAL PARTICLE	DIFFUSION COEFFICIENTS IN PARTICLE	IN FILM
			ML	1/SEC	1/SEC	ML/SEC	CM	CM*CM/SEC	CM*CM/SEC
6	4	16	0.308E 03	0.208E-01	0.208E-01	0.179E 00	0.350000E-01	0.118E-04	0.213E-04
6	4	17	0.318E 03	0.131E-01	0.131E-01	0.411E 00	0.350000E-01	0.118E-04	0.213E-04
6	4	18	0.298E 03	0.906E-02	0.906E-02	0.777E 00	0.350000E-01	0.118E-04	0.213E-04
6	4	19	0.300E 03	0.715E-02	0.715E-02	0.116E 01	0.350000E-01	0.118E-04	0.213E-04
6	4	20	0.313E 03	0.567E-02	0.567E-02	0.170E 01	0.350000E-01	0.118E-04	0.213E-04
CONCENTRATION 0.098 N TEMPERATURE 18.60 C PERCENTAGE DEGRADATION 0. PARTICLE DIAMETER 0.7000E-01 CM									
6	5	21	0.333E 03	0.368E-01	0.368E-01	0.180E 00	0.350000E-01	0.312E-04	0.476E-04
6	5	22	0.338E 03	0.237E-01	0.237E-01	0.399E 00	0.350000E-01	0.312E-04	0.476E-04
6	5	23	0.323E 03	0.161E-01	0.161E-01	0.788E 00	0.350000E-01	0.312E-04	0.476E-04
6	5	24	0.323E 03	0.131E-01	0.131E-01	0.112E 01	0.350000E-01	0.312E-04	0.476E-04
6	5	25	0.328E 03	0.101E-01	0.101E-01	0.174E 01	0.350000E-01	0.312E-04	0.476E-04
CONCENTRATION 0.098 N TEMPERATURE 48.70 C PERCENTAGE DEGRADATION 0. PARTICLE DIAMETER 0.7000E-01 CM									
6	6	26	0.326E 03	0.486E-01	0.486E-01	0.175E 00	0.350000E-01	0.696E-04	0.813E-04
6	6	27	0.321E 03	0.304E-01	0.304E-01	0.411E 00	0.350000E-01	0.696E-04	0.813E-04
6	6	28	0.328E 03	0.214E-01	0.214E-01	0.772E 00	0.350000E-01	0.696E-04	0.813E-04
6	6	29	0.321E 03	0.167E-01	0.167E-01	0.118E 01	0.350000E-01	0.696E-04	0.813E-04
6	6	30	0.328E 03	0.135E-01	0.135E-01	0.171E 01	0.350000E-01	0.696E-04	0.813E-04
CONCENTRATION 0.098 N TEMPERATURE 19.00 C PERCENTAGE DEGRADATION 0. PARTICLE DIAMETER 0.7000E-01 CM									

TABLE 4.13

OBSERVED RESULTS

HYDROXIDE SOLUTION - CHLORIDE RESIN

SERIES	GROUP	RUN	BREAKTHROUGH CURVE OBSERVED MID POINT VOLUME	OBSERVED MID POINT SLOPE	CALCULATED MID POINT SLOPE	SPECIFIC SOLUTION FLOW RATE	RADIUS OF ACTUAL PARTICLE	DIFFUSION COEFFICIENTS IN PARTICLE	IN FILM
			ML	1/SEC	1/SEC	ML/SEC	CM	CM*CM/SEC	CM*CM/SEC
7	1	1	0.257E 03	0.286E-01	0.286E-01	0.178E 00	0.350000E-01	0.370E-05	0.174E-04
7	1	2	0.252E 03	0.232E-01	0.232E-01	0.265E 00	0.350000E-01	0.370E-05	0.174E-04
7	1	3	0.250E 03	0.177E-01	0.177E-01	0.440E 00	0.350000E-01	0.370E-05	0.174E-04
7	1	4	0.245E 03	0.105E-01	0.105E-01	0.117E 01	0.350000E-01	0.370E-05	0.174E-04
7	1	5	0.239E 03	0.816E-02	0.816E-02	0.186E 01	0.350000E-01	0.370E-05	0.174E-04
CONCENTRATION 0.113 N TEMPERATURE 18.70 C PERCENTAGE DEGRADATION 0. PARTICLE DIAMETER 0.7000E-01 CM									
7	2	6	0.255E 03	0.314E-01	0.314E-01	0.171E 00	0.350000E-01	0.391E-05	0.174E-04
7	2	7	0.251E 03	0.240E-01	0.240E-01	0.285E 00	0.350000E-01	0.391E-05	0.174E-04
7	2	8	0.251E 03	0.180E-01	0.180E-01	0.495E 00	0.350000E-01	0.391E-05	0.174E-04
7	2	9	0.244E 03	0.103E-01	0.103E-01	0.142E 01	0.350000E-01	0.391E-05	0.174E-04
7	2	10	0.242E 03	0.924E-02	0.924E-02	0.172E 01	0.350000E-01	0.391E-05	0.174E-04
CONCENTRATION 0.113 N TEMPERATURE 18.70 C PERCENTAGE DEGRADATION 3.74 PARTICLE DIAMETER 0.7000E-01 CM									
7	3	11	0.247E 03	0.352E-01	0.352E-01	0.177E 00	0.350000E-01	0.418E-05	0.174E-04
7	3	12	0.241E 03	0.308E-01	0.308E-01	0.230E 00	0.350000E-01	0.418E-05	0.174E-04
7	3	13	0.239E 03	0.210E-01	0.210E-01	0.479E 00	0.350000E-01	0.418E-05	0.174E-04
7	3	14	0.229E 03	0.122E-01	0.122E-01	0.135E 01	0.350000E-01	0.418E-05	0.174E-04
7	3	15	0.239E 03	0.108E-01	0.108E-01	0.171E 01	0.350000E-01	0.418E-05	0.174E-04
CONCENTRATION 0.113 N TEMPERATURE 18.70 C PERCENTAGE DEGRADATION 10.72 PARTICLE DIAMETER 0.7000E-01 CM									

TABLE 4.14

OBSERVED RESULTS
CHLORIDE SOLUTION - HYDROXIDE RESIN

SERIES	GROUP	RUN	BREAKTHROUGH CURVE OBSERVED MID POINT VOLUME	BREAKTHROUGH CURVE OBSERVED MID POINT SLOPE	BREAKTHROUGH CURVE CALCULATED MID POINT SLOPE	SPECIFIC SOLUTION FLOW RATE	RADIUS OF ACTUAL PARTICLE	DIFFUSION COEFFICIENTS IN PARTICLE	DIFFUSION COEFFICIENTS IN FILM
			ML	1/SEC	1/SEC	ML/SEC	CM	CM*CM/SEC	CM*CM/SEC
7	4	16	0.267E 03	0.238E-01	0.238E-01	0.185E 00	0.350000E-01	0.118 E-04	0.214 E-04
7	4	17	0.262E 03	0.186E-01	0.186E-01	0.285E 00	0.350000E-01	0.118 E-04	0.214 E-04
7	4	18	0.254E 03	0.134E-01	0.134E-01	0.506E 00	0.350000E-01	0.118 E-04	0.214 E-04
7	4	19	0.249E 03	0.803E-02	0.803E-02	0.119E 01	0.350000E-01	0.118 E-04	0.214 E-04
7	4	20	0.248E 03	0.542E-02	0.542E-02	0.223E 01	0.350000E-01	0.118 E-04	0.214 E-04
CONCENTRATION 0.101 N TEMPERATURE 19.50 C PERCENTAGE DEGRADATION 0. PARTICLE DIAMETER 0.7000E-01 CM									
7	5	21	0.286E 03	0.248E-01	0.248E-01	0.187E 00	0.350000E-01	0.141 E-04	0.214 E-04
7	5	22	0.288E 03	0.198E-01	0.198E-01	0.279E 00	0.350000E-01	0.141 E-04	0.214 E-04
7	5	23	0.293E 03	0.141E-01	0.141E-01	0.503E 00	0.350000E-01	0.141 E-04	0.214 E-04
7	5	24	0.295E 03	0.838E-02	0.838E-02	0.120E 01	0.350000E-01	0.141 E-04	0.214 E-04
7	5	25	0.259E 03	0.669E-02	0.669E-02	0.173E 01	0.350000E-01	0.141 E-04	0.214 E-04
CONCENTRATION 0.101 N TEMPERATURE 19.50 C PERCENTAGE DEGRADATION 3.74 PARTICLE DIAMETER 0.7000E-01 CM									
7	6	26	0.238E 03	0.263E-01	0.263E-01	0.196E 00	0.350000E-01	0.232 E-04	0.214 E-04
7	6	27	0.256E 03	0.217E-01	0.217E-01	0.275E 00	0.350000E-01	0.232 E-04	0.214 E-04
7	6	28	0.234E 03	0.138E-01	0.138E-01	0.607E 00	0.350000E-01	0.232 E-04	0.214 E-04
7	6	29	0.251E 03	0.898E-02	0.898E-02	0.124E 01	0.350000E-01	0.232 E-04	0.214 E-04
7	6	30	0.240E 03	0.633E-02	0.633E-02	0.216E 01	0.350000E-01	0.232 E-04	0.214 E-04
CONCENTRATION 0.101 N TEMPERATURE 19.50 C PERCENTAGE DEGRADATION 10.72 PARTICLE DIAMETER 0.7000E-01 CM									

TABLE 4.15

OBSERVED RESULTS
CHLORIDE RESIN - HYDROXIDE SOLUTION

SERIES	GROUP	RUN	BREAKTHROUGH CURVE OBSERVED MID POINT VOLUME	OBSERVED MID POINT SLOPE	CALCULATED MID POINT SLOPE	SPECIFIC SOLUTION FLOW RATE	RADIUS OF ACTUAL PARTICLE	DIFFUSION COEFFICIENTS IN PARTICLE	IN FILM
			ML	1/SEC	1/SEC	ML/SEC	CM	CM*CM/SEC	CM*CM/SEC
8	4	16	0.242E 03	0.295E-01	0.295E-01	0.179E 00	0.350000E-01	0.390E-05	0.174E-04
8	4	17	0.221E 03	0.235E-01	0.235E-01	0.267E 00	0.350000E-01	0.390E-05	0.174E-04
8	4	18	0.213E 03	0.164E-01	0.164E-01	0.497E 00	0.350000E-01	0.390E-05	0.174E-04
8	4	19	0.213E 03	0.843E-02	0.843E-02	0.147E 01	0.350000E-01	0.390E-05	0.174E-04
8	4	20	0.219E 03	0.763E-02	0.763E-02	0.172E 01	0.350000E-01	0.390E-05	0.174E-04
CONCENTRATION 0.101 N TEMPERATURE 19.50 C PERCENTAGE DEGRADATION 17.45 PARTICLE DIAMETER 0.7000E-01 CM									
8	5	21	0.201E 03	0.291E-01	0.291E-01	0.214E 00	0.350000E-01	0.441E-05	0.174E-04
8	5	22	0.201E 03	0.263E-01	0.263E-01	0.257E 00	0.350000E-01	0.441E-05	0.174E-04
8	5	23	0.197E 03	0.191E-01	0.191E-01	0.446E 00	0.350000E-01	0.441E-05	0.174E-04
8	5	24	0.201E 03	0.107E-01	0.107E-01	0.117E 01	0.350000E-01	0.441E-05	0.174E-04
8	5	25	0.197E 03	0.740E-02	0.740E-02	0.209E 01	0.350000E-01	0.441E-05	0.174E-04
CONCENTRATION 0.101 N TEMPERATURE 19.50 C PERCENTAGE DEGRADATION 23.69 PARTICLE DIAMETER 0.7000E-01 CM									

TABLE 4.16

OBSERVED RESULTS
HYDROXIDE RESIN - CHLORIDE SOLUTION

SERIES	GROUP	RUN	BREAKTHROUGH CURVE OBSERVED MID POINT VOLUME	BREAKTHROUGH CURVE OBSERVED MID POINT SLOPE	BREAKTHROUGH CURVE CALCULATED MID POINT SLOPE	SPECIFIC SOLUTION FLOW RATE	RADIUS OF ACTUAL PARTICLE	DIFFUSION COEFFICIENTS IN PARTICLE	DIFFUSION COEFFICIENTS IN FILM
			ML	1/SEC	1/SEC	ML/SEC	CM	CM*CM/SEC	CM*CM/SEC
8	1	1	0.200E 03	0.388E-01	0.388E-01	0.178E 00	0.350000E-01	0.285E-04	0.214E-04
8	1	2	0.198E 03	0.316E-01	0.316E-01	0.265E 00	0.350000E-01	0.285E-04	0.214E-04
8	1	3	0.200E 03	0.228E-01	0.228E-01	0.497E 00	0.350000E-01	0.285E-04	0.214E-04
8	1	4	0.195E 03	0.149E-01	0.149E-01	0.112E 01	0.350000E-01	0.285E-04	0.214E-04
8	1	5	0.189E 03	0.113E-01	0.113E-01	0.190E 01	0.350000E-01	0.285E-04	0.214E-04
CONCENTRATION 0.113 N TEMPERATURE 18.70 C PERCENTAGE DEGRADATION 17.45 PARTICLE DIAMETER 0.7000E-01 CM									
8	2	6	0.181E 03	0.438E-01	0.438E-01	0.171E 00	0.350000E-01	0.281E-04	0.214E-04
8	2	7	0.176E 03	0.303E-01	0.303E-01	0.349E 00	0.350000E-01	0.281E-04	0.214E-04
8	2	8	0.175E 03	0.257E-01	0.257E-01	0.479E 00	0.350000E-01	0.281E-04	0.214E-04
8	2	9	0.176E 03	0.160E-01	0.160E-01	0.117E 01	0.350000E-01	0.281E-04	0.214E-04
8	2	10	0.177E 03	0.126E-01	0.126E-01	0.184E 01	0.350000E-01	0.281E-04	0.214E-04
CONCENTRATION 0.113 N TEMPERATURE 18.70 C PERCENTAGE DEGRADATION 23.69 PARTICLE DIAMETER 0.7000E-01 CM									

latter changes during ion exchange, so also does the selectivity coefficient. In a binary ionic system, where the resin is initially circulated with one ion, three cases must be considered during exchange, depending upon the relation between the assumed constant value and the actual varying selectivity coefficient.

Case a) The selectivity coefficient varies as shown in Fig. 4.7a and the maximum value is taken as the assumed constant value.

Gilliland and Baddour's model (equation,4.8a) shows that the slope of the breakthrough curve at any time decreases with decreasing selectivity coefficient. The breakthrough curve is another name for the effluent concentration history curve. The difference between the observed curve (broken line), and the predicted curve (full line) based on a constant selectivity coefficient is shown in Fig. 4.7a. In the early stages of exchange, the slope of the observed curve is smaller than that of the predicted curve. Later the slopes become equal. In the present work, the selectivity coefficient has a 5% variation as shown in Fig. 4.8 and is independent of the fractional ionic conversion over the upper part of its range, so the assumption of a constant value equal to the maximum is useful.

Case b) The selectivity coefficient varies as in Fig.4.7b and the assumed constant value is taken to be the minimum value.

The effect on the breakthrough curve is as shown in

FIG 4.7

EFFECT OF A VARIABLE SELECTIVITY COEFFICIENT ON THE BREAKTHROUGH CURVE PREDICTED BY A MODEL BASED ON A CONSTANT SELECTIVITY COEFFICIENT.

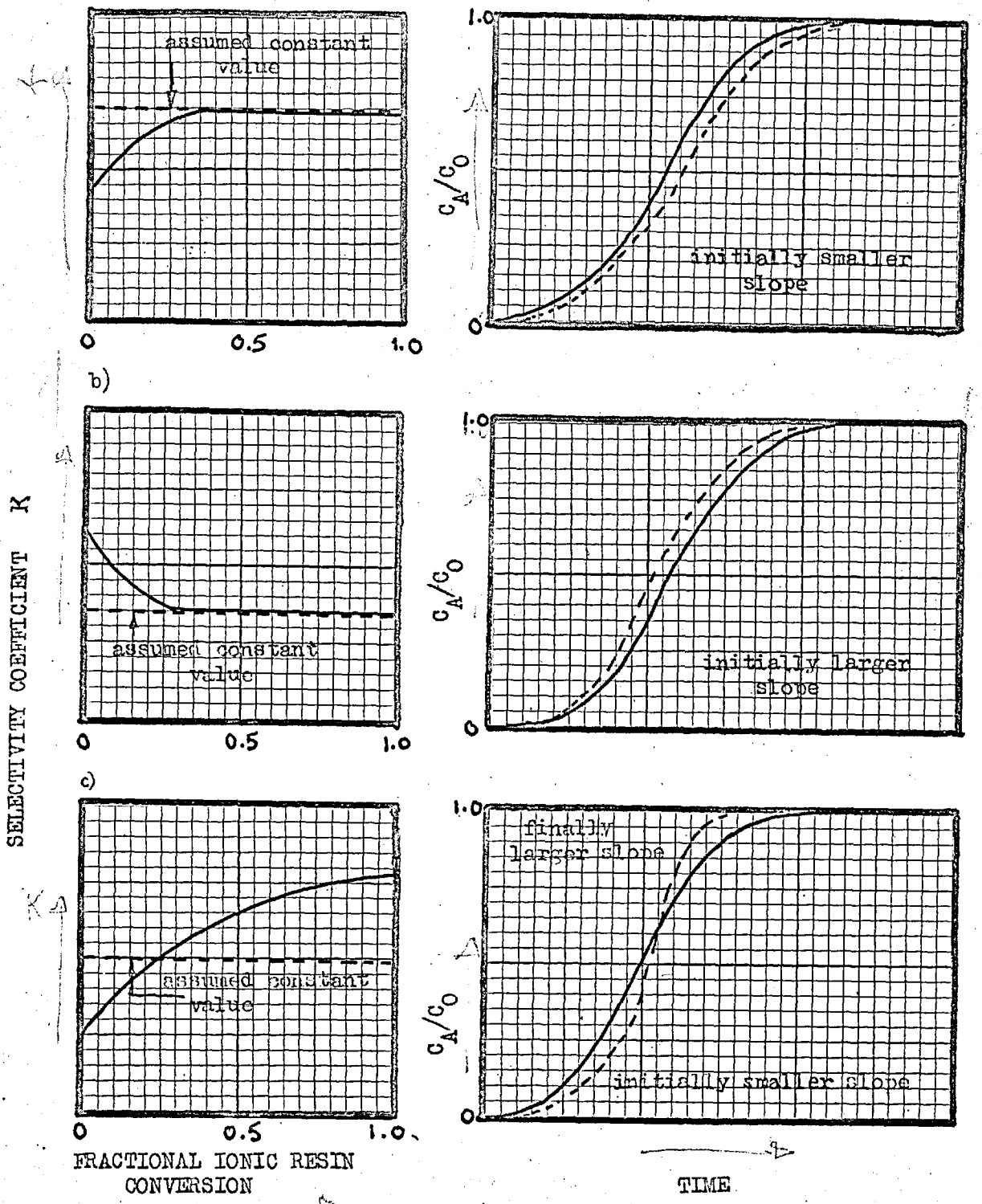

label

FIG 4.8

SELECTIVITY COEFFICIENT VERSUS IONIC COMPOSITION OF THE RESIN
DEACIDITE FF-HYDROXIDE, 20-30 MESH, 7-9% CROSSLINKED.
UNHEATED SAMPLE INITIALLY SATURATED WITH CHLORIDE IONS.
CONCENTRATON 0.1 N, TEMPERATURE 20°C.

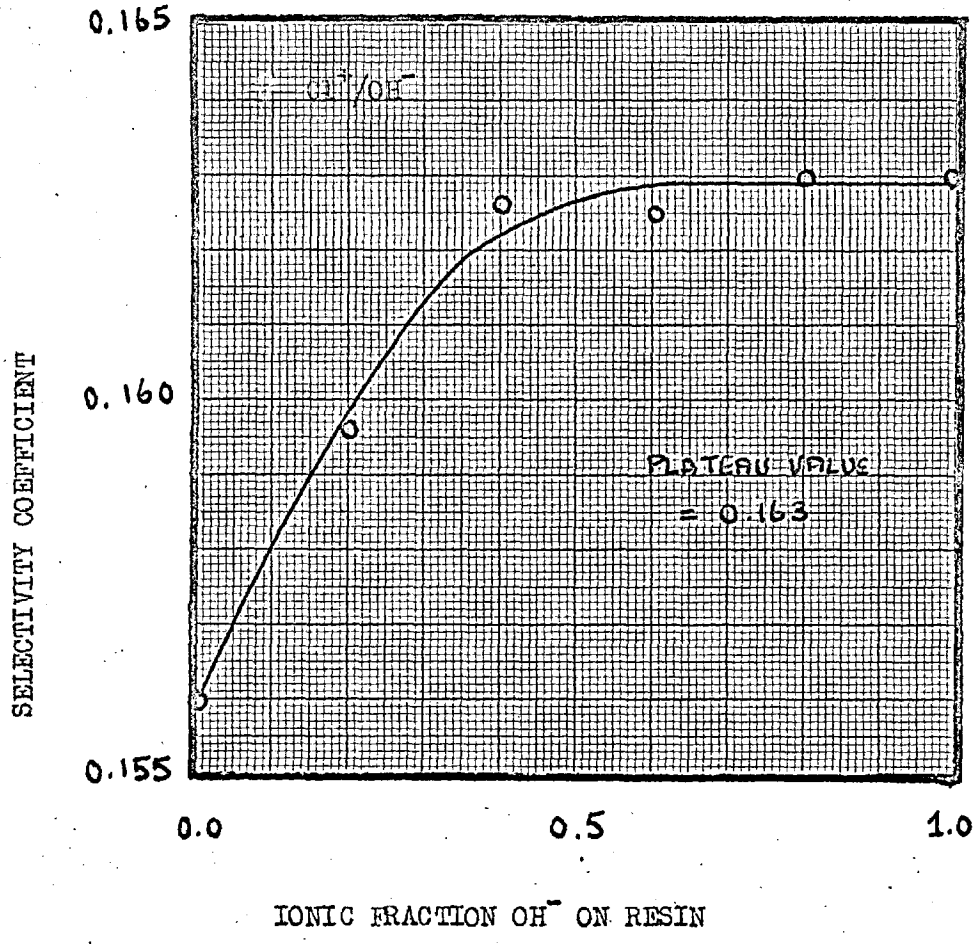

Fig. 4.7b. The observed curve (broken line) at first has a greater slope than is predicted, and later attains the predicted slope.

Case c) The selectivity coefficient varies as in Fig.4.7c and the assumed constant value is an average of the maximum and minimum values.

The difference between the predicted and observed breakthrough curves is shown in Fig. 4.7c. These two curves do not necessarily cross. The assumption should be used where the graph of selectivity coefficient against ionic fraction on the resin shows no regions of constant selectivity coefficient.

A sample experiment on the system used in this work is shown in Fig 4.8. It can be seen that the preference of the resin for the hydroxide ion increases with increasing saturation of the resin phase. This trend was assumed in all the cases of exchange treated in this work and the selectivity coefficient was assumed to have a constant value equal to the maximum value.

4.3.5. Effect of a varying diffusion coefficient on the breakthrough curve predicted assuming a constant value.

Equations 4.5 and 4.8 may be combined to give 4.11.

$$\frac{b\epsilon}{k_{kin}Q(1-\epsilon)} = \frac{1}{A}\left[\frac{1}{k_L} + \frac{C_0 d_0^2}{4\pi^2 D D_P}\right] \qquad \text{--- 4.11}$$

Equation 4.11 indicates that the velocity constant and hence the slope of the breakthrough curve increases with increasing particle diffusion coefficient. This effect becomes important when $C_0 d_0^2/4\pi^2 D D_P$ is comparable to

or greater than $1/k_L$. Because of the factor d_o^2 in the particle diffusion term, variation of the particle diffusion coefficient has greatest effect on the mid point slope for large particles.

Helfferich (ref.H9) states that the particle-diffusion coefficient for binary exchange , when ion A is diffusing into resin initially saturated with a faster moving ion B, decreases with increasing saturation of the resin by ion A. The effect of this change in diffusion coefficient on the slope of the breakthrough curve, calculated with a constant average value is shown in Fig. 4.9.

4.4 Results and discussion.

4.4.1. Diffusion coefficient in the particle phase.

a) Diffusion coefficients of the counter ion.

Experimental changes of the diffusion coefficient with external solution concentration , nature of the diffusing species, temperature, degree of resin crosslinking and percentage loss in strong base capacity caused by thermal degradation were examined.

i. Dependence on external solution concentration.

When the external solution concentration was increased an increase in the counter ion diffusion coefficients was observed (Fig. 4.10). The magnitude of the change was greater than that observed by other workers (ref.S6,R4,T3). It is possible that the method of calculation of particle diffusion coefficients in this work (i.e. Gilliland and Baddour's model) is responsible for the difference.

Helfferich attributes the change of particle diffusion

FIG 4.9 EFFECT OF A VARIABLE PARTICLE DIFFUSION COEFFICIENT ON THE BREAKTHROUGH CURVE PREDICTED BY A MODEL BASED ON A CONSTANT PARTICLE DIFFUSION COEFFICIENT.

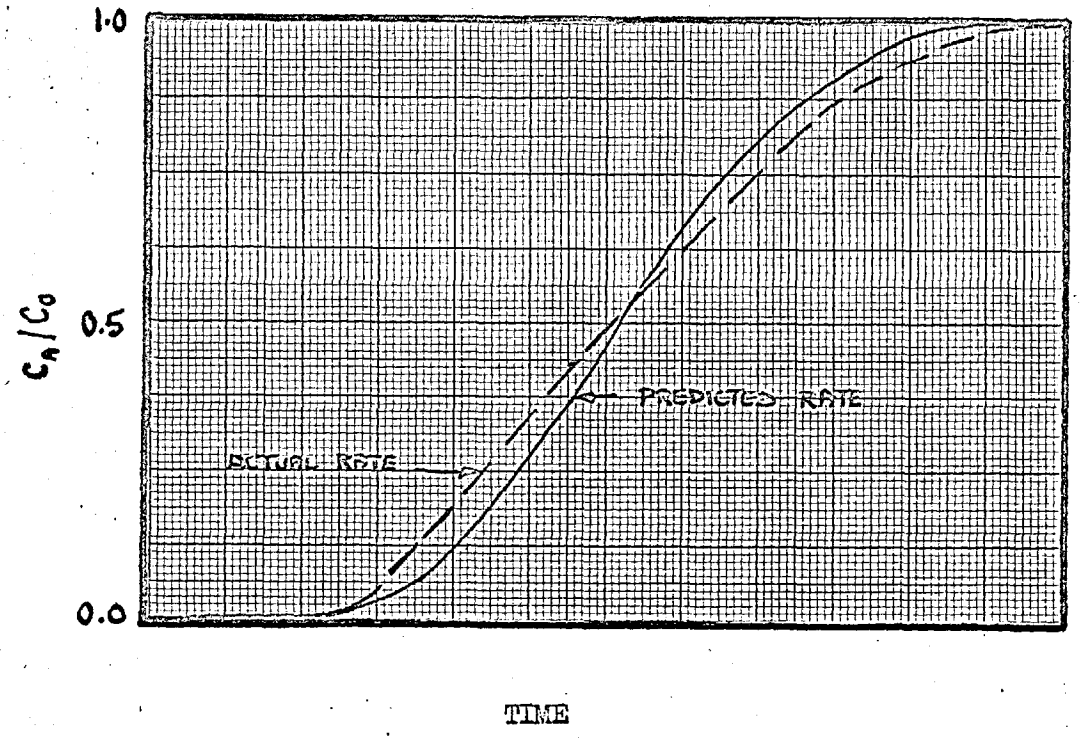

FIG 4.10

PARTICLE DIFFUSION COEFFICIENTS VERSUS EXTERNAL SOLUTION CONCENTRATION.
DEACIDITE FF-HYDROXIDE AND CHLORIDE
20-30 MESH, 7-9% CROSSLINKING,
UNHEATED SAMPLE.
TEMPERATURE 18.5°C.

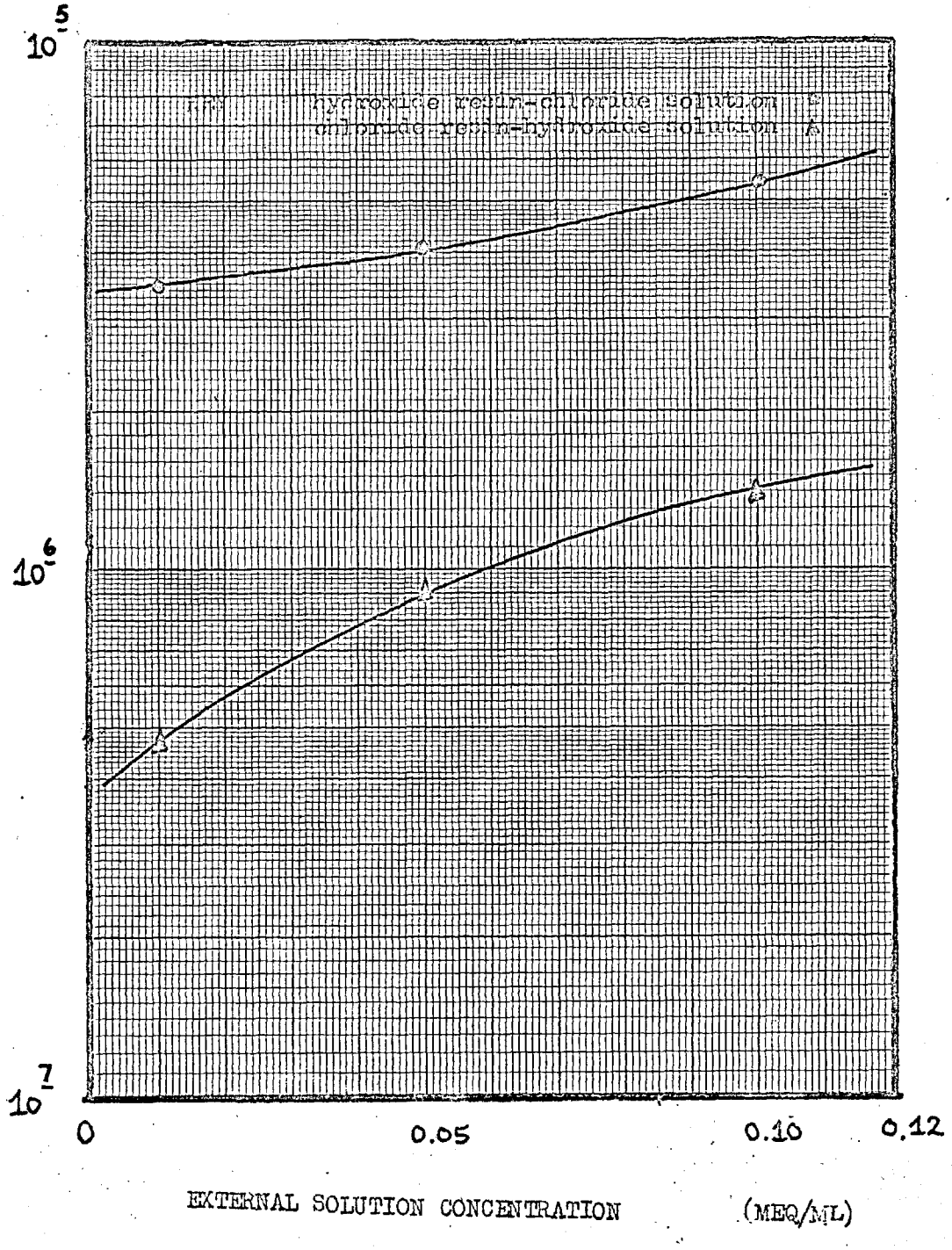

coefficients with external solution concentration to the increased concentration of the co ion in the pores of the resin particles.

ii. Dependence on temperature.

Increased temerature was found to cause an increase in the diffusion coefficient (Fig 4.11 and 4.12). This is probably due to the weakening of specific and electrostatic retardation of the counter ions and reduction of solvation and hence ionic size. Activation energies are given in Table 4.17, and lie in the accepted range below 10 kcal/mole.

iii. Dependence on degree of resin crosslinking .

Diffusion coefficients were found to be higher in the less crosslinked sample (Fig 4.11 and 4.12). Boyd and Soldano (Ref.B8) observed the same effect. Evidently the more open matrix structure in the less crosslinked resin increases the ease with which any species may diffuse through the particle.

iv. Effect of loss of strong base capacity by thermal degradation.

The change in diffusion coefficients with thermal degradation is shown in Fig. 4.13 in terms of the loss in total capacity. It can be seen that a maximum value in the 7-9% crosslinked sample occurs when the total capacity is approximately 3.0 meq/g. for resin initially saturated with hydroxide ions, and at about 2.75 meq/g. for resins initially saturated with chloride ions. Similar maxima may occur at slightly higher values of total capacity in the 2-3% cross linked samples. These observations

FIG 4.11

PARTICLE DIFFUSION COEFFICIENTS VERSUS TEMPERATURE.
DEACIDITE FF-HYDROXIDE AND CHLORIDE.
20-30 MESH, 2-3% CROSSLINKING,
UNHEATED SAMPLE.
EXTERNAL SOLUTION CONCENTRATION 0.1 N.

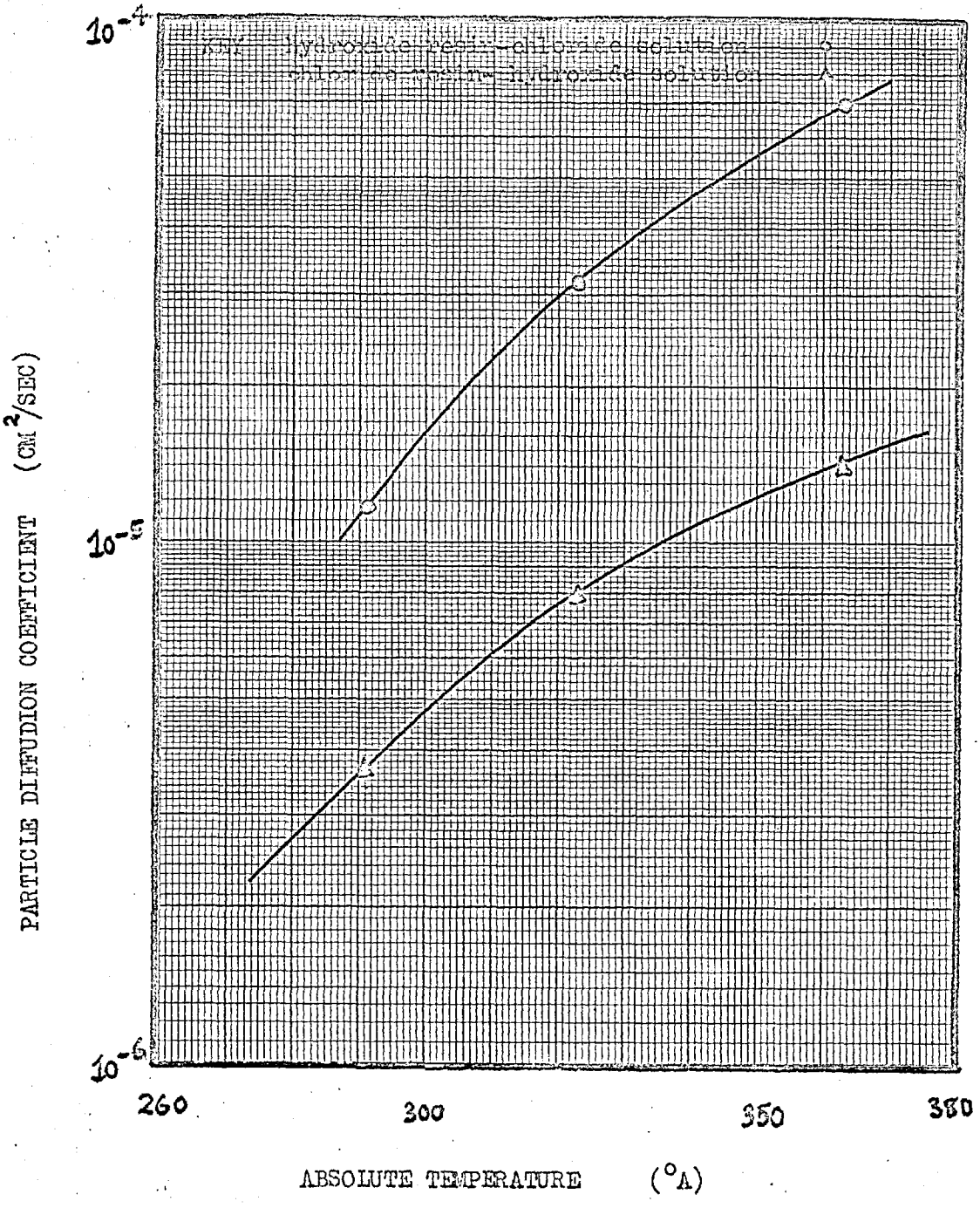

FIG 4.12

PARTICLE DIFFUSION COEFFICIENTS VERSUS TEMPERATURE.
DEACIDITE FF-HYDROXIDE AND CHLORIDE
20-30 MESH, 7-9% CROSSLINKING,
UNHEATED SAMPLE.
EXTERNAL SOLUTION CONCENTRATION 0.1 N.

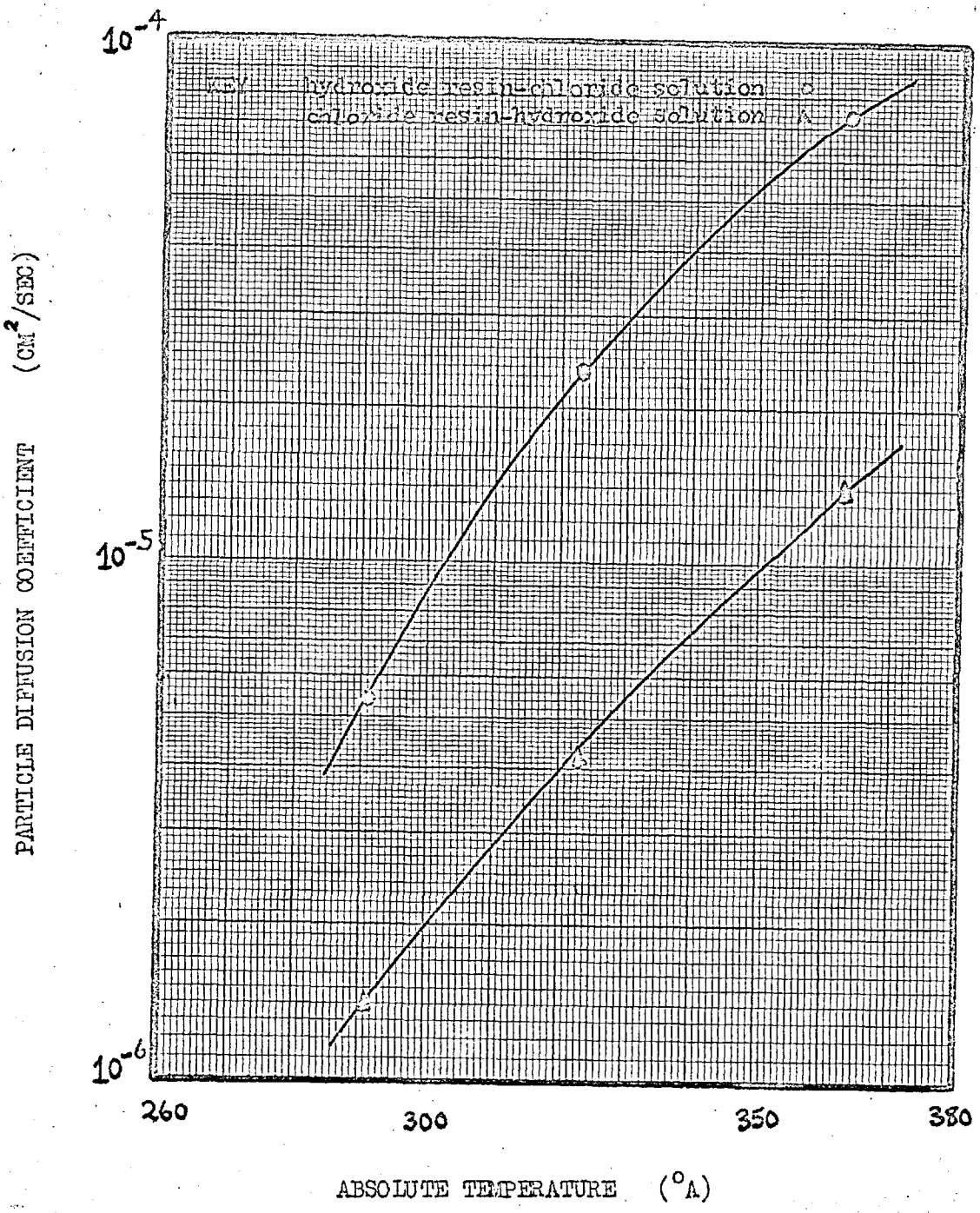

TABLE 4.17 ACTIVATION ENERGIES FOR DIFFUSION IN THE PARTICLE DEACIDITE FF. 20-30 MESH. UNDEGRADED SAMPLES. SOLUTION CONCENTRATION 0.1N.

	RESIN INITIALLY SATURATED WITH HYDROXIDE	RESIN INITIALLY SATURATED WITH CHLORIDE
2-3% CROSSLINKED	5.20 KCAL/MOLE	7.78 KCAL/MOLE
7-9% CROSSLINKED	4.01 KCAL/MOLE	5.90 KCAL/MOLE

are consistent with Creed (ref.C1) who observed the same effect in self diffusion experiments with Deacidite FF and bromide ions from sodium bromide solution. Creed's maximum value occurred when approximately 2.3 meq/g strong base capacity (3.0 meq/g total capacity) remained on the resin samples. Creed found that degradation by heat and radiation produced approximately the same maximum.

Boyd and Soldano (ref. B12) varied the total capacity of sulphonated styrene type cation exchangers by partial thermal desulphonation and found maxima in the curves of self diffusion coefficient versus capacity for various ions. The positions of the maxima were found to be substantially independent of the degree of crosslinking in the resin used. However, as the authors point out, their procedure for varying the capacity is likely to effect the degree of crosslinking and swelling in the resin.

In thermal decomposition at 90°C, it has been observed that no significant change in water regain takes place over a 70 day heating period, and hence it is unlikely that changes in crosslinking and swelling take place to any appreciable extent.

Any changes in the diffusion coefficients within the particle must be caused only by changes in capacity. In addition Creed's work shows that when samples were degraded by radiation, a process which affects the degree of crosslinking, the maxima occurred at the same value of strong base capacity as in thermally degraded samples. The inference again is that capacity changes are the prime

reason for changes in diffusion coefficients during thermal degradation.

Boyd and Soldano (ref.B12) also observe that the maxima occurred at different values of total capacity for self diffusion of different ions, although the difference was small. In the present work the positions of the maxima were also found to vary, slightly dependent upon the ion initially saturating the resin. The magnitude of these differences is such as to throw doubt on their significance.

The reason for the existense of maxima can be explained as follows. Initially a decrease in capacity results in an increase in diffusion coefficients because of the decrease in electrostatic retardation of the diffusing ions. Eventually the decrease in capacity reaches a point where insufficient functional sites are available to react with the entering ions as quickly as they can diffuse inwards. The rate of exchange then becomes controlled by the rate of the chemical reaction of exchange.

If this explanation is correct, reaction rate models such as that of Gilliland and Baddour should fit experimental breakthrough curves with greater accuracy after the maximum in the diffusion coefficient curve has been passed. Fig.4.14 and 4,15 show a series of comparison plots. The improvement in agreement between observed and predicted curves is clearly shown. The velocity constant of a second order reaction becomes valid after the maximum has been passed and is a better way of describing the rate of exchange than the diffusion coefficients.

FIG 4.13

PARTICLE DIFFUSION COEFFICIENTS VERSUS DEGRADATION.
DEACIDITE FF-HYDROXIDE AND CHLORIDE
20-30 MESH, UNHEATED SAMPLES
EXTERNAL SOLUTION CONCENTRATION 0.1 N.
TERMPERATURE 18.5°C.

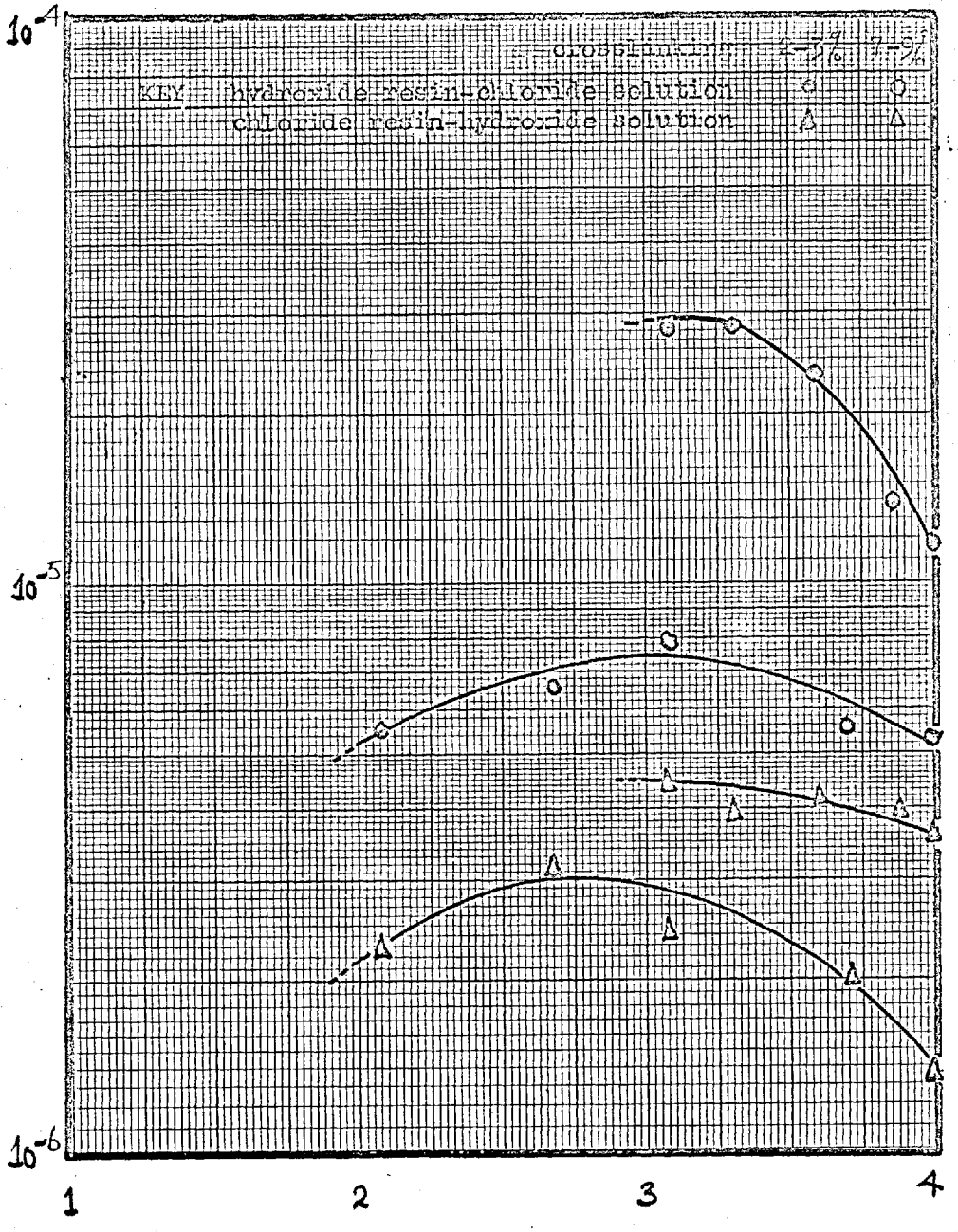

FIG 4.14

COMPARISON OF PREDICTED AND EXPERIMENTAL CURVES AT VARYING PERCENTAGE THERMAL DECOMPOSITION.
DEACIDITE FF - CHLORIDE, 20-30 MESH, 7-9% CROSSLINKING,
EXTERNAL SOLUTION CONCENTRATION 0.1 N SODIUM HYDROXIDE.
SUPERFICIAL FLOW RATE 1.80 CM/SEC.

SERIES 4 RUN 5
PERCENTAGE DEGRADATION 0.00

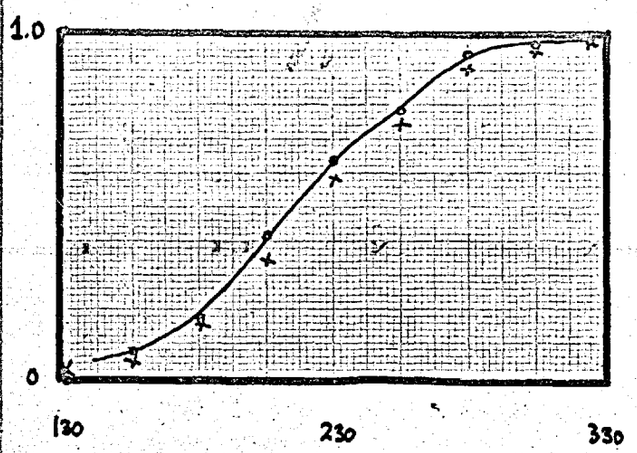

SERIES 4 RUN 10
PERCENTAGE DEGRADATION 7.20

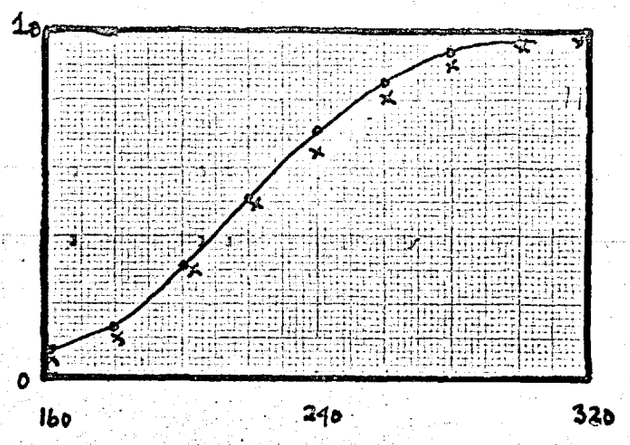

SERIES 4 RUN 15
PERCENTAGE DEGRADATION 23.60

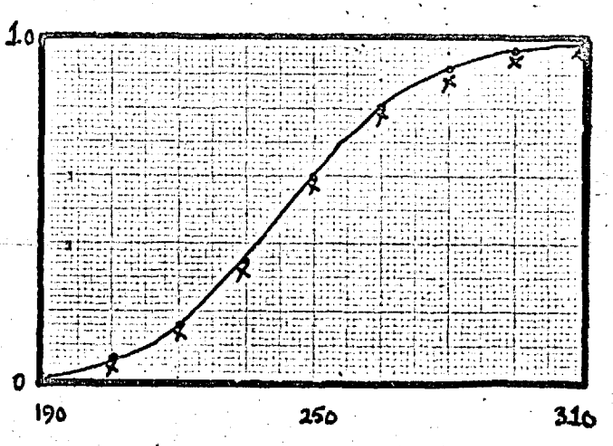

VOLUME OF SOLUTION FED TO COLUMN (ML)

SERIES 5 RUN 5
PERCENTAGE DEGRADATION 33.10

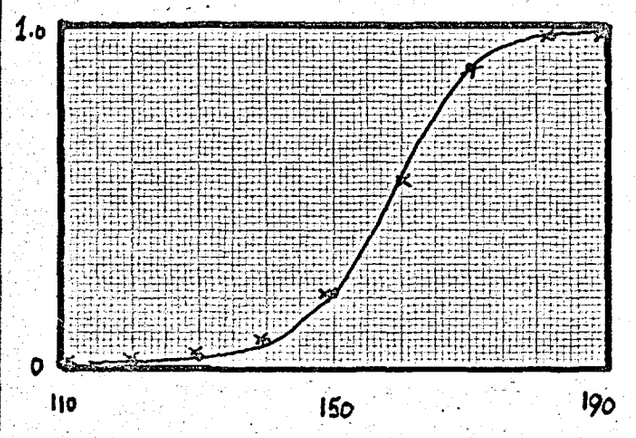

SERIES 5 RUN 10
PERCENTAGE DEGRADATION 48.60

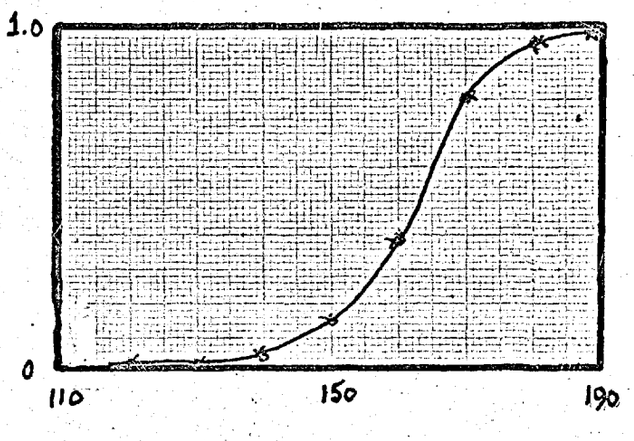

KEY observed x
predicted •

VOLUME OF SOLUTION FED TO COLUMN (ML)

FIG 4.15

COMPARISON OF PREDICTED AND EXPERIMENTAL CURVES AT VARYING PERCENTAGE THERMAL DECOMPOSITION.
[illegible] ACIDITE FF -HYDROGEN, 20-30 MESH, 7-9% CROSSLINKING,
EXTERNAL SOLUTION CONCENTRATION 0.1 N HYDROCHLORIC ACID.
SUPERFICIAL FLOW RATE 0.18 CM/SEC.

SERIES 4 RUN 15
PERCENTAGE DEGRADATION 0.00

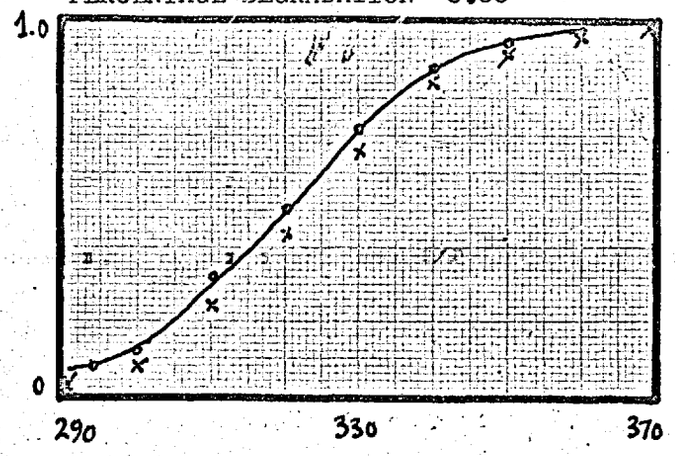

SERIES 4 RUN 21
PERCENTAGE DEGRADATION 7.20

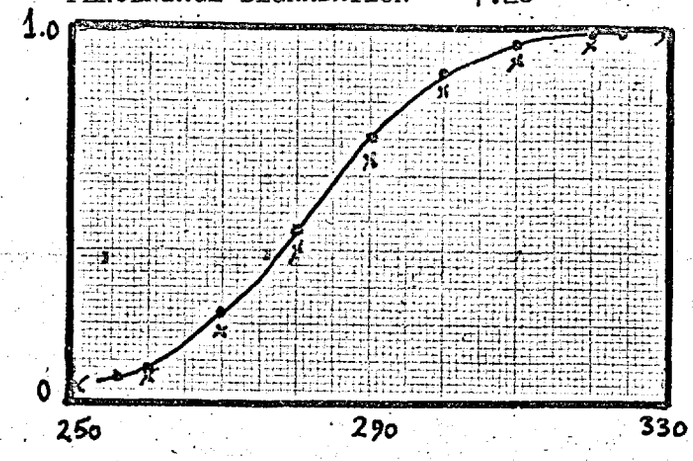

SERIES 4 RUN 26
PERCENTAGE DEGRADATION 23.60

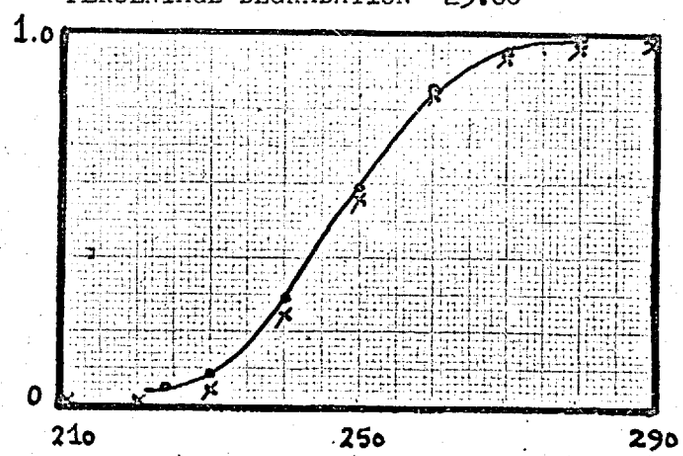

VOLUME OF SOLUTION FED TO COLUMN (ML)

SERIES 5 RUN 15
PERCENTAGE DEGRADATION 33.10

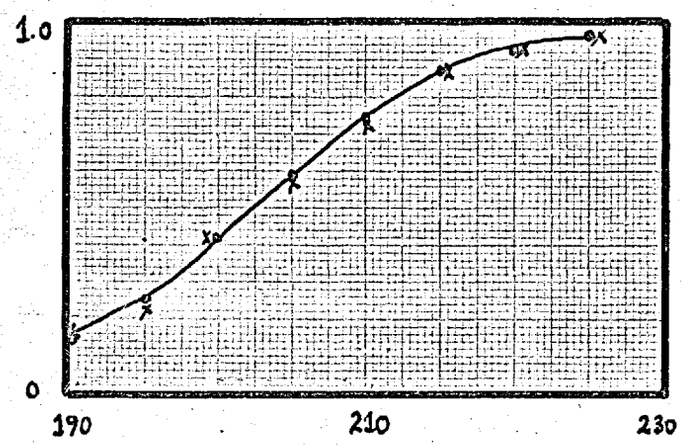

SERIES 5 RUN 21
PERCENTAGE DEGRADATION 48.60

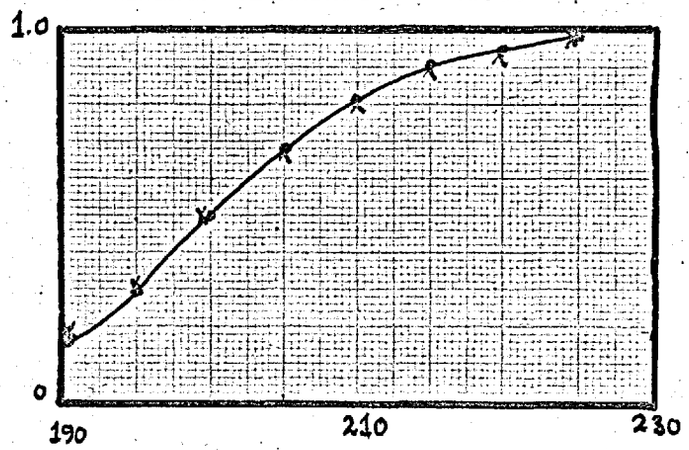

KEY observed x
predicted •

VOLUME OF SOLUTION FED TO COLUMN (ML)

Although no data is available for direct comparison of the present results, the difference between values of diffusion coefficients found in the present work for hydroxide and chloride ions and Creed's (ref.C1) value for bromine or Boyd and Soldano's (ref.B9) values for bromine is consistent with expectation. The hydroxide ion mobility measured in aqueous solution at infinite dilution is considerably greater than that of the bromide ion, whereas chloride and bromide are comparable. Hence the hydroxide ion would be expected to diffuse more rapidly than bromide and chloride within the resin matrix. The rate of ion exchange has been found to be faster when the resin is initially saturated with the faster moving ion (ref. H8) and this is confirmed by the results of this work, although the difference in measured diffusion coefficients is less than one might expect from the mobilities of the ions in solution. This is not altogether surprising in view of the uncertainty as to the degree of ionic solvation within the resin phase and as to the effects of the tortuosity of the pores and specific interactions of different ionic species with the resin matrix.

4.4.2. Diffusion coefficient in the fluid phase.

Diffusion coefficients of electrolytes can be predicted very accurately at infinite dilution using equation 4.12.

$$D_L^{\infty} = 8.931 \times 10^{-10} T \left[\frac{l_+^{\infty} l_-^{\infty}}{\Lambda_{\infty}} \right] \left[\frac{z_+ + z_-}{z_+ z_-} \right] \qquad \text{--- 4.12}$$

due to Nernst (ref.N1). At concentrations other than infinite dilution, Gordon (ref.G4) has derived an equation for the correction of the values at infinite dilutions. Unfortunately fundamental data for this equation is scarce so its use is limited severely.

Equation 4.12 was used to calculate diffusion coefficients at infinite dilution for solutions of hydrochloric acid and sodium hydroxide at the temperatures used in this work.

In general the decrease in diffusion coefficient as the concentration is increased to 1.0 N from infinite dilution is less than 10% of the value at infinite dilution (ref.G5). Therefore an approximate predicted value can be obtained for pure solutions at concentrations other than infinite dilutions. However, in actual binary ion exchange systems the fluid phase is generally a mixture of four ionic species, and diffusion coefficients must therefore differ from those predicted for those of pure solutions. The diffusion of faster species will tend to be retarded by the presence of slower species although the difference is unlikely to be large since ionic mobilities are generally of the same order of magnitude.

In Fig. 4.16 experimental values of liquid phase diffusion coefficients at several concentrations are shown for hydrochloric acid and sodium hydroxide.

In Fig.4.17 experimental variations in liquid phase diffusion coefficients with temperature and the nature of electrolyte are compared with the predicted value at

FIG 4.16 DIFFUSION COEFFICIENTS OF IONS IN THE EXTERNAL SOLUTION (FILM DIFFUSION COEFFICIENTS) VERSUS CONCENTRATION OF THE EXTERNAL SOLUTION. TEMPERATURE 18.5°C.

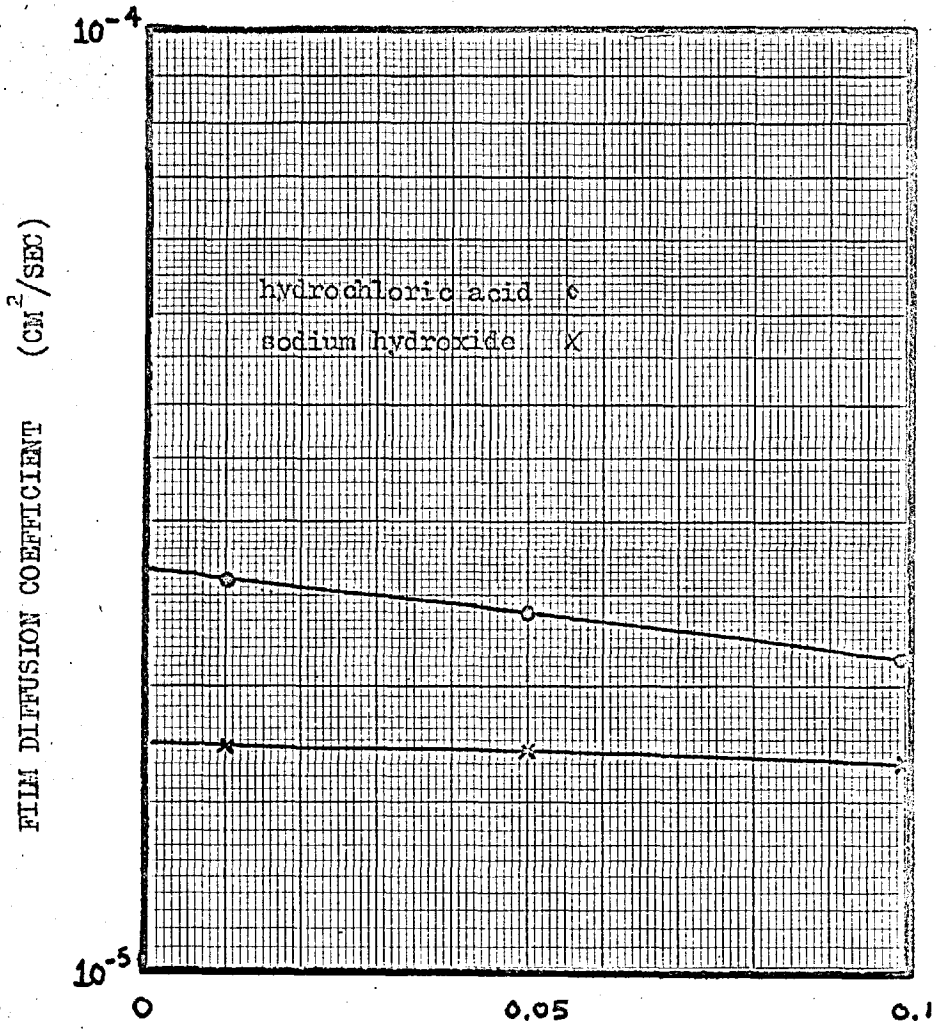

FIG 4.17 DIFFUSION COEFFICIENTS OF IONS IN THE EXTERNAL SOLUTION (FILM DIFFUSION COEFFICIENTS) VERSUS TEMPERATURE.
EXTERNAL SOLUTION CONCENTRATION 0.1 N.

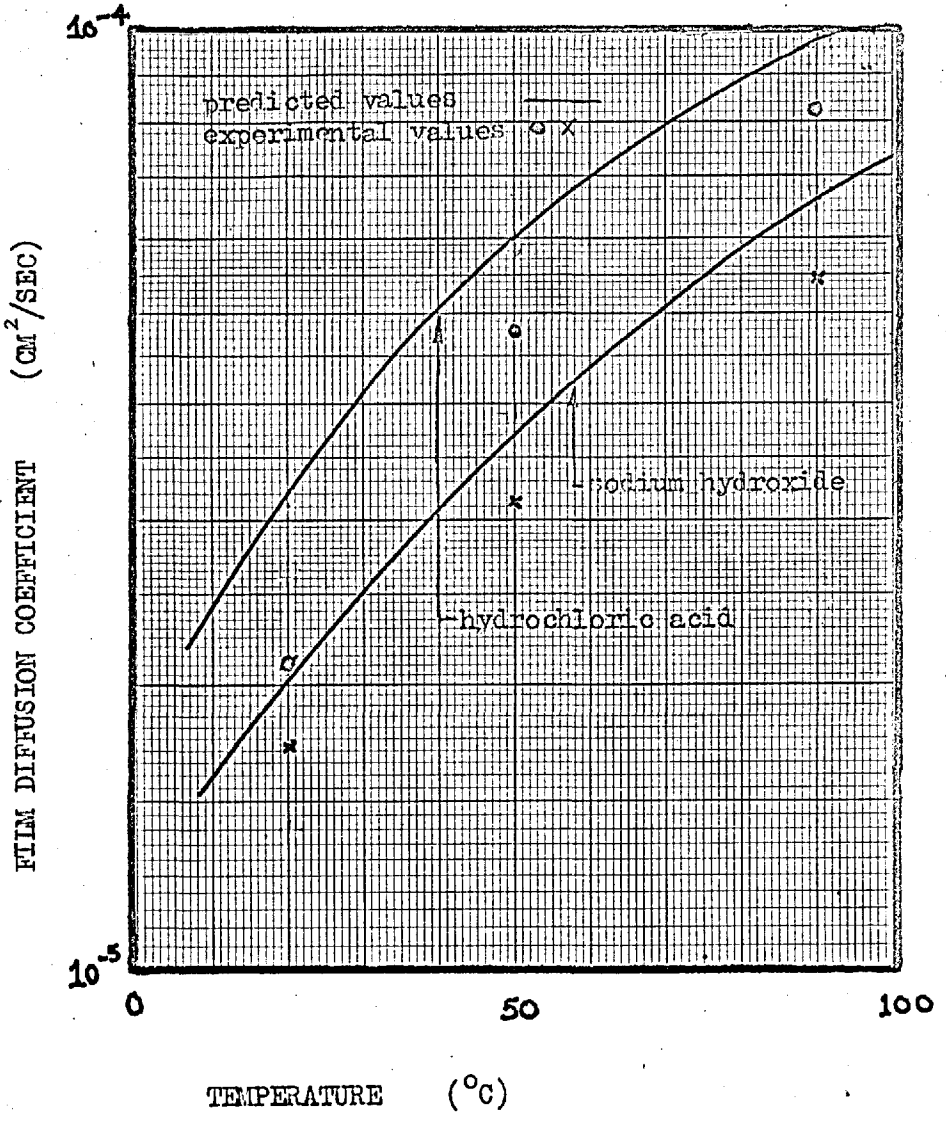

inifinite dilution based on the pure electrolyte entering the column. It can be seen that the experimental values lie reasonably close to the predicted value at infinite dilution and are generally within 10% of the latter. Activation energies for liquid diffusion were found to lie between 3 and 6 kcal/mole. as generally accepted.

4.4.3. Selectivity coefficients.

i, Dependence on temperature.

Generally ion exchange occurs with little evolution of heat and therefore only small changes in equilibrium would be expected as the temperature increases. Activation energies are usually smaller than 2 kcal/mole. (ref.K1). In this work (Fig 4.18) a small change in selectivity coefficient was observed with activation energies of -2.14 and 2.26 kcal/mole. For resin initially in the hydroxide and chloride forms respectively. The effect was substantially independent of the degree of resin crosslinking. In the hydroxide chloride system, the unfavoured hydroxide ion becomes more favoured as temperature increases; the opposite is true of the chloride ion.

ii. The effect of degree of crosslinking and external solution concentration.

Fig. 4.18 shows experimental selectivity coefficients at various temperatures for Deacidite FF resin with 2-3% and 7-9% crosslinking. Selectivity is found to decrease with increasing degree of crosslinking. The effect of varying the external solution concentration is shown in Table 4.20 for 7-9% crosslinked resin. An increase in dilution of the

FIG 4.18 SELECTIVITY COEFFICIENTS VERSUS TEMPERATURE
DEACIDITE FF-HYDROXIDE AND CHLORIDE
20-30 MESH.
UNHEATED SAMPLE.
EXTERNAL SOLUTION CONCENTRATION 0.1 N.
0.8 MOLE FRACTION OF CHLORIDE ION ON THE RESIN.

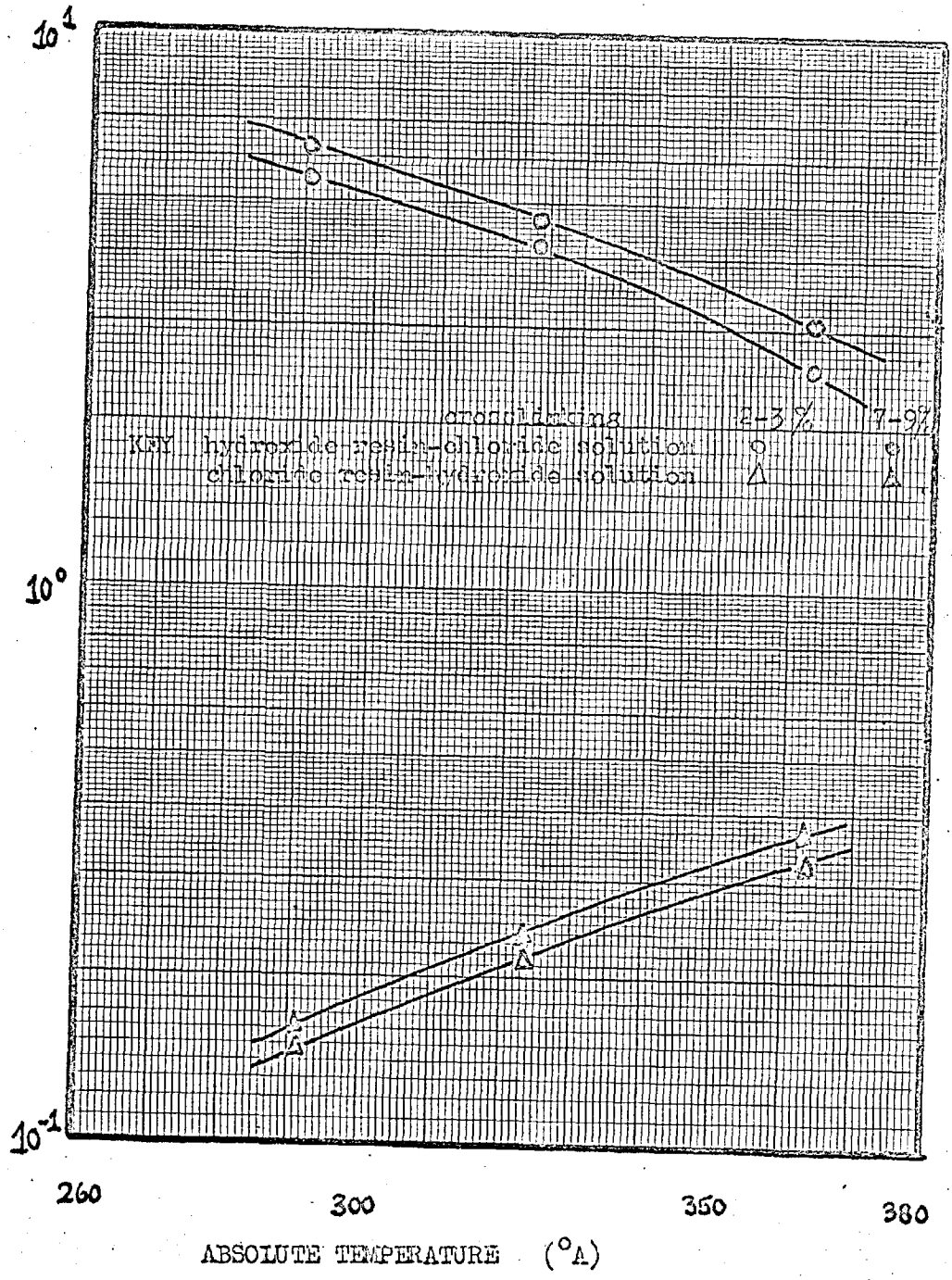

TABLE 4.18 ACTIVATION ENERGIES FOR DIFFUSION IN THE EXTERNAL SOLUTION. SOLUTION CONCENTRATION 0.1N.

EXTERNAL SOLUTION	ACTIVATION ENERGY
HYDROCHLORIC ACID	3.44 KCAL/MOLE
SODIUM HYDROXIDE	3.12 KCAL/MOLE

TABLE 4.19 APPARENT ENTHALPY FOR SELECTIVITY
DEACIDITE FF, 20-30 MESH, UNDEGRADED SAMPLES.
SOLUTION CONCENTRATION 0.1N
0.8 MOLE FRACTION CHLORIDE ON RESIN.

	RESIN INITIALLY SATURATED WITH HYDROXIDE	RESIN INITIALLY SATURATED WITH CHLORIDE
2-3 % CROSSLINKED	2.24 KCAL/MOLE	-2.06 KCAL/MOLE
7-9 % CROSSLINKED	2.26 KCAL/MOLE	-2.14 KCAL/MOLE

TABLE 4.20 SELECTIVITY COEFFICENTS VERSUS CONCENTRATION
DEACIDITE FF. 20-30 MESH. 7-9 %CROSSLINKED.
UNDEGRADED SAMPLES. TEMPERATURE 20° C.
0.8 MOLE FRACTION CHLORIDE ON RESIN.

	SOLUTION CONCENTRATION	SELECTIVITY COEFFICIENT
RESIN INITIALLY SATURATED WITH HYDROXIDE	0.10 N	0.163
	0.05 N	0.182
	0.01 N	0.314
RESIN INITIALLY SATURATED WITH CHLORIDE	0.10 N	5.43
	0.05 N	7.59
	0.01 N	15.63

external solution results in an increase in selectivity. Helfferich (ref.H9) attributes both these observations to the increase in swelling pressure that occurs as the degree of crosslinking and dilution of the external solution are increased. The elastic properties of the resin matrix result in a preference of the ion exchanger for the counter ion of smaller equivalent solvated volume and this tendency is pronounced when the matrix is highly strained (i.e. when the swelling pressure is high).

iii. The effect of thermal degradation.

Table 4.2I shows the change in selectivity coefficient with percentage loss in strong base capacity caused by thermal decomposition. The observed gain in selectivity is small presumably since the loss of functional groups affects both ions. The effect of ionic composition of the resin on the selectivity coefficient is shown in Fig.4.8. The observations are reasonably consistent with Gregor (ref.G1) who investigated Dowex 1. Gregor gives a detailed theoretical explanation of the reasons for the changes.

4.5 Conclusions.

An increase in the operating temperature of a binary ion exchange system leads to an increase in the diffusion coefficients and selectivity changes such that the selectivity coefficient tends to unity.

Considering firstly, changes in diffusion coefficients, it can be seen that an increase in the diffusion coefficient results in a greater mid point slope

TABLE 4.21 SELECTIVITY COEFFICIENTS VERSUS DEGRADATION
DEACIDITE FF, 20-30 MESH.
SOLUTION CONCENTRATION 0.1N, TEMPERATURE 20°C,
0.8 MOLE FRACTION CHLORIDE ON RESIN.

2-3% CROSSLINKED	TOTAL CAPACITY MEQ/G.	INITIAL FORM OF RESIN HYDROXIDE	CHLORIDE
	4.01	6.20	0.150
	3.86	6.50	0.146
	3.58	6.80	0.140
	3.31	6.94	0.138
	3.06	7.10	0.135
7-9% CROSSLINKED	4.01	5.43	0.163
	3.72	5.63	0.151
	3.06	5.81	0.131
	2.68	5.91	0.110
	2.06	6.20	0.102

at any given time, (equation 4.8b and 4.11) and a greater rate of exchange (equation 4.6). Both ions are likely to be affected to much the same extent, since activation energies for diffusion are similar. The result of these changes is an increasing sharpness of the breakthrough curve.

The favoured ion becomes less favoured as the selectivity coefficient tends to unity; the converse is true for the unfavoured ion. As a result the sharpness of breakthrough increases only for the unfavoured ion.

The nett effect of an increased operating temperature is therefore an increase in separation efficiency for the unfavoured ion, whereas the effect on the favoured ion depends on whether the diffusion or selectivity effect is stronger. In normal ion exchange the diffusion effect predominates, since activation energies for diffusion are between 3 and 5 times those for selectivity.

If separation performance alone is important, a good rule is to raise the temperature for unfavourable exchange operations. However, in most practical cases, resin lifetime and product contamination are important and the increase in separation performance must be balanced against decreased resin lifetime and product contamination caused by thermal damage to the resin.

In hydroxide resin operations thermal damage will probably restrict the maximum practicable operating temperature to less than 100°C. The effects of thermal degradation (i.e. andeventual decrease in the particle

Diffusion coefficient and an increase in selectivity) begin to offset the advantages gained in elevated temperature operation if operation is continued to high percentage degradation.

In salt forms, the maximum practical operating temperature is likely to be 200°C.

4.6 Nomenclature.

A	particle surface area per unit volume of packed column	L^{-1}
b	correction factor in equation 4.4	dimensionless
C	ionic concentration in external solution	ML^{-3}
D	distribution parameter = $Q/C_0\epsilon$	dimensionless
D_{ld}	axial dispersion coefficient	L^2T^{-1}
D_L	fluid diffusion coefficient	L^2T^{-1}
D_P	particle diffusion coefficient	L^2T^{-1}
d_0	particle diameter	L
G	term used in Gilliland and Baddour's model = $(-g(Kw,u/K))/g(w,u)$	dimensionless
$g(u,w)$ =	$0.5(1+H(\sqrt{u}+\sqrt{w}))+H'(\sqrt{u}+\sqrt{w})/4(\sqrt{u}+\sqrt{w})$	dimensionless
H	error function	dimensionless
H'	derivative or error function	dimensionless
I_1	modified first order Bessel function of the first kind	dimensionless
K	selectivity coefficient	dimensionless
$\bar{k}$	rate parameter = $k_{kin}(K-1)/K$	$M^{-1}L^3T^{-1}$
k_L	liquid film mass transfer coefficient per unit interfacial area	LT^{-1}
k_{OV}	overall mass transfer coefficient per unit interfacial area	LT^{-1}
k_P	particle mass transfer coefficient per unit interfacial area	LT^{-1}

k_{kin}	second order reaction velocity constant	$M^{-1}L^{-3}T^{-1}$
l	ionic conductance of any ion	$M^{-1}LT$
m	mass	M
n	term in series expansion	dimensionless
P	constant	
Q	ultimate volumetric capacity of resin particles	ML^{-3}
q	ionic concentration in resin	ML^{-3}
$\bar{q}$	average ionic concentration in resin	ML^{-3}
R	external solution flow rate	L^3T^{-1}
R_{ov}	overall mass transfer resistance	T
R_L	film mass transfer resistance	T
R_p	particle mass transfer resistance	T
$\bar{r}$	particle radius	L
r	radius of surface of equal concentration in a spherical particle	L
T	absolute temperature	Θ
t	real time	T
u	dimensionless parameter = $k_{kin}C_o\Theta$	
v	superficial flow rate	LT^{-1}
w	dimensionless parameter = $k_{kin}\bar{x}/Kv$	
X	term used in Fick's law equation $X=C_Ar$	ML^{-2}
x	linear distance from column entrance	L
y	volume of effluent collected	L^3

Z	term used in alternative model $= \left[(K-1)C_A/C_o\right]/(1+(K-1)C_A/C_o)$	dimensionless
z	ionic charge of an ion	dimensionless
$\bar{z}$	equilibrium capacity of the packed column	M
ϵ	void fraction in a packed bed	dimensionless
θ	time measured from time of arrival of solution front at any cross section x cm. from the column entrance = $t-x/v$	T
ϕ	denotes a functional relation	
σ	term in equations 4.8a and 4.8b $=(u/4y)2\sqrt{w/u}\ \exp(-u-w)I_1(2\sqrt{uw})/g(w,u)$	L^{-1}
ρ	fluid density	ML^{-3}
Λ	sum of ionic conductances of all species in solution $= \sum_{n=1}^{n} l^+ + \sum_{n=1}^{n} l^-$	$M^{-1}LT$
μ	fluid viscosity	$ML^{-1}T^{-1}$

Subscripts and superscripts

A	property of ion A
B	property of ion B
o	condition at column entrance
∞	value at infinite dilution
*	equilibrium value
+	cationic property

- anionic property

i conduction at interface

References

A1. Anderson R.E.,Ind. Eng. Chem., 3,(2), 85, (1964).

A2. Arden T.V., private communication.

A3. Robertson R.F.S., Anderson P.G., CRDC - 596
Out Reactor Tests of the HTP loop.

B1. Baumann E.W., J.Chem.Eng. Data., 5, 376,(1960).

B2. Bonner O.D., Pruett R.R., J.Phys.Chem., 63,1417,(1959).

B3. Beaton R.H., Furnas C.C., Ind.Eng.Chem., 33, 1500,(1941).

B4. Bauman W.C., Eichorn J., J.Am.Chem.Soc., 69, 2830,(1947).

B5. Boyd G.E., et al. J.Am.Chem.Soc., 69, 2818, (1947).

B6. British patent, 694,778., (1953).

B7. Boyd G.E., Adamson A.W., Myers L.S., J.Am.Chem.Soc., 69, 2836, (1947).

B8. Boyd G.E., Soldano B.A., J.Am.Chem.Soc., 75,6099, (1953).

B9. Boyd G.E., et al. J.Phys.Chem., 58, 456, (1954).

B10. Breden C.R., ANL-6562, Vol. II, 55.

B11. Boyd G.E., Adamson A.W., Myers L.S., J.Am.Chem.Soc. 69, 2849, (1948).

C1. Creed G.R.B., PhD Thesis., London University, (1965).

C2. Collie N., Schryver S.B., J. Chem.Soc., 57, 767, (1890).

C3. Coates J.I., Gluekauf E., J.Chem.Soc., 1308, (1947).

C4. Corrosion Data Survey., Am. Inst. Chem. Engrs.,(1959).

C5. Colburn A.P., Ind.Eng. Chem., 22, 522, (1930).

C6. Colburn A.P., Hougen O.A., Trans.Am.Inst.Chem.Engrs., 29, 174, (1933).

C7. Carman P.C., Trans.Am.Inst.Chem.Engrs., 15,150, (1937).

C8. Chilton T.H., Colburn A.P., Trans.Am.Inst.Chem.Engrs., 26, 178, (1931).

C9. Carslaw H.S., Jager J.C., Conduction of Heat in Solids, (Oxford, 1950).

D1. Dyer W.J., J. Fisheries. Research. Board.Canada., 7, 576, (1960).

D2. DeVault D., J.Am.Chem.Soc., 65,532, (1943).

D3. Demmitt T.F., HW-65478, High Flow Rate Operation of a Duplex Ion Exchange System.

D4. Dobbs H.E., J.Chromatography., 2, 572, (1959).

F1. Fisher S., Kunin R., Anal.Chem., 27, 1191, (1955).

F2. Freiling E.C., J.Am.Chem.Soc., 77, 2067, (1955).

F3. Furnas C.C., Trans.Am.Inst. Chem.Engrs., 24, 142,(1930).

F4. Faires R.A., private communication.

F5. Freeman D.H., J. Phys.Chem., 64, 1048, (1960).

G1. Gregor H.P., Belle J., Marcus R.A., J.Am.Chem.Soc., 77, 2713, (1959).

G2. Gilliland E.R., Baddour R.F., Ind.Eng.Chem., 45,330, (1953).

G3. Greer A.H., Mindler A.B., Termini J.P., Ind.Eng.Chem., 60, 166, (1958).

G4. Gordon J.B., J.Phys.Chem., 5.522, (1937).

G5. Gordon J.B., Glasstone S., Thermodynamics for Chemists, (Van Nostrand, 1947).

H1. Streat M., PhD Thesis., London University, (1961).

H2. Helfferich F., Ion Exchange, p^P 167,(McGraw Hill,1962).

H3. ibid, p^P 47-61.

H4. Hiester N.K., Vermeulen T., Chem.Eng.Prog.,48,505,(1952).

H5. Hiester N.K., et al. A.I.Ch.E.J., 2, 404, (1956).

H6. Hering B., Bliss H., A.I.Ch.E.J., 9, 495, (1963).

H7. Hanhart W., Ingold C.K., J.Chem.Soc., 997, (1927).

H8. Helfferich F., Ion Exchange,p^P 318, (McGraw Hill, 1962).

H9. ibid, p^P 159.

J1. Juracka F., Chem. Prumysl., 12, 158, (1962).

J2. Juracka F., Stamberg J., Zh.Prik.Khim.,35,10,2295 (1962).

J3. Juracks F., Kaspar K., Chem.Prumysl.,10, 554, (1960).

K1. Kressman T.R.E., Kitchener J.A., J.Chem.Soc.,1190,(1949).

K2. Kraus K.A., Raridon R.J., J.Phys.Chem., 63,1901, (1959).

K3. Kunin R., Ind. Eng.Chem., 3, 404, (1964).

M1. Marinsky J.A., Potter W.D., AECU-3348 (1954), A Stufy of Granular Ion Exchange.

M2. Mayer S.W., Tompkins E.R., J.Am. Chem.Soc., 69, 2866,(1947)

M3. Moller F., Methoden der Organischen Chemie, p^P 848, (Houben-Weyl, 1957).

M4. Miller A.I., PhD Thesis,London University,(1966).

N1. Nernst W. Z.Physik.Chem., 47, 52, (1904).

N2. Nernst W., Z.Physik.Chem., 2, 613, (1888).

P1. Pashkov A.B., Plastickeskie. Massy.,5, 20.

P2. Pepper K.W., Reichenberg D., Hale D.K.,J.Chem.Soc. 3129, (1952.

P3. Polyanskii N.G. Shaburov M.A., Zh.Prik.Khim., 38,115, (1965).

Q1. Q.V.F. Glass for Industry.

R1. Ryan J.L., Wheelwright E.J., Geneva, 1958, Vol 17, P 137.

R2. Rosen J.B., J.Chem.Phys., 20, 387, (1952).

R3. Reichenberg D., J.Am.Chem.Soc., 75, 589, (1953).

R4. Richman D., Thomas H.C., J.Phys.Chem., 60, 237,(1956).

S1. Sivetz P.M., Ind. Eng.Chem., 47,1020, (1955).

S2. Said A.S., A.I.Ch.E.J., 2, 447, (1956).
ibid, 5, 223, (1959).

S3. Sargent R., Rieman W.,J.Phys.Chem., 60,1370,(1956).

S4. Selke W.A., Bliss H., Chem.Eng.Prog., Symposium Series, 46,10, 509, (1950).

S5. Spalding D.B., Internat.J.Heat. and Mass.Transfer., 2, 283, (1951?.

S6. Schlögl R., Z.Elektrochem., 57, 195, (1953).

T1. Thomas H.C., J.Am.Chem.Soc., 66, 1664, (1944).

T2. Tien C., Thodos G., A.I.Ch.E.J., 5, 373, (1959).

T3. Tetenbaum M., Gregor H.P., J.Phys.Chem., 58, 1156,(1954))

V1. Vermeulen T., in Advances in Chemical Engineering Vol II, (Academic Press,1958).

W1. Wheaton R.M., Bauman W.C., Ind.Eng.Chem., 40,1350(1948).

W2. Weiss J., J.Chem.Soc. 297,(1943).

W3. Wilson J.N., J.Am.Chem.Soc., 62, 1538, (1940).

W4. Wheaton R.M., Bauman W.C., Ind.Eng.Chem., 43, 1088,(1951).

W5. Wheaton R.M.,Bauman W.C., Ind.Eng.Chem., 45,228,(1953).

W6. Wheaton R.M.,Chem.Eng.Prog., Symposium Series, 14,43,(1954).

W7. Wilke T., Hougen O.A., Trans.Am.Inst.Chem.Engrs., 41, 445, (1945).

Appendix 1

CONVERSION OF RESIN SAMPLES TO DESIRED IONIC FORM.

99% Conversion to a given ionic form was achieved by carrying out the appropriate cycle between chloride and the desired form four times in a fixed bed before final conversion. A sample from each batch was removed and checked for 99% conversion.

a) Hydroxide form.

A two stage process was used because of the unfavourable equilibrium (ref.W6). A solution of 0.1M sodium carbonate was passed through the bed followed by a 3M solution of sodium hydroxide.

b) Chloride form.

The raw resin as supplied by the manufacturer was predominantly in the chloride form. After pretreatment as described in chapter 2 the resin was washed with 4% hydrochloric acid and washed free of acid with methanol.

c) Nitrate form.

Chloride form resin was treated with 4% nitric acid and washed with methanol . Percentage conversion was checked by eluting a sample with 4% sodium sulphate and estimating the nitrate in the eluate by standard methods.

d) Borate,Thiocyanate and Sulphate form.

These were prepared by treating chloride form resin with 4% solutions of sodium tetraborate, ammonium thiocyanate and sulphuric acid respectively. Percentage conversion was determined by eluting samples with 4% sodium nitrate in the first two cases and 3M sodium hydroxide in the third case. The respective eluates were analysed by standard method.

Appendix 2

DEVELOPMENT OF THE CAPACITY ANALYSIS SCHEME.

The scope of the small scale studies described in Chapter 2 involved the analysis of a large number of samples and would have been very time consuming if carried out by normal volumetric and colourimetric techniques, each requiring individual attention. In addition Stamberg and Juracka (ref.J1) suggested that the standard Fisher Kunin method of capacity analysis was inaccurate. Their conclusions were confirmed by experiment here and the results are given in Table A1. Stamberg claims that whereas the ammonium hydroxide leach is popularly assumed to remove only those ions attached to the weak base groups, in fact some of those attached to the strong base groups are also exchanged and are converted from chloride to hydroxide form during analysis. These hydroxide groups are then released in the subsequent sulphate leach and can be measured by acid base titration. Hence the true weak and strong base capacity can be calculated.

The technique used in this work was Stamberg's, further modified to include the use of chlorine 36 tracer to measure chloride concentration rather than the conventional

TABLE A1.

Comparison of the new method with the Fisher Kunin method for measurement of capacity.

Analytical method used	Salt Splitting Capacity	Weak Base Capacity	Strong Base Capacity	Total Capacity
Fisher Kunin	2.92	1.02	2.22	3.24
"	2.90	0.93	2.31	3.24
"	2.92	1.03	2.21	3.24
" tracer used	2.92	1.05	2.18	3.23
Modified method	2.92	0.31	2.92	3.23
"	2.94	0.30	2.95	3.20
"	2.92	0.25	2.91	3.20
" tracer used	2.92	0.33	2.91	3.24

All capacities are given in milliequivalents per gram of dry resin. The tests were carried out on Amberlite IRA 400 in the hydroxide form. The makers quote the resin as having a total capacity of 3.30 meq/dry g.

Volhard titration, leaving the operator free to perform the relevant colorimetric analyses. In this way the time necessary for a complete analysis of one sample was almost halved.

A survey of counters was carried out to find the most efficient and easiest to use for automatic counting of chlorine 36. The isotope is a beta emmitter of energy 0.708 Mev. A special liquid counter (ref. D4,H4) using a GM4 tube was built and this was compared with a standard liquid Geiger Muller counter using a M6H tube and also with a solid source technique using a GM4 tube. It was found that the solid source technique was the most efficient but difficulty was experienced in making reproducible sources. Of the two liquid counters the special counter was the most efficient but least convenient to use, whereas the liquid M6H counter was much more easily filled and cleaned. The latter was therefore used.

One of the important disadvantages of the Fisher Kunin capacity analysis technique was the poor agreement between strong base and salt splitting capacity. This has been eliminated by using the new method. It can be seen (Table A1) that the salt splitting capacity measurement agrees in all cases as expected since no difference exists in the two schemes for this measurement . However, the value of strong base capacity should agree with the value of the salt splitting capacity and this is only the case where the new method is used. The values of total capacity are in

agreement in all cases. The use of the tracer technique gives the same results as when the chloride ion concentration is measured by Volhard titration.

The weak base capacity as given by the Fisher Kunin method is three times the correct value and the strong base capacity values are proportionatly smaller.

Appendix 3

AN ALTERNATIVE MODEL OF ION EXCHANGE.

a) Model formulation.

For the purposes of this model ion exchange resin beads were assumed to be quasi homogeneous, rather than to consist of a solid frame work with pore spaces as in reality. The effective diffusion coefficient calculated from experimental measurements using such a model is a macroscopic average for a large number of ions in pores of widely different sizes, shapes and directions in the solid matrix at greater and smaller distances from the pore surfaces. As such it expresses the average ability of a species to diffuse in any direction. A model based on such a diffusion coefficient is consistent only if all possible diffusion processes can indeed be described by a single diffusion coefficient . These requirements are met by most ion exchangers since the beads are isotropic and diffusion within them is not limited by slower non diffusional processes. In addition the application of diffusional flux equations based on a quasi homogeneous structure has proved quite successful in the common styrene type polymer ion exchange resin.

Ions originally in the solution must diffuse through the liquid "film" to reach the particle surface. Diffusion through the film depends upon the solution flow rate, which affects the film thickness, while diffusion through the particle remains unaltered. In this alternative approach the liquid film is replaced by an equivalent particle film, and the actual particle and the particle film are compounded into a hypothetical particle. This removes the difficulties normally encountered at the particle solution interface, since the concentration gradient is assumed to be continuous across the hypothetical particle, and to follow Fick's law equations. The concentration profiles in the real case and that assumed in the model are shown in FigwAl. Now, since both the liquid and equivalent particle film are very thin, the nature of the gradient assumed within them is not of great importance. In fact the Fick's law gradient is almost linear at the surface of the hypothetical particle. The thickness of the assumed particle film and hence the hypothetical particle radius vary with the solution flow rate.

Fig. A.1.

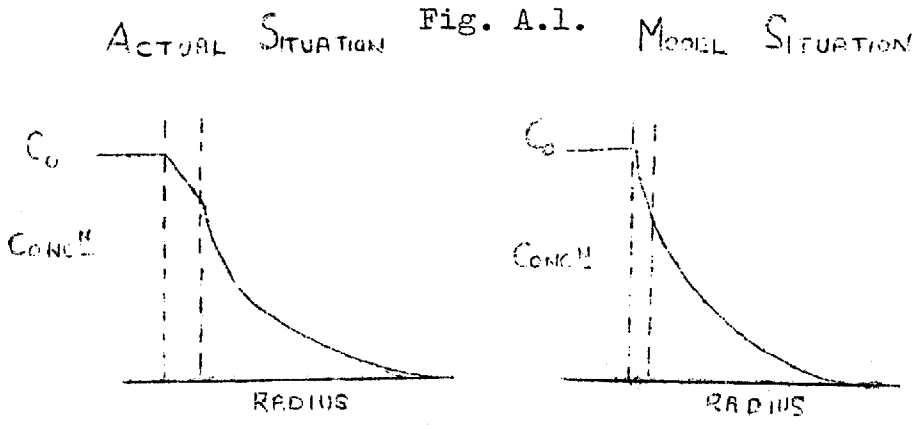

b) Mathematical developments.

The development of this alternative model of ion exchange was attempted but was not completed within the available time. The uncompleted work is described below, because the final solution of the problem is solely one of mathematical manipulation.

The model assumes equimolar counter diffusion within the particle according to Fick's law. This assumption ignores some of the more subtle effects associated with electric coupling between ions, but is otherwise quite satisfactory and has been successful in much past work. No specific interactions (ion-ion, ion-solvent or ion-matrix) are taken into account. The co ions are assumed to have no direct effect on diffusion within the particle because of Donnan exclusion. The diffusion coefficients are assumed to be independent of position within the bed. Variations in solution concentration and velocity over any cross section of the bed are assumed negligible. Concentration within the bed depends on one space variable x, and one time variable t.

i. Conservation of mass.

A mass balance over any cross section in the column;-

$$-\epsilon D_{ld}\frac{\partial^2 C_A}{\partial x^2} + \epsilon\frac{\partial C_A}{\partial t} + \frac{3(1-\epsilon)}{4\pi r_o^3}\frac{\partial M_A}{\partial t} + v\epsilon\frac{\partial C_A}{\partial x} = 0 \qquad \text{---A.1}$$

neglecting longitudinal dispersion i.e.

$$-\epsilon D_{ld}\frac{\partial^2 C_A}{\partial x^2} \ll v\epsilon\frac{\partial C_A}{\partial x}$$

and introducing a new variable $\theta = t - x/v$ where θ is the

time at which the saturating solution reaches any cross section distant x from the column entrance, equation A.1 can be simplified as follows:-

By a fundamental property of partial differentials:-

$$-v\left(\frac{\partial C_A}{\partial x}\right)_t = \left(\frac{\partial C_A}{\partial \theta}\right)_x - v\left(\frac{\partial C_A}{\partial x}\right)_\theta$$

$$= \left(\frac{\partial C_A}{\partial t}\right)_x - v\left(\frac{\partial C_A}{\partial x}\right)$$

and hence

$$\left(\frac{\partial C_A}{\partial x}\right) = \frac{-3(1-\epsilon)}{4\pi r_o^3}\left(\frac{\partial M_A}{\partial t}\right)_x \qquad \text{---A.2}$$

ii. The rate of diffusion into a sphere.

The equasion of diffusion in a homogeneous spherical particle, where the surfaces of equal concentration are concentric spheres is:-

$$\frac{\partial C_A}{\partial t} = D_P\left(\frac{\partial^2 C_A}{\partial r^2} - \frac{2}{r}\frac{\partial C_A}{\partial r}\right) \qquad \text{---A.3}$$

substituting $X=C_A r$ this reduces to:-

$$\frac{\partial X}{\partial t} = D_P \frac{\partial^2 X}{\partial r^2} \qquad \text{---A.4a}$$

If the particle initially saturated with ion B is situated within a column of similar ion exchanging particles, through which a solution of ions A has been passing since zero time, then the concentration of ion A at the surface of the spherical particle will be a function of time and position in the column.

The diffusion equation must be solved with the following boundary condition:-

$X = 0 \quad ; r = 0 ;$ ---A.4b

$X = \phi(t,x) \quad ; r = r_o ;$ ---A.4c

$X = 0 \quad ; t = 0 ;$ ---A.4d

If the parameter $\theta = t - x/v$ is used, the boundary condition become :-

$X = 0 \quad ; r = 0 ;$ ---A.5b

$X = \phi(\theta) \quad ; r = r_o ;$ ---A.5c

$X = 0 \quad ; \theta = 0 ;$ ---A.5d

and equation A.4a becomes :-

$$\frac{\partial X}{\partial \theta} = D_P \frac{\partial^2 X}{\partial r^2} \qquad \text{---A.5a}$$

θ represents time measured from the instant when the solution front reaches a given cross section in the column distant x units from the entrance. At that cross section diffusion begins when $\theta = 0$.

The solution of equation A.5a is given by Carslaw and Jager (ref.C.9) as :-

$$q_A = \frac{2}{rr_{on}} \sum_{n=1}^{\infty} \exp(-D_P n^2 \pi^2 \theta / r_o^2) \sin(n\pi r/r_o) \times -n$$

$$\int_0^{\theta} -n\pi D_P (-1)^n \exp(D_P n^2 \pi^2 (\lambda)/r_o^2) \phi(\lambda) d\lambda \qquad \text{---A.6}$$

The rate of diffusion across the surface of the particle may be obtained by differentiating A.6 with respect to r, substituting for $r=r_o$ and combining the result with equation A.7 to give A.8.

$$\frac{\partial M_A}{\partial t} = -D_P 4\pi r_o^2 \frac{\partial C_A}{\partial r} \qquad \text{---A.7}$$

$$\frac{\partial M_A}{\partial t} = C_1 \sum_{n=1}^{\infty} n^2 \exp(-D_p n^2 \pi^2 \theta / r_o^2) \times \int_o^{\theta} \exp(D_p n^2 \pi^2 \theta / r_o^2)\, q_A(r_o, \theta) \qquad \text{---A.8}$$

where C_1 is a constant.

At the particle surface equilibrium between particle and fluid phases is attained :-

hence $$\frac{q_A^*}{Q} = \frac{KC_A^*}{C_o} \quad (1+(K-1)C_A^* / C_o) \qquad \text{----A.9}$$

combining A.8 and A.9 with the continuity equation for the column A.2 gives the partial differential equation for column operation A.10:-

$$\frac{\partial C_A}{\partial t} = C_2 \sum_{n=1}^{\infty} n^2 \exp(-D_p n^2 \pi^2 \theta / r_o^2) \times \int_o^{\theta} \exp(D_p n^2 \pi^2 \theta / r_o^2)\, (KC_A/(1+(K-1)C_A)) \qquad \text{----A.10}$$

where C_2 is a constant.

The solution to the problem of diffusion into spheres in a deep packed column is given by the integration of A.10 Equation A.10 may only be integrated by trial and error so lo as the integral sign on the RHS remains. Using the substitutions $Y = (K-1)C_A/C_o$ and $Z = Y/(Y+1)$ are used to change A.10 to A.11:-

$$\frac{\partial Z}{\partial t} \frac{1}{(1-Z)^2} = P_3 \sum_{n=1}^{\infty} n^2 \exp(-D_p n^2 \pi^2 \theta / r_o^2) \int_o^{\theta} \exp(D_p n^2 \pi^2 \theta / r_o^2)\, Z \qquad \text{---A.11}$$

Now the LHS may be expanded by the binomial theorem to give the series $\sum_{n=1}^{\infty} nZ^{n-1}$. Subsequently the corresponding terms on each side of the equation A.11 may be equated. Generally this gives A.12.

$$nZ^{n-1}\frac{1}{n^2}\exp(D_p n^2\pi^2\theta/r_o^2) = P_3\int_0^{\theta}\exp(D_p n^2\pi^2\vartheta/r_o^2)\,Z\,d\vartheta \quad \text{---A.12}$$

Differentiation of both sides yields A.13 which can be integrated by the Laplace Transform method in principle.

$$\frac{Z^{n-1}}{n}\frac{\partial^2 Z}{\partial x\partial\theta} + \frac{(n-1)}{n}Z^{n-2}\frac{\partial Z}{\partial x}\frac{\partial Z}{\partial\theta} + nZ^{n-1}\frac{\partial Z}{\partial x} = \bar{G}Z \quad \text{----A.13}$$

where $\bar{G} = 8\pi^3 D_p^2 C_o QK/(K-1)r_o$

Insufficient time was available for the final solution of this problem since it was only a secondary aim of this work. However, at this stage the last step should merely be a matter of time.

Appendix 4

COMPUTER PROGRAMMES.

a) A programme to calculate diffusion coefficients from experimental breakthrough curves using Gilliland and Baddour's model. This comprises the following:-

i. The main programme, which reads in date, accomplishes part of the calculation and prints the results.

ii. A subroutine subprogramme SBGCAL which achieves the controlled trial and error calculations described in Section 4.3.3.

iii. A subroutine subprogramme FMTBGC which calculates the film mass transfer coefficient from Wilke and Hougen's correlation (ref.W7).

iv. A subroutine subprogramme DETECT which is used in minimum detection in conjunction with SBGCAL, in the controlled trial and error calculations.

Variable names used in the main programme.

Common variables.

B	correction factor in equation 4.4.
CAP	ultimate volumetric resin capacity.
CFINIS	external solution concentration at column entrance.

CMDIA	column diameter.
CMHT	column height.
CMPSLP	calculated mid point slope.
COAREA	column cross sectional area.
COLCAP	column volumetric capacity.
DG	percent degradation of strong base capacity.
DENS	external solution density.
DLIQ	external solution diffusion coefficient.
DPAR	particle diffusion coefficient.
EDIA	particle diameter.
EQCON	selectivity coefficient.
FLRATE	external solution flow rate.
IDIR	control variable in trial and error processes.
KBAR	$\bar{k}$ in nomenclature.
KF	film mass transfer coefficient.
KOV	overall mass transfer coefficient.
KPAR	particle mass transfer coefficient.
OMPSLP	observe mid point slope.
RF	film mass transfer resistance.
RFA	assumed film mass transfer resistance.
RN	Reynolds number.
ROV	overall mass transfer resistance.
SC	Schmidt number.
SPFLRT	specific flow rate.
TEMP	temperature .
VALA	constant term in Wilke and Hougen's equation.

VISC external solution viscosity.

VMID volume of effluent collected at mid point.

VOID voidage in resin column.

Dimensioned variables.

HEAD headings.

NGROUP group number.

NSERIS series number.

Undimensioned variables.

I subscript.

IF loop finishing value.

IS loop starting value.

K subscript.

KFACT parameter of KBAR.

PRAD particle radius.

X initial assumed value in trial and error process.

Variable names used in subroutine SBGCAL.

Undimensioned variables.

A assumed value in trial and error process.

BA nth assumed value of parameter.

BB n+1 th assumed value.

BC n+2 th assumed value.

D distribution factor.

DIFF general difference between assumed and actual value.

DIFFA nth difference.

DIFFB n+1 th difference.

DIFFC	n+2 th difference.
EQA	assumed value of parameter. in nth traverse of minimum.
EQB	assumed value in n+1 th traverse.
EQC	assumed value in n+2 th traverse.
IZ	control value.
JDISC	control value.
KDISC	control value.
KFACT	meaning as in main programme.
KTT	initial assumed value of parameter in trial and error process.
KZ	control value.
NDISC	control value.
NDIV	control value.
NQ	control value in minimum defection
NSX	control value in minimum detection.

Variable names used in subroutine FMTBGC.

Undimensioned variables.

EXPA	Reynolds number exponent.
EXPB	Schmidt number exponent.
KFACT	value of film mass transfer coefficient.

Variable names used in subroutine DETECT.

Undimensioned variables.

A	first value.
B	second value.
C	third value.
NA	controlled value transferred to subroutine.

NS control value transferred to calling programme.

The difference between the observed and assumed value of the perameter to be determined by trial and error must be calculated for three consecutive cases to allow the detection of minima and maximal The three difference values are stored in A,B and C. The absolute values of A, B and C must be used since the sign of the difference changes when a minimum or maximum is passed.

b) A programme for the prediction of break through curves from diffusion coefficients by Gilliland and Baddour's model. This comprises the following:-

i. The main programme BGPDN which reads in data calculates overall mass transfer coefficients and prints results .

ii. A subroutine subprogramme FMTBGP which calculates film mass transfer coefficients from Wilke and Hougen's equation .

iii. A subroutine subprogramme FLCVBG which calculates breakthrough curves from data supplied by the main programme.

N.B. This programme is set for a void fraction of 0.37 and a column diameter of 1.5 cm.

Variable names used in the main programme. These are only defined where they are different or additional to those in the previous programme.

Common variables.

RELCN relative effluent concentration C_A/C_o.

VOL volume of solution fed to column.

Undimentioned variables.

RP particle mass transfer resistance.

Variable names used in subroutine FLCVBG.

Dimensioned variables.

GEE	value of g(x,y) as in nomenclature.
UA	parameter x in g(x,y).
V	parameter y in g(x,y).
BIGGEE	value of G as in nomenclature.

c) A programme to calculate the pressure drop across a packed column of particles for any flow rate, particle size, voidage and fluid using the Carman Cozeny correlation. This comprises the following:-

i. The main programme PRESDP , which reads in data calculates the ordinate values from the input data, and calculates the pressure drop per unit bed length from the Carman Cozeny ordinate value supplied by the function subprogramme FRICF and prints results.

ii. A function subprogramme FRICF which determines the Carman Cozeny ordinate for any supplied abcissa value

Variable names used in the main programme.

Common variables.

F	Carman Cozeny abcissa value.
RN	Carman Cozeny ordinate value.

Dimensioned variables.

ROELIQ	Liquid density.
VISC	liquid viscosity.

Undimensioned variables.

X	Carman Cozeny abcissa value. in main programme.
REYNO	Reynolds number.

DELP	pressure drop.

Variable names used in the subprogramme FRICF.

Undimensioned variables.

FRICF	subprogramme returned value.
B	subprogramme argument.
FRF	interpolated value.
I	subscript.

```
IBFTC BGCAL
      REAL KF,KPAR,     KOV,KBAR,KFACT
      COMMON/COMA/EQCON(12),CFINIS(12),          DPAR(12)
     1,DENS(12),VISC(12),DLIQ(12),DEG(12),TEMP(12)
      COMMON/COMB/VMID(60),CMHT(60),FLRATE(60),SPFLRT(60),
     1                  KF(60),          RN(60),SC(60),VALA(60)
      COMMON/COMC/     CMDIA,VOID,COAREA,IDIR,PI,EDIA
      COMMON/COMD/OMPSLP(60),CMPSLP(60),COLCAP(60)
      COMMON/COMX/KPAR(12),KOV(60),KBAR(60),
      COMMON/COMY/RF(60),ROV(60),RFA(60)
      COMMON/COMV/CAP(12),B(12)
      DIMENSION NSERIS(60),NGROUP(60),HEAD(40)
      READ(5,4) (HEAD(I),I=1,30)
    4 FORMAT(6A6)
      VOID=0.37
      CMDIA=1.5
      PI=3.141952
      COAREA=CMDIA**2*PI/4.
      DO 21 K=1,1
      READ(5,2)  EQCON(K),CFINIS(K),PRAD     ,TEMP(K),DEG(K),DENS(K),VISC
     1(K),CAP(K),B(K)
    2 FORMAT(7E10.4,2F4.2)
      EDIA=PRAD*2.
      SQDIA=PRAD**2
      IS=(K-1)*5+1
      IF=IS+4
      DO 21 I=IS,IF
      READ(5,1)  FLRATE(I),CMHT(I),VMID(I),OMPSLP(I)
    1 FORMAT(4E10.4)
      COLCAP(I)=CMHT(I)*COAREA*(1.-VOID)*CAP(K)
      SPFLRT(I)=FLRATE(I)/(COAREA*VOID)
      NGROUP(I)=K
      NSERIS(I)=1
      IDIR=1
      X=0.1
   21 CALL SBGCAL(X,K,I,IS,IF)
      DO 22 K=1,1
      IS=(K-1)*5+1
      IF=IS+4
      IDIR=2
      X=ROV(IF)*B(K)/10.
      CALL SBGCAL (X,K,I,IS,IF)
      DO 23 I=IS,IF
   23 CALL FMTBGC (I,K)
   22 DPAR(K)=KPAR(K)*SQDIA/(4.*PI*PI)
      DO 526 K=1,6
      IS=(K-1)*5+1
      IF=IS+4
      IF(K.EQ.1) WRITE(6,10) (HEAD(I),I=1,6),(HEAD(I),I=13,18)
   10 FORMAT(1H1,5X,6A6/6X,6A6)
      IF(K.EQ.4) WRITE(6,10) (HEAD(I),I=1,6) (HEAD(I),I=19,24)
      IF(K.EQ.1) WRITE(6,916)
      IF(K.EQ.4) WRITE(6,916)
```

```
916 FORMAT(1H0,27X,18HBREAKTHROUGH CURVE,9X,8HSPECIFIC,2X,          6X,
   16HRADIUS,5X,22HDIFFUSION COEFFICIENTS/21X,8HOBSERVED,3X,8HOBSERVED
   2,3X,10HCALCULATED,2X,8HSOLUTION,2X,       8X,2HOF/1X,6HSERIES,2X,5H
   3GROUP,2X,3HRUN,3(2X,9HMID POINT),5X,4HFLOW,4X,                  6X,6
   4HACTUAL,8X,2HIN,9X,2HIN/22X,6HVOLUME,6X,5HSLOPE,6X,5HSLOPE,7X,4HRA
   5TE,4X,          5X,8HPARTICLE,4X,8HPARTICLE,5X,4HFILM//23X,3HML ,8X
   6,5H1/SEC,6X,5H1/SEC,6X,6HML/SEC,3X,      8X,2HCM,7X,9HCM*CM/SEC,2X
   7,9HCM*CM/SEC)
DO 522 I=IS,IF
522 WRITE(6,12) NSERIS(I),NGROUP(I),I,VMID(I),OMPSLP(I),CMPSLP(I),
   1SPFLRT(I),PRAD,                DPAR(K),DLIQ(K)
 12 FORMAT(1H0,I4,I7,I5,E13.3,3E11.3,       E13.6,2E11.3)
526 WRITE(6,13) CFINIS(K),TEMP(K),DEG(K)    ,EDIA
 13 FORMAT(1H0,6X,13HCONCENTRATION,F7.3,2H N,13H  TEMPERATURE,F6.2,
   12H C,24H  PERCENTAGE DEGRADATION,F7.2,19H  PARTICLE DIAMETER,E13.4
   2,3H CM)
    DO 527 K=1,6
    IS=(K-1)*5+1
    IF=IS+4
    IF(K.EQ.1) WRITE(6,10) (HEAD(I),I=1,6) (HEAD(I),I=13,18)
    IF(K.EQ.4) WRITE(6,10) (HEAD(I),I=1,6) (HEAD(I),I=19,24)
    IF(K.EQ.1) WRITE(6,911)
    IF(K.EQ.4) WRITE(6,911)
911 FORMAT(1H0,5X,048HSERIES   GROUP   RUN   OVERALL      FILM          S
   1                                                              ,63H0
   1LUTION    PARTICLE    REYNOLDS    SCHMIDT                      /6X,
   1108HNO       NO       NO    M.T.        M.T.        FLOW        M.T
   1        NUMBER       NUMBER                  /18X,61H
   1COEFF       COEFF        RATE        COEFF        /29X,41HSEC-1
   1   SEC-1         ML/SEC      SEC-1)
    DO 523 I=IS,IF
    WRITE(6,6)   FLRATE(I),CMHT(I),VMID(I),OMPSLP(I)
  6 FORMAT(1HP,4E10.4)
523 WRITE(6,913) NSERIS(I),NGROUP(I),I,KOV(I),KF(I),FLRATE(I),
   1KPAR(K),RN(I),SC(I)
913 FORMAT(1H0,   I7,I9,I8,E14.3,5E12.3)
527 WRITE(6,13) CFINIS(K),TEMP(K),DEG(K)    ,EDIA
```

```
      DO 3071  K=1,6
      IF(KXX.EQ.5.AND.K.EQ.3)   GO TO 3071
      IF(KXX.EQ.5.AND.K.EQ.6)   GO TO 3071
      IF(KXX.EQ.8.AND.K.EQ.3)   GO TO 3071
      IF(KXX.EQ.8.AND.K.EQ.6)   GO TO 3071
      IS=(K-1)*5+1
      IF=IS+4
      IF(K.EQ.1)  WRITE(6,517)  (HEAD(I),I=25,30)
      IF(K.EQ.4)  WRITE(6,517)  (HEAD(I),I=25,30)
  517 FORMAT(1H1,5X,6A6)
      IF(K.EQ.1)  WRITE(6,519)
      IF(K.EQ.4)  WRITE(6,519)
  519 FORMAT(1HO,1X,78HSERIES  GROUP  RUN  FLOW      CONCN      TEMP  DEN
     1SITY   VISCOSITY  DEGRDN  COL,23HUMN   CAPACITY  COLUMN/22X,4HRAT
     2E,51X,2HHT,18X,8HCAPACITY/22X,6HML/SEC,5X,67HN          C      GM/CC
     3    POISE       &         CM        MEQ/ML    MEQ//)
 3071 WRITE(6,3061) (NSERIS(I),NGROUP(I),I,FLRATE(I),CFINIS(K),TEMP(K),D
     1ENS(K),VISC(K),DEG(K),CMHT(I),CAP(K),COLCAP(I) ,I=IS,IF)
 3061 FORMAT(1HO,1X,I1,I8,I7,2X,2E10.2,F6.1,2E10.2,F8.1,3E10.2)
  525 CONTINUE
      STOP
      END
```

```
      SUBROUTINE SBGCAL (X,K,I,IS,IF)
      REAL KF,KPAR,KTT,KOV,KBAR,KFACT
      COMMON/COMA/EQCON(12),CFINIS(12),          DPAR(12)
     1,DENS(12),VISC(12),DLIQ(12),DEG(12),TEMP(12)
      COMMON/COMB/VMID(60),CMHT(60),FLRATE(60),SPFLRT(60),
     1                KF(60),          RN(60),SC(60),VALA(60)
      COMMON/COMC/    CMDIA,VOID,COAREA,IDIR,PI,EDIA
      COMMON/COMD/OMPSLP(60),CMPSLP(60),COLCAP(60)
      COMMON/COMX/KPAR(12),KOV(60),KBAR(60),
      COMMON/COMY/RF(60),ROV(60),RFA(60)
      COMMON/COMV/CAP(12),B(12)
      IZ=1

      JDISC=1
  653 KTT=X
  660 GO TO (640,641,639),JDISC
  640 NQ=-1
      GO TO 642
  641 NQ=1
      GO TO 642
  639 KTT=1.1*KTT
      JDISC=1
      GO TO 660
  642 NDISC=1
  656 KDISC=0
  648 KDISC=KDISC+1
      NDIV=KDISC-1
  655 NDIV=NDIV+1
      GO TO (643,644,645),NDISC
  643 EQA=KTT+FLOAT(NQ)*FLOAT(NDIV-1)*X/2.
      Y=EQA
      GO TO 647
  644 EQB=EQA-FLOAT(NQ)*FLOAT(NDIV-1)*X/4.
      Y=EQB
      GO TO 647
  645 EQC=EQB+FLOAT(NQ)*FLOAT(NDIV-1)*X/8.
      Y=EQC
  647 GO TO (822,823),IDIR
  822 IF(IZ.EQ.1)     KBAR(I)=Y
      IF(IZ.EQ.2.AND.KZ.EQ.1) KBAR(I)=(BB*DIFFA+BA*DIFFB)/(DIFFA+DIFFB)
      IF(IZ.EQ.2.AND.KZ.EQ.2) KBAR(I)=(BC*DIFFB+BB*DIFFC)/(DIFFB+DIFFC)
      KFACT=CFINIS(K)*KBAR(I)/(4.*FLRATE(I))
      KOV(I)=KBAR(I)*EQCON(K)/(EQCON(K)-1.)
      IF(KOV(I).LT.0.)        KOV(I)=-KOV(I)
```

```
      ROV(I)=B(K)*VOID/(KOV(I)*CAP(K)*(1.-VOID))
      CMPSLP(I)=KFACT
      IF(IZ.EQ.2)   RETURN
      DIFF=CMPSLP(I)-CMPSLP(I)
      GO TO 824
  823 A=0.
      DO 20 I=IS,IF
      RF(I)=ROV(I)-Y
      RFA(I)=SPFLRT(I)**(-0.49)
   20 A=A+RF(I)/RFA(I)
      DIFF=ABS(A-5.*RF(IF)/RFA(IF))
  824 IF(NDIV-(KDISC+1))630,631,632
  630 DIFFA=DIFF
      BA=KBAR(I)
      GO TO 655
  631 DIFFB=DIFF
      BB=KBAR(I)
      GO TO 655
  632 DIFFC=DIFF
      BC=KBAR(I)
      IF((DIFFA*DIFFB).LE.0.)     KZ=1
      IF((DIFFC*DIFFB).LE.0.)    KZ=2
      CALL DETECT(DIFFA,DIFFB,DIFFC,NDISC,NSX)
      NDISC=NSX
      GO TO (648,648,648,649,649,650,651,652),NDISC
  652 JDISC=JDISC+1
      GO TO 653
  649 NDISC=NDISC-2
      GO TO 656
  650 GO TO (751,750),IDIR
  751 IZ=2
      GO TO 822
  750 D=CAP(K)*(1.-VOID)/(CFINIS(K)*VOID)
      KPAR(K)=Y*D
      DO 720 I=IS,IF
  720 KF(I)=1./RF(I)
  752 CONTINUE
  651 CONTINUE
      RETURN
      END
```

```
$IBF C FTHICK
      SUBROUTINE FMTBGC  (I,K)
      REAL KF,KPAR,    KOV,KBAR,KFACT
      COMMON/COMA/EQCON(12),CFINIS(12),          DPAR(12)
     ,DENS(12),VISC(12),DLIQ(12),DEG(12),TEMP(12)
      COMMON/COMB/VMID(60),CMHT(60),FLRATE(60),SPFLRT(60),
     1              KF(60),          RN(60),SC(60),VALA(60)
      COMMON/COMC/    CMDIA,VOID,COAREA,IDIR,PI,EDIA
      COMMON/COMD/OMPSLP(60),CMPSLP(60),COLCAP(60)
      COMMON/COMX/KPAR(12),KOV(60),KBAR(60),
      COMMON/COMY/RF(60),ROV(60),RFA(60)
      EXPA=-0.51
      EXPB=-0.67
      SPFLRT(I)=FLRATE(I)/COAREA
      RN(I)=SPFLRT(I)*VOID*EDIA*DENS(K)/VISC(K)
      VALA(I)=1.82*SPFLRT(I)
      SC(I)=((KF(I)*EDIA)/(6.*(1.-VOID)*VALA(I)*(RN(I)**EXPA)))**(1./EXP
     1B)
      DLIQ(K)=VISC(K)/(DENS(K)*SC(I))
      RETURN
      END
```

```
BFTC MINDEC  DECK
      SUBROUTINE DETECT(A,B,C,NS,NA)
      A=ABS(A)
      B=ABS(B)
      C=ABS(C)
      IF(B.LT.A.AND.C.LT.B) GO TO 20
      IF(B.LT.A.AND.C.GE.B) GO TO 21
      IF(B.EQ.A.AND.C.GT.B) GO TO 21
      IF(B.GT.A.AND.C.GT.B) GO TO 22
      IF(B.GT.A.AND.C.LE.B) GO TO 23
   20 NA=NS
      GO TO 24
   21 NA=NS+3
      GO TO 24
   22 NA=8
      GO TO 24
   23 WRITE(6,100)
  100 FORMAT(1H1,6X,15HMAXIMUM PRESENT)
      NA=7
   24 RETURN
      END
```

```
IBFTC BGPDN   NODECK
      REAL KF,KPAR,     KOV,KBAR
      COMMON/COMA/EQCON(12),CFINIS(12),          DPAR(12)
     1,DENS(12),VISC(12),DLIQ(12),DEG(12),TEMP(12)
      COMMON/COMB/VMID(60),CMHT(60),FLRATE(60),SPFLRT(60),
     1                KF(60),          RN(60),SC(60),VALA(60)
      COMMON/COMC/     CMDIA,VOID,COAREA,IDIR,PI,EDIA
      COMMON/COMD/OMPSLP(60),CMPSLP(60),COLCAP(60)
      COMMON/COME/RELCN(400),VOL(400)
      COMMON/COMX/KPAR(12),KOV(60),KBAR(60)
      COMMON/COMY/RF(60),ROV(60),
      COMMON/COMZ/CAP(12),B(12)

      DIMENSION NSERIS(60),NGROUP(60),HEAD(40)
      READ(5,4) (HEAD(I),I=1,30)
    4 FORMAT(6A6)
      VOID=0.37
      CMDIA=1.5
      PI=3.141952
      COAREA=CMDIA**2*PI/4.
      DO 626 K=1,6
      READ(5,2)  EQCON(K),CFINIS(K),PRAD    ,TEMP(K),DEG(K),DENS(K),VISC
     1(K),CAP(K),B(K)
    2 FORMAT(7E10.4,2F4.2)
      EDIA=PRAD*2.
      SQDIA=PRAD**2
      READ(5,3)    DPAR(K),DLIQ(K)
    3 FORMAT(2E10.4)
      D=CAP(K)*(1.-VOID)/(CFINIS(K)*VOID)
      KPAR(K)=4.*PI*PI*DPAR(K)/SQDIA
      RP=1./(KPAR(K)*D)
      IS=(K-1)*5+1
      IF=IS+4
      DO 627 I=IS,IF
      READ(5,3) FLRATE(I),CMHT(I)
      COLCAP(I)=CMHT(I)*COAREA*(1.-VOID)*CAP(K)
      SPFLRT(I)=FLRATE(I)/(COAREA*VOID)
      XOV=CMHT(I)/SPFLRT(I)
      NGROUP(I)=K
      NSERIS(I)=1
```

```
      CALL FMTBGP(I,K)
      RF(I)=PRAD/(KF(I)*3.*(1.-VOID))
      ROV(I)=RP+RF(I)
      KOV(I)=B(K)*VOID/(ROV(I)*CAP(K)*(1.-VOID))
      KBAR(I)=KOV(I)*(EQCON(K)-1.)/EQCON(K)
      IF(KBAR(I).LT.0.)   KBAR(I)=-KBAR(I)
      IF(I.EQ.IS)     WRITE(6,650)   KXX
  650 FORMAT(1H1,6X,I4)
      WRITE(6,18) NSERIS(I),NGROUP(I),I
   18 FORMAT(1HO,5X,13HSERIES NO     ,I3,4X,12HGROUP NO     ,I3,4X,
     19HRUN NO    ,I3//5X,4HC/CO,2X,6HVOLUME)
      CALL FLCVBG (XOV,I,K,IS,IF)
      WRITE(6,9)    FLRATE(I),CMHT(I)
    9 FORMAT(1HP,2E10.4)
      CMPSLP(I)=KBAR(I)*CFINIS(K)/(4.*SPFLRT(I))
      OMPSLP(I)=CMPSLP(I)
  627 CONTINUE
  626 CONTINUE
      DO 526 K=1,6
      IF(K.EQ.1) WRITE(6,10) (HEAD(I),I=1,6) (HEAD(I),I=13,18)
   10 FORMAT(1H1,5X,6A6/6X,6A6)
      IF(K.EQ.4) WRITE(6,10) (HEAD(I),I=1,6) (HEAD(I),I=19,24)
      IF(K.EQ.1) WRITE(6,916)
      IF(K.EQ.4) WRITE(6,916)
  916 FORMAT(1HO,27X,18HBREAKTHROUGH CURVE,9X,8HSPECIFIC,2X,          6X,
     16HRADIUS,5X,22HDIFFUSION COEFFICIENTS/21X,8HOBSERVED,3X,8HOBSERVED
     2,3X,10HCALCULATED,2X,8HSOLUTION,2X,       8X,2HOF/1X,6HSERIES,2X,5H
     3GROUP,2X,3HRUN,3(2X,9HMID POINT),5X,4HFLOW,4X,                  6X,6
     4HACTUAL,8X,2HIN,9X,2HIN/22X,6HVOLUME,6X,5HSLOPE,6X,5HSLOPE,7X,4HRA
     5TE,4X,          5X,8HPARTICLE,4X,8HPARTICLE,5X,4HFILM//23X,3HML  ,8X
     6,5H1/SEC,6X,5H1/SEC,6X,6HML/SEC,3X,       8X,2HCM,7X,9HCM*CM/SEC,2X
     7,9HCM*CM/SEC)
      IS=(K-1)*5+1
      IF=IS+4
      DO 522 I=IS,IF
  522 WRITE(6,12) NSERIS(I),NGROUP(I),I,VMID(I),OMPSLP(I),CMPSLP(I),
     1SPFLRT(I),PRAD,              DPAR(K),DLIQ(K)
   12 FORMAT(1HO,I4,I7,I5,E13.3,3E11.3,      E13.6,2E11.3)
  526 WRITE(6,13) CFINIS(K),TEMP(K),DEG(K)   ,EDIA
   13 FORMAT(1HO,6X,13HCONCENTRATION,F7.3,2H N,13H  TEMPERATURE,F6.2,
     12H C,24H  PERCENTAGE DEGRADATION,F7.2,19H  PARTICLE DIAMETER,E13.4
     2,3H CM)
      DO 527 K=1,6
      IS=(K-1)*5+1
      IF=IS+4
      IF(K.EQ.1) WRITE(6,10) (HEAD(I),I=1,6) (HEAD(I),I=13,18)
```

```
      IF(K.EQ.4) WRITE(6,10) (HEAD(I),I=1,6) (HEAD(I),I=19,24)
      IF(K.EQ.1) WRITE(6,911)
      IF(K.EQ.4) WRITE(6,911)
   11 FORMAT(1HO,5X,048HSERIES   GROUP   RUN   OVERALL      FILM          S
     1                                                              ,63HO
     1LUTION    PARTICLE     REYNOLDS     SCHMIDT                    /6X,
     1108HNO       NO        NO     M.T.          M.T.          FLOW       M.T
     1         NUMBER          NUMBER                      /18X,61H
     1COEFF        COEFF         RATE          COEFF          /29X,41HSEC-1
     1   SEC-1          ML/SEC       SEC-1)
      DO 523 I=IS,IF
  523 WRITE(6,913) NSERIS(I),NGROUP(I),I,KOV(I),KF(I),FLRATE(I),
     1KPAR(K),RN(I),SC(I)
  913 FORMAT(1HO,    I7,I9,I8,E14.3,5E12.3)
  527 WRITE(6,13) CFINIS(K),TEMP(K),DEG(K)    ,EDIA
      DO 3071  K=1,6
      IS=(K-1)*5+1
      IF=IS+4
      IF(K.EQ.1)  WRITE(6,517)  (HEAD(I),I=25,30)
      IF(K.EQ.4)  WRITE(6,517)  (HEAD(I),I=25,30)
  517 FORMAT(1H1,5X,6A6)
      IF(K.EQ.1)  WRITE(6,519)
      IF(K.EQ.4)  WRITE(6,519)
  519 FORMAT(1HO,1X,78HSERIES  GROUP  RUN  FLOW      CONCN      TEMP  DEN
     1SITY   VISCOSITY  DEGRDN  COL,23HUMN    CAPACITY  COLUMN/22X,4HRAT
     2E,51X,2HHT,18X,8HCAPACITY/22X,6HML/SEC,5X,67HN          C      GM/CC
     3    POISE       £         CM          MEQ/ML    MEQ//)
  071 WRITE(6,3061) (NSERIS(I),NGROUP(I),I,FLRATE(I),CFINIS(K),TEMP(K),D
     1ENS(K),VISC(K),DEG(K),CMHT(I),CAP(K),COLCAP(I) ,I=IS,IF)
  061 FORMAT(1HO,1X,I1,I8,I7,2X,2E10.2,F6.1,2E10.2,F8.1,3E10.2)
  525 CONTINUE
      STOP
      END
```

```
      SUBROUTINE FLCVBG (XOV,I,K,IS,IF)
      REAL KF,KPAR,    KOV,KBAR
      COMMON/COMA/EQCON(12),CFINIS(12),          DPAR(12)
     1,DENS(12),VISC(12),DLIQ(12),DEG(12),TEMP(12)
      COMMON/COMB/VMID(60),CMHT(60),FLRATE(60),SPFLRT(60)  ,
     1.                   ,KF(60),          ,RN(60),SC(60),VALA(60)
      COMMON/COMC/    CMDIA,VOID,COAREA,IDIR,PI
      COMMON/COMD/OMPSLP(60),CMPSLP(60),COLCAP(60)
      COMMON/COME/RELCN(400),VOL(400)
      COMMON/COMX/KPAR(12),KOV(60),KBAR(60)
      COMMON/COMY/RF(60),ROV(60),

      DIMENSION V(2),GEE(2),UA(2)
      JA=1
      H=0.1*FLOAT(I-IS+1)*4.*0.1/(CFINIS(K)*5.)
      HB=10.**3*H
      TX=XOV*FLRATE(I)
      YA=0.001
      DO 1020 J=1,1000
      JB=J-JA+1
      VOL(JB)=TX+FLOAT(JB-1)*HB
      Y=YA+FLOAT(JB-1)*HB
      APAR= COLCAP(I)        /CFINIS(K)-Y
      BPAR=APAR*KBAR(I)*CFINIS(K)/SPFLRT(I)
      U=KOV(I)*CFINIS(K)/SPFLRT(I)
      V(2)=KOV(I)*COLCAP(I)          /SPFLRT(I)
      V(1)=V(2)/EQCON(K)
      ID=0
      UA(1)=U*Y
      UA(2)=UA(1)/EQCON(K)
   48 ID=ID+1
      A=SQRT(V(ID))-SQRT(UA(ID))
      C=A*A
      IF(C.GT.80.)          C=80.
      DERF=2.*EXP(-C)/SQRT(PI)
      GEE(ID)=0.5*(1.-ERF(A))+DERF/(4.*SQRT(SQRT(V(ID)*UA(ID)))+4.*SQRT(
     1UA(ID)))
      IF(ID.EQ.1)    GO TO 48
      BIGGEE=(1.-GEE(2))/GEE(1)
      IF(BPAR.GT.80.)     BPAR=80.
      IF(BPAR.LT.-80.)     BPAR=-80.
      RELCN(JB)=1./(1.+BIGGEE*EXP(BPAR))
  546 IF(RELCN(JB)-0.10)   1020,230,230
  230 IF(HB-(H*10.+0.001))231,231,232
  231 IF(RELCN(JB).GE.0.99)  GO TO 1030
      GO TO 1020
  232 JA=J+1
      IF(TX.NE.VOL(JB))  TX=VOL(JB-1)
      IF(YA.NE.Y)    YA=Y-HB
      HB=HB/10.
 1020 CONTINUE

 1030 WRITE(6,1010)  (RELCN(JC),VOL(JC),JC=1,JB)
 1010 FORMAT(1H ,6X,8E12.4)
      DO 1021 J=1,1000
```

```
      IF(RELCN(J)-0.5)  1021,241,242
  241 VMID(I)=VOL(J)
      RETURN
  242 JC=J-1
      VMID(I)=VOL(J)-(VOL(J)-VOL(JC))*(RELCN(J)-0.5)/(RELCN(J)-RELCN(JC)
     1)
      RETURN
 1021 CONTINUE
      RETURN
      END
```

```
IBFTC FTHICK  DECK
      SUBROUTINE FMTBGP (I,K)
      REAL KF,KPAR,     KOV,KBAR
      COMMON/COMA/EQCON(12),CFINIS(12),          DPAR(12)
     1,DENS(12),VISC(12),DLIQ(12),DEG(12),TEMP(12)
      COMMON/COMB/VMID(60),CMHT(60),FLRATE(60),SPFLRT(60)   ,
     1                KF(60),          RN(60),SC(60),VALA(60)
      COMMON/COMC/     CMDIA,VOID,COAREA,IDIR,PI,EDIA
      EXPA=-0.51
      EXPB=-0.67
      RN(I)=SPFLRT(I)*VOID*EDIA*DENS(K)/VISC(K)
      SC(I)=VISC(K)/(DENS(K)*  DLIQ(K))
      VALA(I)=1.82*SPFLRT(I)
      KF(I)=VALA(I)*(RN(I)**EXPA)*(SC(I)**EXPB)
      RETURN
      END
```

```
$IBFTC PRESDP
      COMMON//RN(50),F(50)
      DIMENSION ROELIQ(50),VISC(50)
      PI=3.141592
      READ(5,1)     (RN(I),F(I),I=1,14)
    1 FORMAT(2E7.2)
      READ(5,1)  PDIA,CMDIA
      COAREA=CMDIA**2*PI/4.
      VOID=0.40
      READ(5,1)    ROELIQ(1),VISC(1)
      WRITE(6,10)
   10 FORMAT(1H1,6X,34HPRESSURE DROP IN BEDS OF PARTICLES///
     16X,35HSEE PERRY CHEM ENGRS HANDBOOK,P 394)
      WRITE(6,11)  VOID
   11 FORMAT(1H0,6X,13HBED VOIDAGE=,F6.2////7X,8HFLOWRATE,3X,11HSUPERFIC
     1IAL,2X,8HREYNOLDS,4X,8HFRICTION,14X,8HPRESSURE/3X,11HTHROUGH BED,3
     2X,8HVELOCITY,5X,6HNUMBER,6X,6HFACTOR,3X,18HPER UNIT BED DEPTH)
      DO 20 K=1,50
      FLRATE=FLOAT(K/10)
      SPFLRT=FLRATE/COAREA
      S=6.*(1.-VOID)/PDIA
      REYNO =ROELIQ(1)*SPFLRT/(VISC(1)*S)
      X=FRICF(REYNO)
      DELP=X*S*ROELIQ(1)*SPFLRT**2/(144.*32.2*VOID**3)
   20 WRITE(6,12)  FLRATE,SPFLRT,REYNO,X,DELP
   12 FORMAT(1H0,6X,4E12.4,6X,E12.4)
   21 WRITE(6,13)
   13 FORMAT(1H0,6X,19HUNITS ARE LB,FT,SEC)
      STOP
      END
```

```
$IBFTC FIG35
      FUNCTION FRICF(B)
      COMMON//RN(50),F(50)
      DO 20 I=1,14
      IF(RN(I)-B)  20,40,41
   20 CONTINUE
   40 FRICF=F(I)
      RETURN
   41 N=I-1
      FRF=(ALOG10(RN(I))-ALOG10(B))*(ALOG10(F(I))-ALOG10(F(N)))/
     1(ALOG10(RN(I))-ALOG10(RN(N)))
      FRICF=10.**ABS(ALOG10(F(I))-FRF)
      RETURN
      END
```

```
010E-01048E 03
010E 00052E 02
010E 01050E 01
030E 01018E 01
050E 01012E 01
010E 02072E 00
020E 02052E 00
050E 02037E 00
010E 03030E 00
020E 03026E 00
050E 03021E 00
010E 04019E 00
050E 04017E 00
010E 05015E 00
023E-02060E 00
062E 02070E-03
```

The first fourteen data cards contain the Carman-Cozeny correlation curve as fourteen X and Y values. These cards must be included in the programme. The number of following data cards will depend on the number of separate calculations to be carried out.

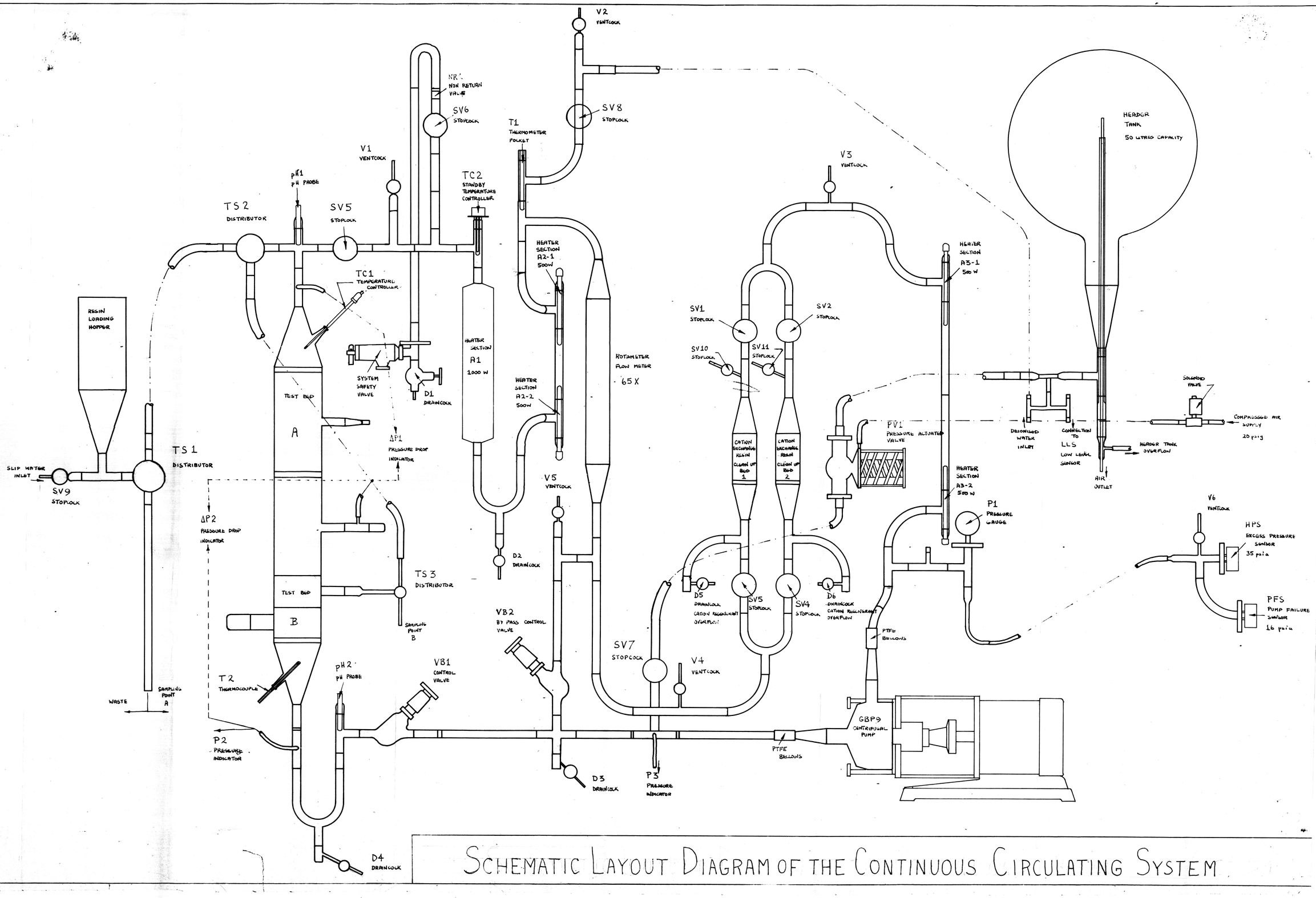

SCHEMATIC LAYOUT DIAGRAM OF THE CONTINUOUS CIRCULATING SYSTEM